APPROVED FOR RELEASE: 2007/02/08: CIA-RDP82-00850R000200030043-9

20 1978 _YA' = 1 OF

APPROVED FOR RELEASE: 2007/02/08: CIA-RDP82-00850R000200030043-9

APPROVED FOR RELEASE: 2007/02/08: CIA-RDP82-00850R000200030043-9

FOR OFFICIAL USE ONLY

JPRS L/8827

20 December 1978

Translation

Seismic Studies with the 'Zemlya' Device

FBIS FOREIGN BROADCAST INFORMATION SERVICE

FOR OFFICIAL USE ONLY

APPROVED FOR RELEASE: 2007/02/08: CIA-RDP82-00850R000200030043-9

APPROVED FOR RELEASE: 2007/02/08: CIA-RDP82-00850R000200030043-9

NOTE

JPRS publications contain information primarily from foreign newspapers, periodicals and books, but also from news agency transmissions and broadcasts. Materials from foreign-language sources are translated; those from English-language sources are transcribed or reprinted, with the original phrasing and other characteristics retained.

Headlines, editorial reports, and material enclosed in brackets [] are supplied by JPRS. Processing indicators such as [Text] or [Excerpt] in the first line of each item, or following the last line of a brief, indicate how the original information was processed. Where no processing indicator is given, the information was summarized or extracted.

Unfamiliar names rendered phonetically or transliterated are enclosed in parentheses. Words or names preceded by a question mark and enclosed in parentheses were not clear in the original but have been supplied as appropriate in context. Other unattributed parenthetical notes within the body of an item originate with the source. Times within items are as given by source.

The contents of this publication in no way represent the policies, views or attitudes of the U.S. Government.

For further information on report content call (703) 351-2938 (economic); 3468 (political, sociological, military); 2726 (life sciences); 2725 (physical sciences).

COPYRIGHT LAWS AND REGULATIONS GOVERNING OWNERSHIP OF MATERIALS REPRODUCED HEREIN REQUIRE THAT DISSEMINATION OF THIS PUBLICATION BE RESTRICTED FOR OFFICIAL USE ONLY.

APPROVED FOR RELEASE: 2007/02/08: CIA-RDP82-00850R000200030043-9

APPROVED FOR RELEASE: 2007/02/08: CIA-RDP82-00850R000200030043-9

JPRS L/8827

20 December 1979

SEISMIC STUDIES WITH THE 'ZEMLYA' DEVICE

Moscow SEYSMICHESKIYE ISSLEDOVANIYA S APPARATUROY "ZEMLYA" in Russian 1977 signed to press 31 Jan 77 pp 1-256

Book by I. V. Pomerantseva and A. N. Mozzhenko, Izdatel'stvo "Nedra," 1400 copies

CONTENTS

PAGE

ANNOTATION 1

INTRODUCTION 2

Part 1. Theoretical Fundamentals of Using Different Wave Fields to Study the Structure of the Earth's Crust and Upper Mantle. 15

CHAPTER 1. PHYSICAL CONCEPTS ON LONGITUDINAL P, TRANSVERSE S AND COMPOSITE PS WAVES ON RECORDINGS FROM EARTHQUAKES AND EXPLOSIONS 15

Wave Fields Observed During the Initial Part of the Earthquake Seismogram Recording. 15

Dynamic Characteristics of Single P and PS Waves from Theoretical Calculations. 27

The Nature of Longitudinal and Transverse Waves from Explosions and Earthquakes and the Field of Their Application. 32

CHAPTER 2. HODOGRAPHS AND VECTORS OF P AND PS WAVE DISPLACEMENTS. . . 35

Equations of Hodographs and of the Recording Times of Single, Multiple and Lateral P and PS Waves 35

Displacement Vector Components of Single Transient P and PS Waves and Their Azimuths in a Two-Layer Three-Dimensional Medium with a Sloping Exchange Boundary 50

Part 2. The "Zemlya" Device, Method of Observations and Interpretation of the Materials 57

APPROVED FOR RELEASE: 2007/02/08: CIA-RDP82-00850R000200030043-9

APPROVED FOR RELEASE: 2007/02/08: CIA-RDP82-00850R000200030043-9

CHAPTER 3. THE "ZEMLYA" DEVICE. 57

Main Characteristics of the Optimum Design of the Device for Continuous Recording of Seismic Signals 57
Block Diagram of the Device for Continuous Recording of Seismic Oscillations 58
The Field Recorder. 62
A Device for Unified Time Marking of Field Recorders (A Radio Channel) 67
A Field Recording Reproduction Apparatus 71
Frequency and Amplitude Characteristics of the Channel 74
Method of Determining the Relative Sensitivity of the Channel 74
The Nature of Oscillations Recorded by the Channel. 80
Checking the Device Prior to the Beginning and During Field Operations. 82
A Device for Processing Magnetic Tapes of "Zemlya" Recording Stations on Analog and Digital Computers. 84

CHAPTER 4. METHOD OF OBSERVATIONS 86

Field Operations. 86
Characteristics of Studies with the "Zemlya" Device 95
The Volume and Conditions for Recording Field Signals 98

CHAPTER 5. WAVE FIELDS ON RECORDINGS FROM EARTHQUAKES AND EXPLOSIONS. 105

Separation and Correlation of the First P and S Waves on Recordings from Local and Near Earthquakes and Explosions 106
Separation and Correlation of P and PS Waves on Recordings From Earthquakes and Explosions 107
The Wave Patterns on Recordings from Local Earthquakes (Δ = 0-40 km) 126
The Wave Pattern on Recordings from Near Earthquakes (Δ = 50-500 km) 128
The Wave Pattern on Recordings from Explosions (Δ = 0-700 km). 130
The Wave Pattern on Recordings from Far Earthquakes (Δ = 10-160°) 136
The Nature of the Wave Field in Fault Zones and in the Presence of Subvertical Contacts of Media of Different Petrographic Composition. 139

CHAPTER 6. DYNAMIC CHARACTERISTICS OF EXPERIMENTAL P AND PS WAVES AND THEIR COMPARISON TO THEORETICAL DATA. 143

The Form of the P and PS Wave Recording. 143
The Ratios of the Amplitudes of PS to P Waves and Their Dependence on the Parameters of the Medium. 146
Visible Periods and Frequency Spectra of P and PS Waves 151
Polarization of PS Waves 152
The Nature of PS Waves of Different Groups and the Criteria for Separating Them on Recordings 163

APPROVED FOR RELEASE: 2007/02/08: CIA-RDP82-00850R000200030043-9

APPROVED FOR RELEASE: 2007/02/08: CIA-RDP82-00850R000200030043-9

CHAPTER 7. METHOD OF INTERPRETING TRANSIENT COMPOSITE PS WAVES ON RECORDINGS FROM NEAR AND FAR EARTHQUAKES 170

Compilation of Time Profiles 170
Formulas for Determining the Depth to the Exchange Boundary (H), Seismic Drifts (L), Approach Azimuths (α), Epicentral Distances (Δ) and Angles of Emergence of Seismic Radiation (E) for Horizontally Layered Media 171
Construction of Depth Charts and Profiles for Horizontally Layered Media 172
Method of Comparing Data of PS Waves to Materials of Explosions and Deep Drilling 179
Characteristics of Interpreting Composite Transient PS Waves Formed on Sloping Interfaces of the Earth's Crust. 180
The Resolution and Accuracy of the Composite Wave Method From Earthquakes 186
The Accuracy of Constructing Interfaces by PS Waves 189

CHAPTER 8. METHOD OF DETERMINING THE COORDINATES OF EARTHQUAKE FOCI AND ACCOMPANYING EXPLOSIONS. 193

Determining the Moment of Occurrence of an Explosion or Earthquake 193
Determining the Location of the Explosion and Earthquake Focus . . 196
The Accuracy of Determining the Coordinates of Earthquake and Explosion Foci 198

CHAPTER 9. METHOD OF DETERMINING THE VELOCITY PARAMETERS OF THE MEDIUM FROM EARTHQUAKE AND EXPLOSION RECORDINGS (Δ = 0-10°). . . 205

Calculating the Propagation Velocities of Longitudinal and Transverse Waves from Recordings of Explosions and Near Earthquakes. 205
Methods of Determining Coefficients K. 209
Determining the Velocity Characteristic of the Medium in the Focal Zones of Recent Earthquakes. 211

Part 3. The Deep Structure of the Earth's Crust and Upper Mantle of Various Geotectonic Zones. 212

CHAPTER 10. THE DEEP STRUCTURE OF THE CRYSTALLINE THICKNESS OF THE EARTH'S CRUST AND UPPER MANTLE IN THE RAYONS OF TASHKENT. . . 212

Criteria of Intrarayon Stratification and Interrayon Correlation of the Interfaces of the Earth's Crust 213
The Velocity Boundaries of the Crust and Mantle of the Tashkent Depression and Their Geological Stratification 215
The Behavior of the Interfaces of the Earth's Crust and Mantle Near Tashkent 215
The Surface Structure of the Paleozoic Basement East and Southeast of Tashkent. 221
The Seismic Activity of the Territory of Investigation and Its Relationship to the Deep Structure 221

APPROVED FOR RELEASE: 2007/02/08: CIA-RDP82-00850R000200030043-9

APPROVED FOR RELEASE: 2007/02/08: CIA-RDP82-00850R000200030043-9

CHAPTER 11. THE DEEP STRUCTURE OF THE EARTH'S CRUST OF THE NORTH GERMAN DEPRESSION. 224

The Velocity Interfaces of the Earth's Crust and Their Stratification 225
Some Data on the Nature of Propagation and the Structural Shapes of the Interfaces of the Earth's Crust. 225
Comparison of the Thickness of the Sedimentary Mantle and the Crystalline Thickness of the Earth's Crust of the German Democratic Republic and Contiguous Countries. 232

CHAPTER 12. THE DEEP STRUCTURE OF THE EARTH'S CRUST AND UPPER MANTLE IN THE SOUTHEAST OF THE RUSSIAN SERIES AND THE NORTHERN PRE-CASPIAN DEPRESSION 236

Velocity Distribution in the Crystalline Thickness of the Earth's Crust and Mantle From Data of the "Zemlya" Station by the Reflected Wave Correlation Method and Deep Seismic Sounding 236
The Structure of the Earth's Crust and Upper Mantle. 238
The Modern Tectonic Activity of the Southeastern Russian Series and the Northern Pre-Caspian Depression 239

CHAPTER 13. THE DEEP STRUCTURE OF THE CRYSTALLINE THICKNESS OF THE EARTH'S CRUST OF THE UPPER MANTLE OF THE AZOV-KUBAN' DEPRESSION 241

The Velocity Interfaces of the Earth's Crust and Upper Mantle and Their Stratification 242
The Relief and Structure of the Interfaces of the Earth's Crust and Upper Mantle 242

CHAPTER 14. PROSPECTS FOR DEVELOPMENT OF THE COMPLEX SEISMIC METHOD OF STUDYING THE STRUCTURE OF THE EARTH'S CRUST AND UPPER MANTLE 245

The Geological Effectiveness of the Studies. 245
Comparison of "Zemlya" Station Data to the Results of Other Types of Geophysical Studies 249
The Economic Effectiveness of the Studies. 252
The Direction of Further Studies with the "Zemlya" Device. 253

CONCLUSIONS 255

BIBLIOGRAPHY. 258

APPROVED FOR RELEASE: 2007/02/08: CIA-RDP82-00850R000200030043-9

APPROVED FOR RELEASE: 2007/02/08: CIA-RDP82-00850R000200030043-9

PUBLICATION DATA

English title	:	SEISMIC STUDIES WITH THE "ZEMLYA" DEVICE
Russian title	:	SEYSMICHESKIYE ISSLEDOVANIYA S APPARATUROY "ZEMLYA"
Author (s)	:	I. V. Pomerantseva and A. N. Mozzhenko
Editor (s)	:	
Publishing House	:	Nedra
Place of Publication	:	Moscow
Date of Publication	:	1977
Signed to press	:	31 Jan 77
Copies	:	1400
COPYRIGHT	:	Izdatel'stvo "Nedra", 1977

APPROVED FOR RELEASE: 2007/02/08: CIA-RDP82-00850R000200030043-9

APPROVED FOR RELEASE: 2007/02/08: CIA-RDP82-00850R000200030043-9

ANNOTATION

A COMPLEX SEISMIC METHOD OF STUDYING THE STRUCTURE OF THE EARTH'S CRUST AND UPPER MANTLE BY USING LONGITUDINAL, TRANSVERSE AND COMPOSITE WAVES EXCITED BY EARTHQUAKES AND EXPLOSIONS AND RECORDED BY THE "ZEMLYA" DEVICE WITH MAGNETIC RECORDING IN THE FREQUENCY RANGE OF 0.5-15 Hz AND EPICENTRAL DISTANCES OF Δ = 0-160° IS DESCRIBED. THE THEORETICAL FUNDAMENTALS OF THE METHOD ARE CONSIDERED AND EQUATIONS OF THE HODOGRAPHS OF TRANSIENT AND LATERAL PS WAVES AND ALSO FORMULAS OF THE VECTOR COMPONENTS OF THEIR DISPLACEMENTS ARE PRESENTED AND ANALYZED AS A FUNCTION OF THE ANGLES OF INCLINATION OF THE INTERFACES IN TWO- AND MULTILAYERED THREE-DIMENSIONAL MEDIA. THE "ZEMLYA" DEVICE WITH MAGNETIC RECORDING AND THE METHOD OF WORKING WITH IT IN DIFFERENT GEOLOGICAL PROVINCES ARE DESCRIBED. BASED ON ANALYSIS OF EXTENSIVE EXPERIMENTAL MATERIAL OBTAINED BY THE "ZEMLYA" DEVICE IN FIVE SIGNIFICANTLY DIFFERENT REGIONS BY HISTORICAL DEVELOPMENT--THE SOUTHEASTERN RUSSIAN PLATFORM, THE PRE-CASPIAN, AZOV-KUBAN' AND NORTH GERMAN DEPRESSIONS AND IN THE RAYONS OF TASHKENT, THE NATURE OF P, S AND PS WAVES IS DETERMINED AND CRITERIA ARE GIVEN FOR SEPARATING THEM ON RECORDINGS FROM EARTHQUAKES AND EXPLOSIONS AND FOR SEPARATION INTO GROUPS. A METHOD OF INTERPRETING P, S AND PS WAVES IN MEDIA WITH HORIZONTAL AND SLOPING INTERFACES OF THE EARTH'S CRUST IS DEVELOPED. THE CAPABILITIES OF THE METHOD ARE ILLUSTRATED BY CHARTS AND PROFILES OF THE EARTH'S CRUST. MATERIALS OBTAINED BY THE "ZEMLYA" APPARATUS ARE COMPARED TO DRILLING DATA, KMPV [REFRACTED WAVE CORRELATION METHOD], GSZ [DEEP SEISMIC SOUNDING] AND OTHER GEOPHYSICAL METHODS.

APPROVED FOR RELEASE: 2007/02/08: CIA-RDP82-00850R000200030043-9

APPROVED FOR RELEASE: 2007/02/08: CIA-RDP82-00850R000200030043-9

INTRODUCTION

Moscow SEYSMICHESKIYE ISSLEDOVANIYA S APPARATUROY "ZEMLYA" in Russian 1977 signed to press 31 Jan 1977 pp 1-13

[Introduction from the book "Seysmicheskiye issledovaniya s apparaturoy 'Zemlya'" by I. V. Pomerantseva and A. N. Mozzhenko, Izdatel'stvo Nedra, 1,400 copies, 256 pages]

[Text] Many studies have been carried out in the USSR and abroad [8, 12, 13, 21, 33, 38, 39, 41, 42, 46, 47, 63, 74, 76, 98, 103, 142, 143, 149, 155] to study the deep structure of the earth's crust and upper mantle, the main purpose of which was to gain an idea about the shape and depths of deposition of the interfaces in the crust and mantle, data on the physical parameters of the crust and mantle and to determine the main relationships between geophysical fields.

The most complete and unambiguous data on the structure of the earth's crust and mantle in the USSR were obtained during regional seismic investigations by the refracted wave correlation method (KMPV) and during deep seismic sounding (GSZ), developed by a group of Soviet scientists under the supervision of G. A. Gamburtsev [38, 67]. The seismic studies conducted in different regions of the Soviet Union during the past 30 years using KMPV and GSZ (G. A. Gamburtsev, Yu. N. Godin, I. P. Kasninskaya, I. S. Berzon, A. M. Yepinat'yeva, P. S. Veytsman, Ye. I. Gal'perin and others) made it possible to gain general concepts about the structure of the earth's crust, to determine the conditions of formation and propagation of waves in its layers, to formulate general relationships between different geophysical fields and so on. The restrictions of their application were also established as the KMPV and GSZ methods were developed. The restrictions included the use of mainly a single class of longitudinal waves, study of the structure of the crust and upper mantle using extended branches of hodographs obtained at distances 2-20 times greater than the distances from the points of explosion to the initial points, which leads to significant averaging to the interfaces of the crust [107]; the difficulty of studying narrow depressions with large angles of inclination (up to 45-60°) and its limbs [125]; and the impossibility of determining recent fault zones which significantly distort waves fields from explosions and earthquakes. Complex and expensive systems of observations

APPROVED FOR RELEASE: 2007/02/08: CIA-RDP82-00850R000200030043-9

APPROVED FOR RELEASE: 2007/02/08: CIA-RDP82-00850R000200030043-9

are necessary for unambiguous determination of the nature of waves recorded by KMPV and GSZ.

All these factors and also the need for rapid study of the enormous areas of the USSR contributed to the search for new ways and methods of seismic study of the structure of the earth's crust and mantle.

The following trends of seismic work to study the deep structure of the earth's crust and upper mantle were noted over the last decade in the USSR: 1) detailed GSZ studies by subcritical reflected waves using ordinary explosions (I. V. Litvinenko, N. I. Pavlenkova, V. B. Sollogub and others); 2) regional point GSZ soundings (N. N. Puzyrev, S. V. Krylov and B. P. Mishen'kin); 3) regional investigations using explosions (Ye. A. Popov, A. V. Yegorkin, N. A. Belyayevskiy, V. Z. Ryaboy, I. S. Vol'volskiy, B. S. Vol'volskiy and N. I. Khalevin); and 4) regional seismological investigations using mobile stations by P and S. waves (I. L. Nersesov, A. S. Alekseyev, T. G. Rautian, A. A. Lukk and others) and also by PS waves (N. K. Bulin and Yu. I. Sytin).

The development of seismology and seismic prospecting and the need to combine them for more detailed study of the structure of the earth's crust and upper mantle with a significant reduction of the cost of seismic studies and the use of a more extensive class of waves led to the development of yet another trend--complex seismic studies with the "Zemlya" device. It was proposed by using these investigations to simultaneously study: 1) the spatial position of the interfaces of the earth's crust and upper mantle by almost vertical rays with an accuracy not below that of studies with KMPV and GSZ; 2) the velocity characteristics of the crust and upper mantle from P and S waves; and 3) the seismicity of the crust and mantle. Among the existing classes of waves, only longitudinal and transverse waves reflected near the point of the explosion and transient composite waves from far earthquakes* satisfied the first condition [6,18, 20,19]. But waves reflected from the surface of the basement and deep boundaries of the crust near the point of the explosion were usually not recorded during KMPV and were very rarely recorded during GSZ studies [51]. The possibility of recording and separation of composite waves, especially from the deep interfaces of the earth's crust, on recordings from far earthquakes was subject to extreme doubt or was absolutely rejected by a number of seismologists and seismic prospectors [3, 4, 31]. However, the first experimental studies conducted with the "Zemlya" apparatus to select the required class of waves on an area known from deep drilling and GSZ data showed the reality of existence of deep transient composite PS waves on recordings from far earthquakes [124]. The rather simple method of recording these waves in the absence of any expenditures on their excitation and also the possibility of statistical accumulation of recordings from different earthquakes made it possible to select composite PS waves as the main ones when studying the interface relief of the earth's crust and upper mantle.

---

*Earthquakes were separated into far, near and local from the values of the epicentral distances Δ. The values of Δ at short distances from the foci are measured in kilometers and those at great distances, where the earth's sphericity begins to be reflected, are measured in degrees. For local earthquakes, Δ = 0-40 km, for near earthquakes Δ = 4-500 km (0.4-5°) and Δ = = 5 - 10° and for far earthquakes Δ = 10-180°

APPROVED FOR RELEASE: 2007/02/08: CIA-RDP82-00850R000200030043-9

APPROVED FOR RELEASE: 2007/02/08: CIA-RDP82-00850R000200030043-9

Table 1. Distribution of Investigations with "Zemlya' Devices by Regions and Years

Номер района исследований (1)	(2) Район исследований	(3) Год проведения работ	(4) Ответственный исполнитель
1 2	(5) Юго-Восток Русской платформы	1962 1963	(6) А. Н. Мозженко, И. В. Померанцева
3 4	Прикаспийская впадина (7)	1965 1966	А. Н. Мозженко, И. В. Померанцева (6) М. С. Эренбург (8)
5	Днепровско-Донецкая впадина (9)	1966	Я. Ф. Бублик (10)
6 7 8 9 10 11 12 13 14	Восточная Сибирь (11)	1964 1965 1966 1967 1966—1967 1967 1967 1968 1969	Л. П. Гришанова (12) Б. Е. Щербакова (13) » » Г. В. Крупская (13а) А. Д. Пугач (14) И. М. Штутин (15) » »
15 16 17	Азово-Кубанская впадина (16)	1964 1965 1966	И. В. Померанцева (17) С. С. Тарасевич (18) К. В. Тригубова (19) »
18 19	Северо-Германская впадина (20)	1968 1969—1970	И. В. Померанцева, В. Ланге (21) А. Н. Мозженко, В. Ланге (22) »
20 21 22 23 24 25	Западная Сибирь (23)	1967—1968 1968 1969 1970 1971 1972	Ю. М. Чемякин (24) » » » В. Ф. Чекалев (25) »
26 27	Закарпатье (26)	1967 1968	В. П. Рудницкий (27) »
28 29 30 31 32 33	Малый Кавказ (28)	1967—1968 1970 1971 1972 1973 1970	Г. В. Егоркина (29) » » » » М. С. Эренбург (30)
34	Юг Туранской плиты, Предкопетдагский прогиб (31)	1964—1967	В. И. Лыков (32)

[Continued on following page]

APPROVED FOR RELEASE: 2007/02/08: CIA-RDP82-00850R000200030043-9

APPROVED FOR RELEASE: 2007/02/08: CIA-RDP82-00850R000200030043-9

Table 1 (Continued)

35 36 37	Юг Туранской плиты, Предкопетдагский прогиб (33)	1967—1968 1968—1969 1969—1971	А. И. Минин (34) В. А. Безгодков (35) »
38 39 40 41 42	Узбекская ССР (36)	1966—1967 1968 1967—1969 1969 1970—1973	И. В. Померанцева (17) Л. С. Шумилина (37) В. И. Пак (38) С. В. Могильникова (39) Е. М. Бутовская (40)
43 44 45 46 47 48 49	Казахстан (41)	1964 1965 1966—1967 1968 1969 1970 1971	В. Ф. Студеникин (42) Л. М. Лысяков (43) М. С. Эренбург (44) » » » К. А. Попов (45)

Key:

1. Number of region of studies
2. Region of studies
3. Year of investigations
4. Responsible executor
5. Southeastern Russian series
6. A. N. Mozzhenko and I. V. Pomerantseva
7. Pre-Caspian depression
8. M. S. Erenburg
9. Dnepr-Donetsk depression
10. Ya. F. Bublik
11. Eastern Siberia
12. L. P. Girshanova
13. B. Ye. Shchepbakova
13a. G. V. Krupskaya
14. A. D. Pugach
15. I. M. Shtutin
16. Azov-Kuban' depression
17. I. V. Pomerantseva
18. S. S. Tarasevich
19. K. V. Trigubova
20. North German depression
21. I. V. Pomerantseva and V. Lange
22. A. N. Mozzhenko and V. Lange
23. Western Siberia
24. Yu. M. Chemyakin
25. V. F. Chekalev
26. Transcarpathian area
27. V. P. Rudnitskiy
28. Minor Caucasus
29. G. V. Yegorkina
30. M. S. Erenburg
31. Southern Turanskaya shield and Pre-Kopet-Dag trough
32. V. I. Lykov
33. Southern Turanskaya shield and Pre-Kopet-Dag trough
34. A. I. Minin
35. V. A. Bezgodkov
36. Uzbek SSR
37. L. S. Shumilina
38. V. I. Pak
39. S. V. Mogil'nikova
40. Ye. M. Butovskaya
41. Kazakhstan
42. V. F. Studenikin
43. L. M. Lysyakov
44. M. S. Erenburg
45. K. A. Popov

APPROVED FOR RELEASE: 2007/02/08: CIA-RDP82-00850R000200030043-9

APPROVED FOR RELEASE: 2007/02/08: CIA-RDP82-00850R000200030043-9

Longitudinal P and transverse S waves on recordings from local and near earthquakes and explosions were used to determine the velocity characteristic and seismicity of the crust. The nature of these waves was established in seismic prospecting and seismology by theoretical and experimental investigations of the last two decades [1, 2, 38, 39]. For complex three-dimensional interpretation of the P, PS and S waves excited by earthquakes and explosions, it became necessary to record them by a three-component apparatus which made it possible to clearly tie in the kinematic and dynamic parameters of different waves propagated in three-dimensional media. This capability was realized by the "Zemlya" apparatus with magnetic recording, developed by A. N. Mozzhenko in 1957. This device has frequency and dynamic bands adequate for simultaneous recording of explosions and earthquakes, high amplification of seismic signals, good resolution, reliable dynamic calibration of the entire record-playback channel, the capability of multiple repetition of the reported signals to select the most optimum conditions for determination of useful oscillations and so on.

Experimental studies on development of the complex seismic method of studying the structure of the earth's crust and upper mantle using the "Zemlya" device were begun in 1962 on the Southeastern Russian series on KMPV and GSZ profiles of past years [124] and the same studies were then carried out on KMPV and GSZ profiles in the Azov-Kuban' (1964) and the Pre-Caspian (1965) depressions using data on the velocity obtained by these methods. Subsequent investigations with the "Zemlya" apparatus in the region of Tashkent and in the German Democratic Republic were carried out without using KMPV and GSZ materials [109, 111].

Studies with "Zemlya" stations begun in 1964-1965 within the Irkutsk ampitheater [126] and inother regions of the USSR and also abroad (Figure 1, Tables 1 and 2). The total length of profiles developed during 1962-1975 by "Zemlya" stations comprised more than 20,000 kilometers

During this same period, the "Zemlya" apparatus complex, initially consisting of five recording stations and one 4-channel reproduction station, was supplemented by survey and marking reproduction stations and an SS-24-61M station. As the method of observations and interpretation of materials were developed, ever greater requirements were placed on the recording and reproduction apparatus, which inevitably led to improvement of it. Thus, the need to reproduce P, S and PS waves of different frequencies determined the appearance of multichannel reproduction; time correlation of data obtained at different stations dispersed in this space resulted in introduction of a radio channel; the need to use the dynamic parameters of the recorded waves in interpretation of materials led to the introduction of relative channel calibration; it was necessary to record precise time checks transmitted by radio broadcast stations and absolute calibration (by displacement) of "Zemlya" channels to compare the materials recorded by "Zemlya" stations and by ordinary seismological apparatus. CDC-3300, Sigma-5 and other computers were used for better separation and correlation of the PS waves. The parts from which the "Zemlya" stations were designed were changed. Amplifiers based on micromodules and integrated circuits were developed instead of tube amplifiers.

APPROVED FOR RELEASE: 2007/02/08: CIA-RDP82-00850R000200030043-9

APPROVED FOR RELEASE: 2007/02/08: CIA-RDP82-00850R000200030043-9

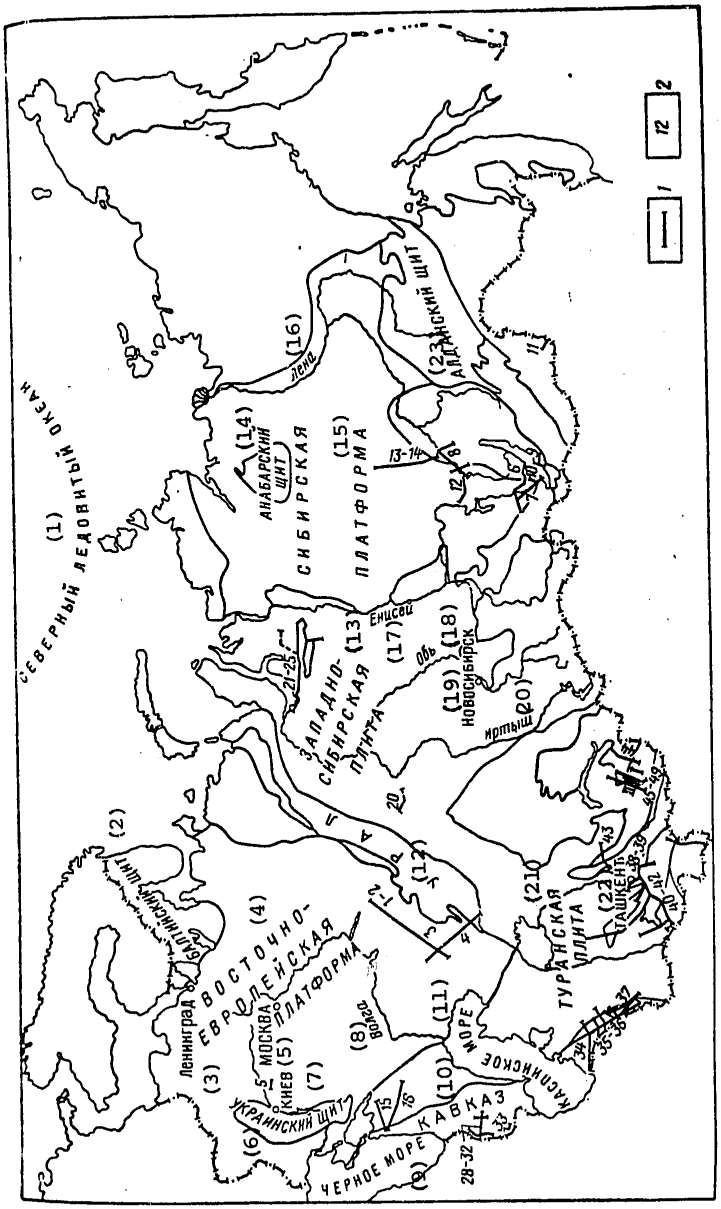

Figure 1. Layout of Regional Seismic Profiles Developed by "Zemlya" Stations: 1--profiles; 2--number of region of studies (see Table 1)

[Key on following page]

APPROVED FOR RELEASE: 2007/02/08: CIA-RDP82-00850R000200030043-9

APPROVED FOR RELEASE: 2007/02/08: CIA-RDP82-00850R000200030043-9

Key:

1. Arctic Ocean
2. Baltic Shield
3. Leningrad
4. Eastern European series
5. Moscow
6. Ukrainian shield
7. Kiev
8. Volga River
9. Black Sea
10. Caucasus Mountains
11. Caspian Sea
12. Ural Mountains
13. West Siberian series
14. Anabar shield
15. Siberian series
16. Lena River
17. Yenisey River
18. Ob' River
19. Novosibirsk
20. Irtysh River
21. Turan platform
22. Tashkent
23. Aldan shield

All the most improved methods of field investigations by KMPV, GSZ, MOV [Reflected wave method] and seismology were used when working out the method. The recording stations were faced by profiles and area with spacing which permitted phase correlation of waves of different types. The presence of correlation stations made it possible to correlate material obtained at different stops and profiles with each other. P and S waves from explosions were correlated by conjugate points and PS waves were correlated by the times and regions of their common points. Simultaneous recording of waves from explosions and earthquakes was carried out. Seismological procedures on spacing the stations around foci were used during observations of earthquake foci with specific ratios of epicentral distances to the depths of the foci (Δ / h_{och}) and seismological calibration of seismographs and channels was carried out according to the polarities of wave arrivals. The main data on the method of field observations with the "Zemlya" device in different regions are presented in Table 2.

The methods of study and interpretation of various waves and primarily of composite PS waves were improved simultaneously with development of field studies. The dynamic and kinetic characteristics of PS waves [52-54, 58, 72, 73, 90, 134, 152, 163, 165], methods of separating them on recordings and correlation from station to station [7, 20, 86, 96, 110] and absorption of P and S waves [146] were determined. Methods of determining the velocity characteristic and seismicity of the crust by P and S waves [8, 22, 36, 70, 77] and PS waves [9] were developed. Methods of interpretation of PS waves for horizontally layered [6, 18, 19, 49, 50, 78, 108, 135] and complexly structured media with inclined interfaces [111] were improved and developed.

A complex seismic method of studying the structure of the earth's crust and upper mantle by longitudinal, transverse and composite waves excited by earthquakes and explosions and recorded by the "Zemlya" device at epicentral distances of 0-160° in the frequency range of 0.5-15 Hc was developed as a result of many years of investigations with the "Zemlya" device, carried out in different regions of the USSR. This method was named the "Zemlya" method for brevity of outline according to the naming of the apparatus used. It combines the method of transient composite waves from remote earthquakes

APPROVED FOR RELEASE: 2007/02/08: CIA-RDP82-00850R000200030043-9

APPROVED FOR RELEASE: 2007/02/08: CIA-RDP82-00850R000200030043-9

Table 2. Main Data on the Method of Field Observations with the "Zemlya" Device in Different Regions

(1) Регион	(2) Район исследований	(3) Номер района исследований по табл. 1	(4) Число полевых выписей за 15 сут							
			(5) всего	(6) от взрывов		(7) от местных и близких землетрясений		(8) от далеких землетрясений		
				(9) зарегистрированные	(10) обработанные	(9) зарегистрированные	(10) обработанные	(9) зарегистрированные	(10) обработанные
(11) Древние платформы	(12) Юго-Восток Русской платформы	1,2	30—60	27	4	8—13	4—13	18	6—15
(13) Внутриплатформенные впадины	(14) Прикаспийская и Днепровско-Донецкая впадины	3, 4, 5 (15)	3—50	1—23	1	6—7	1—5	21	3—13
	Восточная Сибирь (16)	6—14	13—43	1—24	1—6	1—24	1—6	3—36	1—16
(17) Молодые платформы	Азово-Кубанская впадина (18)	15—17	15—41	24—31	4	2—4	2	8	6—8
	Северо-Германская впадина (19)	18, 19	16—29	2—3	2—3	7	—	14—26	13—15
	Западная Сибирь (20)	20—25	5—24	—	—	—	—	4—24	2—11
(21) Сейсмоактивные районы	Закарпатье (22)	26, 27	4—10	3	3	—	—	6	3
	Малый Кавказ (23)	28—33	44—70	6—18	2	24—42	6—16	14—23	6—12
	Туркмения (24)	34—37	7—70	—	—	53	5—6	18	2—13

*Long-term observations were made to study the seismicity of the region

[Continued on following page]

APPROVED FOR RELEASE: 2007/02/08: CIA-RDP82-00850R000200030043-9

APPROVED FOR RELEASE: 2007/02/08: CIA-RDP82-00850R000200030043-9

Table 2. (Continued)

(25) Система расстановки станций записи	(26) Вид исследований	(27) Шаг наблюдений, км	(28) Продолжительность наблюдений на одной расстановке, сут	(29) Число станций записи	(30) Производительность работ, км/сут	(31) Стоимость одной точки наблюдения, тыс. руб.	(32) Стоимость 1 км профиля, тыс. руб
(33) По профилям с выносными станциями	Региональные (34)	10	13—14	4—9	—	—	—
По профилям с выносными станциями (35)	Региональные (34)	3—8	14—20	6—15	5	2,9—3,8	0,43—0,49
(36) По маршрутам с выносными станциями	Региональные	3—12	15—44	5—20	1,5—5,1	2,0—8,4	0,2—0,9
По профилям с выносными станциями (35)	Региональные с детализацией отдельных участков (37)	4—7	14—27	9—12	1,2—3,3	2,4—4,4	0,3—0,9
По профилям с выносными станциями (35)	Региональные с детализацией отдельных участков (37)	5—6	16	9—25	2,0—5,9	—	—
По маршрутам, площадям, в отдельных точках (38)	Рекогносцировочные, региональные, детальные (39)	2—6 и более	16—45	5—15	1,6—3,7	4,6—14,1	0,8—1,1
По профилям в отдельных точках (40)	Рекогносцировочные (41)	0,8?	11?	3—6	0,3	2,4?	—
По профилям с выносными станциями (36)	Региональные с детализацией отдельных участков, долговременные * (42)	5—6 13 *	25—38 135 *	5—10	1,4—1,9 0,5 *	2,9—3,9 31,3 *	0,5—1,6
По профилям с выносными станциями (36)	Региональные (34)	3—5	22—50	5—10	0,8—1,6	2—4,0	0,4—0,6

[Continued on following page]

APPROVED FOR RELEASE: 2007/02/08: CIA-RDP82-00850R000200030043-9

APPROVED FOR RELEASE: 2007/02/08: CIA-RDP82-00850R000200030043-9

Table 2 (Continued)

Регион	Район исследований	Номер района исследований по табл. 1	Число полезных записей за 15 сут						
			всего	от взрывов		от местных и близких землетрясений		от далеких землетрясений	
				зарегистрированные	обработанные	зарегистрированные	обработанные	зарегистрированные	обработанные
(21) Сейсмоактивные районы	Узбекистан (43)	38—42	6—69	8—11	2—4	27—30	2—4	10—32	4—10
	Казахстан (44)	43—49	26—97	2—16	2—4	26—81	20—36	10—38	12—20

Система расстановки станций записи	Вид исследований	Шаг наблюдений, км	Продолжительность наблюдений на одной расстановке, сут	Число станций записи	Производительность работ, км/сут	Стоимость одной точки наблюдения, тыс. руб.	Стоимость 1 км профиля, тыс. руб.
(45) По маршрутам, профилям, площадям	(39) Рекогносцировочные, региональные, детальные	3—10	21—13	8—15	1,1—2,8	1,7—3,8	0,3—0,9
По профилям в отдельных точках (40)	Региональные, детальные, долговременные * (46)	5—11	15—30 80—350 *	5—15	1,4—3,4	2,4—9,3	0,9—2,2

[Key on following page]

APPROVED FOR RELEASE: 2007/02/08: CIA-RDP82-00850R000200030043-9

APPROVED FOR RELEASE: 2007/02/08: CIA-RDP82-00850R000200030043-9

Key:

1. Region
2. Region of investigations
3. Number of region of investigations according to Table 1
4. Number of useful recordings during 15 days
5. Total
6. From explosions
7. From local and near earthquakes
8. From remote earthquakes
9. Recorded
10. Processed
11. Ancient series
12. Southeastern Russian series
13. Depressions within a series
14. Pre-Caspian depression
15. Dneprovsk-Donetsk depression
16. Eastern Siberia
17. Young series
18. Azov-Kuban' depression
19. North German depression
20. Western Siberia
21. Seismically active regions
22. Transcarpathian area
23. Minor Caucasus
24. Turkmeniya
25. System of arranging recording stations
26. Type of investigations
27. Spacing of observations, km
28. Length of observations on one spacing, days
29. Number of recording stations
30. Productivity of operations, km/day
31. Cost of a single observation point, thousand rubles
32. Cost of one kilometer of profile, thousand rubles
33. By profiles with portable stations
34. Regional
35. By profiles with portable stations
36. By traverses with portable stations
37. Regional with detailing of individual sections
38. By traverses, areas and at individual points
39. Preliminary survey, regional and detailed
40. By profiles at individual points
41. Preliminary survey
42. Regional with detailing of individual sections, long-term
43. Uzbekistan
44. Kazakhstan
45. By traverses, profiles and areas
46. Regional, detailed and long-term

and methods based on the use of longitudinal and transverse, refracted and reflected waves from explosions and earthquakes. The following problems can be solved by using this method.

1. The deep structure of the crystalline thickness of the earth's crust and upper mantle can be studied, beginning from the surface of the crystalline base and ending with the interfaces in the upper mantle. The structure of the interfaces in the sedimentary mantle can be determined under favorable conditions.

APPROVED FOR RELEASE: 2007/02/08: CIA-RDP82-00850R000200030043-9

APPROVED FOR RELEASE: 2007/02/08: CIA-RDP82-00850R000200030043-9

2. The velocity characteristic of individual complexes of the earth's crust and upper mantle can be studied.

3. The coordinates of earthquake foci and the velocity characteristic in focal zones and also the mechanism and energy characteristics of foci can be determined.

4. The relationships existing between the deep structure of the earth's crust and displacement of earthquake foci can be established.

Investigations by the "Zemlya" method conducted on the Southeastern Russian Series, in the Pre-Caspian, Azov-Kuban' and North German Depressions and in the rayons of Tashkent made it possible to obtain essentially new data on the deep structure of these regions compared to the results of study of them by KMPV, GSZ and seismological methods. Thus, weak tectonic activity of this region and the adjacent folded system of the Urals was detected during investigations on the Southeastern Russian Series. Besides the crust interfaces in the Pre-Caspian regions, the roof and bottom of the salt-bearing mass in the sedimentary mantle were traced in Pre-Caspian regions along the interfaces of the crust and the position of the boundaries inside the crust was determined. The narrow, but deep (up to 20 km) West Kuban' Trough not determined by KMPV, was established within the Azov-Kuban' Depression along the surface of the basement represented by a Triassic-Jurassic mass. According to KMPV data, the depth to the surface of the basement within the West Kuban' Trough comprised 12 km. An idea of the detailed deep structure of the crust was obtained for the first time in the rayons of Tashkent and the distribution of epicenters and depths of aftershock* foci of the Tashkent earthquake of 26 April 1966 was determined with high accuracy. Reduced values (4-4.4 km/s) of stratal velocities ($v_{P_{pl}}$) of longitudinal waves and ratios (K_{pl}) of stratal velocities of longitudinal and transverse waves (up to 1.61) were discovered within the focal zone located in Paleozoic and Archean basements at a depth of 3-9 km, whereas $v_{P_{pl}}$ = 5.8-6 km/s and $K_{pl} \approx 1.73$ in the zone surrounding the earthquake foci. It was established that the foci are located in a weakened zone of the crust.

A complex heterogenic structure of the basement was established for the North German Depression and a three-level arrangement of the folded phases in it was determined: Variscian, Caledonian and Pre-Cambrian; the deep structure of the northern part of the German Democratic Republic was determined; and a series of structures along the surfaces of different phases of basement folding and deep interfaces of the crust was determined. It is shown that the Eastern Elba gravitational maximum is caused by an uplift of the basaltic and subcrustal layers, while the magnetic maximum is caused by effusive-intrusive formations which fill the trough along the Pre-Cambrian folding.

---

*Tremors following a large earthquake from the same epicenter, less in intensity, are called aftershocks according to H. Jeffries.

APPROVED FOR RELEASE: 2007/02/08: CIA-RDP82-00850R000200030043-9

APPROVED FOR RELEASE: 2007/02/08: CIA-RDP82-00850R000200030043-9

The results obtained in aseismic and seismically active regions permit one to use the "Zemlya" method to study the structure of the earth's crust, the upper mantle and their seismicity both autonomously and in combination with other geophysical methods.*

*The authors are grateful to M. K. Polshkov and Ye. F. Savarenskiy for support and supervision in working out the complex seismic method of studying the structure of the earth's crust and upper mantle and to A. M. Yepinat'yeva and T. I. Oblogina who reviewed the manuscript and made many valuable comments.

APPROVED FOR RELEASE: 2007/02/08: CIA-RDP82-00850R000200030043-9

APPROVED FOR RELEASE: 2007/02/08: CIA-RDP82-00850R000200030043-9

PART 1

THEORETICAL FUNDAMENTALS OF USING DIFFERENT WAVE FIELDS TO STUDY THE STRUCTURE OF THE EARTH'S CRUST AND UPPER MANTLE

PHYSICAL CONCEPTS ABOUT LONGITUDINAL P, TRANSVERSE S AND COMPOSITE PS WAVES ON RECORDINGS FROM EARTHQUAKES AND EXPLOSIONS

Moscow SEYSMICHESKIYE ISSLEDOVANIYA S APPARATUROY "ZEMLYA" in Russian 1977 signed to press 31 Jan 1977 pp 14-34

[Chapter 1 from the book "Seysmicheskiye issledovaniya s apparaturoy 'Zemlya'" by I. V. Pomerantseva and A. N. Mozzhenko, Izdatel'stvo Nedra, 1,400 copies, 256 pages]

[Text] Wave Fields Observed During the Initial Part of the Earthquake Seismogram Recording

The Kinematic Characteristics of Wave Fields

According to Seismological data [43, 48, 132], LR and LQ surface waves, longitudinal (P, PP and PPP), transverse (S, SS and SSS) and composite (PS and PPS) waves refracted singly and multiply in the crust and mantle, for which the multiplicity boundary is the earth's surface, longitudinal (PcP), transverse (ScS) and composite (PcS) waves reflected from the core, transverse waves reflected from the earth's core and surface (ScSP), longitudinal and transverse waves which pass through the earth's core once (PKP and SKS), twice (SKKS) or three times (SKKKS), waves reflected from the earth's core, its surface and which pass through the core (PcPPKP, PcSPKP and ScSPKP) waves reflected from the earth's core and surface and refracted in the crust and mantle (ScSP) and waves which pass through the earth's core once (SKSP) or twice (SKSSKS) and reflected from its surface once may be propagated in the earth from the hypocenter to the recording station at $\Delta = 0.180°$. Photographs of all these waves, compiled by Jeffries and Bullen on the basis of analyzing a large number of experimental recordings from earthquakes, are presented in Figure 2 with regard to a number of theoretical calculations.

The first P waves on the Jeffires-Bullen hodograph (Figure 2) at $\Delta = 0\text{-}110°$ are classified by their nature as refracted in the crust and mantle. Diffracted P waves may first be traced further at $\Delta = 130\text{-}150°$ or a shadow zone will be observed at this range of epicentral distances [84, 132]. The first P waves are refracted in the core (PKP) at $\Delta = 150\text{-}180°$. Moreover, in the initial part of the seismograms according to the Jeffries-Bullen hodograph

APPROVED FOR RELEASE: 2007/02/08: CIA-RDP82-00850R000200030043-9

APPROVED FOR RELEASE: 2007/02/08: CIA-RDP82-00850R000200030043-9

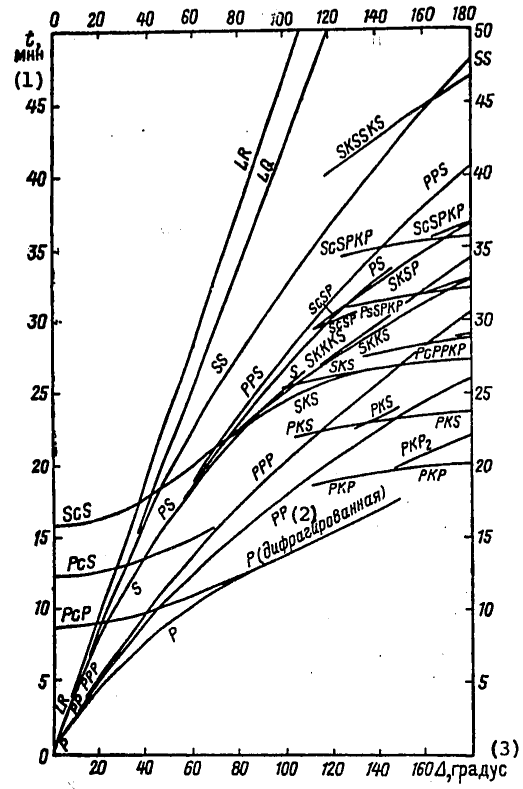

Figure 2. Jeffries-Bullen Hodographs at h_{och} = 0 and Δ = 0-180°

Key:
1. Minutes
2. Diffracted
3. Degrees

and according to [6, 20, 48, 65], the existence of composite SP and PS, transverse S and reflected pP and sP waves related to the interfaces of the earth's crust, the upper mantle and the focus, is possible after the first arrivals of P and PKP waves. The PS waves related to the interfaces of the earth's crust at thickness of 70 km and mean velocity to the Mohorovicic discontinuity of 6.2 km/s are recorded on earthquake recordings not less than 11 seconds after the first arrivals of P or PKP waves. At Δ = 0-5° and h_{och} < < 25 km, sP, pP and S waves related to the focus are recorded in this same time interval [65]. With an increase of Δ and h_{och}, sP, pP and S waves are

APPROVED FOR RELEASE: 2007/02/08: CIA-RDP82-00850R000200030043-9

APPROVED FOR RELEASE: 2007/02/08: CIA-RDP82-00850R000200030043-9

recorded at times greater than the times of recording PS waves, as a result of which a zone of the absence of any waves related to the earth's core and mantle is observed at the first P and PKP waves. This zone is optimum for recording PS waves formed at the interfaces of the earth's crust.

The nature of P, S, sP and pP waves related to the focus has been studied rather thoroughly by seismological investigations. The sP and pP waves are related to composite-reflected and reflected waves in the region of the focus. They emerge from the focus as S or P waves, are exchanged and reflected on the earth's surface and are then propagated to the reception point as longitudinal waves. S waves are transverse types formed as a result of shearing processes at earthquake foci.

The matter with the nature of PS waves recorded on the horizontal components of the recording immediately after the first P waves is more complex. A number of investigators (Ye. M. Butovskaya, S. S. Andreyev, N. K. Bulin, Yu. I. Sytin, N. V. Shebalin and D. N. Rustanovich), who suggested that PS waves be used to study the structure of the earth's crust, feel that they are composite waves which replace a P type for a S type at the interfaces of the earth's crust and upper mantle. Others (I. L. Nersesov, Ye. I. Gal'perin, G. M. Tsibul'chik, I. K. Klushin and others) assume up to the present time that these waves by their nature may be: 1) pS multiple waves related to the upper levels of the sedimentary mantle and incorrectly interpreted as deep composite waves [32, 35]; 2) various types of longitudinal waves recorded due to their own large angles of emergence on the S and Y components [82, 91, 161]; 3) lateral waves of Raleigh type formed from P waves on large uneven areas of relief of the earth's surface and propagated along it for great distances [31]; and 4) additional arrivals formed due to the presence of "projections" and "hollows" on the surface of the P wave fronts during their propagation through an inhomogeneous medium from the focus to the interface and unrelated to the crustal boundaries [62].

The first hypothesis was based on concepts of the low intensity of transient PS waves (from the first erroneous theoretical calculations as was later established) and the high intensity of multiple P and S waves in the sedimentary mantle (from MOV materials).

The second and third hypotheses were based on the fact that the polarization planes of experimental PS waves recorded on recordings from remote earthquakes frequently deviated significantly from the vertical plane passing through the station-epicenter. Theoretical calculations which indicate the possibility of additional arrivals of different waves appearing which are unrelated to the interfaces of the earth's crust and mantle and formed due to curvature of the P wave fronts in complexly structured media were the basis for the fourth hypothesis. The hypothesis on recording of Raleigh wave components formed from P waves on unevennesses of the earth's surface on the X and Y components is hardly probably for series conditions. Thus, it is shown in [61] that Raleigh waves at frequencies of 1-2 Hz at excesses of the earth's surface of 0-400 m above sea level may create only a general microseism background of intensity less than 7 percent of the P wave intensity and consequently 4-10 times weaker than PS waves on the seismograms. These

APPROVED FOR RELEASE: 2007/02/08: CIA-RDP82-00850R000200030043-9

APPROVED FOR RELEASE: 2007/02/08: CIA-RDP82-00850R000200030043-9

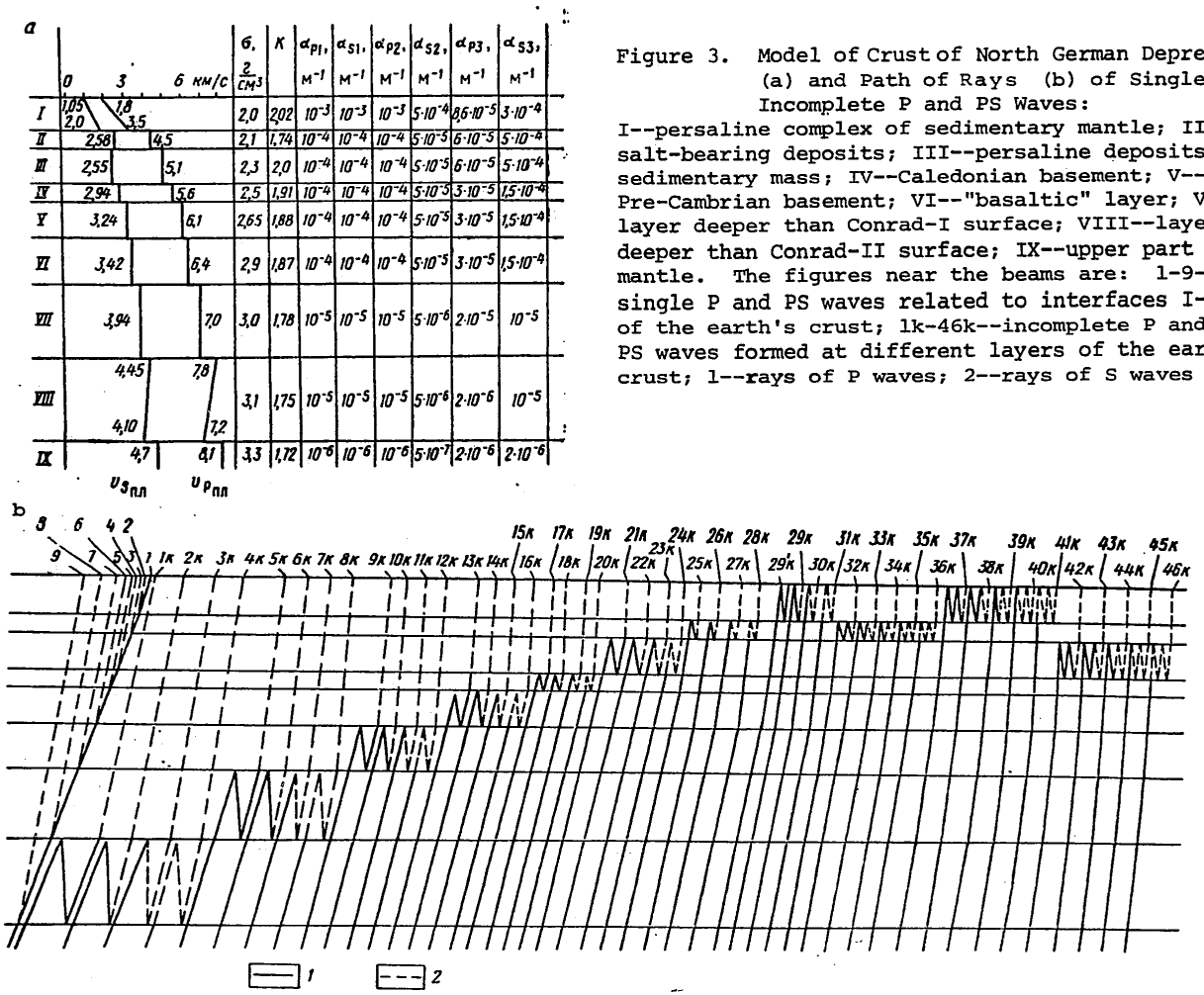

Figure 3. Model of Crust of North German Depression (a) and Path of Rays (b) of Single and Incomplete P and PS Waves:
I--persaline complex of sedimentary mantle; II--salt-bearing deposits; III--persaline deposits of sedimentary mass; IV--Caledonian basement; V--Pre-Cambrian basement; VI--"basaltic" layer; VII--layer deeper than Conrad-I surface; VIII--layer deeper than Conrad-II surface; IX--upper part of mantle. The figures near the beams are: 1-9--single P and PS waves related to interfaces I-IX of the earth's crust; 1k-46k--incomplete P and PS waves formed at different layers of the earth's crust; 1--rays of P waves; 2--rays of S waves

APPROVED FOR RELEASE: 2007/02/08: CIA-RDP82-00850R000200030043-9

APPROVED FOR RELEASE: 2007/02/08: CIA-RDP82-00850R000200030043-9

low-intensive waves cannot be seen on seismograms jointly with PS waves. The hypothesis of the presence of PS waves which can be caused by curvature of the P wave fronts would be valid if the PS waves on the X and Y components were separated only by their first arrivals, as was done, for example, in [91]. Additional PS waves unrelated to the crustal boundaries are eliminated upon separation of PS waves by the shape of the recording of the entire packet of P waves.

Theoretical calculations of hodographs, forms of recording, frequency spectra and intensities of transient longitudinal and composite, single and multiple waves formed at the interfaces of the earth's crust at Δ = 0-160° were made to determine the physics of formation of PS waves at the interfaces of the crust and the nature of their propagation. The calculations were made for models of media which approximate the earth's core of several regions (the North German and Pre-Caspian Depressions, the Tashkent Depression and the Southeastern Russian Series). A diagram of the course of the rays of all types of single and incomplete waves and also one of the variants of models of these media are presented in Figure 3.

Analysis of the theoretical hodographs of transient P and PS waves obtained for models of media of all the enumerated regions showed that the existence of the following secondary waves is possible on the horizontal components of recording in the time interval of 0-11 seconds after the arrivals of P waves from the viewpoint of kinematics: a) single PS waves for all crustal interfaces separated with an interval of 0.2-2 seconds (Figure 4); b) comple PS waves from levels of the sedimentary mantle present at the times of recording PS waves related to the surfaces of basaltic and subcrustal layers; c) incomplete PS and PPSSS waves from levels of the sedimentary mantle recorded at the same times as the first deep single PS waves related to the surface of the crystalline thickness of the earth's crust (see Figure 4); d) incomplete PPSP and PPP waves which occurred at the boundaries of the sedimentary mantle; and e) the horizontal components of P waves in the presence of large angles of emergence of seismic radiation. Based on common physical concepts, one may assume the existence of vertical and inclined contacts of media of different petrographic composition in the upper part of the crystalline thickness of the crust [38, 39, 41, 42, 103]. These structural inhomogeneities of the crust may be sources of various types of lateral waves: transient difrracted and transied reflected waves recorded in the time interval of 0-11 seconds after the arrival of the first transient P wave [133].

The Intensity of P and PS Waves Different in Nature Related to the Earth's Crust

Theoretical calculations of the amplitudes of all probable P and PS waves: single, multiple and lateral, were made from kinematic positions to determine waves dynamically reflected in the initial part of seismograms from earth quakes (Δ = 5-160° and t = 0-11 seconds). It is natural to assume that all the waves differing from the first P and PKP waves by no more than an order or 1.5 orders in amplitude can be seen on the seismograms. Waves

APPROVED FOR RELEASE: 2007/02/08: CIA-RDP82-00850R000200030043-9

APPROVED FOR RELEASE: 2007/02/08: CIA-RDP82-00850R000200030043-9

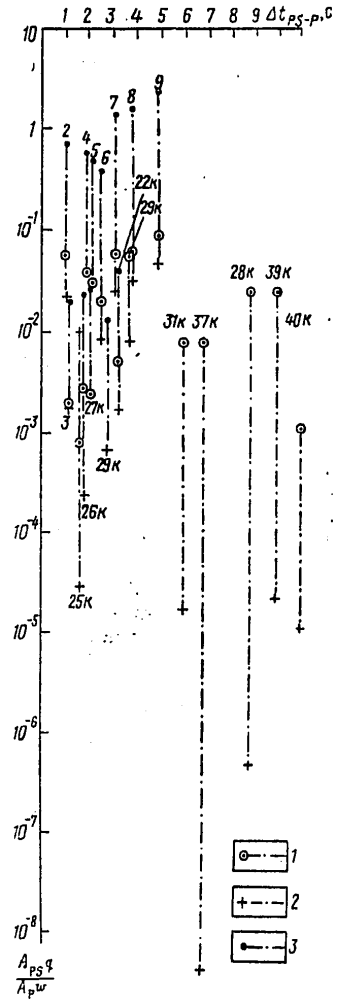

Figure 4. Theoretical Amplitudes A_{PSq}/A_{Pw} for Single and Incomplete PS Waves as a Function of Δt_{PS-P}, Calculated for a Model of the Crust Presented in Figure 3:

1--without regard to P and S wave absorption; 2 and 3--with regard to P and S wave absorption at $\alpha_P = \alpha_S$ and $\alpha_P = 2\alpha_S$, respectively. The figures near the values of A_{PSq}/A_{Pw} correspond to different types of single and incomplete waves, the ray of which is presented in Figure 3.

APPROVED FOR RELEASE: 2007/02/08: CIA-RDP82-00850R000200030043-9

APPROVED FOR RELEASE: 2007/02/08: CIA-RDP82-00850R000200030043-9

which have a greater difference in amplitudes cannot be determined on the same seismogram with P and PKP waves without using some special procedures of accumulation.

The amplitudes of single and multiple P and PS waves were calculated from the programs of T. B. Yanovskaya [166] and L. I. Ratnikova and T. B. Yanovskaya [123]. The amplitudes of lateral P and PS waves were calculated by the program of A. V. Belinosova, A. S. Alekseyev and S. S. Tadzhimukhamedova [10]. All the calculations were made both with and without regard to the absorbing properties of the medium in the layers of the crust. The values of the absorption coefficients for P (α_P) and S (α_S) waves were taken from [146], where they were determined from experimental recordings of P and S waves recorded by the "Zemlya" device from explosions at the same profiles for which the theoretical calculations of P and PS wave intensities were made. The ratios of coefficients α_P/α_S varied from 0.7 to 2.5. Ratios of α_P/α_S equal to 0.286, 1 and 2 were taken during theoretical calculations of amplitudes. The densities σ in calculations of intensity were determined in the layer according to [167]. Theoretical calculations of the amplitudes of single, multiple and lateral PS waves were made for thick-layered models of media with interfaces of first kind and transition zones between individual layers of the crust. Consideration of the ratios of PS wave amplitudes to P wave amplitudes made it possible, on the one hand, to eliminate different intensity of earthquakes and to construct the experimental data on the same graph for earthquakes with different values of mangitudes and energy classes and, on the other hand, to avoid errors in measurements of amplitudes caused by the device (see Chapter 3).

The amplitudes of single and multiple P and PS waves for thick-layered media with interfaces of first kind. The curves of the dependents of the amplitudes of the vertical and horizontal components of longitudinal and composite (single and incomplete) waves are presented in Figure 5, a and b as a function of the epicentral distance Δ and angle of drop of the P wave to the Mohorovicic discontinuity i_M for the model of the medium presented in Figure 3. Analysis of the theoretical amplitudes of P and PS waves calculated without regard to the absorbing properties of the medium for models of the earth's crust of the named regions permits one to make the following conclusions.

1. The vertical Pw components of longitudinal waves have the highest amplitudes among those recorded at epicentral distances of 0-160° in the time interval of 0-11 seconds on the Z, X and Y components (see Figure 5, a).

2. The amplitudes of the horizontal components of composite single PS waves (A_{pq}) recorded on the X and Y components are 1.5-8 times lower than the amplitudes of the vertical components of P waves.

3. The amplitudes of the vertical components of single PS waves are lower than the amplitudes of the horizontal components of the same waves by approximately an order.

APPROVED FOR RELEASE: 2007/02/08: CIA-RDP82-00850R000200030043-9

APPROVED FOR RELEASE: 2007/02/08: CIA-RDP82-00850R000200030043-9

4. The amplitudes of the horizontal components of complete and incomplete PS waves have a very wide range (6 orders) of amplitude variation.

5. The amplitudes of the horizontal components of double PS waves related to levels of the sedimentary mantle have the same order as the horizontal components of single PS waves related to the deep exchange boundaries of the earth's crust. PS waves with multiplicity factor greater than 2 have amplitudes greater than one order lower than single PS waves.

6. The amplitudes of the horizontal components of complete and incomplete PS waves related to the interfaces of the crystalline thickness of the earth's crust are approximately an order less than the amplitudes of single PS waves related to these same boundaries.

7. The amplitudes of incomplete waves related to the interfaces of the crystalline crust are approximately an order less than the amplitudes of incomplete waves related to the levels of the sedimentary mantle.

8. The curves of the amplitudes of the horizontal components of single and multiple PS waves are identical to each other and have a dome shape with very sloping maximum at angles of i_M = 20-70° (Δ = 17-100°). Minimum intensities are noted at i_M = 0 and 90° ($\Delta \approx$ 180 and 3°) on curves A_{PSq}.

Introduction of P and S wave absorption into the calculations significantly alters the concepts obtained about the intensities of single and multiple P and PS waves (Figure 5, b). Consideration of the absorbing properties of the real medium (at $\alpha_P = 0.286\,\alpha_S$ in the uppermost layer of the sedimentary mantle, $\alpha_P = \alpha_S$ and $\alpha_P = 2\,\alpha_S$) leads to the fact that not a multiple wave related to the interfaces of the sedimentary mantle remains in the interval equal to a single dynamic order with single P and PS waves. A similar pattern is also noted for graphs A_{PSq}/A_{PW} (see Figure 4). The values of A_{PSq}/A_{PW} for single deep PS waves and incomplete PS waves formed at the sharp interfaces (v_{P2}/v_{P1} = 1.5) in the sedimentary mantle are similar without regard to the absorbing properties of the medium. Introduction of absorption reduces the value of A_{PSq}/A_{PW} by more than 1-2 orders for incomplete waves. The effect of a sharp decrease of the intensity of multiple PS waves with different combinations of α_P and α_S permits one to assume that incomplete and even more so complete waves related to the sedimentary mantle are absent in the wave pattern observed from earthquakes.

The amplitudes of lateral P and PS waves for thick-layered media with interfaces of first kind. The amplitudes of transient reflected P and PS waves were calculated for two models of two-layered media with the presence of a sloping contact in the second (lower) medium. The P and PS wave velocities in the first medium and its density were assumed constant and those in the second medium were assumed variable with depth according to parabolic law.

The following parameters are used for the first model: H_1 = 3 km, v_{P1} = = 2.8 km/s, v_{P2_n} = 5 km/s and v_{P3_n} = 6 km/s, where v_{P2_n} and v_{P3_n} are the

APPROVED FOR RELEASE: 2007/02/08: CIA-RDP82-00850R000200030043-9

APPROVED FOR RELEASE: 2007/02/08: CIA-RDP82-00850R000200030043-9

velocities near the surface of the gradient layer (initial). The gradient is $\beta_2 = 4 \cdot 10^{-2}$ km$^{-2/3}$ and $\beta_3 = 2 \cdot 10^{-2}$ km$^{-2/3}$. The source of oscillations is located above the medium with greater velocity at a distance of x_0 = 16 and 60 km from the contact. The angle of inclination of the contact φ is equal to 150°. Absorption was not considered.

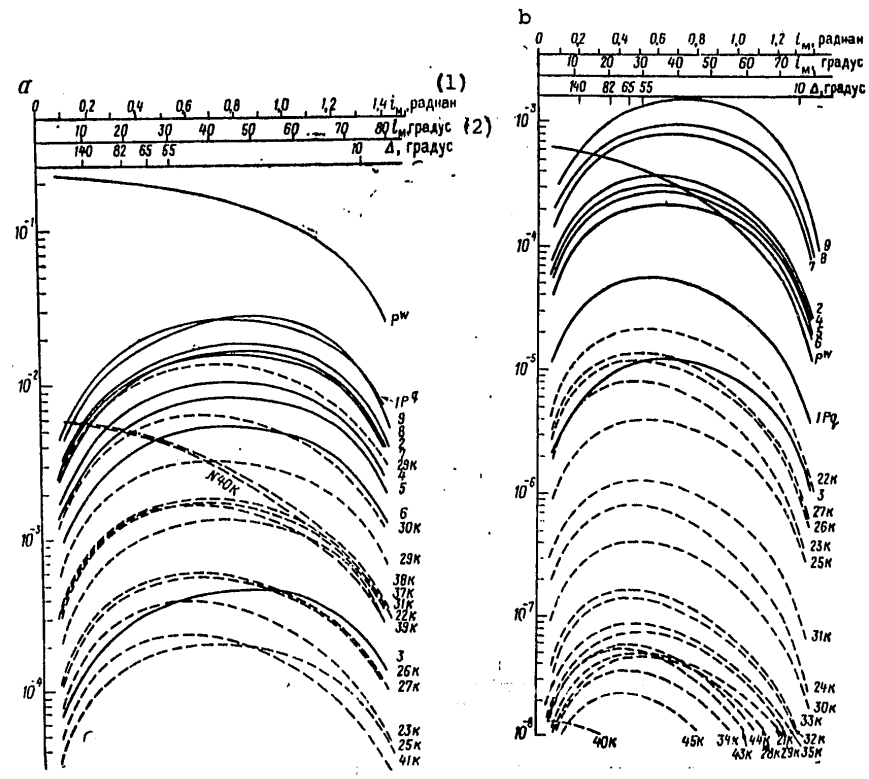

Figure 5. Amplitudes of Vertical A_{pw}, Horizontal A_{pq} and A_{psq} Components of Transient Longitudinal P and Composite PS Waves for a Thick-Layered Model of the Crust Presented in Figure 3 with Interfaces of the First Kind as a Function of Δ and i_M Without Regard to (a) and With Regard to (b) Absorption of P and S Waves by the Real Medium (With Regard to Absorption $\alpha_P = \alpha_S$):
1--single waves; 2--incomplete waves. The numbers near the curves correspond to different types of waves whose rays are presented in Figure 3.

[Continued on following page]

APPROVED FOR RELEASE: 2007/02/08: CIA-RDP82-00850R000200030043-9

APPROVED FOR RELEASE: 2007/02/08: CIA-RDP82-00850R000200030043-9

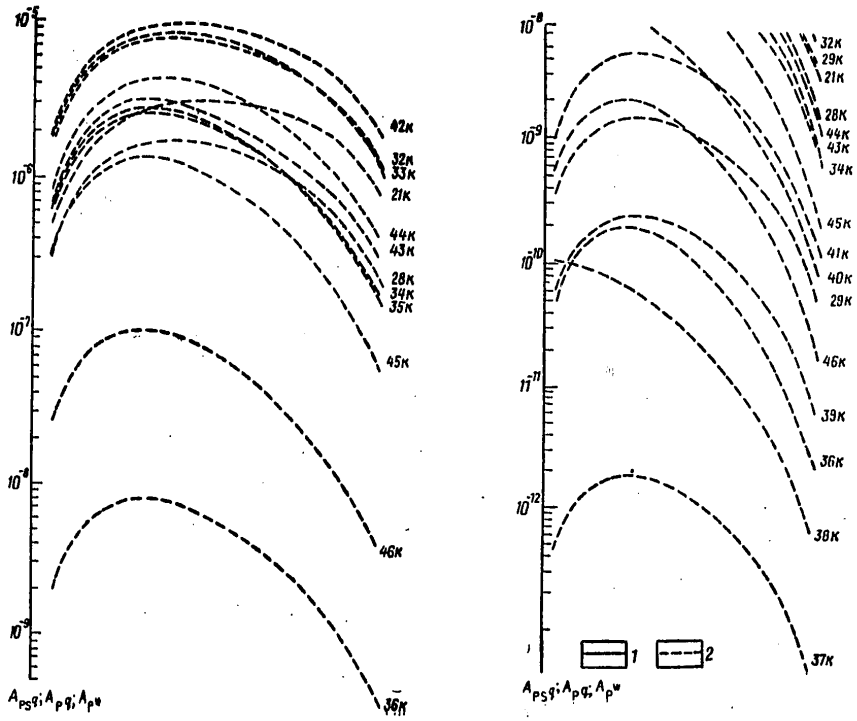

Figure 5. [Continued]

Key:
1. Radians
2. Degrees

The following parameters were taken for the second model: H_1 = 3 km, v_{P1} = = 2.8 km/s, v_{P2_n} = 5 km/s, v_{P3_n} = 6 km/s, φ = 30° and φ = 60°. The sources of oscillations were located on both sides of the contact at distances of 60 (x_0 = 0) and 15 km (x_0 = 45 km). Absorption was not considered. The theoretical calculations showed that the values of the ratios of composite-reflected PS wave amplitudes to the amplitudes of transient P waves may reach 0.5-1.5 and may reach 7.5 at extreme points. The amlitudes of transient diffracted PS waves can be compared to the amplitudes of transient P and PS waves [89, 133].

The amplitudes of transient single P and PS waves for thick-layered media with transition zones between layers represented by a thick-layered bench.

APPROVED FOR RELEASE: 2007/02/08: CIA-RDP82-00850R000200030043-9

APPROVED FOR RELEASE: 2007/02/08: CIA-RDP82-00850R000200030043-9

The ratios of amplitudes of transient single and incomplete PS waves to the amplitudes of transient P waves and the model of a thick-layered media with transition zones between layers represented by a thick-layered bench are presented in Figure 6. The relationship between the thicknesses d of thin layers in the bench and the lengths λ of P and PS waves is expressed by the function $d \ll \lambda$. A model of the medium approximates the crust (Figure 6, III) of the North German Depression. The values of distance from the source are Δx = 0-30 km, which corresponds to angles of incidence of P waves to the Mohorovicic discontinuity of 0-50° and Δ = 20-160°. The amplitudes of all waves were calculated without regard to the absorbing properties of the medium. The derived data indicate that the values of A_{PSq}/A_{Pw} for PS waves formed on the benches of thin layers may reach 1-1.25, i.e, the amplitudes of composite waves may be comparable to and even higher than the amplitudes of P waves passing through the thin-layered bench.

Table 3. Amplitudes of Horizontal and Vertical Components of P Waves

(1) i_P, градус	(2) v_{P1}=3 км/с		v_{P2}=6 км/с		v_{P3}=7 км/с	
	A_{P_Z}	A_{P_X}	A_{P_Z}	A_{P_X}	A_{P_Z}	A_{P_X}
10	0,96	0,05	0,95	0,12	0,95	0,16
20	0,96	0,13	0,94	0,25	0,94	0,31
30	0,96	0,19	0,9	0,36	0,89	0,44
40	0,96	0,25	0,86	0,47	0,82	0,54
50	0,95	0,28	0,80	0,57	0,75	0,66
60	0,94	0,32	0,75	0,62	0,68	0,76
70	0,92	0,35	0,70	0,70	0,60	0,83
80	0,9	0,38	0,66	0,74	0,54	0,87
90	0,9	0,4	0,66	0,75	0,53	0,90

Key:
1. Degree
2. km/s

The amplitudes of the horizontal components of P waves. The amplitude of the horizontal components of P waves, according to Figure 5, are frequently comparable to those of the horizontal components of PS waves. Theoretical calculations of the horizontal and vertical components of P waves were made as a function of the angle of incidence of the wave to the exchange boundary i_P and of the velocity of longitudinal waves near the earth's surface (Table 3) to determine the effect of the parameters of the medium on the amplitudes of the horizontal components of P waves. Analysis of the data showed that the value of the horizontal components of P waves increases with an increase of i_P and v_P. For example, i_P = 80-90° at v_P = 3 km/s, which corresponds to near earthquakes ($\Delta \approx$ 8-10° and $h_{och} \approx 0$) and the ratio of the horizontal component at the P wave to its vertical component does not exceed 0.3. The amplitude of the horizontal component of longitudinal waves becomes comparable to that of the vertical component with an increase of v_P to 6 km/s for angles

APPROVED FOR RELEASE: 2007/02/08: CIA-RDP82-00850R000200030043-9

APPROVED FOR RELEASE: 2007/02/08: CIA-RDP82-00850R000200030043-9

of $i_P = 70°$ ($\Delta \approx 14°$ and $h_{och} \approx 0$) and at $v_P = 7$ km/s for $i_P = 55°$ ($\Delta \approx 18°$ and $h_{och} \approx 0$). The amplitudes of the horizontal components of P waves begin to exceed the amlitudes of the vertical components with a further increase of angles i_P.

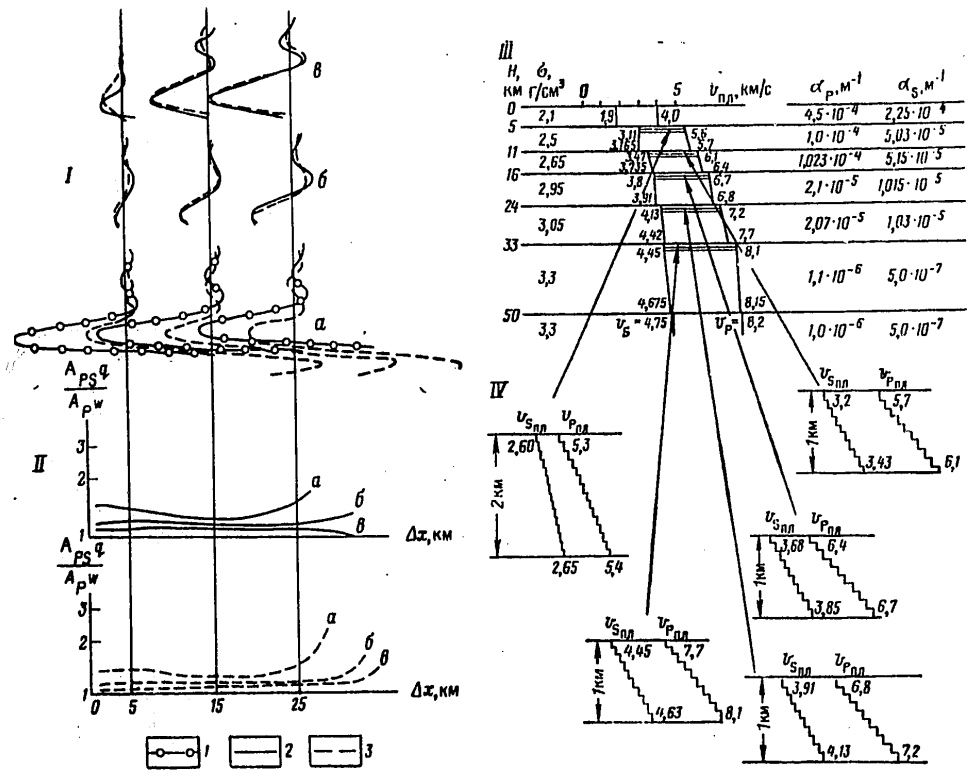

Figure 6. Shape of Recording (I) and Ratio of Amplitudes (II) of P and PS Waves for Model of a Thick-Layered Medium (III) With Thin-Layered Benches (IV): 1--P wave pulse without regard to absorption; 2 and 3--PS wave pulses and curves A_{PSq}/A_{Pw} with and without regard to P and S wave absorption ($\alpha_P = 2\alpha_S$), respectively; a--for basement surface ($v_{Pp1} = 5.6$ km/s); b--for surface of basaltic layer ($v_{Pp1} = 6.7$ km/s); c--for Mohorovicic discontinuity ($v_{Pp1} = 8.1$ km/s)

APPROVED FOR RELEASE: 2007/02/08: CIA-RDP82-00850R000200030043-9

APPROVED FOR RELEASE: 2007/02/08: CIA-RDP82-00850R000200030043-9

The Dynamic Characteristics of Single P and PS Waves from Theoretical Calculations

The dynamic characteristics of P and PS waves include the shape of the recording of recorded waves, their frequency spectra, intensity and polarization.

The Shape of Recording of P and PS Waves

The shape of recording of single P and PS waves formed from P waves at interfaces of the first kind in thick-layered media ($d/\lambda \geqslant 1/2$) is identical [26-28]. The shape of the recording of P and PS waves [72, 73, 164, 165] may undergo changes (see Figure 6) in the case when the interfaces are represented by benches of thin layers and are different for P and PS waves.*

These changes are insignificant even when the velocity drops at the boundaries of the thin layers reach 0.65 [164]. The correlation coefficients of the normalized cross-correlation function, which we calculated by the amplitudes of P and PS waves of the same types of phases which passed through the zone of the interface with different structure, were rather high: 0.73 - 0.95 for $\Delta = 20°$ and 0.56-0.91 for $\Delta = 70°$ (Table 4).

The Frequency Spectra of P and PS Waves

The frequency spectra of P and PS waves for models of thick-layered media with interfaces of first kind are identical [26-28]. The frequency spectra of P and PS waves, according to theoretical calculations [164] and our data, also remain identical, but differ in amplitude in the presence of zones represented by transient layers or by a bench of thin layers between the layers of the crust. The amplitude of a maximum frequency spectrum of composite PS waves may be 2.5-3.5 times less than that of the maximum frequency spectrum of P waves. Displacements of the maximum frequency spectra of P and PS waves during passage through thin-layered transient zones of different structure at different values of d/λ do not exceed 10 percent, i.e., they are essentially located within the accuracy of determining the periods of P and PS waves on seismograms.

Theoretical Amplitudes of P and PS Waves and Their Dependence on the Parameters of the Medium

The corresponding theoretical calculations were made for three models of two-layered and a number of multi-layered media with the presence of interfaces of the first kind and also benches of layers which approximate the transition zones from one layer of the crust to another** to determine the effect of various parameters of the medium on the amplitudes of P and PS

---

* We considered P and PS waves only with frequency of 1-2 Hz.

** The effect of the structure of the exchange zone on the amplitudes of P and PS waves in the case of its representation in the form of a transition layer or bench of layers is given in more detail in [72, 73, 165].

APPROVED FOR RELEASE: 2007/02/08: CIA-RDP82-00850R000200030043-9

APPROVED FOR RELEASE: 2007/02/08: CIA-RDP82-00850R000200030043-9

Table 4. Values of Cross-Correlation Coefficients K Between Amplitudes of the Same Type of P and PS Waves for Transition Zones]164]

Модель (1)	v_{P1}	v_{S1}	v_{P2}	v_{S2}	v_{P3}	v_{S3}	σ_1	σ_2	σ_3	d, км	K	
	км/с (2)						г/см³ (3)				$\Delta=20°$	$\Delta=70°$
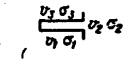	8,62	5,0	6,9	4,0	8,62	5,0	3,6	2,9	2,7	—	0,93	0,83
	5,52	3,2	6,9	4,0	5,52	3,2	2,34	2,9	2,34	—	0,8	0,56
	8,0	4,6	6,4	3,7	7,0	4,0	3,2	2,7	2,9	—	0,95	—
	8,0	4,6	6,4	3,7	7,0	4,0	3,2	2,7	2,9	—	0,92	—
	—	—	—	—	—	—	—	—	—	2,0	0,81	0,91
	—	—	—	—	—	—	—	—	—	1,0	0,73	0,88
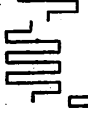	6,3	3,6	—	—	6,1	3,5	2,7	—	2,7	—	0,83	0,91
	6,3	3,6	—	—	6,1	3,5	2,7	—	2,7	—	0,73	0,83
	8,1	4,6	—	—	7,0	4,0	3,2	—	2,9	—	0,87	0,77

Key:
1. Model
2. km/s
3. g/cm3

APPROVED FOR RELEASE: 2007/02/08: CIA-RDP82-00850R000200030043-9

APPROVED FOR RELEASE: 2007/02/08: CIA-RDP82-00850R000200030043-9

and the ratios A_{PSq}/A_{PW}. The first and second two-layered models with interfaces of first kind approximated the sedimentary mantle and the crystalline crust of the North German Depression. The studied boundary in the first model corresponded to the surface of the Variscian basement and that in the second model corresponded to the surface of basaltic layer. The third model approximated the crust and mantle. The studied boundary approximated the Mohorovicic discontinuity.

Analysis of the data on the amplitudes of P and PS waves showed that the absorbing properties of the media, which alter them by 1-1.5 orders, mainly affect the amplitudes of the vertical components of P waves. The structure of the overlying mass (the number of boundaries, the velocity drop on them and replacement of the gradient medium by a homogeneous medium) changes the amplitudes of P waves within slight limits. Thus, when the number of overlying boundaries changes from 2 to 9, the velocity drop on them changes from 0.4 to 1 and the velocity gradient changes from 0.07 to 0.5 km^{-1}, the amplitudes of P waves vary by a total of 0.04-0.06.

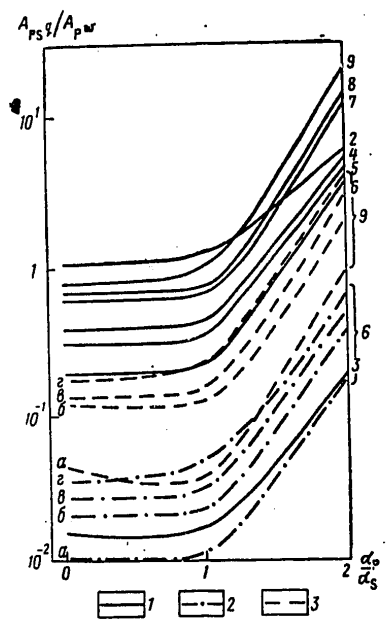

Figure 7. Graphs of the Dependence of A_{PSq}/A_{PW} on α_P/α_S for the Model of the Crust Presented in Figure 3: 1--for PS waves exchanged at all interfaces of the crust at Δ = 72°; 2 and 3--for PS waves changed on the basement and Mohorovicic discontinuities, respectively, at different values of Δ: a--140°; b--72°; c--55°; d--20°. The numbers near the curves correspond to the types of PS waves in Figure 3.

APPROVED FOR RELEASE: 2007/02/08: CIA-RDP82-00850R000200030043-9

APPROVED FOR RELEASE: 2007/02/08: CIA-RDP82-00850R000200030043-9

The ratio of amplitudes of composite PS waves to the amplitudes of longitudinal P waves are also mainly affected by the absorbing properties of the medium and primarily by the difference of the absorption coefficients of P and S waves. Thus, the value of A_{PSq}/A_{PW} for the models presented in Figure 8 varies by approximately 1-2 orders upon variation of α_P/α_S from 0.5 to 2 (Figure 7).

The second factor affecting the value of A_{PSq}/A_{PW} is variation of the velocity drop of P and S waves at the interface of the two media. Variation of v_{P1}/v_{P2} from 0.535 to 0.98 leads to a decrease of A_{PSq}/A_{PW} from 0.26 to 0.01 (see Figure 8). Variation of v_{S1}/v_{S2} from 0.45 to 0.8 on the exchange boundary leads to variation of A_{PSq}/A_{PW} from 0.3 to 0.1 at $\Delta = 20°$.

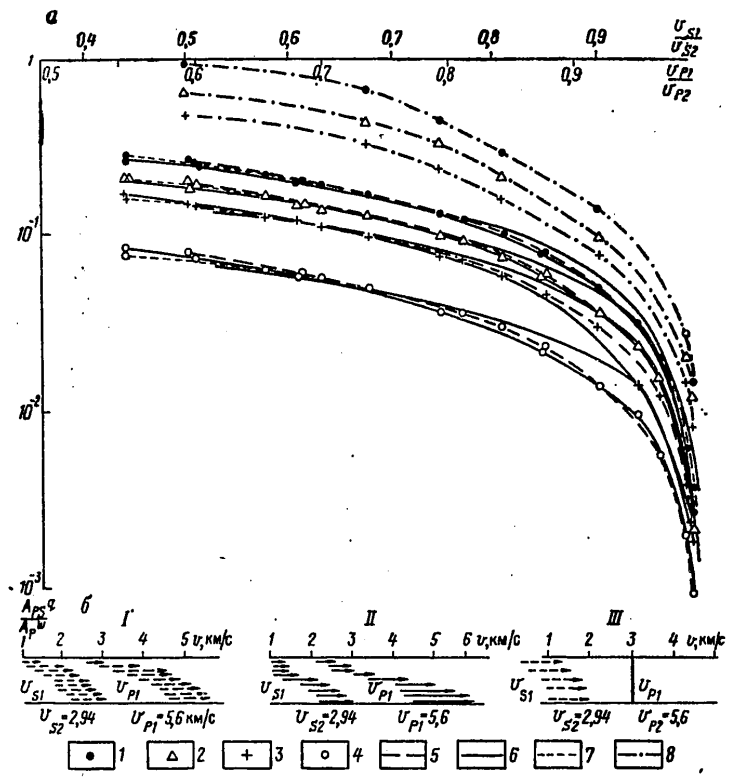

Figure 8. Graphs of the Dependence of A_{PSq}/A_{PW} on the Velocity Drop of Longitudinal v_{P1}/v_{P2} and Transverse v_{S1}/v_{S2} Waves at the Exchange Boundary (a) and the Profiles for which the Theoretical Calculations were Made (b): 1-- $\Delta = 20°$; 2-- $\Delta = 55°$; 3-- $\Delta = 72°$; 4-- $\Delta = 140°$; 5-7-- curves for models of the sedimentary mantle I, II and III, respectively, without regard to absorption of P and S waves; 8-- curve for variant I with regard to absorption of P and S waves ($\alpha_P = 2\alpha_S$)

APPROVED FOR RELEASE: 2007/02/08: CIA-RDP82-00850R000200030043-9

APPROVED FOR RELEASE: 2007/02/08: CIA-RDP82-00850R000200030043-9

The third important factor which significantly affects the value of A_{PSq}/A_{PW} is variation of the value of coefficient K at the exchange boundary which characterizes the ratio of the velocities of longitudinal to transverse waves in the layers. Variation of this parameter from 1.06 to 1 or from 0.95 to 1 at a constant value of Δ leads to a decrease of the ratio A_{PSq}/A_{PW} by a factor of 30. Unlike longitudinal waves, the amplitudes of composite waves and consequently the ratio A_{PSq}/A_{PW} depend somewhat more strongly on the number of boundaries located above the exchange boundary and on the velocity drop on these boundaries. An increase of the number of overlying boundaries, velocity drop and velocity gradients on them within the same limits, which was presented above for P waves, changes the values of A_{PSq}/A_{PW} by a factor of 4-5. Variation of the density of rock σ at the exchange boundary and replacement of a homogeneous covering medium by a gradient medium weakly or essentially does not affect the value of A_{PSq}/A_{PW}. Variation of the value of σ by 0.3 g/cm^2 leads to variation of the value of A_{PSq}/A_{PW} by 0.005. Replacement of the gradient medium by a homogeneous medium at $v_{P1}/v_{P2} = 0.6$ and $\Delta = 72°$ changes the value of A_{PSq}/A_{PW} from 0.12 to 0.131.

Polarization of PS Waves

There are now two points of view on polarization of PS waves. According to the first, PS waves are close to linearly polarized with regard to the accuracy of determining their delay times on seismograms (Δt_{PS-P}) with respect to P waves. The phase shifts of PS waves recorded on the X and Y components do not exceed 0.1-0.2 seconds. An exception are fault zones where they may reach 0.4 second. According to the second point of view [52, 54], PS waves are polarized elliptically due to the anisotropy of the medium. Their phase shifts on the X and Y components reach values of 0.7-1.5 seconds.

We made theoretical calculations of the phase shifts of PS waves recorded on the X and Y components determined by the effect of anisotropy or quasi-anisotropy of the medium [120, 131, 167]. Theoretical calculations of the quasi-anisotropy coefficients* $\varkappa$ of a layered medium, made by formulas of [131] for PS waves with $\lambda \ll d$, showed that $\varkappa$ will comprise 1.01-1.05 for the sedimentary mantle and 1.005 for the entire crust at angles of inclination of the interfaces up to 20° and for earthquakes with $\Delta > 20°$. These values of coefficient $\varkappa$ lead to a time different of recording PS waves on the X and Y components of 0.1-0.12 second for the basement surface at depths of its deposition of 5 km and of 0.1-0.4 second for the horovicic discontinuity at depths of deposition of 33 km. Since the angles of inclination of the Mohorovicic discontinuity φ do not exceed 10° under platform conditions, the value of the time delay of recording PS waves on the X and Y components from this surface will also not exceed 0.1-0.15 second. A similar pattern

*Coefficient $\varkappa$ is denoted in [131] as $\varkappa_3$ and is considered for longitudinal waves. The assumption of the proximity of the values of $\varkappa_3$ for P and S waves was used in our investigation.

APPROVED FOR RELEASE: 2007/02/08: CIA-RDP82-00850R000200030043-9

APPROVED FOR RELEASE: 2007/02/08: CIA-RDP82-00850R000200030043-9

is also observed for P and S waves propagated from remote earthquakes in anisotropic media. The low effect of anisotropy or quasi-anisotropy of the medium on composite transient waves polarized in the plane of the beam (PS_V) and in the plane perpendicular to the beam (PS_H) is determined by their propagation in directions close to vertical. Consequently, the anisotropy and quasi-anisotropy of the crystalline and sedimentary masses of the earth's crust (with the exception of fault zones) may not lead to significant phase shifts (up to 0.7-1.5 second) between PS waves recorded on the X and Y components. Taking into account that the error of reading the times Δt_{PS-P} on seismograms comprises $\pm$ 0.05-0.1 second, uninterpreted PS waves from remote earthquakes may be regarded as linearly polarized with a specific error.

The Nature of Longitudinal and Transverse Waves from Explosions and Earthquakes and the Area of Their Application

The Nature of Waves

The nature of P waves recorded from explosions at distances from 0 to 300 km from the point of the explosion has been rather thoroughly studied during the past 10-15 years [38, 39, 55-57, 68, 69, 104, 106]. It was established as a result of the investigations that there are two types of waves in wave fields from explosions at distances from 0 to 300 km: those reflected before and after critical points and refracted waves related to deep interfaces of the earth's crust. Refracted waves are mainly traced in the first arrivals, although the existence of reflected waves is also possible in the "visible" first arrivals. Reflected waves are mainly traced in the next part of the recording. Since the observations were usually made during extensive investigations in seismic prospecting only by means of vertical seismographs, essentially no one was involved with S waves and determination of their nature. However, S waves apparently have the same nature as longitudinal waves.

During seismological investigations, observations were made by using three-component installations which record intensive S waves occurring at earthquake foci [48, 132, 141]. Direct and refracted P and S waves are recorded in the first arrivals on earthquake recordings as a function of epicentral distance and reflected and refracted waves are recorded in subsequent recordings. Direct P and S waves in the region of the first arrivals are observed at those values of Δ for which the condition $\Delta \leqslant h_{och}$ is fulfilled.

The Area of Application of P and S waves

The presence of refracted and reflected rather than leading [1, 38, 39, 106] P and S waves during KMPV and GSZ led to variation of views on the physics of formation and propagation of P and S waves in the medium from explosions. Consideration of the process of formation of refracted waves during KMPV and GSZ [30] and the nature of propagation of refracted and reflected waves in the block structure of the crust showed that the use of refracted and subcritically reflected waves obtained at great distances from their initial

APPROVED FOR RELEASE: 2007/02/08: CIA-RDP82-00850R000200030043-9

APPROVED FOR RELEASE: 2007/02/08: CIA-RDP82-00850R000200030043-9

points is complicated for construction of the relief of the crustal interface and leads to their significant averaging [1, 107]. Taking the nature of P and S waves into account, it was more correct to use them in investigations with the "Zemlya" device to determine the velocity characteristics of the medium.

Determination of velocities by P and S waves is possible only by hodographs of the first arrivals of refracted waves or by hodographs of reflected P and S waves from the interfaces of the earth's crust mainly to the initial points.

The correctness of constructing hodographs of reflected P and S waves recorded during subsequent arrivals is determined by the reliability of correlating these waves along the profile lines. The latter in turn depends on the distance between the observation points (seismograms) and the frequency spectrum of the recorded oscillations. Confident phase correlation of any types of waves is possible if the following condition is adhered to [14, 45]: $\Delta x = (Tv_k)/2$ or $\Delta x = (Tv_k/4)$, where Δx is the distance between seismographs, T is the period of the wave and v_k is the seeming velocity of the wave along the hodograph. The maximum frequency spectra of P waves recorded during GSZ (Δ = 0-300 km) are located at frequencies of 5-8 and 12-16 Hz [38, 39]. The maximum frequency spectra of the first P waves from explosions and near earthquakes were determined at frequencies of 5-8 Hz during the initial stage of investigations with the "Zemlya" device and those of S waves were determined at frequencies of 3-5 Hz [124]. The apparent velocities of P and S waves from earthquakes on the hodographs at $\Delta > 5°$ varied from 8-10 to 20 km/s. Consequently, the distance between the observation points Δx should be given as 0.5-1 km to find a reliable base correlation of reflected P and S waves. At the same time, if the same device is used to record P and PS waves from remote earthquakes, which are optimum for construction of the crustal interfaces, then Δx for them can be brought up to 2.5-5 km or more. These distances are unsuitable for finding the continuous phase correlation of P and S waves reflected from the crustal interfaces. At the same time it is unprofitable to decrease the distances between the observation points to 0.5-1 km during regional investigations in order to be able to accomplish phase correlation of reflected P and S waves. Moreover, a decrease of distances to 0.5-1 km, based on the experience of GSZ operations [38], does not lead to reliable axes of cophasality of P and S waves from the deep crustal interfaces since their hodographs consist of individual unextended axes of cophasality (up to 1-3 km) even at distances of 100 m between seismographs. Based on these concepts, it was decided to rely on the first arrivals of P and S waves refracted in the crust to study the velocity characteristic of the medium. Determination of the beginning of oscillations of P and S waves on the recordings from earthquakes and explosions and tracing them from station to station with distances of 5 km between them is quite realistic. Thus, the first area of application of P and S waves during development of a rational complex method of studying the structure of the earth's crust was study of its velocity characteristic. It was assumed in this case that P and S waves be used both from special and

APPROVED FOR RELEASE: 2007/02/08: CIA-RDP82-00850R000200030043-9

APPROVED FOR RELEASE: 2007/02/08: CIA-RDP82-00850R000200030043-9

accompanying explosions (KMPV, GSZ, MOV, quarry and so on) and from local and near earthquakes. The next tasks, solution of which was possible by using P and S waves, were seismological: determination of the coordinates of earthquake foci and study of their dynamic characteristics (energy, class, magnitude, intensity and so on).

APPROVED FOR RELEASE: 2007/02/08: CIA-RDP82-00850R000200030043-9

APPROVED FOR RELEASE: 2007/02/08: CIA-RDP82-00850R000200030043-9

HODOGRAPHS AND DISPLACEMENT VECTORS OF P AND PS WAVES

Moscow SEYSMICHESKIYE ISSLEDOVANIYA S APPARATUROY "ZEMLYA" in Russian 1977 signed to press 31 Jan 1977 pp 34-53

[Chapter 2 from the book "Seysmicheskiye issledovaniya s apparaturoy 'Zemlya'" by I. V. Pomerantseva and A. N. Mozzhenko, Izdatel'stvo Nedra, 1,400 copies, 256 pages]

[Text] Equations of Hodographs and Recording Times of Single, Multiple and Lateral P and PS Waves

Equations of surface hodographs of all these waves and equations of their delay times with respect to transient P waves for two- and multilayered three-dimensional models of media were derived to study the kinematic characteristics of single, multiple and lateral P and PS waves from remote earthquakes.

Difference Equations of Recording Times on the Surfaces of Various Horizontally Layered Media of Transient Sincle P and PS Waves

Difference equations of the recording times of single P and PS waves (Δt_{PS-P}) were derived for two-, three- and multilayered homogeneously stratified media and also for a gradient medium covering the exchange boundary. Since clear P and PS waves can be separated both on recordings from near (Δ = 1-10°) and from remote (Δ = 10-160°) earthquakes, it makes sense to present formulas of Δt_{PS-P} for $\Delta < 10°$ and $\Delta > 10°$. The difference in these formulas includes the following. Since the front of transient P waves may be assumed flat and the angles of incidence of these waves to the exchange boundaries may be assumed small at $\Delta > 10°$ on spacing of recording stations of 100-200 km, they can be simplified when deriving equations of Δt_{PS-P}. As a result, the Hasegawa formula [176] will be found for a two-layered model of the medium. Making use of a similar procedure for multilayered media as well, the formulas for Δt_{PS-P} can be reduced to a more convenient simplified variant. The formulas derived below, prior to expansion of them into a series by sines, can be used for $\Delta < 10°$ [108].

APPROVED FOR RELEASE: 2007/02/08: CIA-RDP82-00850R000200030043-9

APPROVED FOR RELEASE: 2007/02/08: CIA-RDP82-00850R000200030043-9

A two-layered medium. Let us denote the velocities of longitudinal waves in the first (covering) and second (underlying) media by v_{P1} and v_{P2}. The delay times Δt_{PS-P} of the PS wave with respect to the P wave enter their approach to O according to Figure 9, a after a number of mathematical transformations [108] can be written in the form

$$\Delta t_{PS-P} = \frac{H_1}{v_{P1}}(K_1 - 1)\left(1 + \frac{K_1}{2}\sin^2\frac{\bar{i}_{P1}}{2}\right), \tag{2.1}$$

where H_1, v_{P1} and K_1 are the depth, velocity and mean coefficient of the velocity ratio of P waves, respectively, to the velocities of S waves in the first medium covering the exchange boundary and $\bar{i}_{P1}$ is the apparent angle of emergence of the P wave to the surface of a two-layered medium. Taking into account that $e_{P1} = K_1 \sin\frac{\bar{i}_{P1}}{2}$ [141], one can find

$$\Delta t_{PS-P} = \frac{H_1}{v_{P1}}(K_1 - 1)\left(1 + \frac{1}{2K_1}\cos^2 e_{P1}\right), \tag{2.2}$$

where e_{P1} is the angle of emergence of seismic radiation.

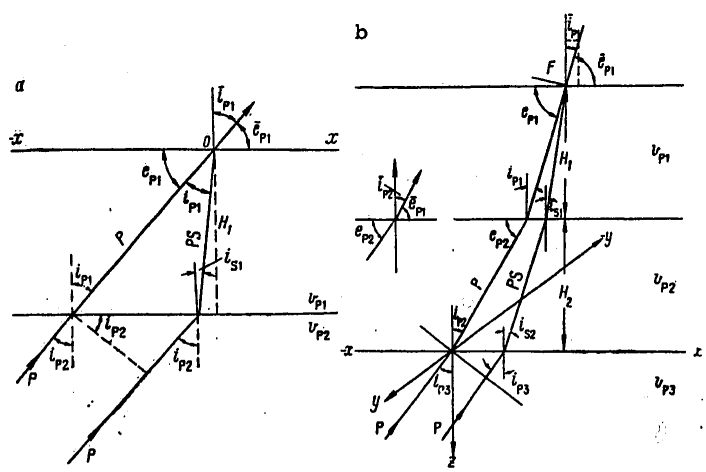

Figure 9. Diagram of Path of Single P and PS Waves in Two- (a) and Three-Layered (b) Media With Horizontal Interfaces

Formula (2.1) was derived by Hasegawa [176] in 1930, but in a somewhat different manner than was done in [108]. This formula was subsequently distorted: the apparent angle of emergence of waves to the earth's surface $\bar{i}_{P1}$ was taken

APPROVED FOR RELEASE: 2007/02/08: CIA-RDP82-00850R000200030043-9

APPROVED FOR RELEASE: 2007/02/08: CIA-RDP82-00850R000200030043-9

by investigators who used this formula as the angle of incidence of the P wave to the exchange boundary. This error was noted and corrected [108].

The three-layered medium. The velocity distribution in the medium is as follows (Figure 9, b): $v_{P3} > v_{P2} > v_{P1}$ and $v_{S3} > v_{S2} > v_{S1}$. The delay time of the PS wave with respect to the P wave at point F can be written in the form

$$\Delta t_{PS-P} = \frac{H}{v_{P2}}(K_2-1)\left(1+\frac{K_2}{2}\sin^2\frac{\bar{i}_{P2}}{2}\right) + \frac{H_1}{v_{P1}}(K_1-1)\left(1+\frac{K_1}{2}\sin^2\frac{\bar{i}_{P1}}{2}\right) \tag{2.3}$$

or

$$\Delta t_{PS-P} = \frac{H_2}{v_{P2}}(K_2-1)\left(1+\frac{1}{2K_2}\cos^2 e_{P2}\right) + \frac{H_1}{v_{P1}}(K_1+1)\left(1+\frac{1}{2K_1}\cos^2 e_{P1}\right), \tag{2.4}$$

where the parameters contained in the first term characterize the first layer and those contained in the second term characterize the second layer (see Figure 9, b); $\bar{i}_{P2}$ is the apparent angle of incidence of the P wave to the bottom of layer I (Figure 9, b).

The multilayered medium. By analogy with formula (2.3), the formula for determination of Δt_{PS-P} for a multilayered medium (n layers above a half-space) will have the form

$$\Delta t_{PS-P}^{n+1} = \sum_{m=2}^{n}\frac{H_m}{v_{P\,m}}(K_m-1)\left[1+\left(\frac{v_{P\,m}}{v_{P\,(m+1)}}\right)^2 \times \frac{1}{2K_m}\sin^2 i_m\right], \tag{2.5}$$

where i_m is the angle of incidence of the P waves to the exchange boundary or

$$\Delta t_{PS-P}^{n+1} = \sum_{m=1}^{n}\frac{H_m}{v_{P\,m}}(K_m-1)\left(1+\frac{1}{2K_m}\cos^2 e_m\right). \tag{2.6}$$

Gradient media. If there is a gradient of velocity variation with depth, formula Δt_{PS-P} can be derived from formulas (2.5) and (2.6) by an unlimited increase of the number of layers with simultaneous approach of their thickness to zero. As a result of derivation, the formula for a gradient medium will have the form

APPROVED FOR RELEASE: 2007/02/08: CIA-RDP82-00850R000200030043-9

APPROVED FOR RELEASE: 2007/02/08: CIA-RDP82-00850R000200030043-9

$$\Delta t_{PS-P} = \int_{m=1}^{n} \frac{H_m}{v_{P\,m}} (K_m - 1) \left[1 + \left(\frac{v_{P\,m}}{v_{P\,(m+1)}} \right)^2 \times \right. \\ \left. \times \frac{1}{2K_m} \sin^2 i_m \right] dH, \tag{2.7}$$

where v_m and K_m are the variable values which vary with depth by some law.

The Equation of Hodographs of P and PS Waves and Time Differences of Their Recording on the Surface of a Two-Layered Three-Dimensional Medium with Inclined Exchange Boundary

The equations of surface hodographs of P waves at $\Delta > 10°$, according to [45, 112], can be written in the form (Figure 10)

$$t'_P = \frac{\sin i_{P2}}{v_{P2}} \left[\sqrt{(x'_P \cos\varphi)^2 + (y'_P)^2} - \frac{x'_P \sin\varphi - H_{P1}}{\operatorname{tg} i_{P1}} \right], \tag{2.8}$$

where i_{P1} and i_{P2} are the angles between the paths of the P waves and to the normal to the exchange boundary in the first and second media, x'_P and y'_P are the coordinates of the point of emergence of the rays of P waves to surface Q in the x'y'z' system and H_{P1} is the depth along the normal at the point of separation of the P wave from the exchange boundary.

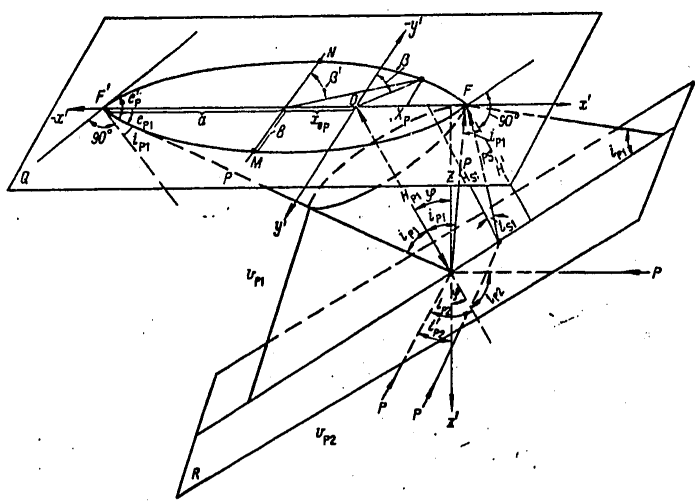

Figure 10. Diagram of Ray of P Waves in a Two-Layered Medium With Inclined Interface:
R--inclined interface; Q--horizontal surface of earth

APPROVED FOR RELEASE: 2007/02/08: CIA-RDP82-00850R000200030043-9

APPROVED FOR RELEASE: 2007/02/08: CIA-RDP82-00850R000200030043-9

The value of H_{P1} is determined by the formula

$$H_{P1} = \frac{Z}{\cos\varphi_K}. \tag{2.9}$$

Here Z is the depth along the vertical drawn through the point of separation of the P wave from the exchange boundary and φ_K is the apparent angle of inclination of the exchange boundary

$$\cos\varphi_K = \sqrt{\cos^2\varphi\sin^2\beta + \cos^2\beta},$$
$$\sin\varphi_K = \sin\varphi\sin\beta,$$

where β is the approach azimuth of the P wave counted from the line of strike of the boundary for the coordinaty system x'Oy'.

Equation (2.8) can be written in the form

$$t'_P = \frac{\sin i_{P1}}{v_{P1}}\left[\sqrt{(x'_P\cos\varphi)^2 + (y'_P)^2} - \frac{x'_P\sin\varphi - H_{P1}}{\operatorname{tg} i_{P1}}\right]. \tag{2.10}$$

The equation of the surface hodograph of the PS wave, by analogy with (2.8) can be written as

$$t'_{PS} = \frac{\sin i_{P2}}{v_{P2}}\left[\sqrt{(x'_S\cos\varphi)^2 + (y'_S)^2} - \frac{x'_S\sin\varphi - H_{S1}}{\operatorname{tg} i_{S1}}\right], \tag{2.11}$$

where i_{S1} is the angle between the path of the S wave and to the normal to the exchange boundary in the first medium, x'_S and y'_S are the coordinates of the point of emergence of the rays of the P waves to surface Q in the system x'y'z' and H_{S1} is the depth along the normal at the point of separation of the S wave from the exchange boundary.

The difference equations of the arrival times of PS and P waves to the surface of a two-layered medium with inclined exchange boundary at $\Delta > 10°$ have the form:

$$\Delta t^*_{PS-P} = \frac{H_{P1}}{v_{P1}}(K_1 - 1)\left(1 + \frac{1}{2K_1}\cos^2 e'_{P1}\right) - \\ - \frac{1}{v_{P1}}(K_1 - 1)\left(1 + \frac{1}{2K_1}\cos^2 e'_{P1}\right)X_P\sin\varphi, \tag{2.12}$$

where e'_{P1} is the angle of emergence of the seismic radiation of P waves to the boundary inclined at angle φ to the earth's surface and X_P is the coordinate of the point of emergence of the P wave to the Q surface along the Ox' axis.

APPROVED FOR RELEASE: 2007/02/08: CIA-RDP82-00850R000200030043-9

APPROVED FOR RELEASE: 2007/02/08: CIA-RDP82-00850R000200030043-9

The relationship of angle e'_{P1} to the ordinary angle e_{P1} is expressed by the formula

$$e_{P1} = e'_{P1} \pm \varphi,$$

where the plus corresponds to a dip of the boundary and the minus corresponds to a rise. Coordinate X_P is determined by the formula

$$X_P = a \sin \beta' + x_{0P}, \tag{2.13}$$

where a is the major axis of the ellipse MF'NF, x_{0P} is the extent of displacement of the center of the ellipse MF'NF with respect to the center O of the coordinate system x'Oy' and β' is the approach azimuth of the P wave counted from the minor axis of the ellipse (see Figure 10) parallel to the strike of the boundary.

The relationship between the values of β' and β is expressed by the function

$$\sin \beta' = \frac{-a x_{0P} + \operatorname{tg} \beta \sqrt{-x_{0P}^2 + a_P^2 (1 + \operatorname{tg}^2 \beta)}}{a_P (1 + \operatorname{tg}^2 \beta)}. \tag{2.14}$$

At $\varphi = 0$, the second term of equation (2.12) approaches zero, the depth (H) along the perpendicular to the interface coincides with the depth along the vertical and the entire formula (2.12) is transformed to a Hasegawa formula for a two-layered medium with horizontal interface [108, 176]:

$$\Delta t_{PS-P} = \frac{H_1}{v_{P1}} (K_1 - 1) \left(1 + \frac{1}{2K_1} \cos^2 e_{P1}\right). \tag{2.15}$$

The value of $\Delta t'_{PS-P}$ from formula (2.12) can be written as

$$\Delta t'_{PS-P} = \frac{H'}{v_{P1}} (K_1 - 1) \left(1 + \frac{1}{2K_1} \cos^2 e'_{P1}\right), \tag{2.16}$$

where H' is the depth along the normal eliminated from the point of reception to the exchange boundary (Figure 11).

If angle i_{P2} (denoted by i'_{P2} in Figure 10) is located between the ray and the vertical to the point of incidence of the ray to the sloping interface, then for the same value of Δ, but for different values of β', we will have different values of the angles formed by the rays of the P waves and by the normal to the interface, equal to $i'_{P2} \pm \varphi$ along the rise and dip of the boundary, respectively. Formula (2.12) for Δt_{PS-P} remains the same; the values of i_{P1}, x_{0P}, a_P, b_P, $\sin \beta'$ and X_P become variable for different

APPROVED FOR RELEASE: 2007/02/08: CIA-RDP82-00850R000200030043-9

APPROVED FOR RELEASE: 2007/02/08: CIA-RDP82-00850R000200030043-9

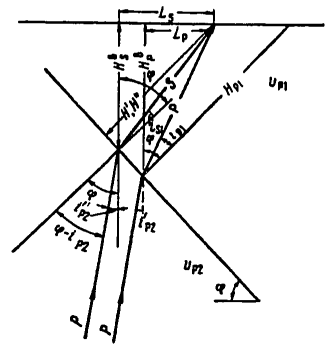

Figure 11. Diagram of Rays of Single P and PS Waves in a Two-Layered Medium with Sloping Interface

values of β, but for the same angle φ_K. In this case an ellipse with its own parameters a_P, b_P and x_0 must be calculated for each value of β' and φ_K. The value of X_P will be determined each time in this case for each value of φ_K as the coordinate of the major axis of the ellipse. At $\beta' = 90°$, $X_P = \pm a_P + x_{0P}$. Angle i_{P1} is determined in this case for each value of φ_K as

$$\sin i_{P1} = \frac{v_{P1}}{v_{P2}} \sin (i'_{P2} \pm \varphi_K).$$

Moreover, the plus inside the parentheses corresponds to the rise of the boundary and the minus corresponds to a dip.

Equations of the Lines of Intersections of the Aggregate of Rays of P and PS Waves with the Daytime Surface of a Two-Layered Medium

For P waves

$$(x'_P)^2 [\cos^2 \varphi - \sin^2 \varphi \operatorname{tg}^2 i'_{P1}) + (y'_P)^2 + 2x'_P \sin \varphi H_P \operatorname{tg}^2 i_{P1} = \\ = (H_P \operatorname{tg} i_{P1})^2. \tag{2.17}$$

In the case of a horizontal interface ($\varphi = 0$), equation (2.15) assumes the form

$$(x'_P)^2 + (y'_P)^2 = (H_P \operatorname{tg} i_{P1})^2, \tag{2.18}$$

APPROVED FOR RELEASE: 2007/02/08: CIA-RDP82-00850R000200030043-9

APPROVED FOR RELEASE: 2007/02/08: CIA-RDP82-00850R000200030043-9

i.e., the line of intersection of the rays of the P waves with the surface of a two-layered medium will be a circle with radius $H\mathrm{tg}i_{P1}$. The line of intersection of the rays of P waves for a sloping interface [equation (2.17)] with second-order invariants of curves [17] Δ' and δ equal to $\Delta \neq 0$, $\delta > 0$ and $i_{P1} < (90° - \varphi)$ is an ellipse, while that at $\Delta' \neq 0$, $\delta < 0$ and $i_{P1} > (90° - \varphi)$ is a hyperbola. The rays of the P waves will be described by ellipses for earthquakes with epicentral distances of $\Delta > 20°$ and at $\varphi = 40\text{-}80°$. The axes of the ellipses and the displacements of their centers with respect to the axes of coordinate system x'Oy' are expressed by the formulas

$$a_P = \pm \frac{H_{P1}\,\mathrm{tg}\,i_{P1}\cos\varphi}{\cos^2\varphi - \sin^2\varphi\,\mathrm{tg}^2 i_{P1}},$$
$$b_P = \pm \frac{H_{P1}\,\mathrm{tg}\,i_{P1}\cos\varphi}{\sqrt{\cos^2\varphi - \sin^2\varphi\,\mathrm{tg}^2 i_{P1}}}, \qquad (2.19)$$
$$x_{0P} = -\frac{\sin\varphi H_{P1}\,\mathrm{tg}^2 i_{P1}}{\cos^2\varphi - \sin^2\varphi\,\mathrm{tg}^2 i_{P1}}.$$

For the PS wave, the equation of the line of intersection of their paths with the daytime surface of a two-layered medium with sloping interface has the form

$$(x_S')^2[\cos^2\varphi - \sin^2\varphi\,\mathrm{tg}^2 i_{S1}] + (y_S')^2 + \\ + 2x_S'\sin\varphi H_{S1}\,\mathrm{tg}^2 i_{S1} = (H_{S1}\,\mathrm{tg}\,i_{S1})^2. \qquad (2.20)$$

In the case of a horizontal interface ($\varphi = 0$), equation (2.20) assumes the form

$$(x_S')^2 + (y_S')^2 = (H_{S1}\,\mathrm{tg}\,i_{S1})^2, \qquad (2.21)$$

i.e., the equation of the projection of the ray of the PS wave to the earth's surface is a circle of radius $H_{S1}\mathrm{tg}i_{S1}$.

Equation (2.20) for PS waves is an ellipse provided that $\Delta' \neq 0$; $\delta < 0$; $90° - \varphi > i_{S1}$ [17].

Equation (2.20) is a hyperbola provided that $\Delta \neq 0$; $\delta < 0$; $(90° - \varphi) < i_{S1}$.

The axes of the ellipses and the displacements along the x' axis for PS waves are determined by the formulas

$$a_S = \pm \frac{H_{S1}\,\mathrm{tg}\,i_{S1}\cos\varphi}{\cos^2\varphi - \sin^2\varphi\,\mathrm{tg}^2 i_{S1}},$$

APPROVED FOR RELEASE: 2007/02/08: CIA-RDP82-00850R000200030043-9

APPROVED FOR RELEASE: 2007/02/08: CIA-RDP82-00850R000200030043-9

$$b_S = \pm \frac{H'_{S1} \operatorname{tg} i_{S1} \cos\varphi}{\sqrt{\cos^2\varphi - \sin^2\varphi \operatorname{tg} i_{S1}}},$$
$$x_{0S} = -\frac{\sin\varphi H'_{S1} \operatorname{tg}^2 i_{S1}}{\cos^2\varphi - \sin^2\varphi \operatorname{tg}^2 i_{S1}}. \tag{2.22}$$

Equations Δt_{PS-P} at $\Delta < 10°$ for a two-layered medium with sloping interface can be written in the form

$$\Delta t'_{PS-P} = \frac{H'}{\cos i_{S1} v_{S1}} - \frac{H'}{\cos i_{P1} v_{P1}} + \frac{H'(\operatorname{tg} i_{P1} - \operatorname{tg} i_{S1}) \sin(\varphi - i_{P1})}{v_{P2}} \tag{2.23}$$

or

$$\Delta t'_{PS-P} = \frac{H'}{v_{P1}} (K_1 \cos i_{S1} - \cos i_{P1}). \tag{2.24}$$

Equations of Hodographs and the Time Difference of the Arrival of Multiple P and PS Waves and Single P Waves to the Surface of a Two-Layered Three-Dimensional Medium with Horizontal and Sloping Interface

If multiple waves of types $P_2P_1^n$, ($P_2P_1P_1P_1$, $P_2P_1P_1P_1P_1P_1$ and so on), $P_2S_1^m$ and $P_2P_1^nS_1^m$ (Figure 12, a) occur at some special geological conditions, the equations of their surface hodographs with horizontal exchange boundary in a two-layered medium can be written in the form

$$t_{P_2P_1^n} = \frac{(n-1) H_1}{v_{P1}} \cos i_{P1} + t_P, \tag{2.25}$$

$$t_{P_2S_1^m} = \frac{(m-1) H_1}{v_{S1}} \cos i_{S1} + t_{PS}, \tag{2.26}$$

$$t_{P_2P_1^nS_1^m} = \frac{nH_1}{v_{P1}} \cos i_{P1} + \frac{(m-1) H_1}{v_{S1}} \cos i_{S1} + t_{PS}, \tag{2.27}$$

where n is the number of segments of rays of the way included between the surface of a two-layered medium and the multiplicity boundary (n = 1, 3, 5, 7 and so on) and m is the number of multiple reflections without the first single wave. There is the following relationship between the values of m and n: n = 1 and m = 0, n = 3 at m = 1, n = 5 at m = 2, n = 7 at m = 3 and so on. At n = 1 and m = 1, equations (2.25)-(2.27) change to equations of

APPROVED FOR RELEASE: 2007/02/08: CIA-RDP82-00850R000200030043-9

APPROVED FOR RELEASE: 2007/02/08: CIA-RDP82-00850R000200030043-9

the surface hodographs of single transient P and PS waves. The equations of the surface hodographs of single transient P and PS waves for a two-layered medium with horizontal exchange boundary have the form

$$t_P = \frac{\sin i_{P2}}{v_{P2}} \left(\sqrt{(y')^2 + (x')^2} + \frac{H_1}{\operatorname{tg} i_{P1}} \right), \tag{2.28}$$

$$t_{PS} = \frac{\sin i_{P2}}{v_{P2}} \left(\sqrt{(y')^2 + (x')^2} + \frac{H_1}{\operatorname{tg} i_{S1}} \right). \tag{2.29}$$

With a sloping interface, the equations of the surface hodographs of $P_2P_1^n$, $P_2S_1^m$ and $P_2P_1^nS_1^m$ waves (Figure 12, b) for a two-layered medium have the form

$$t'_{P_2P_1^n} = T_1 + t''_{P_2P_1^n}, \tag{2.30}$$

$$t'_{P_2S_1^m} = T_2 + t''_{P_2S_1^m}, \tag{2.31}$$

$$t_{P_2P_1^nS_1^m} = t''_{P_2P_1^n} + t''_{P_2S_1^m}, \tag{2.32}$$

where T_1 and T_2 are the transit times of multiple P and PS waves from point A to point N and $t''_{P_2P_1^n}$ and $t''_{P_2S_1^m}$ are the equations of the surface hodographs of single longitudinal or composite PS waves whose wave fronts comprise angles $i_{P1} - (n-1)\varphi$ and $i_{S1} - (m-1)\varphi$, respectively, with boundary R.

The time difference of recording multiple $P_2P_1^n$, $P_2S_1^m$ and $P_2P_1^nS_1^m$ waves and single P waves can be written in the following form.

A horizontal interface

$$t_{P_2P_1^n} - t_P = \frac{(n-1)H_1}{v_{P1}} \cos i_{P1}, \tag{2.33}$$

$$t_{P_2S_1^m} - t_P = \frac{(m-1)H_1}{v_{S1}} \cos i_{S1} + \frac{H_1}{v_{P1}} (K_1 - 1) \left(1 + \frac{1}{2K_1} \cos^2 e_{P1} \right), \tag{2.34}$$

$$t_{P_2P_1^nS_1^m} - t_P = \frac{nH_1}{v_{P1}} \cos i_{P1} + \frac{(m-1)H_1}{v_{S1}} \cos i_{S1} + \frac{H_1}{v_{P1}} (K_1 - 1) \left(1 + \frac{1}{2K_1} \cos^2 e_{P1} \right). \tag{2.35}$$

A sloping interface

$$t'_{P_2P_1^n} - t'_P = \frac{h_1}{v_{P1}} \cos i_{P1} + T_1, \tag{2.36}$$

$$t'_{P_2S_1^m} - t'_P = \frac{h_1}{v_{S1}} \cos i_{S1} + T_2. \tag{2.37}$$

APPROVED FOR RELEASE: 2007/02/08: CIA-RDP82-00850R000200030043-9

APPROVED FOR RELEASE: 2007/02/08: CIA-RDP82-00850R000200030043-9

[redacted]

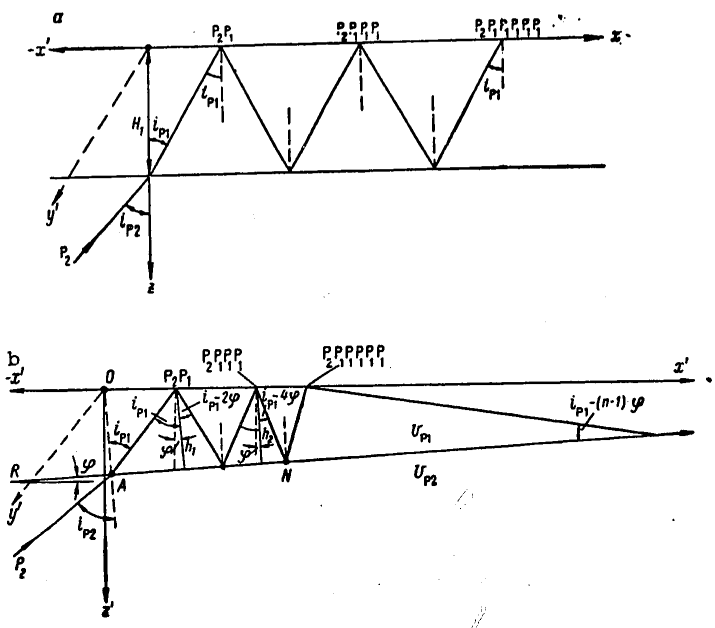

Figure 12. Diagram of Path of Multiple P Wave Rays in a Two-Layered Medium with Horizontal (a) and Sloping (b) Interface

The equations of the lines of intersection of a series of rays of multiple P and PS waves with the surface of a two-layered medium will, as for single P and PS waves, be ellipses or hyperbolas as a function of the ratio of the invariants of these lines and angles of inclination of the multiplicity boundaries. At $\Delta \neq 0$, $\delta < 0$, which is possible at $n\varphi > i_{P1}$, we find a hyperbola. At $\delta > 0$, which is possible at $n\varphi < i_{P1}$, we find an ellipse. The axes of the ellipses x_{0P} can be calculated by the method, as for single transient P and PS waves, outlined in detail in [112].

Equations of the Arrival Times of Single P and PS Waves in Multilayered Three-Dimensional Media with Sloping Parallel Interfaces

A three-layered three-dimensional medium. The time difference of recording PS and P waves at point F (Figure 13) is determined by the formula

$$\Delta t'_{PS-P} = \frac{H_{P2}}{v_{P2}}(K_2-1)\left(1+\frac{1}{2K_2}\cos^2 e_{P2}\right) + \frac{H_{P1}}{v_{P1}}(K_1-1)\left(1+\frac{1}{2K_1}\cos^2 e_{P1}\right) - \frac{1}{v_{P1}}(K_1-1)\left(1+\frac{1}{2K_1}\cos^2 e_{P1}\right) X_P \sin\varphi, \quad (2.38)$$

APPROVED FOR RELEASE: 2007/02/08: CIA-RDP82-00850R000200030043-9

APPROVED FOR RELEASE: 2007/02/08: CIA-RDP82-00850R000200030043-9

[redacted]

where H_{P1} and H_{P2} are the depths along the perpendiculars to the interfaces, e_{P1} and e_{P2} are the angles of emergence of seismic radiation (see Figure 13) in the first and second media and X_P is the coordinate x' along the major axis of the ellipse.

Multilayered three-dimensional media. By analogy with (2.38), the equation of the delay times of PS waves with respect to P waves for an n-layered medium with sloping and parallel interfaces has the form

$$\Delta t'_{PS-P} = \sum_{i=2}^{n-1} \frac{H_i}{v_{Pi}} (K_i - 1) \left(1 + \frac{1}{2K_i} \cos^2 e_{Pi}\right) + \\ + \frac{H_1}{v_{P1}} (K_1 - 1) \left(1 + \frac{1}{2K_1} \cos^2 e_{P1}\right) + \\ + \frac{1}{v_{P1}} (K_1 - 1) \left(1 + \frac{1}{2K_1} \cos^2 e_{P1}\right) X_P \sin\varphi, \tag{2.39}$$

where

$$X_P = A \sin\beta' + x_{0P}. \tag{2.40}$$

Unlike (2.19), here the parameters A and x_{0P} are determined by the formulas

$$A = \frac{\sum_{i=2}^{n-1} (H_i \operatorname{tg} i_{Pi} \cos\varphi)}{\sum_{i=2}^{n-1} (\cos^2\varphi - \sin^2\varphi \operatorname{tg} i_{Pi})}, \\ x_{0P} = -\frac{\sum_{i=2}^{n-1} (H_i \sin\varphi \operatorname{tg}^2 i_{Pi})}{\sum_{i=2}^{n-1} (\cos^2\varphi - \sin^2\varphi \operatorname{tg}^2 i_{Pi})}. \tag{2.41}$$

Equations of Hodographs of Lateral P and PS Waves

Transient diffracted P waves. Let us consider the case when the interface of two media is horizontal and diffraction of P waves is from the edge of the bench (Figure 14). The equations of the surface hodographs of transient diffracted (longitudinal P and composite PS) waves from edge AA' on the surface of a two-layered medium can be written in the form

$$t^{\text{диф}}_{P_2P_1} = \frac{1}{v_{P1}} \left\{\sqrt{x^2 + H_1^2} + y \frac{v_{P1}}{v_{P2к}}\right\}, \tag{2.42}$$

$$t^{\text{диф}}_{P_2S_1} = \frac{1}{v_{S1}} \left\{\sqrt{x^2 + H_1^2} + y \frac{v_{S1}}{v_{P2к}}\right\}. \tag{2.43}$$

APPROVED FOR RELEASE: 2007/02/08: CIA-RDP82-00850R000200030043-9

APPROVED FOR RELEASE: 2007/02/08: CIA-RDP82-00850R000200030043-9

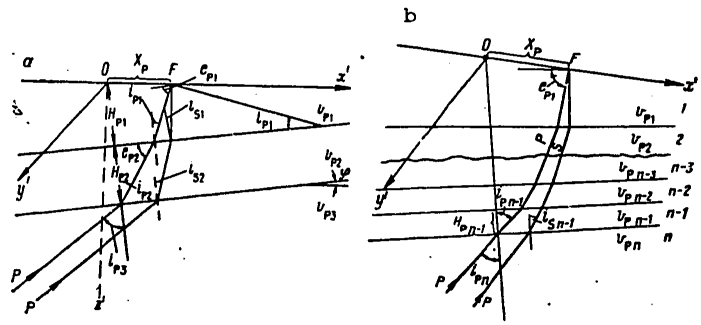

Figure 13. Diagram of Ray Path of P and PS Waves in Three-Layered (a) and Multilayered (b) Media with Sloping Interfaces

The value of v_{P2K} along the edge is determined by the formula

$$v_{P2K} = \frac{v_{P2}}{\cos \eta}, \tag{2.44}$$

where v_{P2} is the velocity of longitudinal waves in the second layer and $\cos \eta$ is the direction cosine for the incident ray of the P wave (see Figure 14)

$$\cos \eta = \sin i_{P2} \sin \psi_1. \tag{2.45}$$

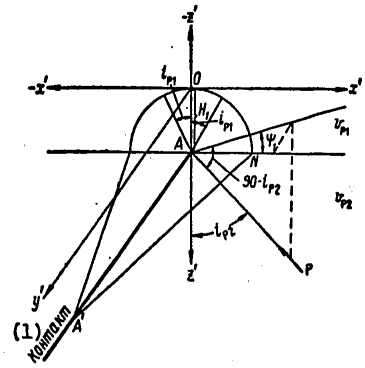

Figure 14. Diagram of Ray Path of Transient Diffracted P Waves

Key:
1. Contact

APPROVED FOR RELEASE: 2007/02/08: CIA-RDP82-00850R000200030043-9

APPROVED FOR RELEASE: 2007/02/08: CIA-RDP82-00850R000200030043-9

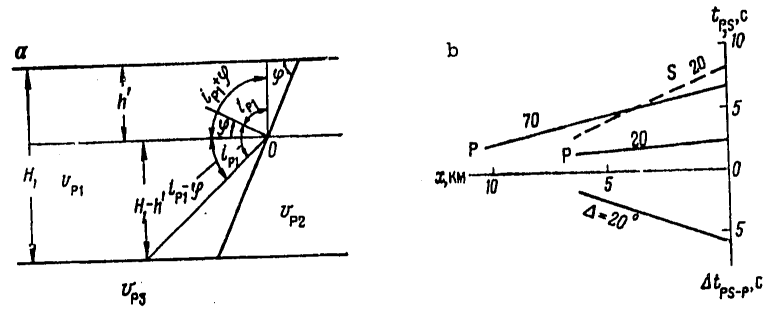

Figure 15. Diagram of Rays of Transient P Waves Reflected From a Sloping Contact (a), Hodographs of P and S Waves and the Time Profile Δt_{PS-P} at $\varphi = 10°$ (b)

Transient reflected P and PS waves from sloping contacts. Let us consider a two-layered medium with horizontal interface. The contact of the medium with different velocities is included between two horizontal boundaries (Figure 15, a) and is a plane sloping toward the horizon at angle φ. The equations of the hodographs of transient reflected P and PS waves were derived in a plane perpendicular to the strike of the contact. According to Figure 15, a, the equations of the recording times of the P and PS waves reflected from the sloping contact have the form

$$t^{\text{отр}}_{P_1P_1} = \frac{1}{v_{P1}}\left\{\frac{h'}{\sin(i_{P1}-\varphi)} + \frac{H_1-h'}{\sin(i_{P1}+\varphi)}\right\}, \tag{2.46}$$

$$t^{\text{отр}}_{P_1P_1} = \frac{1}{v_{S1}}\left\{\frac{h_1}{\sin(i_{S1}-\varphi)} + \frac{H-h_1}{\sin(i_{S1}+\varphi)}\right\}, \tag{2.47}$$

where v_{P1} and v_{S1} are the velocities of the P and S waves in the first layer, h' is the depth along the vertical to the point of reflection in the first layer, H_1 is the depth to the interface in the two-layered medium, i_{P1} and i_{S1} are the angles of incidence of the reflected to the waves to the sloping contact for P and PS waves, respectively and φ is the angle of inclination of the contact.

The Effect of the Angle of Inclination of the Crustal Boundaries on the Difference of the Delay Times of Single, Multiple and Lateral PS Waves with Respect to Single P Waves

Single waves. Let us consider the case when the aggregates of the rays of P and PS waves describe ellipses on the surface of a two-layered three-dimensional medium. The differences of the values of $\Delta t'_{PS-P}$ were calculated by formulas (2.2) and (2.12) for two models of the medium to analyze

APPROVED FOR RELEASE: 2007/02/08: CIA-RDP82-00850R000200030043-9

APPROVED FOR RELEASE: 2007/02/08: CIA-RDP82-00850R000200030043-9

the time difference of recording the P and PS waves on the surface of a two-layered medium with horizontal and sloping interfaces. Model I: $Z = 5$ km, $v_{P1} = 3.6$ km/s, $K_1 = 2.1$ and $v_{P2} = 5.35$ km/s. Model II; $Z = 33$ km, $v_{P1} = 5.8$ km/s, $K_1 = 1.8$ and $v_{P2} = 8.1$ km/s. The value of angle φ varied from 0 to 80° every 10°. Angles i'_{P2} (with the vertical to the interface) comprised 40°55', 30°36', 17°15' and 8°38' and corresponded to Δ equal to 10, 20, 70 and 140°; angles β' varied from 0 to 360° every 30°.

The dependence of the value of $\delta\Delta t_{PS-P}$, which is the difference of Δt_{PS-P} for horizontal and sloping interfaces, on φ, Δ and β', is presented in Figure 16. The theoretical dependence of the relative error ($\delta\Delta t_{PS-P}$) on φ along the dip and rise of the interface in percent is given in Figure 17.

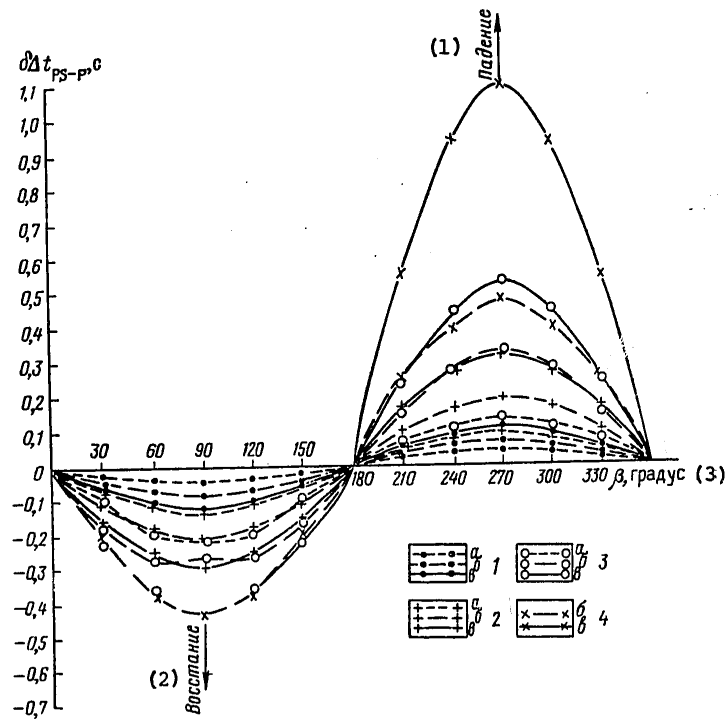

Figure 16. Theoretical Graphs of the Dependence of $\delta\Delta t_{PS-P}$ on Azimuth β' for Two Models of Media:
1-3--model I for φ = 10, 30 and 50°, respectively; Model II for φ = 10°; a-- Δ = 70°; b-- Δ = 20°; c-- Δ = 10°

Key:
1. Dip
2. Rise
3. Degree

APPROVED FOR RELEASE: 2007/02/08: CIA-RDP82-00850R000200030043-9

APPROVED FOR RELEASE: 2007/02/08: CIA-RDP82-00850R000200030043-9

Analysis of the graphs of Figure 16 made it possible to reach the following conclusions. At β' equal to 0, 180 and 360°, which corresponds to the condition of the strike of the boundary ($\varphi_K = 0$), there is no difference in Δt_{PS-P} for sloping and horizontal boundaries at H_{P1} dependent on φ_K. The maximum differences between Δt_{PS-P} for sloping and horizontal interfaces are observed at β' equal to 90 and 270°, which corresponds to the rise and dip of the boundary ($\varphi_K = \varphi_{max}$). Thus, at $\Delta = 10°$ and $\varphi = 70°$, they reach +0.75 second along the dip with a total value of Δt_{PS-P} of 1.61 and +8.5 seconds for a horizontal interface and 5.25 seconds at Δt_{PS-P} for a horizontal interface. The values of $\delta \Delta t_{PS-P}$ are approximately of the same order along the rise as along the dip, but are negative. This corresponds to the fact that the values of Δt_{PS-P} for a horizontal boundary is greater than those of Δt_{PS-P} for a sloping boundary. The ratio between Δt_{PS-P} for horizontal and sloping boundaries changes to the opposite along the dip: Δt_{PS-P} for a sloping boundary is greater than for a horizontal boundary.

According to the graph of Figure 17, the difference in Δt_{PS-P} for sloping and horizontal interfaces at φ = 10-80° may reach 20-100 percent or more of Δt_{PS-P} for a horizontal interface. This circumstance requires that the angles of inclination of the interfaces be considered when constructing the profile at $\varphi > 10°$ for $\Delta < 70°$ and at $\varphi > 20$-40° for $\Delta > 70°$.

Multiple P and PS waves. In the case of a horizontal interface of two-layered media, multiple $P_2P_1^n$ and $P_2S_1^m$ waves are distinguished from each other by values equal to $t_{P_2P_1^n} - t_P$, determined by the type of wave and the parameters of the medium. The dependence of the difference of arrival times of multiple waves Δt on the angle of incidence of P waves to the interface i_{P1} for four variants of models of the media is presented in Figure 18. The parameters of the models were as follows. Model I: v_{P1} = 3 km/s, H_1 = = 3.5 km, K_1 = 2.2 and v_{P2} = 4.5 km/s. Model II: v_{P1} = 3.6 km/s, H_1 = 5 km, K_1 = 2.1 and v_{P2} = 5.35 km/s. Model III: V_{P1} = 4.73 km/s, H_1 = 14 km, K_1 = 1.96 and v_{P2} = 6.4 km/s. Model IV: V_{P1} = 5.8 km/s, H_1 = 33 km, K_1 = = 1.86 and v_{P2} = 8.1 km/s.

As can be seen from Figure 18, the interval Δt between the multiple waves is reduced with an increase of the angle of incidence i_{P1} to the interface. The distribution Δt of multiple waves is subordinated to the same principles as single P and PS waves in the presence of a sloping interface.

Lateral P and PS waves. Transient diffracted P and PS waves on the surface of a two-layered medium have the shape of hodographs varying from a hyperbola (y' = 0) to a straight line (x' = 0) (Figure 19) as a function of the approach azimuth of the front or rays of the P and PS wave to the dislocation line (see Figure 14). The time profiles [$\Delta t_{PS-P} = f(R)$] are either almost horizontal straight lines (x' = 0) or second-order curves intersecting the universal cophasal axes at large angles of inclination, corresponding to crustal interfaces from the basement surface to the interfaces in the mantle on comparatively small (up to 30 km) tracking intervals of the PS wave.

APPROVED FOR RELEASE: 2007/02/08: CIA-RDP82-00850R000200030043-9

APPROVED FOR RELEASE: 2007/02/08: CIA-RDP82-00850R000200030043-9

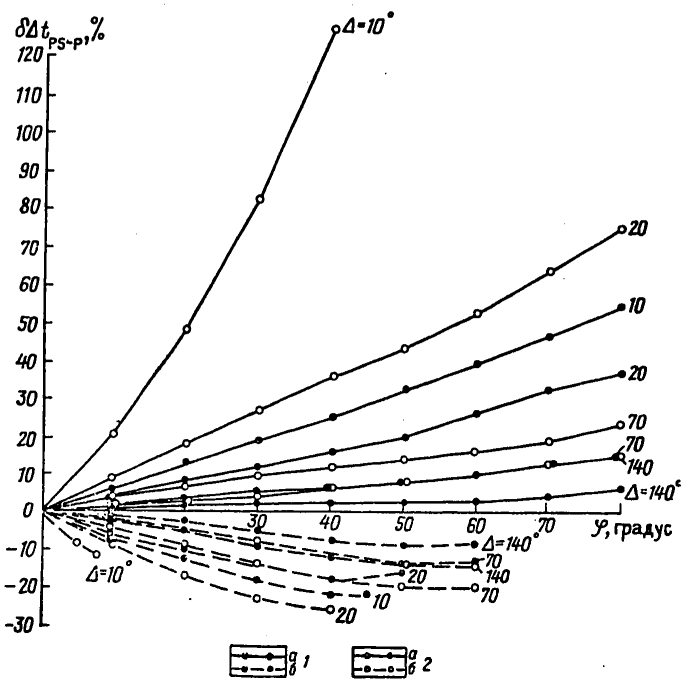

Figure 17. Theoretical Graphs of the Dependence $\delta \Delta t_{PS-P}$ on the Angle of Inclination of the Boundary Upon Approach of the P Wave to the Interface Along its Dip and Rise for Two Models of Media: 1--curves for model I; 2--curves for model II; a--along the dip of the boundary; b--along the rise of the boundary

Transient reflected P and PS waves have the shape of hodographs which are straight lines with different angular coefficients dependent on the parameters of the studied medium and the angle of inclination of the reflecting contact. The hodographs of transient reflected P and PS waves and the time profile [$\Delta t_{PS-P} = f(x)$] are presented in Figure 15, b. As can be seen from the time profile, the transient-reflected PS waves at a short distance (up to 5 km) from the contact may intersect all the time profiles (from 1 to 5.5 seconds) related to the interfaces of the entire earth's crust.

Displacement Vector Components of Single Transient P and PS Waves and Their Azimuths in a Two-Layered Three-Dimensional Medium with Sloping Interface

Calculating Formulas

The displacement vector components of P($\bar{U}^P$) and PS($\bar{U}^{PS}$) waves for the right-handed coordinate system xyz located on the surface of a two-layered

APPROVED FOR RELEASE: 2007/02/08: CIA-RDP82-00850R000200030043-9

APPROVED FOR RELEASE: 2007/02/08: CIA-RDP82-00850R000200030043-9

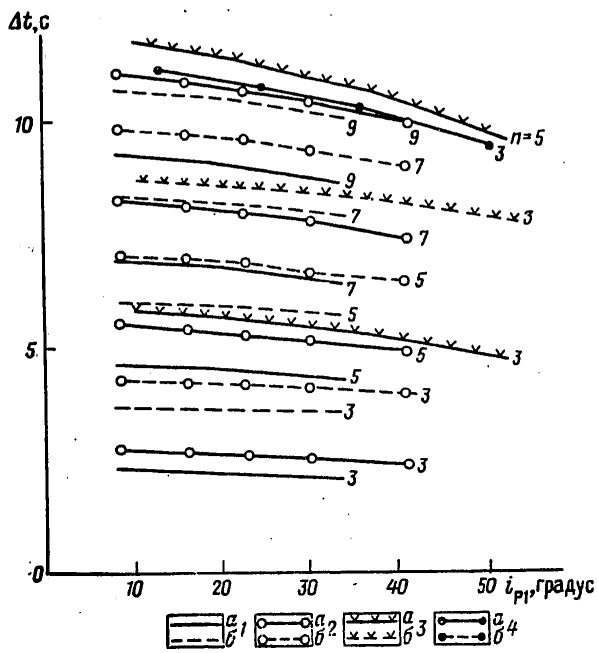

Figure 18. Graphs of Dependence of Δt on i_{P1} for Difference Models of Media:
1-4--graphs for models I-IV, respectively; a--for multiple P waves; b--for multiple PS waves

three-dimensional medium with sloping interface (Figure 20) can be calculated by formulas similar to those presented in [90].

For P waves

$$\left.\begin{aligned} \overline{U}_{P_X} &= \overline{U}_P q_P \cos(\psi_1' + \omega), \\ \overline{U}_{P_Y} &= -\overline{U}_P q_P \sin(\psi_1' + \omega), \\ \overline{U}_{P_Z} &= -\overline{U}_P W_P. \end{aligned}\right\} \tag{2.48}$$

For PS waves

$$\left.\begin{aligned} \overline{U}_{PS_X} &= \overline{U}_{PS}\,[\cos\eta q_S \cos(\psi_1 + \omega) - 2\sin\eta \sin(\psi_1 + \omega)], \\ \overline{U}_{PS_Y} &= \overline{U}_{PS}\,[2\sin\eta \cos(\psi_1 + \omega) + q_S \cos\eta \sin(\psi_1 + \omega)], \\ \overline{U}_{PS_Z} &= \overline{U}_{PS} \cos\eta W_S, \end{aligned}\right\} \tag{2.49}$$

APPROVED FOR RELEASE: 2007/02/08: CIA-RDP82-00850R000200030043-9

APPROVED FOR RELEASE: 2007/02/08: CIA-RDP82-00850R000200030043-9

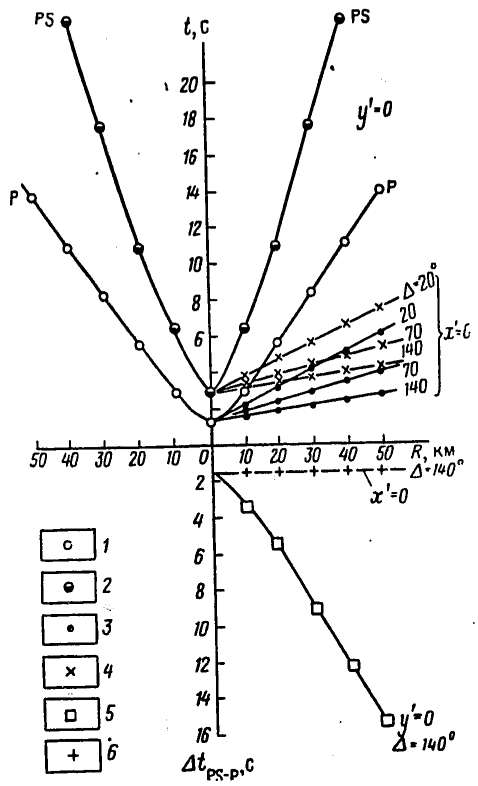

Figure 19. Theoretical Hodographs of Transient Diffracted Longitudinal P and Composite PS Waves for the Model of Figure 14:
1 and 2--hodographs of transient diffracted P and PS waves for the plane x'Oz'; 3 and 4--hodographs of transient diffracted P and PS waves for the plane y'Oz'; 5--time profile Δt_{PS-P} of transient diffracted PS wave for the plane x'Oz'; 6--time profile of Δt_{PS-P} of transient diffracted PS wave for the plane y'Oz'

where $\bar{U}_{PX}$, $\bar{U}_{PY}$, $\bar{U}_{PZ}$, $\bar{U}_{PSX}$, $\bar{U}_{PSY}$, $\bar{U}_{PSZ}$ are the displacement vector components of P and S waves on the axis of a rectangular coordinate system, q_P, q_S, W_P and W_S are the horizontal and vertical components of the conversion coefficients determined by the formulas of [28], ψ_1' and ψ_1 are the ray azimuths of refracted P and PS waves, ω is the angle between the direction of dip-rise of the interface and the axes in coordinates xOy and η is the angle between the vertical and normal planes passing through the ray of the PS wave.

APPROVED FOR RELEASE: 2007/02/08: CIA-RDP82-00850R000200030043-9

APPROVED FOR RELEASE: 2007/02/08: CIA-RDP82-00850R000200030043-9

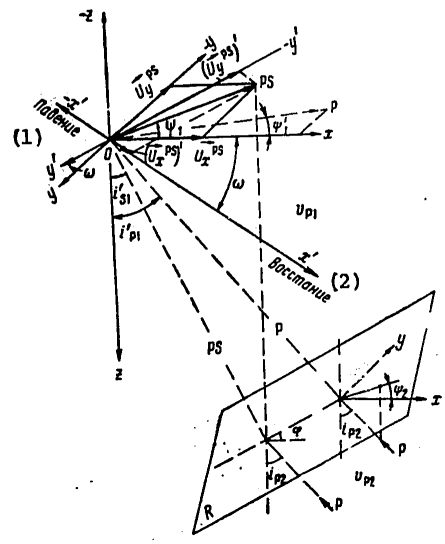

Figure 20. Diagram of Ray Path of P and PS Waves and Distribution of their Displacement Vector Components in a Three-Dimensional Medium with Sloping Interface R

Key:
1. Dip
2. Rise

The values of ψ_2 and ψ_1 are determined by the formula [90]

$$\sin\psi_1 = \frac{K' \sin i'_{P2} \sin\psi_2}{\sin i'}, \tag{2.50}$$

where $\psi_1 = \psi_{P1}$ or $\psi_1 = \psi_{S1}$, $K' = v_{P1}/v_{P2}$ or $K' = v_{S1}/v_{P2}$, $i' = i'_{P1}$ or $i' = i'_{S1}$ as a function of for which wave the calculations are made--P or PS, ψ_2 is the azimuth of the ray of the P wave impinging on the interface and i'_{P1} and i'_{S1} are the angles between the rays of the P and PS waves in the first medium and the vertical to the interface.

Angle i' is calculated by the formula

$$\cos i' = C \sin\varphi + \cos\varphi \sqrt{B - C^2}, \tag{2.51}$$

where

APPROVED FOR RELEASE: 2007/02/08: CIA-RDP82-00850R000200030043-9

APPROVED FOR RELEASE: 2007/02/08: CIA-RDP82-00850R000200030043-9

$$C = K'(\cos i' \sin \varphi - \sin i' \cos \psi_2 \cos \varphi);$$
$$B = 1 - (K')^2 \sin^2 i' \sin^2 \psi_2.$$

The Effect of the Angle of Inclination of the Interface on the Horizontal Components of the Displacement Vectors and Ray Azimuths of P and PS Waves

The theoretical curves of the ratio of the horizontal components of PS waves ($\bar{U}_{PSY}/\bar{U}_{PSX}$) and the angles between the ray azimuths of PS waves and their P waves formed as a function of α, determined by formulas of seismology at different values of Δ and φ were calculated to determine the effect of the angles of inclination of the interfaces on the displacement vector components of PS waves and the ray azimuths of P and PS waves.

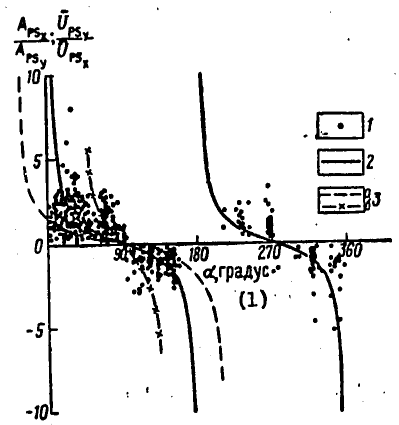

Figure 21. Ratios of Horizontal Displacement Vector Components of PS Waves A_{PSX}/A_{PSY} and $\bar{U}_{PSY}/\bar{U}_{PSX}$ as a Function of α:
1--experimental values of A_{PSX}/A_{PSY} for regions of the North German Depression; 2 and 3--theoretical curves of $\bar{U}_{PSY}/\bar{U}_{PSX}$ for horizontal and sloping interface, respectively, at φ = = 20°; a--along the dip of the interface; b--along the rise of the interface

Key:
1. Degree

The graph of the theoretical value of $\bar{U}_{PSY}/\bar{U}_{PSX}$ is presented in Figure 21 as a function of the approach azimuth α of P waves to the recording station [136] at angles of inclination of the interface of 0 and 20° (Δ = 20°, i'_{P2} = 30°36' and K = 0.32). Since the coordinate system selected during field investigations differs from the theoretical system (see Figure 20),

APPROVED FOR RELEASE: 2007/02/08: CIA-RDP82-00850R000200030043-9

APPROVED FOR RELEASE: 2007/02/08: CIA-RDP82-00850R000200030043-9

then the Y components of the theoretical displacement vectors of P and PS waves correspond to the X components of the displacement vectors determined by the amplitudes of experimental PS waves, while the X components correspond to the Y components. At $\varphi = 0$, the value of $\bar{U}_{PSY}/\bar{U}_{PSX}$ varies by the law of the tangent. At $\varphi = 20°$, the curve $\bar{U}_{PSY}/\bar{U}_{PSX}$ is located to the left and right of the curve $\bar{U}_{PSY}/\bar{U}_{PSX}$ plotted for $\varphi = 0$ as a function of the slope of the interface.

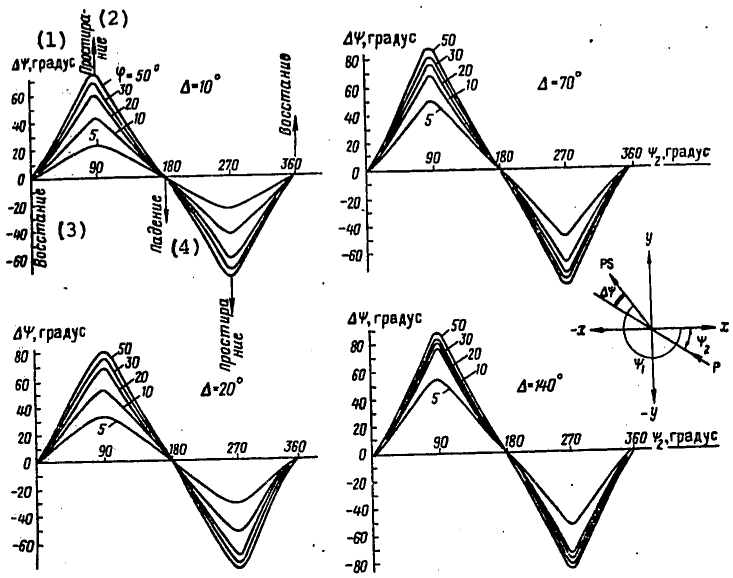

Figure 22. Dependence of $\Delta\psi$ and ψ_2 at Different Values of φ and Δ.

Key:

1. Degree
2. Strike
3. Rise
4. Dip

Theoretical graphs of variation of the angles between the ray azimuths of PS waves and the P waves forming them ($\Delta\psi$) are presented in Figure 22 as a function of ψ_2. The calculations were made for a model of a medium with v_{P2} = 5.3 km/s, v_{P1} = 3.6 km/s, v_{S1} = 1.71 km/s, K = 0.32, φ equal to 5, 10, 20, 30 and 50° and Δ equal to 10, 20, 30 and 140°. As can be seen from Figure 22, the value of $\Delta\psi$ is sign-variable. It is equal to zero at angles of ψ_2 equal to 0, 180 and 360°, reaching maximum values at ψ_2 equal to 90 and 270°. In other words, the ray azimuths of PS waves lie in the vertical plane in the plane of the dip and rise of the interface, coinciding with the azimuths of the P waves impinging on the interface. The

APPROVED FOR RELEASE: 2007/02/08: CIA-RDP82-00850R000200030043-9

APPROVED FOR RELEASE: 2007/02/08: CIA-RDP82-00850R000200030043-9

maximum deviations of the ray azimuths of refracted PS waves from ray azimuths of P waves impinging on the interface are observed along the strike of the interface. The values of these deviations will reach 70-85° with angle of inclination of the interface of $\varphi = 50°$. The values of $\Delta\psi$ increase with an increase of the angle of inclination of the interface and of the epicentral distance.

APPROVED FOR RELEASE: 2007/02/08: CIA-RDP82-00850R000200030043-9

APPROVED FOR RELEASE: 2007/02/08: CIA-RDP82-00850R000200030043-9

PART 2

THE "ZEMLYA" DEVICE, METHOD OF OBSERVATION AND INTERPRETATION OF MATERIALS

THE "ZEMLYA" DEVICE

Moscow SEYSMICHESKIYE ISSLEDOVANIYA S APPARATUROY "ZEMLYA" in Russian 1977 signed to press 31 Jan 1977 pp 54-80

[Chapter 3 from the book "Seysmicheskiye issledovaniya s apparaturoy 'Zemlya'" by I. V. Pomerantseva and A. N. Mozzhenko, Izdatel'stvo Nedra, 1,400 copies, 256 pages]

[Text] The Main Characteristics of the Optimum Design of a Device for Continuous Recording of Seismic Signals

Continuous recording of seismic signals arriving at the reception point at any time of day requires a special design of recording apparatus operating for a long time without maintenance personnel. It should have sufficiently wide frequenty and dynamic ranges and have the capability of recording signals for a long time and maintaining given parameters.

These problems are being solved either by discrete recording of the useful information or by continuous recording of all seismic signals arriving at the reception point. Discrete recording of signals is accomplished either on a magnetic drum or on a magnetic tape loop, where the signals recorded on the magnetic carriers are erased at the end of a single revolution of the drum or magnetic tape loop and new information is recorded on the erased track. The useful signals are read and sent to the non-volatile storage unit before erasure. This recording system makes it possible to carry out prolonged sampling of useful information, limited only by capacity of the storage unit. One of the main disadvantages of the discrete method of recording is the difficulty of identifying the moment of arrival of signals with useful information. The known method of separating signals by amplitude-frequency features sharply limits the capabilities of this method of recording since the signals of microseism background are frequently comparable to useful signals in both frequency and amplitude. More complex systems of separating the useful information result in complication of the design and an increase of power supply consumption, which significantly worsens the technical-economic indicators as a whole.

Continuous recording of all seismic signals arriving at the observation point is technically simpler but requires continuous supplementation of the

APPROVED FOR RELEASE: 2007/02/08: CIA-RDP82-00850R000200030043-9

APPROVED FOR RELEASE: 2007/02/08: CIA-RDP82-00850R000200030043-9

information carrier. In the case when the information carrier can be restored and used again after laboratory sampling of the useful information, the continuous method of recording seismic signals is sufficiently effective.

Seismic signals are recorded continuously on magnetic tape for 100 hours or more in the "Zemlya" apparatus complex. Frequency recording in the band of 0.5-15 Hz is provided at magnetic tape speed of 1 mm/s. Accelerated speed of the magnetic tape is used during reproduction of the recorded signals [84]. In this case the emf and frequency of the reproduced signal are increased in proportion to this acceleration.

The use of this phenomenon made it possible to use direct magnetic recording to record infralow frequencies without introduction of any modulation methods. The use of some type of modulation is based on the use of an auxiliary high-frequency signal which varies its parameters as a function of variation of the frequency of the recorded low-frequency signal. The auxiliary signal should have a frequency tens of times higher than the recorded frequency in all types of modulation recordings. If the recorded signal is limited by a frequency of 20Hz, the auxiliary signal will be within the range of 400-800 Hz. In this case signal recording will be provided at a magnetic tape speed of 10-12 mm/s when using magnetic heads with working gap width of 10 microns. This magnetic head provides direct signal recordings at magnetic tape speed of 0.25-0.3 mm/s. Variation of the frequency of the reproduced signal (frequency transformation) permits conversion of the superlow frequencies of the recorded signals to the seismic prospecting frequency band of reflected waves. This makes it possible to utilize standard seismic prospecting apparatus for subsequent information processing both in analog and in discrete variants.

Block-Diagram of Apparatus for Continuous Recording of Seismic Oscillations

A block-diagram of a device having all the necessary components for continusou recording of seismic oscillations for a long time is presented in Figure 23. A group of seismic receivers 1 is connected by a calibration device 2 to the inputs of seismic signal amplifiers 3. The calibration device 2 transmits a series of signals to the seismic detectors and amplifier inputs at given time intervals, which makes it possible to determine the parameters of the recording channels during reproduction.

The outputs of amplifiers 3 are loaded by magnetic recording heads 4, the number of which is determined as a function of the number of working channels and required two auxiliary magnetic heads which record time signals taken from the output of the radio receiver 8 and quartz frequency standard 5. The radio receiver receives time signals transmitted by a special ratio station 18 or by some other radio station. Time signals from the internal quartz frequency standard 5, which are individual for each recording station, are recorded on the second magnetic head. The time signals received by the radio receivers turned to a single transmitting radio station are reference signals for the entire recording network and are usually tied to world time

APPROVED FOR RELEASE: 2007/02/08: CIA-RDP82-00850R000200030043-9

APPROVED FOR RELEASE: 2007/02/08: CIA-RDP82-00850R000200030043-9

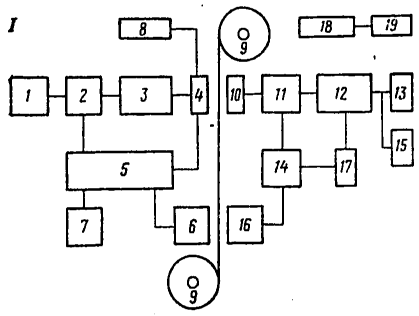

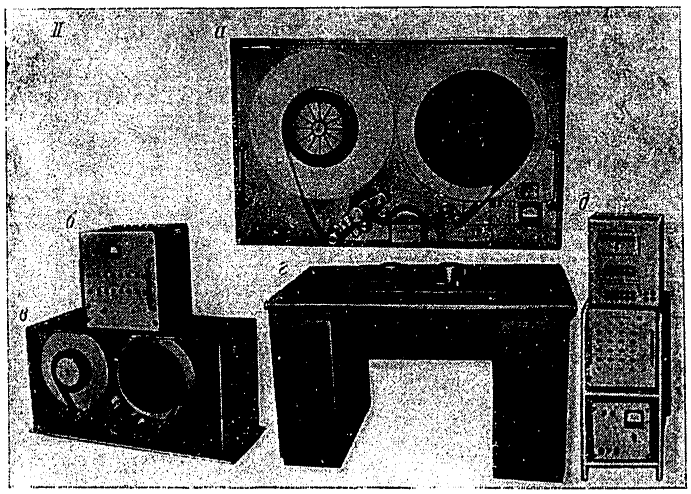

Figure 23. Block-Diagram of Device for Continuous Recording of Seismic Oscillations (I) and Overall View of "Zemlya" Station (II):

1--seismic detectors; 2 and 11--calibration device for recording and reproduction; 3 and 12--recording and reproduction amplifiers; 4 and 10--magnetic head unit for recording and reproduction; 5 and 14--quartz recording and reproduction frequency station; 6 and 16--tape-feed mechanism; 7 and 17--power supply batteries; 8--time-marker radio receiver; 9--magnetic tape; 13--recording galvanometers; 15--monitoring the magnetic tape speed; 18--radio station; 19--quartz clocks

APPROVED FOR RELEASE: 2007/02/08: CIA-RDP82-00850R000200030043-9

APPROVED FOR RELEASE: 2007/02/08: CIA-RDP82-00850R000200030043-9

(GMT). The quartz frequency standard 5 is a signal source with stable frequency. It is designed to supply power to the synchronous tape-feed mechanism 6 and to create a high-frequency magnetizing field in the magnetic recording heads 4. The tape-feed mechanism 16 sets the magnetic tape 9 into motion at the same speed in the reproduction device according to the frequency signal triggered in the quartz frequency standard 14. The magnetic reproduction heads 10, equal in number to the recording heads, are connected to the amplifier inputs 12 through calibration circuits 11. Each amplifier 12 is loaded by several filter-amplifiers with different bandpasses.

Table 5. Parameters of "Zemlya" "Zemlya-73" and "Zemlya-75" Devices

Параметры (1)	(2) «Земля»	(3) «Земля-73»	(4) «Земля-75»
(5) Полевой регистратор (рис. 23, *II*, *а*)			
Число каналов (6)	4	(7) 4 на двух уровнях усиления	8
Динамический диапазон, дБ (8)	40—42	40—70	42—44 на 8 каналах (9) 74—75 на 4 каналах (10)
Частотный диапазон, Гц (11)	0,5—12	0,5—15,0	0,35—15,0
Тип магнитной пленки (12)	6	6; 10	6; 10; Сигма (13)
Ширина магнитной пленки, мм (14)	35	35	25,4
Длина рулона магнитной пленки, м (15)	1000	1000	1000
Потребляемая мощность аккумулятора, Вт (16)	20	10	8
Тип сейсмоприемника (17)	ВЭГИК «Земля» (18)	ВЭГИК «Земля», НСП-3 (19)	Трехкомпонентная установка, разработка ВНИИГеофизики (20)
Сопротивление входа усилителя, кОм (21)	240	1000	1500
Скорость движения магнитной пленки, мм/с (22)	1,25—3	1	1
Стабильность средней скорости движения пленки, % (23)	5	0,01	0,01
Марки времени от собственного датчика времени (24)	(25) 1 с; (26) 1 мин; (27) 1 ч	0,2 с; 1 с; 1 мин	0,2 с; 1 с; 1 мин
Внешний датчик времени (радиоканал) (28)	Нет (29)	(30) Есть	Есть
Калибратор канала записи, работающий в автоматическом режиме (31)	(32) Нет (калибровка в момент пуска и остановки регистратора)	(33) Есть (калибровка тракта усиления и сейсмоприемников)	Есть (калибровка тракта усиления и сейсмоприемников)
Масса полевого регистратора без сейсмоприемников, кг (34)	35	21	15

[Continued on following page]

APPROVED FOR RELEASE: 2007/02/08: CIA-RDP82-00850R000200030043-9

APPROVED FOR RELEASE: 2007/02/08: CIA-RDP82-00850R000200030043-9

Table 5. (Continued)

Станция обзорного воспроизведения (рис. 23, *II*, *б*, *в*)

Число одновременно воспроизводимых магнитных лент (36)	1	2	2
Скорость воспроизведения, мм/с (37)	50—100	100	100
Полоса воспроизводимых частот, Гц (38)	25—600	50—1000	50—1000

Станция основного воспроизведения (рис. 23, *II*, *г*, *д*) (39)

Число фильтровых каналов, подключенных к одному основному каналу (40)	5	5	4
Полоса воспроизводимых частот, Гц (41)	5—600	7,5—600	7,5—600
Скорость движения магнитной пленки, мм/с (42)	10; 20; 30; 40; 50	15; 20; 30; 40	15; 20; 30; 40
Минимальный воспроизводимый сигнал, мкВ (43)	0,25	0,5	0,5
Автоматика для запуска осциллографа (44)	Нет	Есть	Есть

Key:

1. Parameters
2. "Zemlya"
3. "Zemlya-73"
4. "Zemlya-75"
5. Field recorder (Figure 23, 2,a)
6. Number of channels
7. 4 at two amplification levels
8. Dynamic range, dB
9. On 8 channels
10. On 4 channels
11. Frequency range, Hz
12. Type of magnetic tape
13. Sigma
14. Width of magnetic tape, mm
15. Length of magnetic tape reel
16. Consumed power of storage battery, W
17. Type of seismic detector
18. VEGIK "Zemlya"
19. VEGIK "Zemlya," NSP-3
20. Three-component installation developed by VNIIGeofizika
21. Amplifier input resistance, kohms
22. Magnetic tape speed, mm/s
23. Stability of average tape speed, percent
24. Time marks from internal time sensor
25. Seconds
26. Minutes
27. Hours
28. External time sensor (radio channel)
29. No
30. Yes
31. Recording channel calibrator operating in automatic mode
32. No (calibration at moment of starting and stopping recorder)
33. Yes (calibration of amplification and seismic detector channel)
34. Mass of field recorder without seismic detectors, kg
35. Survey reproduction station (Figure 23, 2, b and c)
36. Number of simultaneously reproduced magnetic tapes
37. Reproduction speed, mm/s
38. Band of reproduction frequencies, Hz

[Key continued on following page]

APPROVED FOR RELEASE: 2007/02/08: CIA-RDP82-00850R000200030043-9

APPROVED FOR RELEASE: 2007/02/08: CIA-RDP82-00850R000200030043-9

[Key continued from preceding page]

39. Main reproduction station (Figure 23, 2, d and e)
40. Number of filter channels connected to a single main channel
41. Band of reproduction frequencies, Hz
42. Magnetic tape speed, mm/s
43. Minimum reproduced signal, μV
44. Automatic device for starting oscillograph

This block-diagram of the recording-reproduction device was proposed in 1958 [85] and achieved further development in the "Zemlya" apparatus complex. A number of additional devices: survey reproduction and an analog apparatus for correlation re-recording, was subseqeutnly introduced into the device to accelerate the process of separating the signals recorded on magnetic tape. The parameters of the different versions of the "Zemlya" device are given in Table 5.

The Field Recorder

The field recorder is a self-contained design which accomplishes prolonged recording of seismic signals (see Figure 23, 2, a). The main technical parameters of the field recorder are presented in Table 5.

The seismic detector. Three or four seismic detectors are installed as a function of the recording conditions at the recording amplifier input. VEGIK or NSP-3 seismic detectors are mainly used. Both seismic detectors are pendulum type devices and the overall dimensions and mass of the VEGIK device is approximately 1.5 times greater than those of the NSP-3, while their sensitivity is approximately identical.

The advantages of the devices should include their design simplicity and the capability of repair and tuning under field conditions. The disadvantage of the NSP-3 seismic detector is the absence of adjusting screws to change the inclination of the device in the horizontal state. The overall disadvantage of pendulum type devices is the significant path of the vertical pendulum due to temperature effects. This path reaches 1 mm at 10°C in the VEGIK device. The path of the vertical pendulum in the NSP-3 seismic detector should be compensated for by a special bimetal plate-spring, but this system, which requires careful selection of the spring material and the corresponding temperature path of the plate-temperature regulator, usually operates unstably.

O. I. Kovalev recently developed a seismic detector specially for the "Zemlya" device which utilizes a forward-return system where the working coil, which is the pendulum, is suspended on two iris, flat springs rather than on a lever suspension. In this case the coil can be moved in the magnetic field along a straight line rather than around the circumference, which makes it possible to achieve a greater path of it in the magnetic system. Expansion

APPROVED FOR RELEASE: 2007/02/08: CIA-RDP82-00850R000200030043-9

APPROVED FOR RELEASE: 2007/02/08: CIA-RDP82-00850R000200030043-9

of the temperature range is achieved by this, even if the pendulum has a temperature path of the VEGIK or NSP-3 devices. The electromechanical coupling coefficients (KEMS) and some technical data of seismic detectors are presented in Table 6.

Table 6

Тип сейсмоприемника (1)	Сопротивление, кОм (2)	КЭМС, В·м/с (3)	Температурный ход, градус/мм (4)
ВЭГИК (5)	2	140	±0,1
НСП-3 (6)	2	120	±0,1
Возвратно-поступательный, (7) 1975 г.	18	500—600	Не установлен (8)

Key:
1. Type of seismic detector
2. Resistance, kohms
3. KEMS, V·m/s
4. Temperature path, degrees/mm
5. VEGIK
6. NSP-3
7. Forward-return
8. Not installed

When conducting field operations, the seismic detectors are turned to a frequency of 1Hz, which is maintained within a range of ± 5 percent. The natural frequency of the pendulum is monitored by means of the recording channel calibrator.

Calibration recording device. The calibrator in the "Zemlya" device is designed for systematic monitoring of the amplification level of the recording amplifier, sensitivity and the natural frequency of the seismic receivers. The calibrator may operate in the automatic mode and may also be switched on by maintenance personnel. A diagram which explains the operating principle of the device is presented in Figure 24.

There is brief closing of contact K5, by means of which the time relay T_{30} and T_{60} is started, during movement of the magnetic every 12-15 hr. Contact K5 is closed either from a mechanical reducer operating from the tape-feed system or from a photorelay triggered when light penetrates through holes punched in the magnetic tape.

The time relay T_{30} switches on and maintains the commutation relays P1 and P4 for 30 seconds, while relay P_{60} contraols the coils of relays P2 and P3 with duration of switching on current of 60 seconds. The time relay circuit is set to the initial position and is ready for the next cycle after 60 seconds. Since time relays T_{30} and T_{60} are switched on simultaneously, relays P1-P4 switch on the corresponding contacts K1-K4. At this moment the seismic detector winding L1, previously connected to the recording amplifier input, is connected by resistor K3 and contact K1 to a stable direct current voltage source (U_{st}). The current occurring in the coil circuit L1 deflects it from the equilibrium point by the given angle. If the number of turns of

APPROVED FOR RELEASE: 2007/02/08: CIA-RDP82-00850R000200030043-9

APPROVED FOR RELEASE: 2007/02/08: CIA-RDP82-00850R000200030043-9

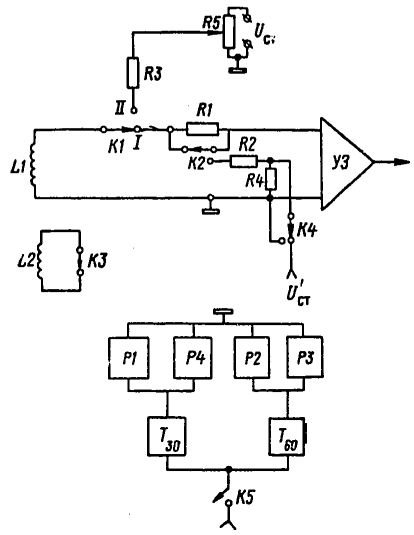

Figure 24. Block-Diagram of Calibrator of "Zemlya" Recording Channel:
L1--working coil of seismic receiver; L2--damping coil of seismic detector; U_{st}--stabilized direct voltage for deviation of seismic detector pendulum; U'_{st}--stabilized alternating voltage at frequency of f = 1 Hz; P1-P4--commutation relays; K1-K4--contacts of commutation relays; K5--starting contact of time relay

the coils, magnetic fields of the magnetic systems and the current admitted to the coil windings are identical in all the monitored seismic detectors, the angle of deflection of the coils will also be identical. A voltage divider with ratio of 1:100 is created by means of resistors R1 and R2 and a signal stable in voltage with frequency of 1 Hz is taken from resistor R4 through contact K4. A signal with frequency of 1 Hz and with strictly defined (150 μ V) and stabilized value in all the field recorders is fed to the amplifier inputs during the first period with duration of 30 seconds. The windings of coil L1 is connected to voltage divider R1 or R2 and the voltage of the monitored signal is deflected with frequency of 1 Hz 30 seconds after relays P1 and P4 are switched off. During the next 30 seconds, until relays P1 and P3 are switched off, a signal attenuated by a factor of 100 is fed from the coils of slowly attenuating seismic detectors to the recording amplifier inputs. The accuracy of adjusting the seismic detector pendulums, their freedom of movement and the relative sensitivity of the devices are established by recording this process. All these operations can be carried out by an operator without the use of automatic equipment. The possibility of visual monitoring of the amplification level and the process

APPROVED FOR RELEASE: 2007/02/08: CIA-RDP82-00850R000200030043-9

APPROVED FOR RELEASE: 2007/02/08: CIA-RDP82-00850R000200030043-9

of moving the seismic detector pendulum by different voltage levels of the field recorder circuit is also provided in the circuit.

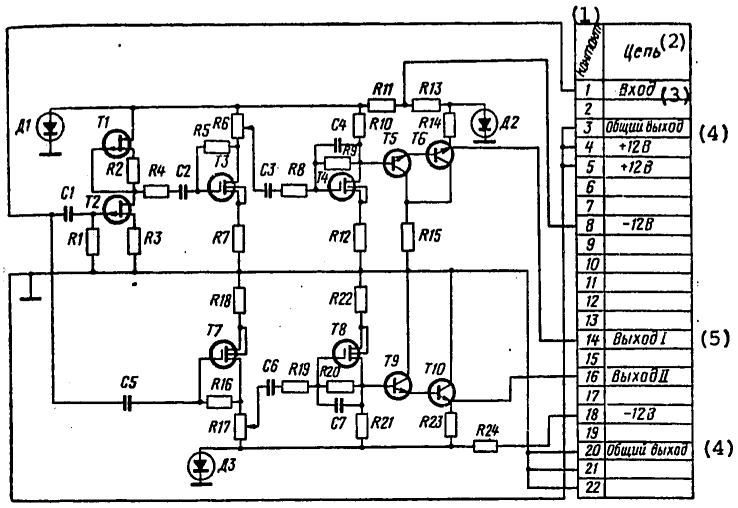

Figure 25. Recording Amplifier:
Resistors: R1-1 mohms; R2 and R3-- 1 kohm; R4--270 kohms; R5--2 mohms; R6--22 kohms; R7--2.4 kohms; R8--360 kohms; R9--3.6 mohms; R10--62 kohms; R11--270 kohms; R12--3.3 kohms; R13--150 kohms; R14--820 kohms; R15--430 kohms; R16--2 mohms; R17--22 kohms; R18--2.4 kohms; R19--360 kohms; R20--3.6 mohms; R21--62 kohms; R22--3.3 kohms; R23--820 kohms; R24--150 kohms; Capacitors: C1-C3--1 mF; C4-C7--0.1 mF; Transistors: T1 and T2--KP-103E; T3, T4, T7 and T8--KP-301P; T5, T6, T9 and T10--MP-113A; D1-D3--D-81 Stabilitrons

Key:
1. Contact
2. Circuit
3. Input
4. Common output
5. Output

The recording amplifier. The signals from the seismic detector winding enter the recording amplifier inputs through the KIP [Monitoring and measuring device] circuits. The recording amplifiers are designed to amplify the seismic detector signals and to create the corresponding current in the winding circuit of the magnetic recording head. Various types of amplifiers were used in field "Zemlya" recorders. Let us consider one of the recent circuits of transistorized amplifiers with two amplified signal output levels (Figure 25).

APPROVED FOR RELEASE: 2007/02/08: CIA-RDP82-00850R000200030043-9

APPROVED FOR RELEASE: 2007/02/08: CIA-RDP82-00850R000200030043-9

The seismic detector signal is transmitted to the input of transistors T2 and T7 through capacitors C1 and C5. Transistor T2 is the lower arm of the amplifier with dynamic loading (T1 and T2). The amplified signal is fed to the gate of transistor T3 through resistor R4 and capacitor C2, is amplified and is fed to the input of active filter T4 through resistor R8 and capacitor C3. The signal taken from the channel of transistor T4 is fed to the winding of the magnetic recording head by means of the compound emitter repeater T5 and T6. This part of the amplifier is designed to amplify signals from 5 to 500-600 μV and is called a highly sensitive amplifier.

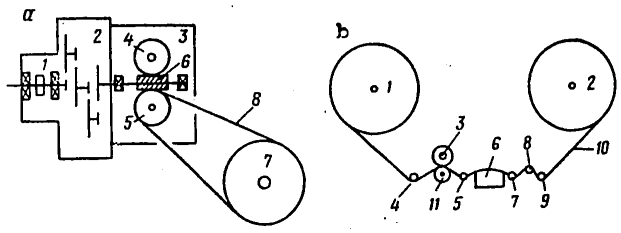

Figure 26. Diagram of Field Recorder Tape-Feed Mechanism: a--diagram of tape-feed reducer and drive: 1--SD-54 synchronous motor; 2--gear reducer of SD-54 motor (retardation of 1:137); 3--"Zemlya" worm reducer; 4--drive shaft worm gear; 5--worm gear of winding subassembly; 6--worm shaft connected to reducer output shaft; 7--winding device of take-up cassette; 8--rubber drive of tape-up cassette (plastic); b--overall kinematic diagram: 1--take-up cassette; 2--feed cassette; 3--pressure roller; 4, 5 and 7-9--guide pins; 6--magnetic head block; 10--tape; 11--driveshaft

The signal entering the input of resistor T7 through capacitor C5 is amplified 30-35 times less since there is no preamplification stage in this part of the amplifier. The remaining part of the circuit is similar to that of the highly sensitive amplifier. This amplifier is called a low--sensitive amplifier and is designed to amplify signals with voltage from 160 to 16,000 μV. Thus, using two amplifiers with a single common input, one can record signals up to 70 dB.

Correction of high-frequency signals with steepness of right-hand cut-off of 6 dB/octave is provided in the amplifier.

The tape-feed mechanism. The amplified signals of the seismic detector are fed to the recording head windings. The magnetic tape is set into continuous motion at a speed of 1 mm/s by means of the tape-feed mechanism. The forward motion of the magnetic tape is accomplished by a single-motor two-cassette version of the tape-feed mechanism. The tape-feed mechanism (Figure 26) is set it motion by a synchronous motor 1 through reducers 2 and 3 with reduction

APPROVED FOR RELEASE: 2007/02/08: CIA-RDP82-00850R000200030043-9

APPROVED FOR RELEASE: 2007/02/08: CIA-RDP82-00850R000200030043-9

of the number of revolutions by a factor of 1,500. Worm gears 4 and 5 are installed at the reducer output. Gear 4 sets the driveshaft in motion and gear 5 sets the take-up cassette in motion through a rubber pulley. Mechanical separation of the forces of the motor between the shaft and the winding device by means of worm gears makes it possible to use a single motor to feed the tape and to wind it onto the take-up cassette without transfer of jolts of the take-up cassette to the capstain. Electric power is supplied to the synchronous motor by means of a power amplifier which emits a signal with frequency of 50 Hz at the output.

A similar power amplifier for supplying power to the magnetic head high-frequency magnetization circuits emits a voltage with frequency of 2,500 Hz. Both the power amplifier of the synchronous motor and the high-frequency amplifier are controlled by heavy-current voltage in frequency taken from the outputs of the quartz frequency standard.

Time marking. Quartz with a resonance frequency of 10 kHz stabilizes the generator oscillation, the signal from whose output is fed to the flip-flop counting device. Signals with frequency of 2,500, 50, 5, 1 and 1/60 Hz are taken from the given device. Signals with frequency of 2,500 and 50 Hz control the operation of the power amplifier, while signals with frequency of 5, 1 and 1/60 Hz are applied to the magnetic tape by means of the time marker magnetic head and are marking signals with scale division of 0.2 and 1 second and 1 min, respectively. The given type of time marking has been called internal marking. This marking is inadequate during group operation of a system of field recorders and it becomes necessary to achieve unified time marks at all recording stations and to tie them in to unified world time. There is an additional magnetic time head in the field recorder by means of which signals for tying to absolute time can be introduced into the magnetic recording.

Device for Unified Time Marking of Field Recorders (Radio Channel)

Individual field recorders located in the area of investigation are sections of a multichannel seismic station in which the coupling element is time marks. As was already noted, two service channels have been allocated in the field recorder for time marks. One of them records the time pulses from the internal time sensor and the other is used to record the time signals, unified for all the field recorders.

The internal time sensor emits pulses every 0.2 and 1 second and 1 min. The second and minute time marks are distinguished by the amplitude of the recorded signals. With regard to the fact that the quartz frequency standard of the field recorder is not thermally stabilized, the path of its frequency due to temperature comprises $3 \cdot 10^{-6}$ per $\pm$ 1°C. A number of precise time transmission circuits by radio (Figure 27) is used to tie the internal time sensors to unified world time. The most convenient and accurate is the circuit (Figure 27, a) where the radio receiver 3 emits signals upon instructions from the time device 4. Unlike the device of the internal time mark

APPROVED FOR RELEASE: 2007/02/08: CIA-RDP82-00850R000200030043-9

APPROVED FOR RELEASE: 2007/02/08: CIA-RDP82-00850R000200030043-9

channel of the field recorder, the amplitude system of separating the time intervals is unsuitable here. This is related mainly to the desire to operate the radio transmitter in kilograph mode at maximum power. Half-second intervals, minute, hourly and daily signals are separated in transmission of time signals by radio by means of admission of several half-second pulses. Thus, a minute is noted by a pause of 2-2.5 seconds, the hour marker is noted by a pause of 30 seconds and the daily intervals are noted by combination admission of a number of seconds at some time intervals. Continuous recording of time signals on paper tape is carried out to maintain the coding signals and those for monitoring the operation of the radio channel at the radio center. Automatic recording voltmeters, for example, the N-379, are used for this purpose. The recording speed is selected within the range of 0.1-0.2 mm/s.

A radio receiver (Figure 28) which is assembled on microcircuits U1-U3 and transistors T1-T5 and which has real sensitivity of 2.5-3 μV, is installed in the field recorder. The signal taken from the antenna is amplified by two high-frequency stages L2 and L4 and is fed to the input of the frequency converter U1, in which the intermediate frequency of 465 kHz, which is the difference frequency between the signal of the first heterodyne stabilized by crystal oscillator E1 and the radio transmitter signal, is separated. The bandpass is constricted upon passage of the signal through the piezoceramic filter F, from whose output the signal is fed to the input of amplifier U2. The signal is detected at the output of circuit L6 by means of diode D2. The signal is also separated here with frequency of 1 kHz, achieved as a result of adding the frequencies of 465 kHz and 464 kHz. The separated signal is amplified by amplifier U3 and is fed to the filter input (L7 and T4) with frequency of 1,000 Hz. The signal is fed from the filter output to transistor T5 and is introduced into the field recorder circuit through capacitor C35. With regard to the fact that the signal with frequency of 1,000 Hz cannot be recorded in the field recorder, the given signal is detected and its initial and final fronts are recorded.

The radio channel time sensor is strictly monitored by the accurate time signals and is connected to GMT time. This unified time system can be used where it is economically justified and advantageous. If 5-10 field recorders are operating, the use of this type of radio channel is difficult due to the need to allocate a special radio detachment working continuously. Therefore, one should recommend the use of a number of circuits selected by the technical capabilities of the executors and suitable for the region of investigations.

A circuit which utilizes accurate time signals transmitted by the "Mayak" radio station is presented in Figure 27, b. The given stations are heard over almost the entire territory of the USSR and emit an hourly time check with transmission of six precise time signals at signal frequency of 1,000 Hz. The second heterodyne (T3E2) is disconnected in the radio receiver for this purpose (see Figure 28) and the frequency of circuit L1 and C3 and of crystal oscillator E1 should correspond to the frequency of the "Mayak" radio station. The filter with frequency of 1,000 Hz will separate the time

APPROVED FOR RELEASE: 2007/02/08: CIA-RDP82-00850R000200030043-9

APPROVED FOR RELEASE: 2007/02/08: CIA-RDP82-00850R000200030043-9

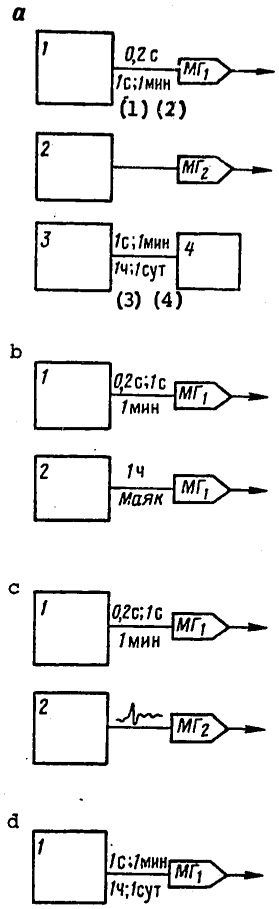

Figure 27. Diagram of Time Mark Signal Transmission and Recording:
a--diagram of radio channel with self-contained transmitter; b--diagram of hourly time signal reception from "Mayak" radio station; c--diagram of signal reception from any radio broadcast station; d--diagram of marking channel with heavy-current time sensor; 1--time sensor of "Zemlya" stations; 2--radio receiver of time marks; 3--radio transmitter; 4--time sensor; MG_1 and MG_2--magnetic recording heads

Key:
1. Second
2. Minute
3. Hour
4. Day

APPROVED FOR RELEASE: 2007/02/08: CIA-RDP82-00850R000200030043-9

APPROVED FOR RELEASE: 2007/02/08: CIA-RDP82-00850R000200030043-9

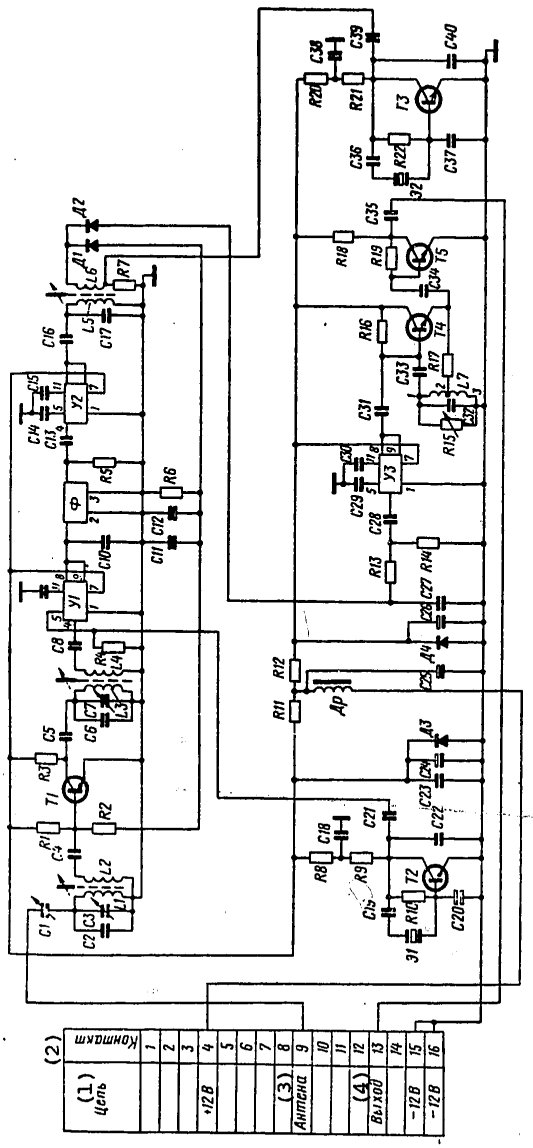

Figure 28. Time Mark Radio Receiver:

L1-L4--high-frequency circuit; L5 and L6--intermediate frequency circuit; L7--coil of 1,000-Hz filter; Dr--noise filter choke; F--PF1P-2 filter; E1 and E2--crystal vibrators; resistors: R1--120 kohms; R2--5.8 kohms; R3--4.7 kohms; R4--5.6 kohms; R5--1.2 kohms; R6--4.7 kohms; R7--270 kohms; R8--3.0 kohms; R9--20 kohms; R10--5.6 kohms; R11 and R12--91 kohms; R13--1 kohm; R14--6.8 kohms; R15--15 kohms; R16--62 kohms; R17--390 kohms; R 18--1.2kohms; R19--82 kohms; R20--3 kohms; R21--20 kohms; R22--5.6 kohms; capacitors: C1--3-20 pF; C2--130 pF; C3--3-20 pF; C4--2,200 pF; C5--30 pF; C6--132 pF; C7--3/20 pF; C8--2,200 pF; C9--100 pF; C10--2,200 pF; C11--0.047 F; C12--10 mF; C13--82 pF; C14--3,300 pF; C15--0.33 pF: C16--240 pF; C17--510 pF; C18--3,300 pF; C19-C22--300 pF; C23--0.047 mF; C24--20.0 mF; C25 and C26--5.0 mF; C27--68,000 pF; C28--5.0 mF; C29--10.0 mF; C30--0.33 mF; C31--0.047 mF; C32--0.1 mF; C33--0.33 mF; C34--0.0047 mF; C35--10.0 mF; C36-C40--300 pF; C41--10.5 mF; D1, D2 and D5--D9D diodes; D3 and D4--D-810 stabilitrons; transistors: T1-T3--KT-316-D; T4 and T5--MP-113A; microcircuits: U1--1UB221; U2 and U3--1US-221

Key:
1. Circuit 2. Contact 3. Antenna 4. Output

APPROVED FOR RELEASE: 2007/02/08: CIA-RDP82-00850R000200030043-9

APPROVED FOR RELEASE: 2007/02/08: CIA-RDP82-00850R000200030043-9

check signals and will effectively suppress all signals differing from the given frequency.

There are regions where the "Mayak" radio station operates irregularly, changes frequency during the day or is generally not heard. In this case one can recommend the circuit presented in Figure 27, c and almost similar to the circuit shown in Figure 27, b. Its main difference is that the radio receiver is tuned to any continuously operating radio station. In this case the modulation signals, close to or equal to frequency of 1,000 Hz, will penetrate the filter and be recorded on the magnetic tape of the field recorder. Due to the fact that all the radio receivers are tuned to a single radio station and the filters have identical bandpass, the shape of the recorded signals will be identical on all the field recorders. The precise time signals transmitted 1-2 times per day have a typical shape and are easily distinguishable on summary seismograms. Further identification of the modulation signals and time tying of the seismic signals present no difficulties, but require more time than in the case of using a self-contained radio channel. If the radio transmitting station does not emit time check signals, then one may, having two additional radio receivers and an automatic recording voltmeter (for example, the N-379), periodically record the precise time signals from another transmitting radio station with simultaneous recording of the modulation curve recorded by the field recorders. In the other case, this periodic tying of the modulation signals to the precise time signals is possible on the fourth working channel of the field recorder where the signal from the radio receiver tuned to the radio station transmitting the precise time signals is transmitted.

If it is possible to provide the corresponding accuracy of the course of the hours, one can use the circuit presented in Figure 27, d. Here the signals from the quartz clocks coming to the counting device which separates the second, minute, hour and day time intervals, are recorded on a single channel. The clocks can maintain the necessary accuracy of the rate if the corresponding temperature conditions are provided. The time signal on all the field recorders will be identical within the rate tolerances if starting of the clocks is synchronized. The given time sensor circuits may be the main ones in precise time storage with development of integrated electronics. The difference of heavy-current time sensors from the quartz frequency standard of the "Zemlya" field recorder is the use of heavy-current quartz stabilizers and a thermostat with temperature stability within the range of $\pm$ 0.2°C.

Field Recording Reproduction Apparatus

As already noted, the main characteristic of the "Zemlya" apparatus complex is the use of the principle of frequency transformation, achieved by accelerated motion of the magnetic tape with respect to the recording. An increase of the speed during magnetic recording reproduction is dictated by the need to raise the level of amplification of the read signal and conversion of ultra-low frequencies (0.5-15 Hz) to frequencies convenient for amplification and visualization by means of ordinary seismic prospecting apparatus.

APPROVED FOR RELEASE: 2007/02/08: CIA-RDP82-00850R000200030043-9

APPROVED FOR RELEASE: 2007/02/08: CIA-RDP82-00850R000200030043-9

The main reproducing station. A block-diagram of a reproduction device is shown in Figure 29, a. The magnetic head block MG is connected to the inputs of amplifiers U1-U4 of the main channels and the time marker amplifiers of radio channel U5 and signal amplifier U6 (service channel amplifiers) with frequency of 5 Hz. The amplified signals of amplifiers U1-U4 are then fed to filter-amplifiers F1-F4. Amplifier F1 has four outputs connected to galvanometers G1-G4. The outputs of the filter amplifiers F2-F4 are connected to galvanometers G5-G16, respectively. The outputs of the service amplifiers U5 and U6 and loaded by galvanometers G17 and G18.

A kinematic diagram of the tape-feed mechanism is presented in Figure 29, b. The magnetic tape is moved through the magnetic head block 7 from the feed cassette 2 to the take-up cassette 1. The pressure roller 6 clamps the magnetic tape to the drive shaft 5, while the guide pins 3 and 4 restrict its lateral motion. The drive shaft is set in motion by a synchronous motor supplied by alternating current with frequencies of 25, 33, 50 and 66 Hz.

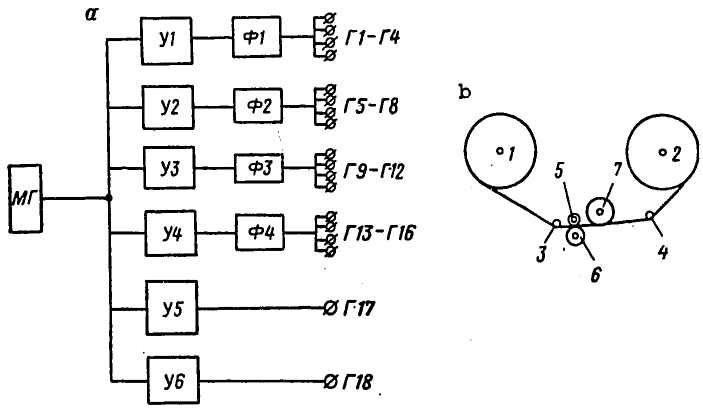

Figure 29. Block-Diagram of Reproduction Device (a) and Kinematic Diagram of Tape-Feed Mechanism (b)

The magnetic tape speed varies within the range of 15-40 mm/s according to the frequency of the synchronous motor power supply. Alternating voltage with frequency of 25 Hz can be transmitted to the amplifier inputs to calibrate the amplification level. The supplied voltage levels may vary intermittently in the range of 5-320 μV. The given voltages are equivalent to those developed in the magnetic reproduction head at signal frequency of 25 Hz.

Summary reproduction. It is extremely difficult to separate the useful oscillations directly on the magnetic tape with recording length of 3-5 days. For this purpose the "Zemlya" apparatus complex is supplied with a special device which makes it possible to summarize all the information recorded on the magnetic tape within a short time.

APPROVED FOR RELEASE: 2007/02/08: CIA-RDP82-00850R000200030043-9

APPROVED FOR RELEASE: 2007/02/08: CIA-RDP82-00850R000200030043-9

This device has been called the summary reproduction apparatus. A kinematic diagram of the tape-feed device is presented in Figure 30. The tracking path of the magnetic tape from the feed cassette 2 to the take-up cassette 1 is shown in Figure 30, a. The tape is moved along the magnetic head 5 by means of the drive shaft 6 and pressure roller 7. The guide pins 3 and 4 prevent the tape from moving laterally.

As can be seen from the diagram of Figure 30, b, two drive shafts 6 are set in motion from a single motor 3 through a worm pair 5 in the summary reproduction tape-feed device. The take-up cassette 1 is set in motion through the pulleys mounted on the axle of the drive shaft by means of a rubber capstain. Thus, the summary reproduction device permits one to simultaneously re-record two magnetic tapes installed on the feed cassettes 2. The signals are amplified by the corresponding number of amplifiers with bandpass of 50-1,-00 Hz; the transformation coefficient is K = 100. Two channels (left and right), which serve to amplify the signals of the Z components are duplicated by the filter-amplifiers having bandpass of 0.5-12.5 Hz in the recording frequency.

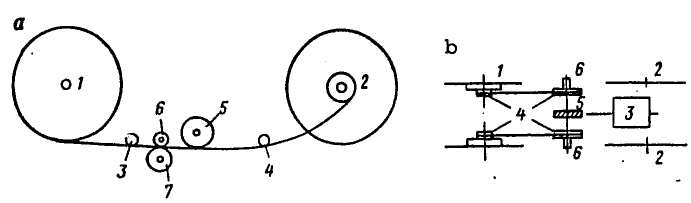

Figure 30. Block-Diagram of Tape-Feed Mechanism (a) and Kinematic Diagram of Tape-Feed Mechanism (b)

The use of these filters is necessary if there is strong microseism noise which makes the search for useful information difficult. If there is severe high-frequency noise recorded on the tape, a teflon film from 40 to 200 microns thick is applied to the magnetic heads. In this case, attenuation of the high-frequency part of the signal occurs as a result of separation of the magnetic tape from the surface of the magnetic head. The degree of attenuation depends on the ratio of the backing thickness to the length of the signal wave and is determined by the formula

$$\frac{U_2}{U_1} = 10^{-2,73d/\lambda}, \tag{3.1}$$

where U_2 is the voltage at the device output corresponding to a signal with wavelength λ, U_1 is the voltage corresponding to an infinitely large wavelength and D is the thickness of the backing filter. Attenuation (in decibels) can be calculated by the formula [99]

$$N = -54,6\frac{d}{\lambda}. \tag{3.2}$$

APPROVED FOR RELEASE: 2007/02/08: CIA-RDP82-00850R000200030043-9

APPROVED FOR RELEASE: 2007/02/08: CIA-RDP82-00850R000200030043-9

This signal filtration system has been called an air filter and is being used with great success to suppress high-frequency noise.

Frequency and Amplitude Characteristics of the Channel

Each channel of the "Zemlya" device consists of a seismic detector, field recorder amplifier, magnetic recording head, magnetic tape, magnetic reproduction head, amplifier, filter and galvanometer. All the enumerated components participate in formation of the frequency and amplitude characteristics of the channels.

The frequency characteristic of the channel. The frequency characteristic of the channel of the "Zemlya" station is made up of the frequency characteristics of all the described components and also varies from the ratio of the reproduction speed to the recording speed (K) and from use during reproduction of the air filter ("filter-backing").

The transformation coefficient permits the frequency characteristics of the channels to be shifted to the right or to the left. Therefore, it makes sense to consider the frequency characteristics of the section of the "seismograph-magnetic reproduction head" channel (Figure 31, a) and the frequency characteristics of the reproduction amplifiers (Figure 31, b) separately. The channel has a set of characteristics by means of which the signals distinguished from each other by units and even by fractions of a hertz can be confidently separated as a result of the presence of four reproduction speeds and four filters in the amplifiers. An air filter whose frequency characteristics are presented in Figure 31, a (curves I-III) is used during operations in regions with high level of high-frequency noisy background.

Amplitude characteristic of the channel. The resulting amplitude characteristic of the channel is presented in Figure 32. The maximum signal recorded with comparatively low nonlinear distortions (4 percent) and with maximum amplification of the recording stations corresponds to some generalized earthquake with magnitude of M = 5.4, epicentral distance of $\Delta = 70°$ and depth of the hypocenter of approximately 100 km (these data were obtained on the basis of 46 determinations). The minimum recorded signal is determined by the natural noise of the device and the magnetic tape (approximately 5 μV). The dynamic range of the main channel is equal to approximately 40 dB (100 times). It is natural that the lower boundary of the recorded useful signal range was determined during field recording by the microseism noisy background, which sometimes reached $(1\text{-}3) \cdot 10^{-4}$ mm on the studied areas, rather than by apparatus noise.

Method of Determining the Relative Sensitivity of the Channel

Calibration of the Device

As can be seen from the foregoing, the "Zemlya" channel consists of three separate sections: the seismic detector, recording station and reproduction

APPROVED FOR RELEASE: 2007/02/08: CIA-RDP82-00850R000200030043-9

APPROVED FOR RELEASE: 2007/02/08: CIA-RDP82-00850R000200030043-9

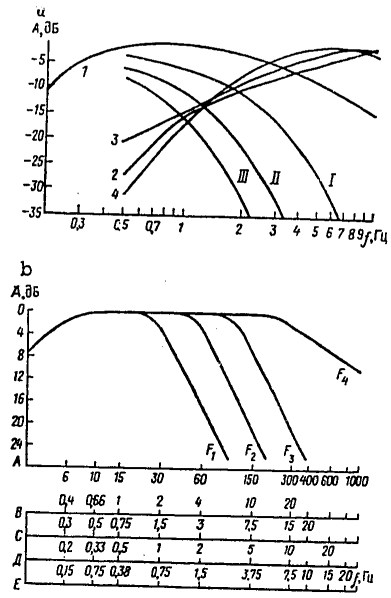

Figure 31. Frequency Characteristics of Main Channel (a) and Reproduction Channel (b) of "Zemlya" Device: 1--for recording amplifier; 2--for VEGIK seismic detector; 3--for section of "magnetic recording head-magnetic reproduction head" channel; 4--for "seismograph-magnetic reproduction head" section; I-III--for air filters with thickness of 0.12, 0.24 and 0.36 mm, respectively; F_1--filtration I; F_2--filtration II; F_3--filtration III; F_4--filtration IV (open channel); A--reproduced signal frequencies; B-E--recorded signal frequencies at K equal to 15, 20, 30 and 40, respectively

station. There may be different amplification of the recorded signals in different stations and seismographs with identical frequency and amplitude characteristics. Control signals whose level is either strictly constant (for seismic detectors and recording amplifiers) or may vary, but is always known (for reproduction amplifiers),* are fed to the inputs for systematic monitoring (calibration) and determination of the sensitivity of individual sections of the "Zemlya" channel. The overall sensitivity of the "Zemlya" channel is proportional to the amplification factors (sensitivities) of the individual sections:

---

*The channels were calibrated by A. N. Mozzhenko and V. P. Danilin.

APPROVED FOR RELEASE: 2007/02/08: CIA-RDP82-00850R000200030043-9

APPROVED FOR RELEASE: 2007/02/08: CIA-RDP82-00850R000200030043-9

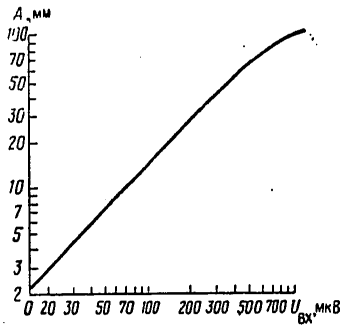

Figure 32. Amplitude Characteristic of Channel of "Zemlya" Device

$$K_к = K_c K_з K_в, \tag{3.3}$$

where K_k is the sensitivity of the entire channel; K_s is the sensitivity of the seismic detector; K_z is the sensitivity of the recording station and K_v is the sensitivity of the reproduction station.

The essence of determining the relative sensitivity of seismic detectors includes the following. A block diagram of delivery of calibration current to the winding of the seismic detector coil L1 is presented in Figure 24. Current is fed to the working windings of the seismographs from a direct-voltage source U_{st} through resistor R3, whose resistance is many times greater than that of winding L1. When current is supplied, the seismograph coil L1 is shifted by a value proportional to the KEMS:

$$a = C_1 i \mathfrak{M}, \tag{3.4}$$

where a is the bias amplitude of the seismograph coil, C_1 is the proportionality constant which takes into account the mechanical properties of the springs of the system (identical for all seismographs), i is the current in the coils from the calibration pulse and $\mathfrak{M}$ is the KEMS.

When the working coil is switched to the amplifier input, the movable system of the seismic detector makes free oscillations (with attenuation coil L2 switched off). In this case the emf at the coil output is proportional to the bias and KEMS:

$$U_{вых} = a\mathfrak{M} = C_1 i \mathfrak{M}^2. \tag{3.5}$$

APPROVED FOR RELEASE: 2007/02/08: CIA-RDP82-00850R000200030043-9

APPROVED FOR RELEASE: 2007/02/08: CIA-RDP82-00850R000200030043-9

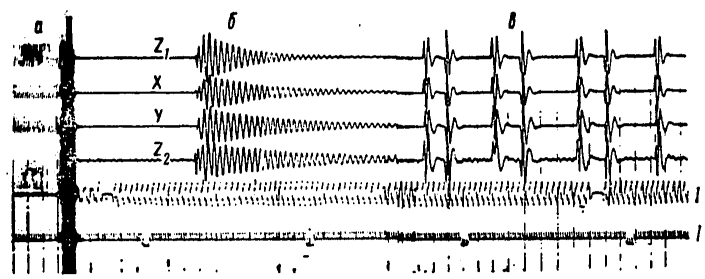

Figure 33. Oscillograms of Calibration Pulses of Reproduction Station Generator (a), Natural Processes of Undamped Seismographs (b) and Recording Station Amplifiers (c):
I--recording of pulses from contact on reproduction station capstan; II--recording of time markers from radio channel

When this process is reproduced, the deviation of the galvanometer spot A_s is proportional to U_{bykh} and to the amplification factors during recording K_z and reproduction K_v:

$$A_c = U_{вых} K_з K_в = C_2 K_з K_в \mathfrak{M}^2, \tag{3.6}$$

where A_s is the amplitude of one of the extreme values of the seismogram of free pendulum oscillations (Figure 33).

A series of single pulses or a generator signal with stable voltage (U_{st}) is fed to the amplifier input after recording the process of the seismic detectors to take into account the amplification of the station. The natural processes of the recording amplifier and of the seismic detector are reproduced on the same oscillogram with the same parameters of the reproduction station. Consequently, coefficients K_z and K_v in (3.6) can be replaced by $A_{u.z}$--the amplitude of deviation of the galvanometer when re-recording the natural process of the amplifier (Figure 33, c):

$$A_г = C_3 A_{у.з} \mathfrak{M}^2. \tag{3.7}$$

APPROVED FOR RELEASE: 2007/02/08: CIA-RDP82-00850R000200030043-9

APPROVED FOR RELEASE: 2007/02/08: CIA-RDP82-00850R000200030043-9

Hence, the sensitivity of the seismograph proportional to the KEMS in some arbitrary units is equal to:

$$K_c = \sqrt{\frac{A_c}{A_{y.s}}}. \qquad (3.8)$$

The natural processes of undamped seismic detectors are usually recorded during calibration of the recording channel--this permits systematic monitoring of their tuning frequency. The seismographs were tuned to frequency of 1 ± 0.05 Hz. Deviation of attenuation during checking the seismic detectors and recording the calibration processes are accomplished automatically at the station. However, recording the processes of normally damped seismic detectors is also provided.

The bias amplitude of the seismograph coil is controlled by the order of 200 microns, which significantly exceeds the bias caused by noise, to prevent distortions of the calibration signals by the noisy background. Voltage divider R1 and R2 reduces the total signal by a factor of 200. Because of this, the useful signal at the amplifier input corresponds to a displacement of 1 micron.

Amplification of the reproduction stations is calibrated by means of a signal from a low-frequency generator transmitted to the inputs of the reproduction amplifiers (through the voltage divider). The amplification factor of the amplifier (in conditional units) is achieved as partial amplification due to division of the output signal level to the input signal. The value of the monitoring signal can be varied from units to several tens of microvolts. Knowing the amplification factors during reproduction, one can calculate the amplification of the recording station by the amplitude of the natural process from a single pulse transmitted to the input of the recording amplifier.

Method of Processing Calibration Pulses and Construction of Correcting Amplitude Graphs

The method of processing calibration pulses A_s, $A_{u.z}$ and A_g^v is accomplished in the following manner.

Amplitudes A_s are measured by the maximum deviation of the galvanometer spot, after which attenuation of their oscillations begins (Figure 33). This is usually the fourth or fifth extreme value. The amplitudes are not taken prior to these extreme values since they correspond to oscillations of the seismic detector pendulum in the unsteady mode.

Amplitude $A_{u.z}$ is measured by the second phase. The first arrivals are also eliminated since they characterize the operation of the amplifiers in the unsteady mode. The amplitude of the extreme value of recording from the low-frequency generator A_g^v is determined as the mean value on a section of 3-5 seconds. All the amplitudes A_s, $A_{u.z}$ and A_g^v must be measured from their maximum to their minimum values.

APPROVED FOR RELEASE: 2007/02/08: CIA-RDP82-00850R000200030043-9

APPROVED FOR RELEASE: 2007/02/08: CIA-RDP82-00850R000200030043-9

All the corrections described above are introduced into the recording of each channel to compare the amplitudes of the useful signals recorded on different channels of the "Zemlya" device.

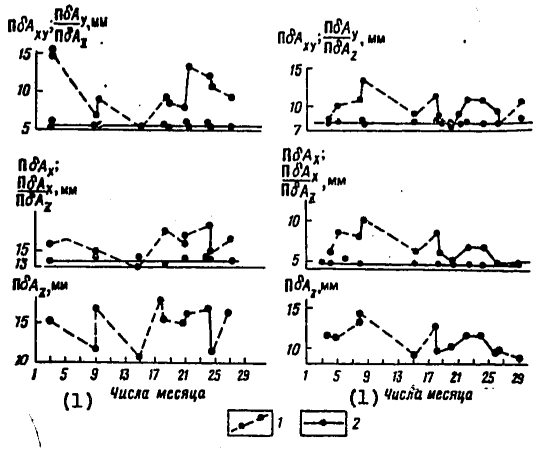

Figure 34. Amplitudes of Corrections $\Pi\delta A_{X,Y,Z}$ and Their Ratios $\Pi\delta A_{X,Y}/\Pi\delta A_Z$ on Various Dates of the Month:

1 — $\Pi\delta A_{X,Y,Z}$; 2 — $\Pi\delta A_{X,Y}/\Pi\delta A_Z$

Key:
1. Dates of month

If one denotes the amplitude of the useful recording on the Z channel by A_{PZ} and that on the X and Y channels by A_{PX} and A_{PY}, then the values of A_{PZ}, A_{PX} and A_{PY} must be separated to products of the corresponding calibration pulses, i.e., corrections must be introduced for the seismic detectors, recording station and reproduction station, to compare these amplitudes with each other. Thus, we find the following formulas:

$$\left.\begin{aligned}
(A_{PZ})' &= \frac{A_{PZ}}{\left(\frac{A_{y.з}}{A_г^в}\sqrt{\frac{A_c}{A_{y.з}}}A_г\right)_Z},\\
(A_{PX})' &= \frac{A_{PX}}{\left(\frac{A_{y.з}}{A_г^в}\sqrt{\frac{A_c}{A_{y.з}}}A_г\right)_X},\\
(A_{PY})' &= \frac{A_{PY}}{\left(\frac{A_{y.з}}{A_г^в}\sqrt{\frac{A_c}{A_{y.з}}}A_г\right)_Y},
\end{aligned}\right\} \qquad (3.9)$$

APPROVED FOR RELEASE: 2007/02/08: CIA-RDP82-00850R000200030043-9

APPROVED FOR RELEASE: 2007/02/08: CIA-RDP82-00850R000200030043-9

A_g^e is the amplitude of the extreme value from the low-frequency generator on a seismogram from an earthquake or explosion.

Having denoted the denominators of the fractions in formulas (3.9) by $\Pi\delta A_Z$, $\Pi\delta A_X$ and $\Pi\delta A_Y$, we find

$$A_{P_Z} = A_{P_Z}/\Pi\delta A_Z,$$
$$A_{P_X} = A_{P_X}/\Pi\delta A_X,$$
$$A_{P_Y} = A_{P_Y}/\Pi\delta A_Y.$$

The curves of corrections $\Pi\delta A_Z$, $\Pi\delta A_X$ and $\Pi\delta A_Y$ are presented in Figure 34. Variation of these curves* may be related to nonuniform magnetization of the tape, by variation of the storage battery voltage and so on. In those cases when the pulses were not recorded for some technical reasons, it is impossible to make a correction to the amplitudes of useful recordings by the pulse curve. In this case the correction ratio $\Pi\delta A_X/\Pi\delta A_Z$ and $\Pi\delta A_Y/\Pi\delta A_Z$ must be used.

As can be seen from Figure 34, the correction ratios for any recording station are stable over the entire period of its operation. Using the correction ratios is also justified by the fact that the effect of the difference of foci energies on them must be eliminated when studying the dynamic characteristics of PS waves from earthquakes. This is accomplished by studying the ratios of PS to P wave amplitudes.

The Nature of Oscillations Recorded by the Channel

The nature of the oscillations recorded by the channel of the "Zemlya" device was determined by the method outlined in [15, 139] for steady harmonic waves. For this purpose the amplitude-frequency characteristics of the channel were approximated by the expression

$$\alpha(f) = (2\pi f)^n, \tag{3.10}$$

where $\alpha(f)$ is the channel sensitivity at the frequency of the recorded oscillations equal to f and n is the exponent which determines the order of differentiation ($n > 0$) or integration ($n < 0$) of the signals.

At n = 0, the signal is recorded by the device without distortions.

The formula

$$n(f) = \frac{\lg \frac{\alpha(f_{i+1})}{\alpha(f_i)}}{\lg \frac{f_{i+1}}{f_i}}, \tag{3.11}$$

* These variations of the curves were observed at "Zemlya-66" stations and were completely eliminated at "Zemlya-73" stations.

APPROVED FOR RELEASE: 2007/02/08: CIA-RDP82-00850R000200030043-9

APPROVED FOR RELEASE: 2007/02/08: CIA-RDP82-00850R000200030043-9

was used to calculate the values of n as a function of f for channels of "Zemlya" stations at different filtrations and recording transformation coefficients and also for the VEGIK seismic detector (Figure 35). It was determined as a result of calculations that the channel of the "Zemlya" device records the displacement (table-like parts of the characteristics), velocity, acceleration and one-third the product (the left side of the amplitude-frequency characteristic) and also integrates the signals (the right side of the amplitude-frequency characteristic). The capability of changing the frequency band with small spacing, existing in the device, by selecting different frequency characteristics and transformation coefficients permits one to select the region of amplitude of the frequency characteristics for each wave where its displacement will be recorded. For example, one must use K_{tr} = 20 (filtration I) to find the displacement due to waves with visible frequency of 0.8 Hz; one should use filtration II for waves with frequency of 1.2 Hz at the same value of K_{tr} = 20 and so on.

The values of the soil displacements by wave recordings from explosions and earthquakes, recorded by the "Zemlya" device, can be determined by the empirical formula derived during the operations:

$$a = \frac{A_c U_r}{A_r BC},$$

where a is the soil displacement in microns, A_s is the amplitude of the reproduction generator calibration signal in mm, U_g is the reproduction generator signal voltage in microvolts, B is the signal transfer coefficient from the recording amplifier input to the reproduction amplifier input and C is the signal at the seismic detector output during soil displacement equal to 1 micron on a frequency of 1 Hz per μV.

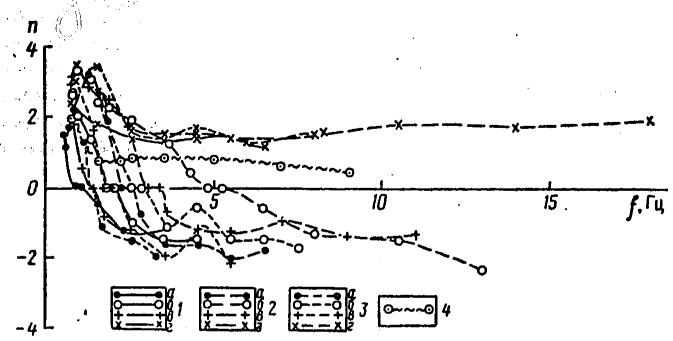

Figure 35. Curves of Function n(f) for Channels of "Zemlya" Device (1-3) and for VEGIK Seismograph (4): 1--K = 21.5; 2--K = 15; 3--K = 7.5; a--filtration I; b--filtration II; c--filtration III; d--filtration IV

APPROVED FOR RELEASE: 2007/02/08: CIA-RDP82-00850R000200030043-9

APPROVED FOR RELEASE: 2007/02/08: CIA-RDP82-00850R000200030043-9

If the signal frequency differs from 1 Hz, the multiplier C_F determined by the frequency characteristics of the channel as the ratio of the single pulse amplitude at frequency of 1 Hz to the amplitude at frequency F, must be introduced to determine the soil displacement. The extent of displacements by the waves recorded by the "Zemlya" stations is determined under stationary conditions. We checked it in 1968-1970 when setting up the "Zemlya" recording stations at locations of seismological stations of the Central Institute of Physics of the Earth of the German Democratic Republic Academy of Sciences. Kirnos M-III seismographs were located simultaneously at the same spot. The following parameters of the recording apparatus were established when measuring the soil displacements at a frequency of 1 Hz: 1) $K_s = 300$ μV/micron; 2) $K_{u.z} = 1$ μA/μV; and 3) B = 0.4 at $K_{tr} = 20$.

Comparison of the extent of soil displacement (by P waves) from a number of earthquakes obtained by using the Kirnos M-III seismographs and the "Zemlya" device showed their good agreement with a correlation coefficient close to unity.

Checking the Apparatus Before the Beginning and During Field Operations

Seismograms are obtained prior to the beginning of field operations and the following graphs are constructed: a) the frequency characteristics of the seismic detectors used; b) seismograms with attenuation of the seismic detectors; c) the frequency and amplitude characteristics of the channel of the reproduction summary station; and d) the frequency and amplitude characteristics of all the recording and reproduction stations.

A tuning error by resonance frequency (at $f_{rez} = 1$ Hz) no greater than $\pm$ 5 percent is permitted, while attenuation is optimum when monitoring the seismic detectors.

The frequency characteristics of the channels (Z, X, Y_1 and Y_2) of the summary reproduction station should admit signals in the frequency band of 0.5-6 Hz. A second channel Z_2 with bandpass of 0.5-1.5 Hz is also introduced to separatedthe recordings from remote earthquakes at a high level of industrial microseism noise (Figure 36).

The most effective type of monitoring the device is installation of all the "Zemlya" recording stations at the same point and simultaneous recording of seismic waves from different energy sources: earthquakes and explosions. In this case all the seismic detectors are installed on the same foundation. Horizontal devices are oriented by one azimuth and later by different azimuths. The phase identity of all the recording channels, the identity and polarity of switching on the time marking channels, the polarity of swtiching on the seismic detectors for corresponding calibration of the wave arrivals by quadrants (see Chapter 4) and the amplitude identitity of the channels are established for the recordings obtained.

APPROVED FOR RELEASE: 2007/02/08: CIA-RDP82-00850R000200030043-9

APPROVED FOR RELEASE: 2007/02/08: CIA-RDP82-00850R000200030043-9

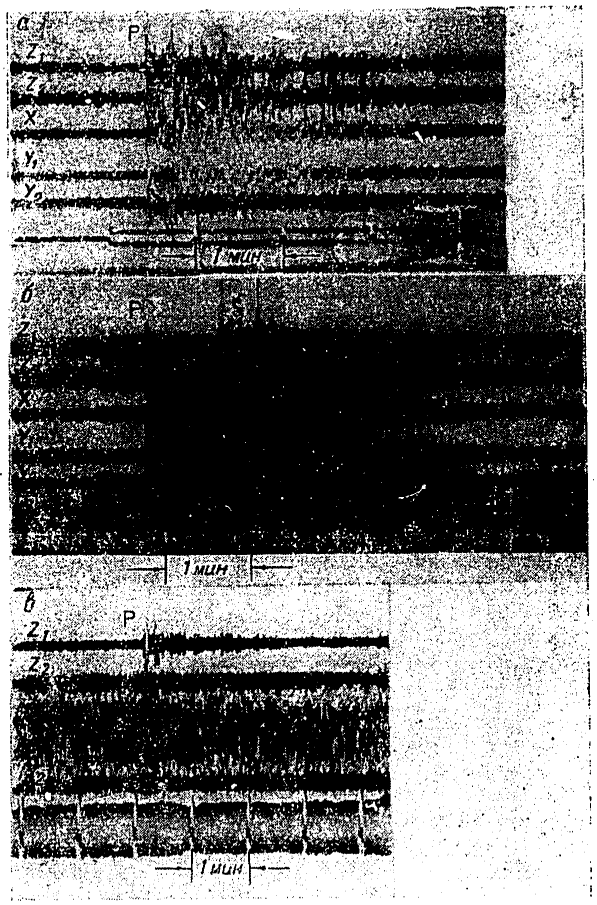

Figure 36. Recordings from Remote (a and b) and Near (b) Earthquakes on Summary Seismograms with Low and High Level of Microseism Noise:
a--T = 1400 , 24 Sep 1967, Δ = 53°, α = 138.4°; b--T = = 2217, 25 Oct 1967; c--T = 1648, 30 Jul 1967; Z_1--frequency band of 0.5-1.5 Hz; Z_2--frequency band of 0.5-6Hz; X, Y1 and Y_2--channels with horizontal seismographs and frequency band of 0.5-6 Hz

APPROVED FOR RELEASE: 2007/02/08: CIA-RDP82-00850R000200030043-9

APPROVED FOR RELEASE: 2007/02/08: CIA-RDP82-00850R000200030043-9

A check of the status of the "Zemlya" device during field observations was made mainly from recordings of calibration pulses. The polarity of switching on the seismic detectors is determined at each new layout of the recording stations.

Apparatus for Processing the Magnetic Tapes of the "Zemlya" Recording Stations on Analog and Digital Devices

An enormous number of seismograms recorded at different, but simultaneously operating recording stations dispersed over great distances is received when conducting field operations with the "Zemlya" device. Summary seismograms must be compiled to correlate the waves from station to station. This is accomplished either by drawing and combining components of the same type of different recording stations or by magnetic re-recording of the signals on multichannel magnetic recorders.

A special device was developed for automatic construction of summary seismograms and the use of modern methods of machine processing of materials directly from magnetic tapes. It was carried out on the basis of the SS-24-61M re-equipped standard seismic station. A six-channel variational magentic drum installed on the common axis of the magnetic recorder was added to the station. The signals from magnetic tapes of the "Zemlya" stations were re-recorded by using this drum onto the magnetic tapes of the SS-24-61M station. The channels of different "Zemlya" recording stations are combined by the first phase of the P wave or by time marks with an error of $\pm$ 0.02 second when re-recording the signals from the variational drum on the main drum. The transformation coefficient K_{tr} of the "Zemlya" reproduction stations is selected with regard to the frequency range of the SS-24-61M station. Pin re-recording of all signals on the summary correlation seismogram is accomplished after the capacity of the main drum is filled. The signal shifting system, grouping and so on may be included at this moment. The derived recordings on magnetic tapes can be processed on computers having the appropriate drums.

Another system was also developed to enter the magnetic tapes of the "Zemlya" stations into the computer. Analog information taken from the output of all the magnetic heads of the reproduction device is fed to the input of the standard digital seismic station. The transformation coefficient K_{tr} = 20, the recording time comprises 3 seconds, the enciphering interval is 2 ms, initial amplification is 48 dB and delay of the initial amplification is eliminated. The preamplifier filtration is set in the frequency band of 10-125 Hz with the filter having frequency of 50 Hz which cuts the noise from the lighting system switched on. Connecting the digital station to the "Record" mode is accomplished by means of a relay, triggering of which occurs from a photoelement. The latter is lighted up through a perforated opening on the magnetic tape of the "Zemlya-75" reproduction device. The holes are punched with calculation of start signal delivery within 0.7-0.8 second prior to the beginning of seismic recording. The given encipherment versions showed that a standard digital seismic device in simplified form without special

APPROVED FOR RELEASE: 2007/02/08: CIA-RDP82-00850R000200030043-9

APPROVED FOR RELEASE: 2007/02/08: CIA-RDP82-00850R000200030043-9

automatic signal regulation systems can be used to enter the analog information of the "Zemlya" stations into a computer since the dynamic range of the field recording does not exceed 40-42 dB.

APPROVED FOR RELEASE: 2007/02/08: CIA-RDP82-00850R000200030043-9

APPROVED FOR RELEASE: 2007/02/08: CIA-RDP82-00850R000200030043-9

METHOD OF OBSERVATIONS

Moscow SEYSMICHESKIYE ISSLEDOVANIYA S APPARATUROY "ZEMLYA" in Russian 1977 signed to press 31 Jan 1977 pp 80-97

[Chapter 4 from the book "Seysmicheskiye issledovaniya s apparaturoy 'Zemlya'" by I. V. Pomerantseva and A. N. Mozzhenko, Izdatel'stvo Nedra, 1,400 copies, 256 pages]

[Text] Field Operations

Field operations with the "Zemlya" stations include the type of surveying, location of the investigation profiles, layout and operation of the recording stations on the terrain (number of simultaneously operating stations, space in between them, average length of observations on one spacing, number of correlation stations, installation of stations at observations points, recording and reproduction of useful signals, orientation of seismographs in the container and production of explosions).

The type of surveying is determined by the postulated problems. Recognizance, regional and detailed observations are distinguished as a function of this. Recognizance studies are conducted to determine the overall nature of the wave fields and the microseism background, noise recorded in a given region and also to determine the main features of the deep structure of the region and the behavior of the surface relief of the crystalline foundation. These studies are conducted mainly on traverses accessible for rapid movement of people and equipment. Regional studies are conducted to determine structures of first and second orders noted during recognizance investigations or previously planned from data of other, less accurate geophysical methods, and also to detect the epicenters of local and near earthquakes. These studies are conducted mainly along straight or broken lines (profiles) with the presence of portable stations or by a system of mutually perpendicular profiles. Area operations are carried out to detail the structures and foci of earthquakes determined during regional studies. Detailed studies for an area are frequently combined with regional operations, refining the complex tectonics of the region, especially within zones of fusion of large regional blocks of the crust.

The profiles are laid out transversely and along the strike of large elements of gravitational and magnetic fields and also by structures proposed from

APPROVED FOR RELEASE: 2007/02/08: CIA-RDP82-00850R000200030043-9

APPROVED FOR RELEASE: 2007/02/08: CIA-RDP82-00850R000200030043-9

geological data during regional studies. The distances between profiles comprise 20-30 km during regional studies and 3-7 km during detailed studies.

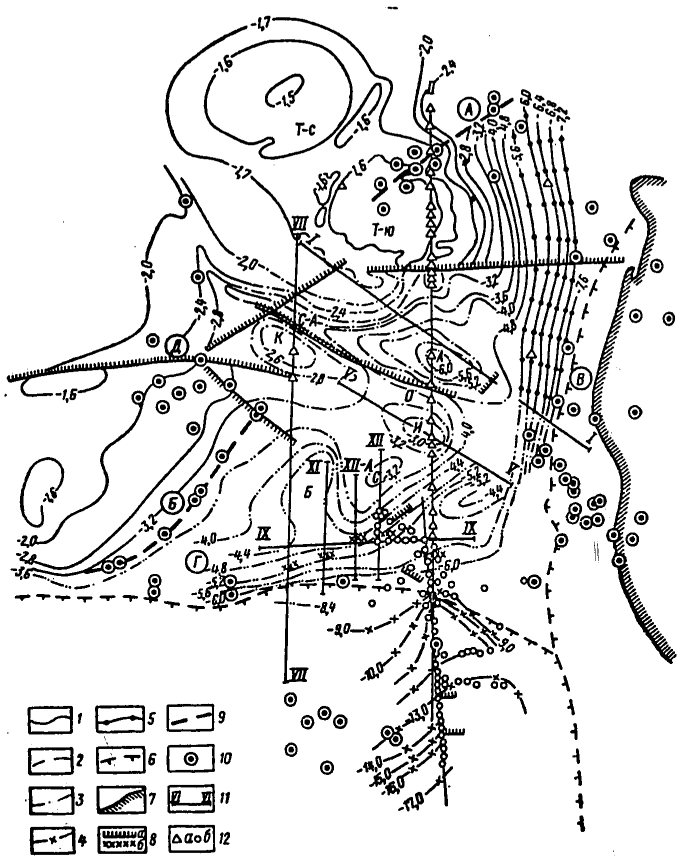

Figure 37. Diagram of Layout of "Zemlya" Recording Stations and Epicenters of Local Earthquakes Recorded on the Southeastern Russian Series and the Northern Pre-Caspian Depression

The surface isolines of the Precambrian basement are from data: 1--of deep drilling according to P. A. Blokhin; 2--KMPV according to Yu. N. Godin et al; 3--reinterpretation of KMPV materials according to I. A. Sokolova and others; 4--"Zemlya" stations according to I. V. Pomerantseva et al; 5--other geophysical methods according to P. A. Blokhin; 6--line separating the Russian series with the Precaspian Depression and Pre-Urals Trough; 7--boundary of folded Urals; 8--fault zones from geological data (a) and KMPV data (b); 9--fault zones from materials of "Zemlya"

[Continued on following page]

APPROVED FOR RELEASE: 2007/02/08: CIA-RDP82-00850R000200030043-9

APPROVED FOR RELEASE: 2007/02/08: CIA-RDP82-00850R000200030043-9

[Continued from preceding page]

stations; 10--epicenters of local earthquakes; 11--KMPV and GSZ profiles; 12--locations of installation of "Zemlya" stations in 1962 (a) and in 1965 (b); T-s--northern apex of Tatarskiy Vault; T-yu--southern apex of Tatarskiy Vault; A and S-A--Abdullinskaya and Sernovodsko-Abdullinskaya Depressions; O--Orenburg Vault; I and S--Ivanovsk and Sorochinsk Projections; K--Kinel'skiy Vault; B--Buzuluk Depression; the zones of local earthquake epicenters are denoted by the letters in circles.

The number of simultaneously operating recording stations comprises 10-15 during recognizance studies, 10-15 during regional studies and 15-25 during detailed studies. The different number of recording stations used is determined by the concepts of their mobility and cost of operations in combination with the accuracy and reliability of the results obtained. The technique of operations is simplified with a smaller number of stations, but the cost of 1 km of profile and 1 physical point increases, the method of interpreting the materials is complicated and their accuracy is reduced. An increase of the number of recording stations permits a reduction of the cost per unit measurement, an increase of the reliability of the information obtained by processing it at computer centers, but complicates the conditions of organizing the operations.

The spacing between the recording stations may vary from 1 to 30 km as a functionof the type of surveying (Figures 37 and 38). It may reach 20-30 km during recognizance studies and 5-10 km during regional studies. The optimum spacing during regional studies comprises 5-7 km and 0.5-5 km during detailed studies. The optimum spacing permits phase correlation of P and PS waves. The distances between recording stations at the boundaries of blocks are reduced to 1-2 km during detailed study of small basement blocks measuring 2 X 2 km^2 and with depths from 300 m to 3 km.

The average length of observations on a single spacing of recording stations is determined by the postulated problems and by the accuracy of this study.

The length of observations depends on the number of recorded remote earthquakes necessary to construct the time and depth profiles by P and PS waves during regional and detailed operations on study of the structure of the earth's crust. It is always possible during this time to register a sufficient number of recordings from near earthquakes and explosions used to determine the velocity characteristic of the medium. The optimum length of the stopover is determined by the accuracy of the given studies and can be determined from the graph of the dependence of the relative confidence interval of existence of the boundary on the number of PS waves with P-wave surfaces equal to 0.9, 0.95 and 0.99 (Figure 39). An instrument was made for a model of the crust presented in Figure 3. The number of PS waves on a single point should comprise 5-7 with error of plotting the boundaries of $\pm$ 2.5

APPROVED FOR RELEASE: 2007/02/08: CIA-RDP82-00850R000200030043-9

APPROVED FOR RELEASE: 2007/02/08: CIA-RDP82-00850R000200030043-9

1978 _YA' DEVICE 2 OF 3

APPROVED FOR RELEASE: 2007/02/08: CIA-RDP82-00850R000200030043-9

APPROVED FOR RELEASE: 2007/02/08: CIA-RDP82-00850R000200030043-9

percent. The number of observations may be reduced to 3-4 with an increase of error up to ± 10 percent. Obtaining 5-7 values of PS waves connected to all the main interfaces of the earth's crust (besides the fault zones) in regions with low level of microseism noise background where the signal to noise ratio is equal to 5-10 in the frequency band of 0.5-1.5 Hz, based on operating experience, is possible over a period of 8-15 days.

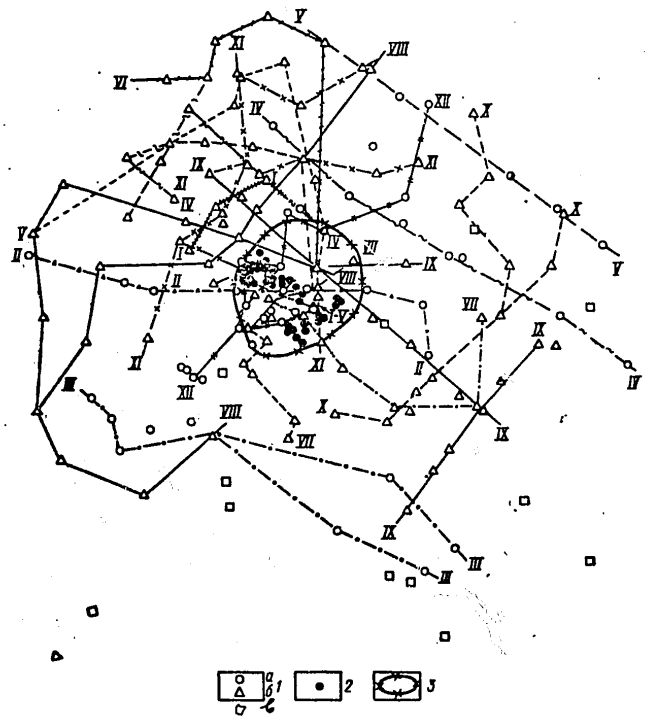

Figure 38. Diagram of Layout of "Zemlya" Recording Stations at Tashkent with Number of Stopovers (I-XII): 1--observation points in 1966 (a), 1967 (b) and in 1968 (c); 2--aftershock epicenters of the Tashkent earthquake of 26 April 1966, registered by "Zemlya" recording stations; 3--zone of reduced velocities in the mass of the Paleozoic basement.

The length of a stopover of recording stations is increased to 20-25 days in regions with high background of microseism noise, where the signal to noise ratio in the frequency band of 0.5-1.5 Hz comprises 1-5. An increase of the number of observations to obtain more than 7 PS waves makes no sense at a single recording station for each interface, since this does not lead to a further increase of investigation accuracy (see Figure 39).

APPROVED FOR RELEASE: 2007/02/08: CIA-RDP82-00850R000200030043-9

APPROVED FOR RELEASE: 2007/02/08: CIA-RDP82-00850R000200030043-9

The length of observations may be any length as a function of the seismological tasks during detailed studies to determine the seismicity of a region.

Upon travelling from one stopover to another, from one to three recording stations are left in place for correlation tying in time Δt_{PS-P} of the time profiles of the earth's crust obtained at different stopovers of recording stations and hodographs of P and S waves from special explosions.

The "Zemlya" recording stations are installed at the observation point either in special containers (Figure 40) measuring 2 X 2 X 2 m^2 without a base, installed in holes dug in the ground or in the basements of houses. A reinforced concrete slab oriented by the directions of light, measuring 0.8 by 0.8 by 0.3 m^3, is placed on the earth base in the container, on which the seismographs are installed. The recording station and the power supply for it are also located in the container. The antenna for the recording station detector is the wire surrounding the container hole (see Figure 40).

The recordings at each station are registered by using four VEGIK seismographs (Z_1, X, Y_1, Z_2 or Y_2). The Z_1 and Z_2 devices are vertical and the X, Y_1 and Y_2 devices are horizontal. The mobile systems of the latter devices fluctuate within the following planes: X--north-south; Y_1--west-east; and Y_2--northeast and southwest. The Y_2 component permits recording of the horizontal components of PS waves from Japanese earthquakes at the ray azimuth with horizontal interfaces of the crust.

The polarity of the devices is tuned so that the soil displacements due to the compression wave upward (Z) to the north (X), to the east (Y_1) or to the northeast (Y_2) corresponded to the light point displacements upward on the seismogram. As a result of this calibration of the apparatus, the polarity of wave arrival on the X and Y components with respect to their arrival polarity on the Z components (assuming arrivals on the Z channel as positive) is distributed by quadrants in the following manner:

Quadrant	Channel Z	Channel X	Channel Y
I (α=0—90°)	+	−	−
II (α=90—180°)	+	+	−
III (α=180—270°)	+	+	+
IV (α=270—360°)	+	−	+

The coincidence of the wave arrival signs on the X and Y components indicates that the polarity of their arrivals is identical and disagreement of signs indicates that their polarity is different.

Reproduction of the useful signals from magnetic to paper tape is accomplished in the frequency band of 0.5-10 Hz. The use of a higher frequency band during operations with the "Zemlya" stations under conditions of nonstationary seismological installations is not feasible since in this case the microseism noise

APPROVED FOR RELEASE: 2007/02/08: CIA-RDP82-00850R000200030043-9

APPROVED FOR RELEASE: 2007/02/08: CIA-RDP82-00850R000200030043-9

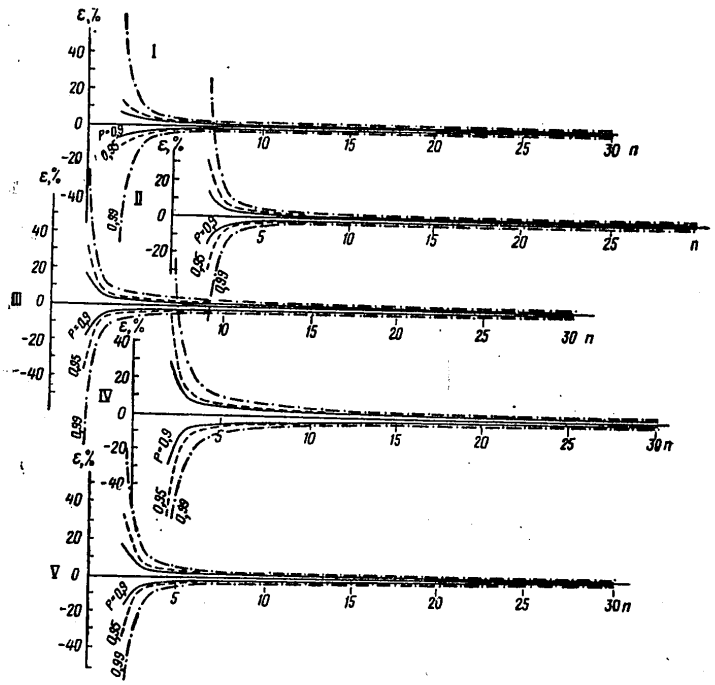

Figure 39. Dependence of Relative Confidence Interval ε of the Existence of Interfaces at Different Probabilities P on the Number of Recorded Composite Waves n for Regions of the North German Depression and Tashkent:
I--for a Variscian Basement; II--for a Precambrian Basement; III--for a Paleozoic Basement; IV--for a transition zone from a granite to basaltic layer; V--for a transition zone from the crust to the mantle

background increases sharply and the recordings become inoperative. Expansion of the frequency band to the low-frequency region when recording P, PS and S waves from earthquakes also makes no sense since the microseism background of first kind [7] increases approximately 100-fold at frequencies below 0.5 Hz, which sharply worsens the possibility of recording useful signals.

Seismograms obtained within Tashkent and reproduced by means of air filters and without them are presented in Figure 41. Channels Z_1, Z_2, X_1 and Y_1 were re-recorded in the frequency band of 0.5-1.5 Hz (upper tracks) and at 0.5-10 Hz (lower tracks). The two intermediate tracks were re-recorded in

APPROVED FOR RELEASE: 2007/02/08: CIA-RDP82-00850R000200030043-9

APPROVED FOR RELEASE: 2007/02/08: CIA-RDP82-00850R000200030043-9

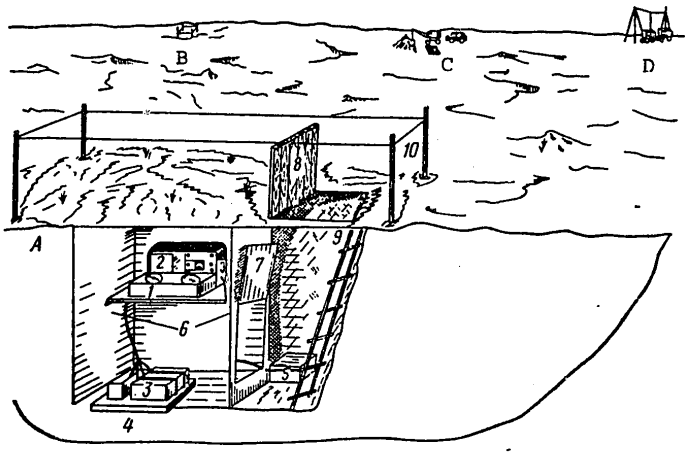

Figure 40. Installation of "Zemlya" Recording Stations at Observation Points:
a--container for installation of apparatus; 1--recorder; 2--power supply block; 3--seismic detectors; 4--concrete slab for installation of seismographs; 5--power supply storage batteries; 6--container walls; 7--door to container; 8--hatch; 9--ladder; 10--enclosure (antenna); B--container in profile; C--equipment which installs container; D--radio center (radio channel)

in the average frequency band between 0.5-10 Hz. Pulse recordings from the reproduction station generator are presented to the left of the seismograms, which indicate the difference in the amplifications of its channels. The following are recorded on the three lower tracks below the seismograms from bottom to top: pulses from the reproduction station capstan and time markers from the generator with frequency of 5 Hz and from the radio channel. The minute mark on the recording is determined by the absence of second marks. Pulse recording from the reproduction station capstain permits direct determination of the transformation coefficient during reproduction on the seismogram. The use of air filters (Figure 41, b) removes all high-frequency signals (background, capstan pulses and generator) from the recordings and also smooths out the time marks from the ratio channel. If a reduction of the microseism background is a positive phenomenon, distortion of the time signals is negative. A window opposite the service channels must be left to use air filters without distortion of the serivce signal recordings in the teflon film used in the air filter and inserted between the magnetic tape and the reproduction station head. Similar distribution of all the working and service tracks on the recordings will be subsequently maintained upon illustration of seismograms obtained within Tashkent. The distribution of the service and working tracks

APPROVED FOR RELEASE: 2007/02/08: CIA-RDP82-00850R000200030043-9

APPROVED FOR RELEASE: 2007/02/08: CIA-RDP82-00850R000200030043-9

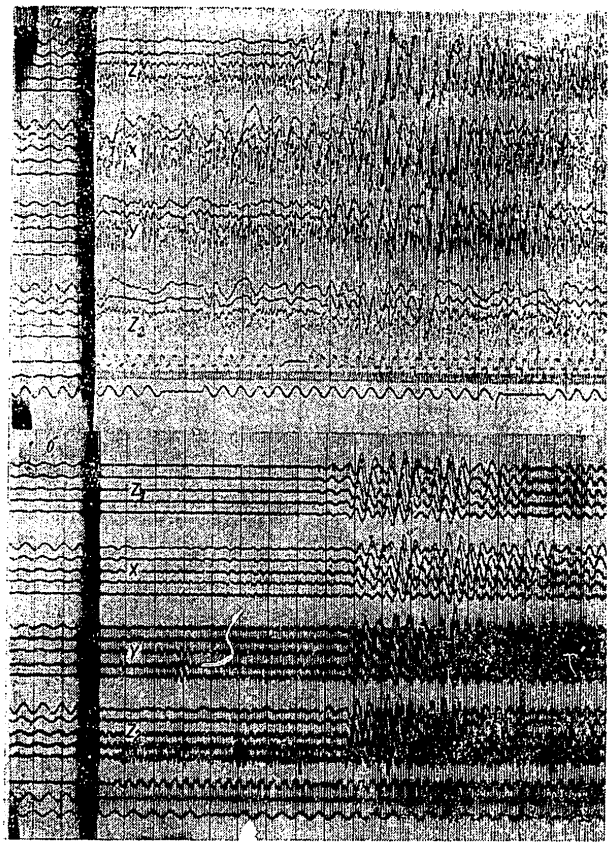

Figure 41. Seismogram From Remote Earthquake Recorded at Tashkent and Reproduced without (a) and with the Use (b) of an Air Filter. The time of recording the earthquake was 0925 (Greenwich Time) on 15 Aug 1967.

is somewhat different on seismograms obtained within the North German Depression. The difference is that a second horizontal channel Y_2 was used instead of a vertical seismograph Z_2; the higher frequency track (0.5-10 Hz) was located

APPROVED FOR RELEASE: 2007/02/08: CIA-RDP82-00850R000200030043-9

APPROVED FOR RELEASE: 2007/02/08: CIA-RDP82-00850R000200030043-9

on the bottom in a group of four tracks; the time marks from the generator with frequency of 5Hz were recorded at the top of the seismogram; the capstan pulses were not suppressed.

The seismic detectors in the container were oriented with respect to the meridian by means of a theodolite compass of mark TT-5. Since the containers are manufactured from iron, an auxiliary attachment is used upon application of the lines along which the horizontal seismographs are installed on the slab. It is (Figure 42) an extensible bar 4 on the upper end of which a sighting rule 3 is attached and on the lower end of which, parallel to the sighting rule, a ruler 6 is attached, which serves to mark the lines of orientation of horizontal seismographs on the seismograph plate. There is an opening in the cover of the metal container for installation of the device through which the upper end of the extensible rod with the sighting rule emerges. The lower end of the rod is installed on the seismograph plate. During orientation of seismographs, the theodolite is installed 100-200 m from the instrument hole to eliminate the effect of the metal container on the magnetic arrow of the compass. The azimuth of the hole is measured by the theodolite compass by combining the zero mark of the compass with the north end of the magnetic pointer. The north-south (N-S) line is determined by the value of the hole azimuth Az (correction to the hole-theodolite line). The north-south direction is determined in the container hole by rotating the upper end of the extensible rod by angle Az. The north-south and west-east directions are drawn on the plate. If there is a second seismograph Y_2 which should be oriented at angle α to the north-south line, this direction is also noted. The error of determining the direction comprises $\pm$ 1-3°.

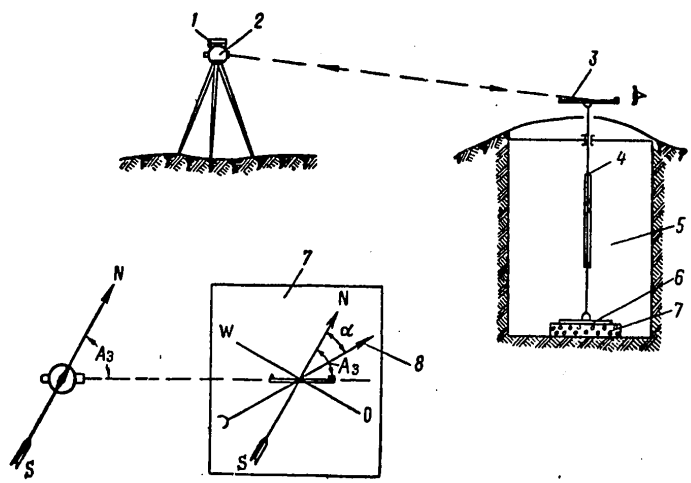

Figure 42. Orientation of Seismic Detector Installation in Container: 1--compass; 2--theodolite; 3--sighting rule; 4--extensible rod; 5--container; 6--rule for noting the orientation lines of horizontal seismic detectors; 7--concrete slab; 8--orientation line

APPROVED FOR RELEASE: 2007/02/08: CIA-RDP82-00850R000200030043-9

APPROVED FOR RELEASE: 2007/02/08: CIA-RDP82-00850R000200030043-9

Special explosions are produced in aseismic regions when laying out the station along the profiles.* The main purpose of these investigation is to obtain data on the propagation velocities of P and S waves in the earth's crust. The optimum number of special explosions comprises 4-5 with a single layout of the recording stations to study the velocity characteristic of the medium and the stratification of the interfaces.

A system of straight lines and counter hodographs of the first arrivals of P and S waves, indicated at conjugate points (Figure 43), is constructed from explosion seismograms. The distances between the explosion points vary from 40 to 90 km. The minimum lengths of the hodographs necessary to find the velocity distribution curves of P and S waves should comprise 230-240 km with depth of 40-50 km for the entire crust and upper mantle. Charges up to 1,500 kg are usually employed to obtain these lengths of hodographs (Figure 44). The mass of charges may be reduced to 300-100 kg near the explosion point to obtain a readable recording, especially for S waves recorded on a background of longitudinal waves. The mass of a medium charge in a single shot hole is equal to approximately 350 kg. The number of shot holes is determined by the total mass of a charge and varies from 1 to 6. It should be noted that experimental investigations to select the conditions for P and S wave excitation from explosions have never been carried out during operations with the "Zemlya" stations. Therefore, the used values of the charges may be assumed maximum, but not optimum. The explosions are set off either during the evening (2000-2100) or at night (2300-0600) when the noise background is least.

When setting off explosions, the moment of the explosion is recorded at the explosion point by recording the interruption of the detonator circuit on the oscillograph paper of the N-700 oscillograph. The time marks from the radio channel are recorded on the oscillograph paper at the same time to tie in the moment of explosion to the recording stations (Figure 45). The recording method used makes it possible to determine the moment of the explosion with an error of $\pm$ 0.002 second. The explosions are registered by recording stations in the frequency range of 0.5-10 Hz.

In seismically active regions, the explosions can be produced on regional profiles by a similar or facilitated method by using the foci of permanently active near and local earthquakes as the explosion point.

Characteristics of Studies with the "Zemlya" Device

The characteristics of working with the "Zemlya" device include: 1) continuous field recording of seismic signals and separate laboratory reproduction from recording of the sections of magnetograms with useful information and 2) all simultaneously operating recording stations are isolated channels

---

*Explosions can also be produced during area studies. In these cases isochronal and velocity charts to the crustal interfaces can be used.

APPROVED FOR RELEASE: 2007/02/08: CIA-RDP82-00850R000200030043-9

APPROVED FOR RELEASE: 2007/02/08: CIA-RDP82-00850R000200030043-9

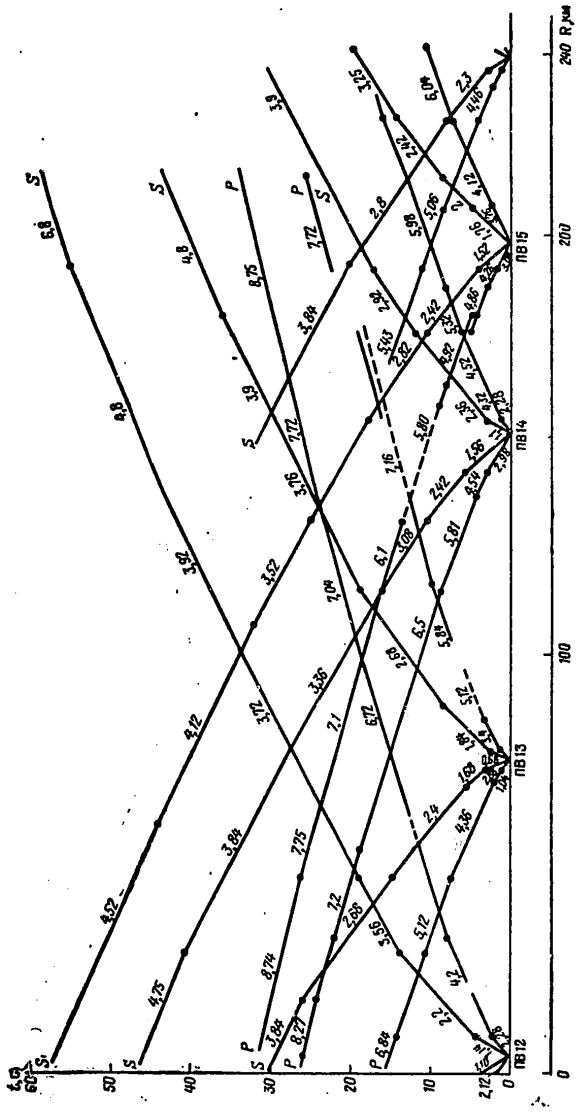

Figure 43. Hodographs of First Arrivals of P and S Waves (The Values of the Apparent Velocities in km/s are Indicated on the Hodographs)

APPROVED FOR RELEASE: 2007/02/08: CIA-RDP82-00850R000200030043-9

APPROVED FOR RELEASE: 2007/02/08: CIA-RDP82-00850R000200030043-9

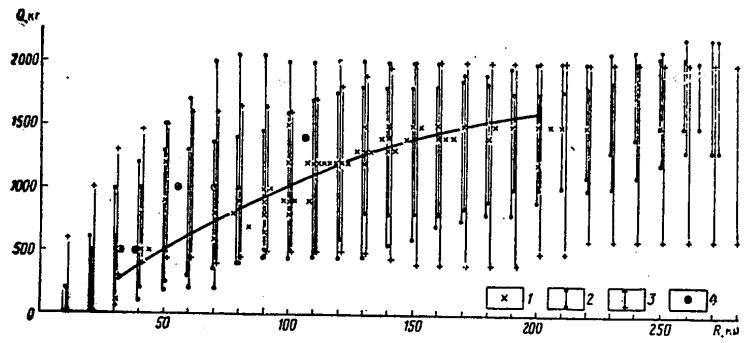

Figure 44. Graph of Dependence of Charge Mass Q on Distance R to Explosion Point During Investigations by KMPV, GSZ and with "Zemlya" Stations:
1--regions of North German Depression (data of "Zemlya" stations); 2 and 3--regions of the Southeastern Russian Series (data of KMPV and GSZ from profiles VII and IX, respectively); 4--regions of the Pre-Caspian Depression (data of "Zemlya" stations)

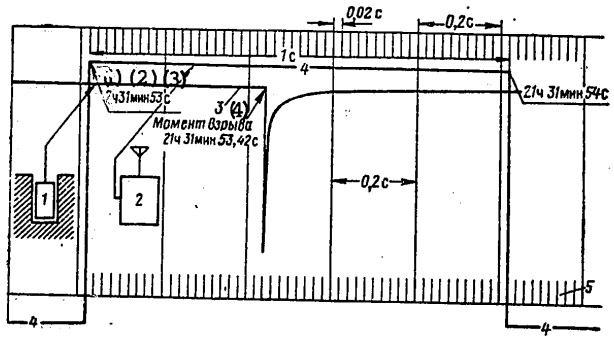

Figure 45. Oscillogram and Diagram of Explosion Time Marker: 1--charge with moment line; 2--radio receiver for reception of radio channel signals; 3--recording of moment of explosion; 4--radio channel signals (1 second); 5--time marks from tuning for generator

Key:

1. Hours
2. Minutes
3. Seconds
4. Moment of explosion

APPROVED FOR RELEASE: 2007/02/08: CIA-RDP82-00850R000200030043-9

APPROVED FOR RELEASE: 2007/02/08: CIA-RDP82-00850R000200030043-9

dispersed in space of seemingly a single multichannel seismic station. These two characteristics require, on the one hand, operational monitoring of the materials obtained on magnetic tapes and, on the other hand, exceptional operating stability of all the recording station channels. Operational monitoring of the device operation is accomplished only on a stationary base where the magnetic tapes are processed on survey, marking and multichannel reproduction tables. The magnetic tapes obtained every 2-3 days* from the profile are rerecorded on the summary table. Sections with useful recordings are further separated on the summary seismograms recorded oscillographically. These sections are noted on the magnetic tape and are reproduced on the multichannel reproduction table with the corresponding selected speeds and filters. After the entire cycle of processing the magnetic tape has been completed, one can reach conclusions about the quality and quantity of the material obtained. This process occupies from 2 to 6 days in time.

The operation of the device on the profile is monitored by recording a series of standard pulses transmitted to the recording station amplifiers connected in parallel and to undamped seismographs at the beginning and end of each magnetic tape (see Chapter 3). Preliminary processing of these pulses is accomplished by the summary seismograms after the arrival of the magnetic tapes at the base. Data on operation of the device are reported on the profile by radio. The latter provides essentially continuous operation of the device at the observation points. As a result of this organization of operations, the inoperative time of the "Zemlya" stations, including days of transporting the stations from one stopover to another, did not exceed 2 percent.

The Volume and Conditions of Recording Useful Signals

The number of useful recordings registered by the "Zemlya" device. The number of earthquakes and explosions registered by the "Zemlya" device in different regions is presented in Figure 46. Aseismic and seismically active regions are distinguished by the total number of useful recordings N_{obshch} obtained during 15 days. The number of useful recordings in the seismically active regions is increased two- to threefold or more due to the presence of near and local earthquakes (N_z) compared to aseismic regions. The number of registered recordings from explosions N_{vzr} is approximately identical in both regions. The number of remote earthquakes $N_{d.z}$ is either identical or somewhat reduced in seismically active regions. The number of recordings from remote earthquakes in the mountain regions of Central Asia and Siberia varies out of proportion to the length of observations on a single layout. This may be related both to the method of observations (the absence of backing-filters and other methodical procedures directed toward improving the conditions of useful signal separation) and to the increase of volumetric wave absorption from remote earthquakes during their passage through the complex tectonics of mountains.

---

*The "Zemlya-66" recording stations have an operating period of 2-3 days. The "Zemlya-73" stations have a period of 12 days.

APPROVED FOR RELEASE: 2007/02/08: CIA-RDP82-00850R000200030043-9

APPROVED FOR RELEASE: 2007/02/08: CIA-RDP82-00850R000200030043-9

Comparison of the number of remote earthquakes recorded by "Zemlya" stations at mobile observation points to the number of earthquakes presented in the earthquake bulletins of the USSR and United States showed that the "Zemlya" device records 1.5-2 times fewer earthquakes (magnitude of $M > 5$) than regional seismological stations. This is explained by the fact that observations of "Zemlya" stations are made within the range of small individual regions considerably remote from earthquake foci, while data of a large number of regional stations located around the entire globe are included in seismological catalogs. When the "Zemlya" stations are installed at staionary seismological points, the number of remote earthquakes registered by this and standard seismological apparatus is identical. The number of local, weak earthquakes recorded by the "Zemlya" apparatus under these conditions of installation exceeds the number of local earthquakes registered by ordinary seismological stations by more than 30 percent.

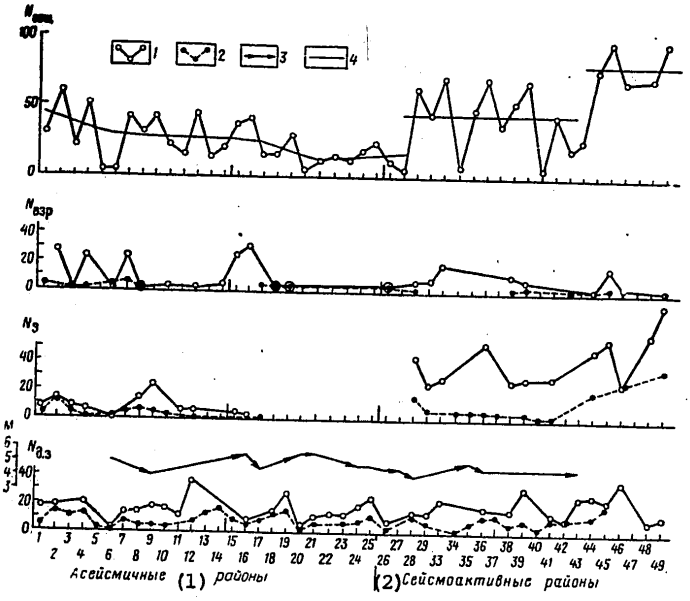

Figure 46. Graphs which Characterize the Seismicity of the Regions of Study (Compiled by I. V. Pomerantseva and L. P. Barskova):
1--number of registered recordings; 2--number of recordings accepted for processing; 3--level of minimum magnitudes for recorded earthquakes of a region; 4--averaging lines. The numbers on the X-axis denote the numbers of the regions of operations (See Table 1)

Key:
1. Aseismic regions
2. Seismically active regions

APPROVED FOR RELEASE: 2007/02/08: CIA-RDP82-00850R000200030043-9

APPROVED FOR RELEASE: 2007/02/08: CIA-RDP82-00850R000200030043-9

The useful signal to background ratio (A_s/A_f) and the methodical-apparatus procedures of separating useful waves on a microseism background. The useful signal to background ratio (A_s/A_f) plays a significant role in different regions in separation of useful recordings on summary and working seismograms. This is especially true of the least intensive recordings from remote earthquakes. The background and signal to background ratio was studied most fully from data obtained within Tashkent and the North German Depression. The noise observed in these regions had a sufficiently wide spectrum (0.5-20 HZ or more). They were determined both by the industrial background (operation of factories, plants, railroads and airfields) and by the storms and waves of the Baltic Sea which cause microseism oscillations of the soil (apparently Rayleigh waves). The industrial background has a spectrum from 2 Hz or more in its frequency composition and the background* caused by microseism oscillations of the soil has a range of 0.5-2 Hz. A background of primarily high-frequency noise was observed on the recordings during operations in the rayons of Tashkent. Soil displacements caused by this background reached 750 microns in some cases. Both types of noise were present during operations in the regions of the North German Depression.

The high-frequency noise background behaves identically both within the North German Depression and in the rayons of Tashkent. An increase of it is observed during daytime hours and a decrease is observed at night. The maximum background occurs at 1100 and the minimum occurs at midnight. The amplitude of the background varies by a factor of 3-4 during this period.

Graphs A_f/A_s and A_s/A_f in the frequency band of 0.5-1.5 and 0.5-10 Hz were constructed (Figure 47) to determine the separate effect of the low- and high-frequency noise background on the useful recordings during the entire period of working with the "Zemlya" device within the North German Depression. The graphs in the frequency band of 0.5-1.5 Hz indicate the effect of only the low-frequency background, while those in the frequency band of 0.5-10 Hz are the sum of the low- and high-frequency noise background. Each point of the graph in Figure 47 is constructed from 5-8 recordings from Japanese earthquakes with $\Delta = 75°$ and magnitude (M) equal to 5.3, registered at each installation of field stations. The ratio A_s/A_f in the frequency band of 0.5-1.5 Hz is 2-8 times higher than the ratio of A_s/A_f in the frequency band of 0.5-10 Hz, i.e., the presence of a high-frequency background makes it difficult to separate the signals on a noisy background by a factor of 2-8.

Several methodical procedures were developed to separate the useful signals from remote and near earthquakes on a background of intensive high-frequency noise: a) the corresponding low-frequency filters with maximum frequency characteristic at 1.3 Hz were introduced in the recording stations; b) air filters on summary and main reproduction tables were used when reproducing the recordings; and c) the locations for installing the recording stations

---

* Possibly the frequency spectrum of this background is also continued into the frequency range lower than 0.5 Hz. But these frequencies are not recorded by the "Zemlya" device.

APPROVED FOR RELEASE: 2007/02/08: CIA-RDP82-00850R000200030043-9

APPROVED FOR RELEASE: 2007/02/08: CIA-RDP82-00850R000200030043-9

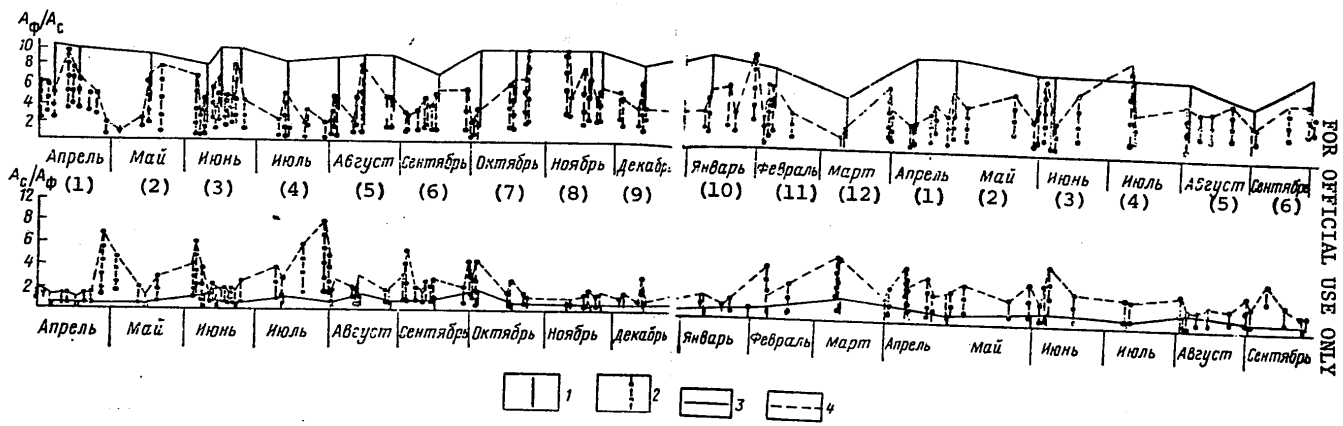

Figure 47. Graphs of Ratio of Background Amplitude and Useful Signal Amplitude (A_f/A_s and A_s/A_f):
1--graphs of A_f/A_s and A_s/A_f in the frequency band of 0.5-10 Hz; 2--graphs of A_f/A_s and A_s/A_f in the frequency band of 0.5-1.5 Hz; 3 and 4--curves plotted through the maximum values of A_f/A_s and A_s/A_f for the frequency band of 0.5-10 and 0.5-1.5 Hz, respectively

Key:

1. April
2. May
3. June
4. July
5. August
6. September
7. October
8. November
9. December
10. January
11. February
12. March

APPROVED FOR RELEASE: 2007/02/08: CIA-RDP82-00850R000200030043-9

APPROVED FOR RELEASE: 2007/02/08: CIA-RDP82-00850R000200030043-9

were selected with special care. The level of the microseism noise background at the selected site of the recording station installation should not exceed 50-60 microns. From the experience of operating in many regions, this microseism background is observed for sites of recorder installations separated from construction sites and trees at a distance of 100-300 m, 2km from highways and 10-12 km from railroads. The use of an air filter was optimum for separating P and S waves from remote and near earthquakes (f = = 1-3 Hz) on a high-frequency noisy background. A seismogram obtained within Tashkent without and with the use of an air filter which take high-frequency oscillations from the recordings is presented in Figure 41. As can be seen from Figure 41, the use of an air filter reduces the high-frequency noise background by a factor of 5-8 and makes the seismogram suitable for processing. Similar recordings were obtained in other regions as well where an air filter was used.

Study of the low-frequency noise background carried out for regions of the North German Depression (Figures 47 and 48) showed that the value of A_s/A_f decreases during winter (from the middle of October to the middle of January) by a factor of 3-4 compared to the summer season. A decrease of the low-frequency background is also observed during the summer season when the recording stations are remote from the shore line of the sea.

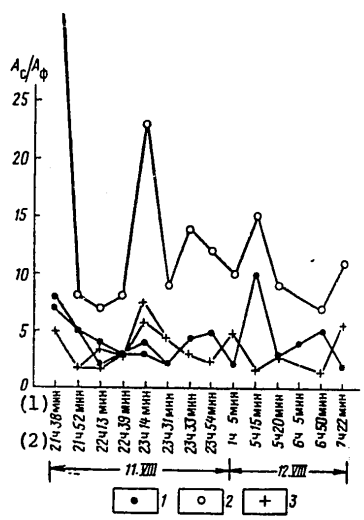

Figure 48. Graphs of Ratio of Useful Signal Amplitude to Background Amplitude A_s/A_f for Earthquakes Recorded at Different Distances R from the Baltic Sea Coast: 1--R_1 = 0-20 km; 2--R_2 = 70-120 km; 3--$(A_s/A_f)_{R_1}/(A_s/A_f)_{R_2}$

Key:
1. Minutes
2. Hours

APPROVED FOR RELEASE: 2007/02/08: CIA-RDP82-00850R000200030043-9

APPROVED FOR RELEASE: 2007/02/08: CIA-RDP82-00850R000200030043-9

A graph of variation of the ratio A_s/A_f for earthquakes recorded at different distances R from the Baltic Sea coast is presented in Figure 48. The graph was constructed from 14 remote earthquakes with α = 32-32.8° and Δ = = 75.8-76.3°, recorded simultaneously by 12 stations on the coast and by 13 stations at a distance of 100-120 km from it. Each point of the graph in Figure 48 shows the mean value of the ratio A_s/A_f calculated for 12-13 recording stations. As can be seen from the figure, the low-frequency background at distances of 100-120 km from the coast decreases by an average factor of 5.

Seismograms of the same earthquake recorded with spacing of the stations on the sea coast and 120 km from the coast are presented in Figure 49. The intensive low-frequency noise background, comparable to useful waves in amplitudes, is observed on seismogram I prior to the arrival of waves from the earthquake. This background is essentially absence on seismogram II, although the amplification of the recording reproduction is two times higher than that of the first station.

The ratio A_s/A_f is considerably dependent on the magnitude of the recorded earthquake. Thus, the value of A_s/A_f comprised 3-6 at M = 5 and Δ = 75°. The ratio reached 18-21, i.e., it increased by a factor of 2-7, at M = 6.

The characteristic features of the low-frequency background made it possible to suggest specific methodical and apparatus procedures of controlling it. The methodical features include processing profiles located in the band of 0-100 km from the coast only during the summer season and the apparatus procedures include the use of grouping, displacement and other seismic means directed toward improving the separating and correlation of useful seismic signals during reproduction of the recordings.

APPROVED FOR RELEASE: 2007/02/08: CIA-RDP82-00850R000200030043-9

APPROVED FOR RELEASE: 2007/02/08: CIA-RDP82-00850R000200030043-9

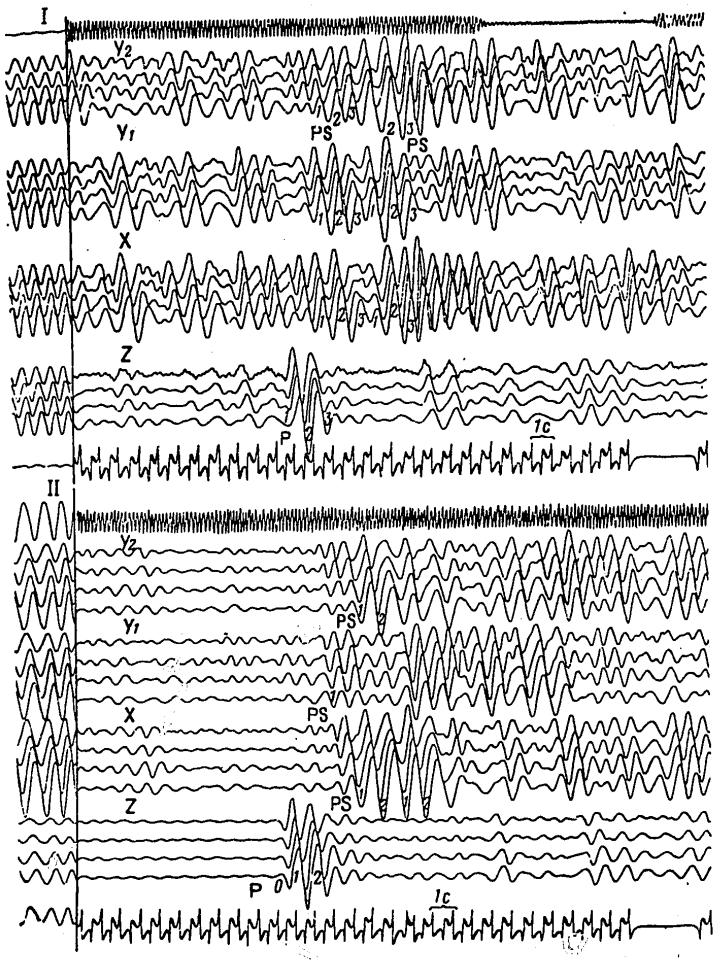

Figure 49. Seismograms Which Illustrate the Nature of the Low-Frequency Background at Different Distances R From The Baltic Sea Coast:
I--R = 0-20 km; II--R = 120 km

APPROVED FOR RELEASE: 2007/02/08: CIA-RDP82-00850R000200030043-9

APPROVED FOR RELEASE: 2007/02/08: CIA-RDP82-00850R000200030043-9

WAVE FIELDS ON RECORDINGS FROM EARTHQUAKES AND EXPLOSIONS

Moscow SEYSMICHESKIYE ISSLEDOVANIYA S APPARATUROY "ZEMLYA" in Russian 1977 signed to press 31 Jan 1977 pp 98-134

[Chapter 5 from the book "Seysmicheskiye issledovaniya s apparaturoy 'Zemlya'"by I. V. Pomerantseva and A. N. Mozzhenko, Izdatel'stvo Nedra, 1,400 copies, 256 pages]

[Text] Let us consider the wave fields recorded by the "Zemlya" stations within the Southeastern Russian series, the Pre-Caspian, Azov-Kuban' and North German Depressions and in the city of Tashkent from earthquakes and explosions at epicentral distances Δ = 0-160° and in the frequency band from 0.5 to 10 Hz.

The wave pattern from local earthquakes was described on the example of recordings of 356 aftershocks of the Tashkent earthquake of 26 April 1966. The wave fields from near earthquakes were analyzed in detail for approximately 200 Pamir, Hindu-Kush and other earthquakes recorded during observations at Tashkent during 1966-1967. The wave fields from the explosions were studied in all the enumerated regions from recordings of 650 incidental (Δ = 0-700 km) and 123 special (Δ = 0-250 km) explosions. Analysis of the wave fields from remote earthquakes was carried out from recordings of approximately 1,400 earthquakes (Table 7). All the explosions and earthquakes were recorded by 9-25 stations simultaneously.

Only the first arrivals of longitudinal and transverse waves were studied and interpreted on seismograms from local and near earthquakes and explosions. The interval of 0-11 seconds after the first arrivals of P waves was analyzed on seismograms from remote earthquakes to determine the structure of the earth's crust. Longitudinal P waves and their components on the Z (P_Z), X (P_X) and Y (P_Y) channels, transverse S waves, surface Rayleigh R_1 and R_2 waves, composite transient PS waves formed at the interfaces in the sedimentary mantle (PS_{OS}), the surface of the Variscian (PS_{PZ2}), Caledonian (PS_{PZ1}), Archean (PS_{AR}) and Pre-Cambrian (PS_{PR+AR}) basements, the surface of effusive-intrusive bodies a layer with increased velocities in the upper part of the crystalline mass of the crust, roof (PS_{B0}) and bottom (B_I) of the transition zone from the granite layer to the basaltic layer on the Pre-Cambrian (PS_J), the surface of the gabbro-diabasic (PS_G) and roof and bottom (PS_I) to the boundaries within the basaltic layer (B_{II}), the Conrad-I layer

APPROVED FOR RELEASE: 2007/02/08: CIA-RDP82-00850R000200030043-9

APPROVED FOR RELEASE: 2007/02/08: CIA-RDP82-00850R000200030043-9

(K_1), Conrad-II layer (K_{II}), roof (M_I) and bottom (M_{II}) of the transition zone from the crust to the mantle and to the interfaces in the mantle (M_M) were considered on recordings from all sources. Transient diffracted waves (PS_{dif}) formed at the interfaces in the earth's crust were also considered.

Separation and Correlation of the First P and S Waves from Local and Near Earthquakes and Explosions

The first arrivals of P waves on recordings from explosions and earthquakes are usually easily separated with high accuracy by the first sharp beginning of oscillations (Figure 50). The degree of reliability of separating the first arrival of P waves is determined by the ratio of the signal to background amplitude of high-frequency noise. The first arrivals of waves on recordings from explosions and near earthquakes are confidentaly separated at $A_s/A_f = 5-10$. Separation of the first arrivals becomes unstable with a decrease of this ratio to three. However, even in these cases when the P waves have higher frequencies than background (Figure 51) or when a sharp disappearance (Figure 52) of it is observed within 0.5-0.8 second prior to the first arrivals, separation of the first arrivals of P waves remains rather reliable. Disappearance of the background prior to the first arrivals of P waves was noted for a number of recordings of aftershocks of the Tashkent earthquake of 26 April 1966. This effect remained unstudied, although one may assume that it is related to variation of some physical parameters of the medium on the focus-recording station path.

S waves are always recorded on a background of previous longitudinal, surface, composite and other types of waves. Therefore, separation of the first arrivals of S waves is frequently more complex than separation of the first arrivals of P waves. The relationship of the intensities of S and P waves has a significant role in this case. In those cases when the S waves are more intensive by an order than P waves, separation of them causes no complications. If the intensities of the P and S waves are comparable or the intensity of S waves is 2-3 times greater than that of the previous P waves, separation of the first arrivals of S waves presents serious difficulties. Since the ratio of the intensities of P and S waves on recordings from explosions and earthquakes is different, the complexity of separating P and S waves from these sources of seismic energy is not identical. S waves on recordings from explosions are less reliably separated than those on recordings from earthquakes, since the intensity of the P waves on recordings from explosions is either comparable or the S waves are not much more intensive (by a factor of 2-3) than P waves (Figure 53). S waves on earthquake recordings are usually more intensive by an order of 0.5-1 than P waves (Figure 54). However, in those cases when S waves are very intensive and fall into the nonlinear part of the amplitude characteristic of the "Zemlya" device, their separation again becomes difficult. This is related to the fact that the amplitudes of S waves are significantly distorted in shape and are reduced in size to the dimensions of the amplitudes of the preceding P waves. This phenomenon was noted on recordings of aftershocks of the Tashkent earthquake of 26 April 1966 during their magnitude of more than 4-5 (see Figure 52).

APPROVED FOR RELEASE: 2007/02/08: CIA-RDP82-00850R000200030043-9

APPROVED FOR RELEASE: 2007/02/08: CIA-RDP82-00850R000200030043-9

Table 7. Number of Useful Recordings Registered by "Zemlya" Station in Different Regions

(1) Район работ	(2) Сроки работ	(3) Записи от			
		(4) далеких землетрясений	(5) близких землетрясений	(6) местных землетрясений	(7) взрывов
(8) Юго-Восток Русской платформы	(9) С 3 июля по 25 октября 1963 г.	89	170 (близких и взрывов)	—	—
(11) Азово-Кубанская впадина	(12) С 16 июля по 23 ноября 1964 г.	96	—	(10) 40	280
(13) Прикаспийская впадина	С 6 июля по 26 октября 1965 г. (14)	88	—	20	160
г. Ташкент (15)	С 13 июля по 22 декабря 1966 г. (16)	151	189	356	110
Северо-Германская (17) впадина	С 1 апреля 1969 г. по 1 сентября 1970 г. (18)	946	7	—	118

Key:

1. Regions of operations
2. Periods of operations
3. Recordings from
4. Remote earthquakes
5. Near earthquakes
6. Local earthquakes
7. Explosions
8. Southeastern Russian series
9. From 3 July through 25 October 1963
10. Near earthquakes and explosions
11. Azov-Kuban' Depression
12. From 16 July through 23 November 1964
13. Pre-Caspian Depression
14. From 6 July through 26 October 1965
15. Tashkent
16. From 13 July through 22 December 1966
17. North German Depression
18. From 1 April 1969 through 1 September 1970

P and S waves are correlated from station to station by the first arrivals. The exchanges of longitudinal and transverse waves related to different crustal interfaces are determined mainly by the breaks of the hodographs of P and S waves caused by variation of the apparaent velocities of P and S waves (V_{Pk} and V_{Sk}).

Determination and Correlation of P and PS Waves During Recordings of Earthquakes and Explosions

Let us consider the recordings from remote earthquakes recorded in platform regions in the presence of the sedimentary mantle from 1 to 15 km thick and at angles of inclination of the interfaces of not more than 10-20°. Separation and correlation of P and PS waves in these regions differ significantly

APPROVED FOR RELEASE: 2007/02/08: CIA-RDP82-00850R000200030043-9

APPROVED FOR RELEASE: 2007/02/08: CIA-RDP82-00850R000200030043-9

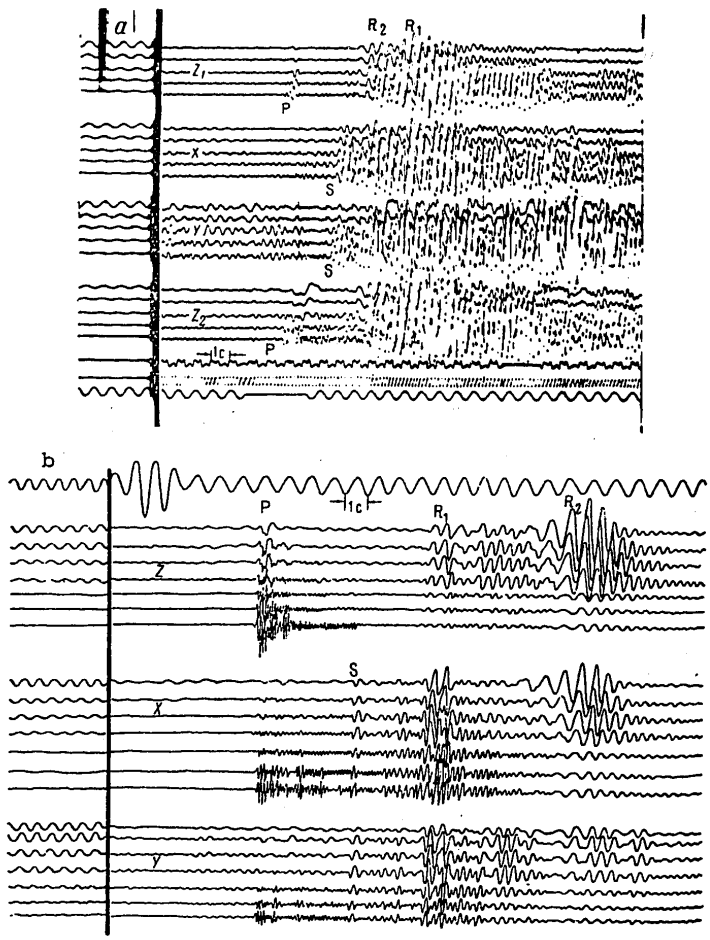

Figure 50. Recordings from Explosions at $\Delta \approx 5$ km Obtained Within Tashkent (a) and Within the Azov-Kuban' Depression (b)

from separation and correlation of P and PS waves in mountain regions where the angles of inclination of the structures may reach 80°. Whereas separation and correlation of PS waves in platform regions are possible from recordings of individual earthquakes, they are determined and correlated in mountain regions by a series of seismograms or even by the histograms or the statistical time profiles $\Delta t_{PS-P} = f(N)$ [113].

APPROVED FOR RELEASE: 2007/02/08: CIA-RDP82-00850R000200030043-9

APPROVED FOR RELEASE: 2007/02/08: CIA-RDP82-00850R000200030043-9

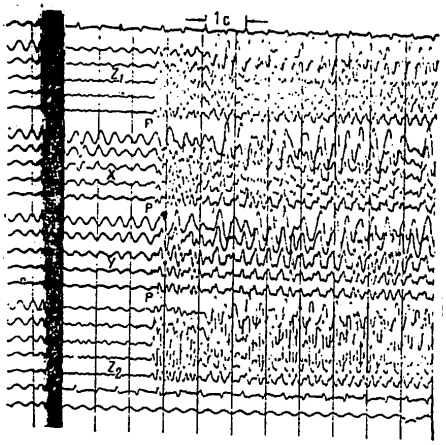

Figure 51. Seismogram from Aftershock of Tashkent Earthquake with Clear Arrival of P Waves: T = 1949, 17 Sep 1967

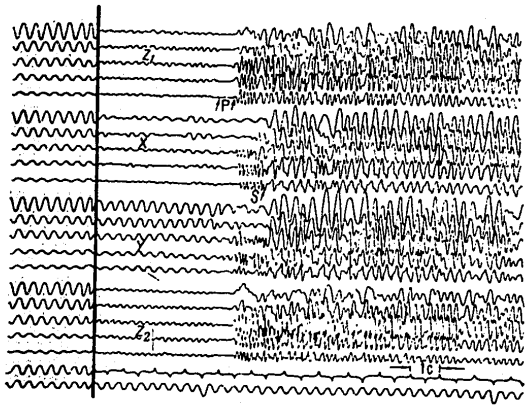

Figure 52. Seismogram from Aftershock of Tashkent Earthquake of 26 April 1966 with Disappearing Low Microseism Background Prior to Arrival of P Waves

APPROVED FOR RELEASE: 2007/02/08: CIA-RDP82-00850R000200030043-9

APPROVED FOR RELEASE: 2007/02/08: CIA-RDP82-00850R000200030043-9

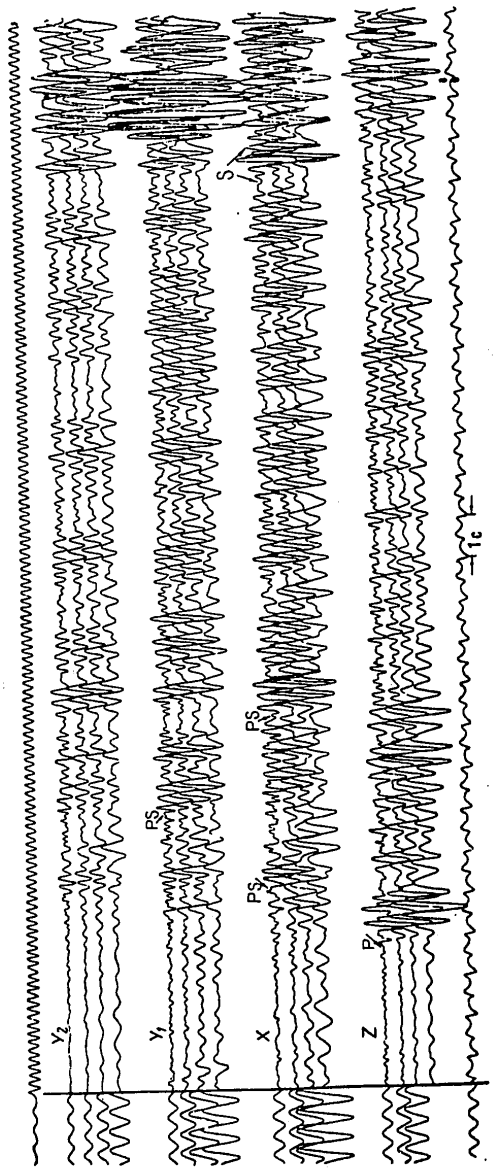

Figure 53. Seismogram from Explosion in the Region of the North German Depression (R = 140.2 km and Q = 1,492 km)

APPROVED FOR RELEASE: 2007/02/08: CIA-RDP82-00850R000200030043-9

APPROVED FOR RELEASE: 2007/02/08: CIA-RDP82-00850R000200030043-9

Separation of PS waves on recordings of earthquakes and explosions and identification of them with P waves is accomplished by the following criteria [6, 18, 20, 108]: recording of PS waves on the horizontal components of the recording, identity of the shapes of recordings of PS waves and the generatrix of their P wave, the proximity of the recording times of P and PS waves, the nature of polarization of PS waves and the distribution of their arrival polarity (at $\varphi < 10°$) mainly by quadrants as in P waves and usually reduced intensity of PS waves by a factor of 2-5 compared to the intensity of P waves.

The reliability of determining PS waves on recordings depends on the shape of oscillations of the generatrices of their P waves. PS waves are clearly determined on recordings of those earthquakes for which only a single P wave or packet of P waves having amplitude 3-5 times or more greater than the amplitude of the preceding microseism background and subsequent P waves (Figure 55) is recorded on the Z components. In these cases the first composite wave is clearly determined on all the earthquake recordings. The first P wave must be time-limited (1-3 periods) to determine the subsequent PS waves outside the interference zone.

The characteristics of P waves forming composite PS waves. All earthquake recordings with Δ = 1.5-10°, h_{och} = 100 m and $\Delta > 10°$ can be divided into four groups by the nature and shape of P wave oscillations.

Group I includes recordings with a single clearly defined P wave in amplitude, recorded in the region of the first arrivals and having 1-3 phases (see Figure 55). The epicenters of these earthquakes are located within Kamchatka, the Kuriles-Kamchatka arc, Japan, in the Pamirs and in the Aegean Sea. The foci of these earthquakes are located in the upper mantle and their average depths are 200 km. Some of the epicenters are located within the Tonga and Kermadec Islands ($\Delta \approx 140°$) and in the regions of the Aegean Sea ($\Delta \approx 20°$),* also with foci in the upper mantle (Figure 56). The P waves are, by their nature, transient waves refracted in the crust (P) and mantle (PKP). The nature of P waves which form clear composite PS waves at the crustal interfaces outside their interference zone were determined in the following manner. The time differences $T-T_0$ of recording the first phases of P waves from earthquakes (T) and the times at the foci (T_0) were applied to the Jeffries-Bullen hodograph. As can be seen from Figure 57, the arrival times of the first phases of P waves recorded by "Zemlya" stations with errors caused by the structural characteristics of the earth's crust and upper mantle under the observation points coincide with the arrival times of longitudinal waves refracted in the crust and mantle (P) and which passed through the earth's core (PKP).

Group II includes recording in which a packet of intensive P waves rather than a single wave is recorded on the Z component (Figure 58, II). These are PKP waves by their nature. The epicenters of these earthquakes are located within the Kermadec Depression and Tonga Islands ($\Delta \approx 140°$). The depths of earthquake foci vary from 120 to 450 km.

*The values of the epicentral distances are given for recording stations operating in the region of the Azov-Kuban' and North German Depressions.

APPROVED FOR RELEASE: 2007/02/08: CIA-RDP82-00850R000200030043-9

APPROVED FOR RELEASE: 2007/02/08: CIA-RDP82-00850R000200030043-9

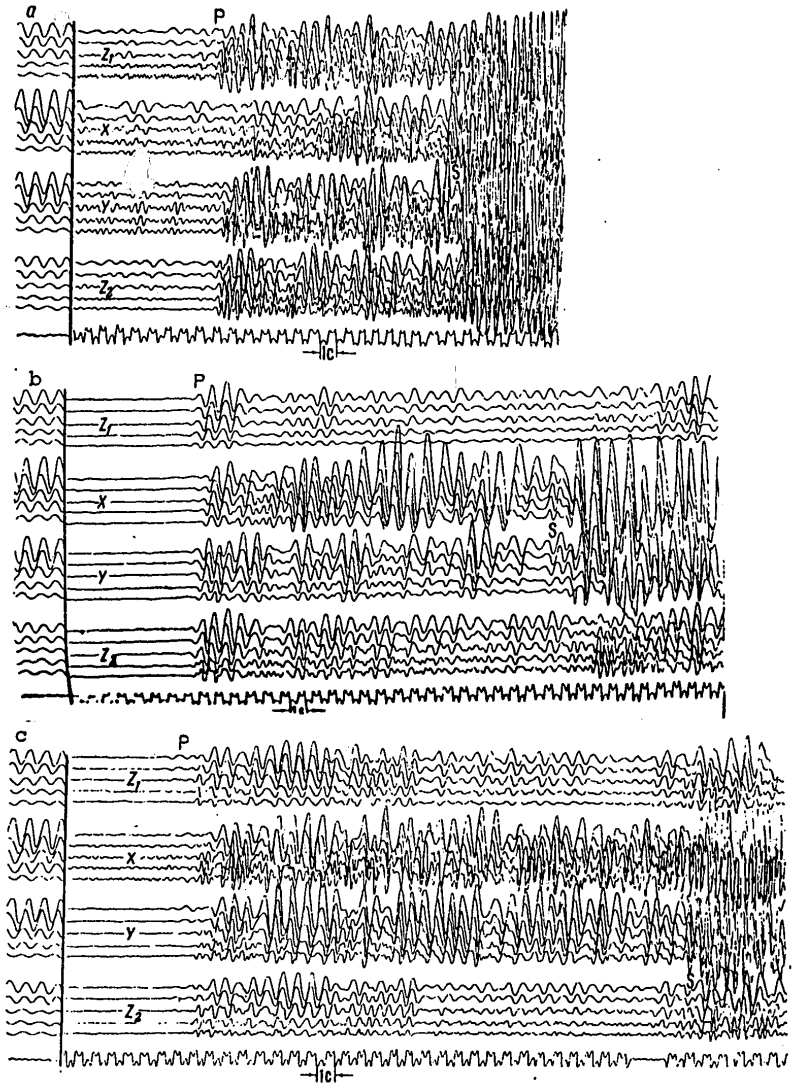

[Caption on following page]

APPROVED FOR RELEASE: 2007/02/08: CIA-RDP82-00850R000200030043-9

APPROVED FOR RELEASE: 2007/02/08: CIA-RDP82-00850R000200030043-9

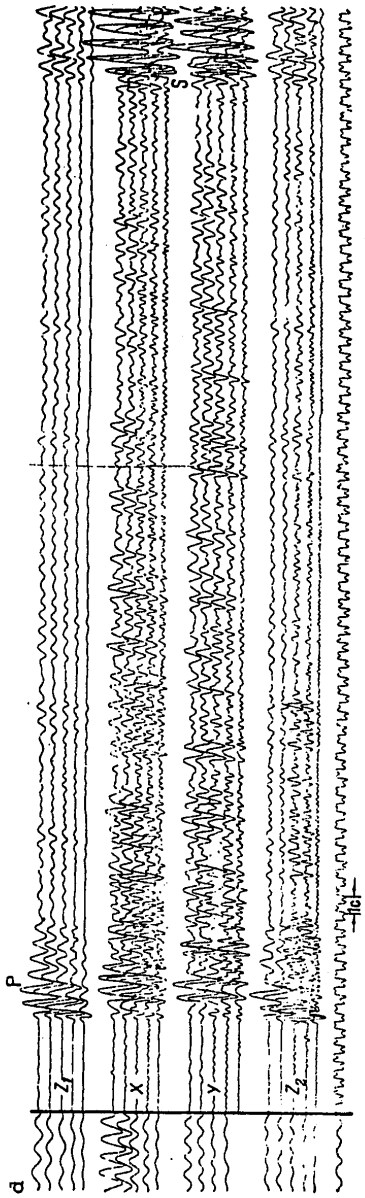

Figure 54. Nature of Wave Pattern on Recordings from Near Earthquakes: a--T = 1939, 3 Sep 1967, Δ = 60 km; b--T = 2108, 7 Sep 1967, Δ = 179.8 km; c--T = 2108, 7 Sep 1967, Δ = 226.4 km; d--T = 0457, 27 Aug 1967, Δ = 500 km

APPROVED FOR RELEASE: 2007/02/08: CIA-RDP82-00850R000200030043-9

APPROVED FOR RELEASE: 2007/02/08: CIA-RDP82-00850R000200030043-9

Group III includes recordings in which two clear P waves separated by a time interval up to 8-15 seconds are recorded on the Z components (Figure 58, III). The epicenters of these earthquakes are located within the Kuriles-Kamchatka arc ($\Delta \approx$ 66-86°) and the depths of the foci are appxoimately 80-100 km. The first P wave is one refracted in the crust and mantle by its nature (see Figure 57) and the second P wave, according to seismological data [65], is a composite-reflected sP wave.

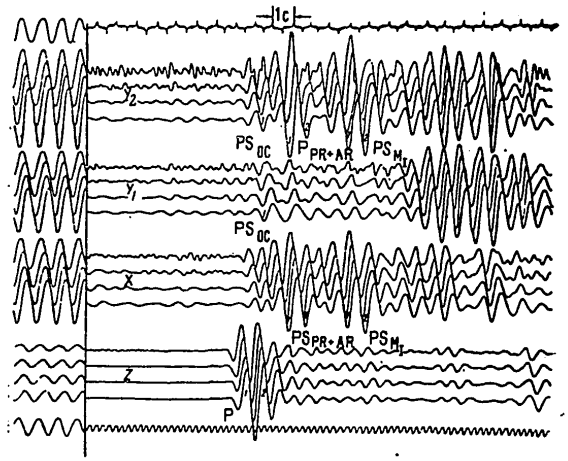

Figure 55. Seismogram with Clear Recording of First P Wave From Earthquake in the Region of the North German Depression:
T = 2305, 11 Aug 1969, Δ = 75.8° and α = 30.8°

Group IV may include recordings on which a large number of P waves comparable in intensities and continuously following each other is recorded (Figure 58, IV). The epicenters of these earthquakes are located within the Mediterranean Sea and transasiatic belt of seismisity, in western Europe and within the Atlantic Ridge. The depths of the foci vary from 20 to 185 km.

The distribution of the total number of earthquakes recorded by the "Zemlya" device by groups of P waves is as follows. If all the clear recordings registered by "Zemlya" stations from remote earthquakes are taken as 100 percent, the number of earthquakes related to group I comprises 15-50 percent in aseismic regions. The maximum number of remote earthquakes ($\Delta >$ 10°) of this type comprised 30-40 percent in seismically active regions (Tashkent). Their number increases to 60 percent with regard to recordings from near earthquakes (Δ = 1-10°). The number of earthquakes of groups II and III is also low and varies from 10 to 15 percent and from 10 to 30 percent, respectively.

APPROVED FOR RELEASE: 2007/02/08: CIA-RDP82-00850R000200030043-9

APPROVED FOR RELEASE: 2007/02/08: CIA-RDP82-00850R000200030043-9

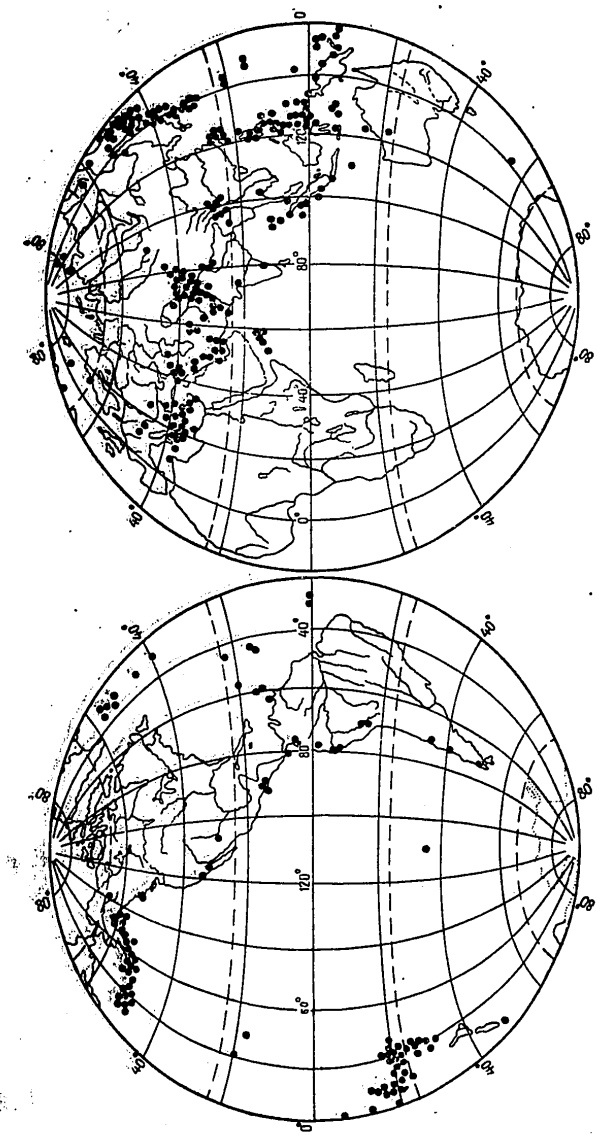

Figure 56. Layout of Epicenters of Remote Earthquakes From Which Clear Composite PS Waves Were Recorded by Means of "Zemlya" Stations in 1962-1971

APPROVED FOR RELEASE: 2007/02/08: CIA-RDP82-00850R000200030043-9

APPROVED FOR RELEASE: 2007/02/08: CIA-RDP82-00850R000200030043-9

Group IV of earthquakes is the most numerous and comprises 50-60 percent, and sometimes 30 percent of the total number of recorded earthquakes. Recordings of most catastrophic earthquakes are related to this group.

Analysis of material obtained from the "Zemlya" stations permits one to assume that the shape of the P-wave recording is apparently determined by processes occurring at the foci at the moment the earthquakes occur and is determined only at zones of large disturbances by seismogeological conditions of the region of investigation and is essentially independent of Δ. The greatest length of recording P waves is observed for focal depths up to 50 km, i.e., for foci located in the crust, and the shortest length is noted for foci with H $\approx$ 200 km (regions of the Kurile arc, Kamchatka, the Pacific Ocean, the Aegean Sea, Hindu-Kush and the Pamirs) and with H = 20-60 km (regions of the Japanese Depression, the Aegean Sea and the Pacific Ocean). The earthquake foci are mainly located in the mantle in both cases. No clear dependence of the length of recording P waves on Δ is observed for the same earthquakes. A similar dependence of the length of recording P waves on the Z component on the depth of the focus is determined upon comparison of recordings from earthquakes obtained at significantly different values of Δ, but with shallow depths of foci [110].

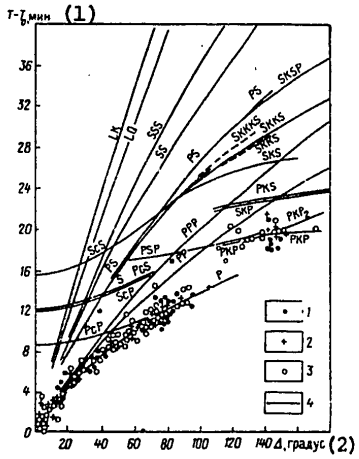

Figure 57. Comparison of the Values of $T-T_0$ for P Waves Recorded by "Zemlya" Stations within the North German (1) and Azov-Kuban' (2) Depressions and in the City of Tashkent (3) to Jeffries-Bullen Hodographs (4) at $h_{och} = 0$.

Key:
1. Minutes
2. Degrees

APPROVED FOR RELEASE: 2007/02/08: CIA-RDP82-00850R000200030043-9

APPROVED FOR RELEASE: 2007/02/08: CIA-RDP82-00850R000200030043-9

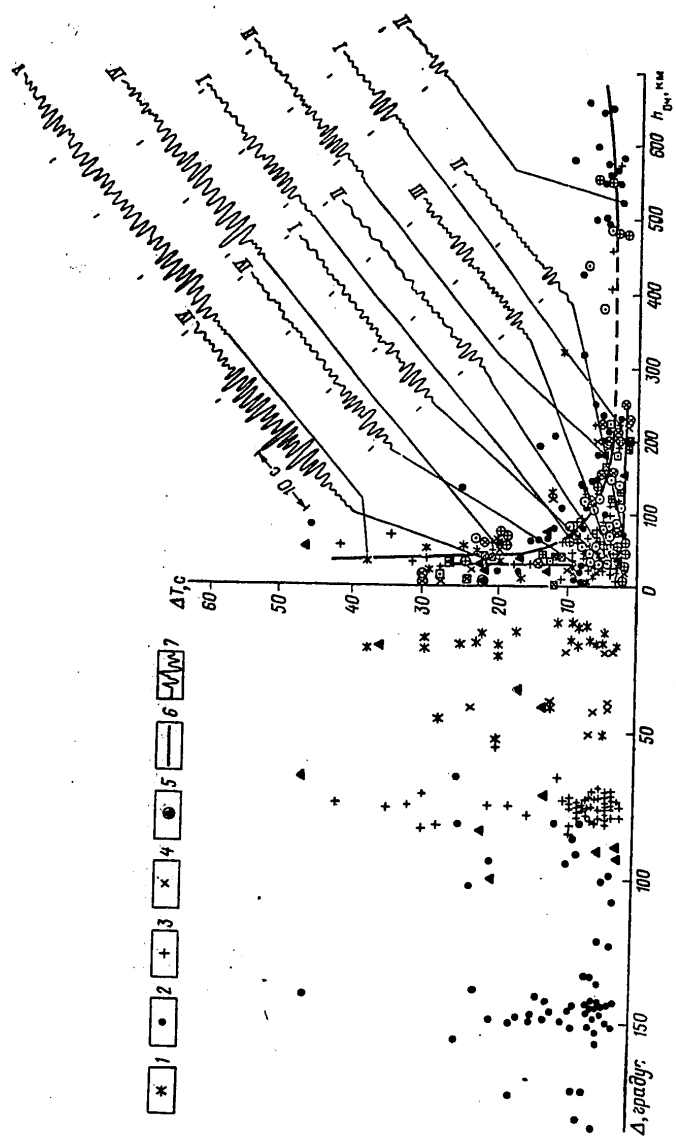

Figure 58. Graphs of Dependence of Recording Time ΔT of First P Waves on hoch and Δ for Different Regions: 1--Turkey and Mediterranean Sea; 2--southern part of Pacific Ocean; 3--Japan, Kurile Islands, Kamchatka and northern part of Pacific Ocean; 4--Hindu-Kush and the Pamirs; 5--Atlantic Ocean and Greenland; 6--averaging lines; 7--shape of P-wave recording with number of its group

APPROVED FOR RELEASE: 2007/02/08: CIA-RDP82-00850R000200030043-9

APPROVED FOR RELEASE: 2007/02/08: CIA-RDP82-00850R000200030043-9

Analysis of recordings registered in different regions, but from the same earthquakes, showed that the shape of the recording of the P wave on the wideband channel (f = 0.5-10 Hz) does not vary significantly upon variation of the epicentral distance from 30 to 100° when operating in sections with sufficiently thick sedimentary mass, excluding regions with salt-dome tectonics. A complex shape of the P-wave recording is observed in regions with salt-dome tectonics and outcrops of crystalline rock to the earth's surface for these same values of Δ. Multiple P waves apparently appear over the domes. An additionally large number of longitudinal waves of rather large amplitude which interfere with each other appears in regions with outcrops of crystalline rock. One may assume that complication of the nature of recording of P waves is related to complication of the P-wave front due to the inhomogeneities of the upper part of the crystalline crust and superposition of additional lateral P waves and also due to the appearance of intensive vertical components of PS waves [110].

Characteristics of recording and determination of composite PS waves. Composite PS waves in the presence of a sedimentary mantle with velocities up to 5 km/s are recorded only on the horizontal components (see Figure 55). Composite PS waves are separated on recordings of local, near and remote earthquakes from explosions. However, confident separation of them and tracking are possible on recordings from remote and partially from deep-focus near earthquakes of the groups analyzed above. The complexity of determining PS waves on recordings from explosions and local earthquakes is explained in the following manner. PS waves on a recording from explosions may be confidently separated at the same distances and times where there are not other waves of any kind and when a single wave or a packet of P waves is recorded on the Z component. A large number of waves: surface, reflected and single and multiple refracted whose total length exceeds 10-20 seconds (Figure 59) is usually registered in the initial part of the seismogram recording upon excitation of oscillations by explosions (Δ = 0-250 km). The angles of emergence of all these waves are close to 45°, as a result of which the same complex wave pattern is observed on the X and Y components as on the Z components. With a time difference of recording PS waves from different crustal interfaces of 0.5-1 second, PS waves with length of 10-20 seconds will be complexly interpreted between each other from each of these boundaries. It is impossible to visually separate and distinguish PS waves related to different boundaries in this zone. The existing program of V. N. Troyan [44] does not operate under these conditions. A similar complex wave pattern is observed on recordings from local and near earthquakes with foci at the crust [110]. Moreover, PS waves from explosions and near and local earthquakes have visible frequencies from 3 to 10 Hz. Ordinary phase correlation of composite waves cannot be carried out for these waves with spacing of 5-7 km between the recording stations and v_k = 6-9 km/s. Therefore, recordings from explosions and near and local earthquakes located in the crust cannot be used as the main recordings for separation and tracking of PS waves from station to station.

APPROVED FOR RELEASE: 2007/02/08: CIA-RDP82-00850R000200030043-9

APPROVED FOR RELEASE: 2007/02/08: CIA-RDP82-00850R000200030043-9

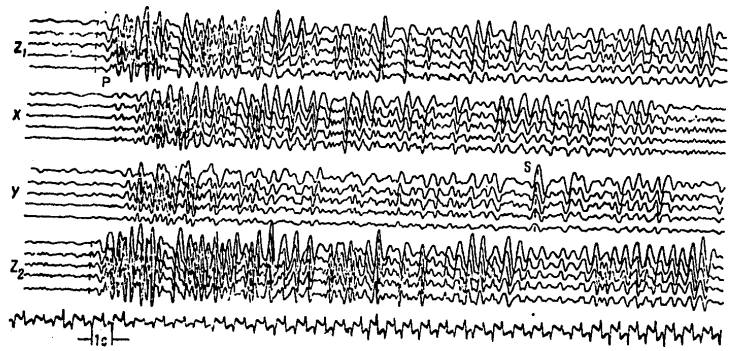

Figure 59. Nature of P-Wave Recording Registered from Explosion in the Region of the Pre-Caspian Depression: T = 0219, 15 Sep 1965, Δ = 140°

The PS waves (f $\approx$ 1-3 Hz) are separated more systematically and reliably on recordings of deep-focus near (Δ = 1-10°) (Figure 60) and remote (Δ = 10-160°) earthquakes. The shape of the P-wave recording from these earthquakes on the same recording station spacing (approximately 100 km) essentially does not vary (Figures 60 and 61). A correlation seismogram obtained by means of SS-24-61M stations is presented in Figure 61; the spacing between recording stations is 5-6 km and the total length of the installation is approximately 100 km. The reproduction recordings have both the use of 100 percent mixing of three channels with overlapping of two channels and without the use of these channels. A recording of one of the Z channels is presented for comparison of the shape of the P and PS wave recordings and the tie-ins of them in time over the groups of channels X and Y.

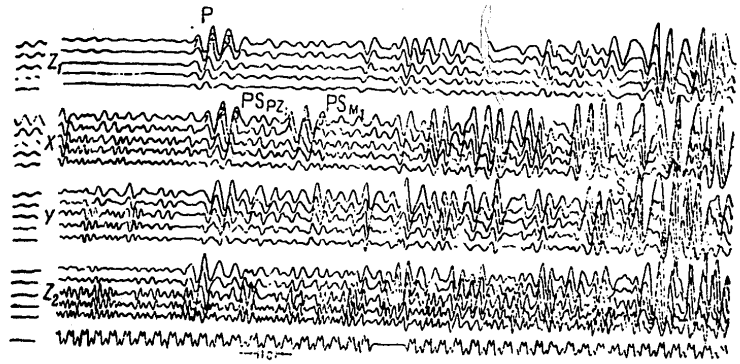

Figure 60. Recordings of Longitudinal, Transverse and Composite Waves Registered from Near and Deep-Focus (H $\approx$ 200 km) Earthquakes in the Region of Tashkent: T = 0755, 28 Sep 1967, Δ = 7.8° and α = 40°

APPROVED FOR RELEASE: 2007/02/08: CIA-RDP82-00850R000200030043-9

APPROVED FOR RELEASE: 2007/02/08: CIA-RDP82-00850R000200030043-9

PS waves are most clearly determined on recordings from earthquakes related by the shape of the P wave to groups I and III. The first P waves on the Z components of these earthquakes are unique on the recordings; therefore, all the waves at times of 0-11 seconds can be formed at the crustal interfaces only from these P waves. One can usually determine only the first phases of the first PS wave on earthquake recordings of group II (see Figure 58), characterized by the presence of a packet of P waves of long length (up to 6-8 seconds). Finally, the least promising for determining clear composite waves are earthquake recordings of group IV. One can confidently determine, with rare exceptions, only the first composite wave on recordings of these earthquakes (see Figure 58, IV). The presence of P waves with low intensity in time, the clear recording of PS waves from the crustal interfaces outside the interference zone and the possibility of fulfilling the conditions of phase correlation of P and PS waves permits one to consider recordings from deep-focus near and remote earthquakes of groups I and III as the most optimum for study of the structure of the earth's crust and mantle.

Correlation of P and PS waves. It is impossible to correlate PS waves from station to station by the shape of the recording. All PS waves related to different crustal interfaces are similar to the P waves from which they were formed. However, despite the similarity of the shape of recording, each reference boundary places its own mark on the amplitude, nature of polarization and the order of recording the composite wave which was formed on it. Based on this, we proposed that phase correlation of PS waves and correlation by the regions of their common deep points be used and also that the nature of variation of the amplitudes, polarization properties and sequence of registering PS waves on recordings be taken into account to trace PS waves from station to station (mainly for simple, platform regions with $\varphi < 10°$).

The necessary condition for phase correlation of P and PS waves is that the time displacements of recording the maximums of these waves of the same type may not exceed 1/4 or 1/2 of their period. This is possible for remote earthquakes when the recording stations are spaced no more than every 5-6 km, since $\Delta x = v_k T/2$ ($v_k \geqslant 10$ km/s and T = 1 second).

Phase correlation of P and PS waves is accomplished both by separate seismograms and by correlation seismograms specially compiled for each earthquake (see Figure 61). The latter are obtained by using the modernized SS-24-61M attachment and at computer centers (Figures 61 and 62).

A series of standard programs designed to separate and correlate reflected waves: mixing, various types of filters, deconvolution and so on (Figure 62, c) was used to improve phase correlation of PS waves at sigma-5 and CDC-3300 computer centers. Signal mixing and grouping are used at the SS-24-61M station. Phase correlation is carried out in sequence for each earthquake. The results for all earthquakes are applied to ordinary or statistical time profiles (Figure 63). Since recordings from 4 to 20 earthquakes of groups I and III are registered at the same stopover, the number of time profiles for all deep crustal boundaries on the same spacing of stations is no less than 4.

APPROVED FOR RELEASE: 2007/02/08: CIA-RDP82-00850R000200030043-9

APPROVED FOR RELEASE: 2007/02/08: CIA-RDP82-00850R000200030043-9

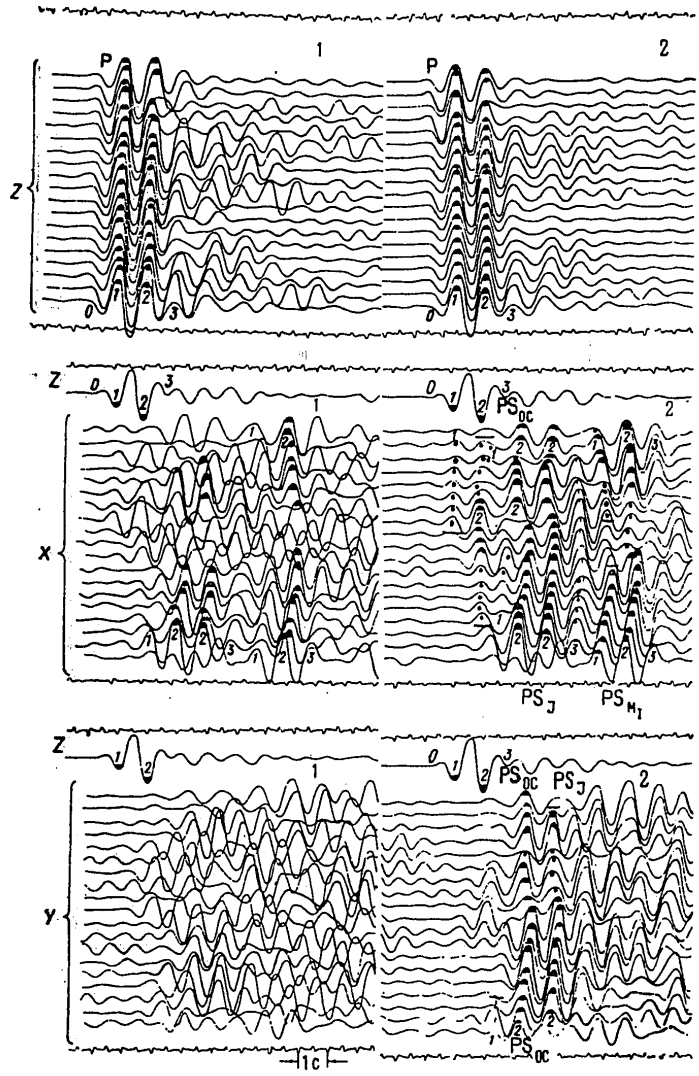

Figure 61. Correlation Seismogram Obtained by Using SS-24-61M Stations: T = 0828, 16 Jul 1969, Δ = 71° and α = 21°; 1--reproduction without mixer; 2--reproduction with mixer

APPROVED FOR RELEASE: 2007/02/08: CIA-RDP82-00850R000200030043-9

APPROVED FOR RELEASE: 2007/02/08: CIA-RDP82-00850R000200030043-9

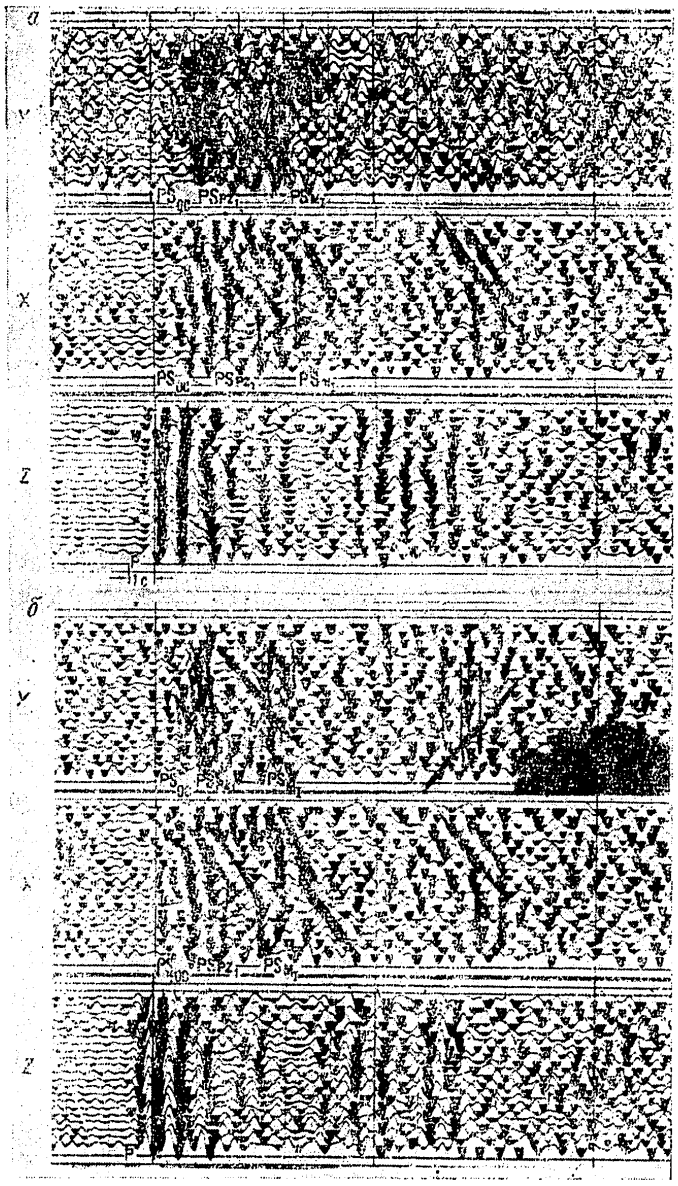

[Caption on following page]

APPROVED FOR RELEASE: 2007/02/08: CIA-RDP82-00850R000200030043-9

APPROVED FOR RELEASE: 2007/02/08: CIA-RDP82-00850R000200030043-9

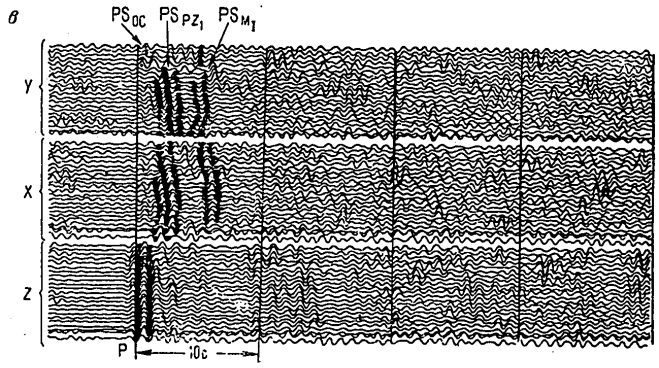

Figure 62. Correlation Seismograms of Earthquakes Obtained at a Computer Center with Sigma-5 Computers Using Band Filtration of 10-35 Hz (a), Band and Reverse Filtration of 10-60 Hz (b) and 100 Percent Mixing of the Three Sequential Channels with Overlapping of Two Channels (c): T = 1354, 14 Jun 1969, Δ = 21° and α = 150°

The coincidence of time profiles from different earthquakes, but having similar values of Δ, indicates the correctness of phase correlation by single earthquakes. A check of the correctness of phase correlation may also be the coincidence of depths to the interfaces in regions of their common points (Figure 64).

Fault zones are observed when working in mountain regions where there is no sedimentary mantle and the angles of inclination of the interfaces may reach 80°. Separation and especially phase correlation of the PS wave for individual seismograms are significantly complicated in these regions. This is related to the time scattering effects Δt_{PS-P} (see Chapter 2) due to the effect of the angle of inclination of the interface and the presence of lateral waves (transient diffracted and transient reflected PS waves) on transient PS waves. Separation and correlation of PS waves on statistical time profiles (Figure 63) are possible by their maximum values. Special processing methods must also be used during detailed study of the structure of the crust in these regions in addition to statistical accumulation of PS waves (see Chapter 7).

APPROVED FOR RELEASE: 2007/02/08: CIA-RDP82-00850R000200030043-9

APPROVED FOR RELEASE: 2007/02/08: CIA-RDP82-00850R000200030043-9

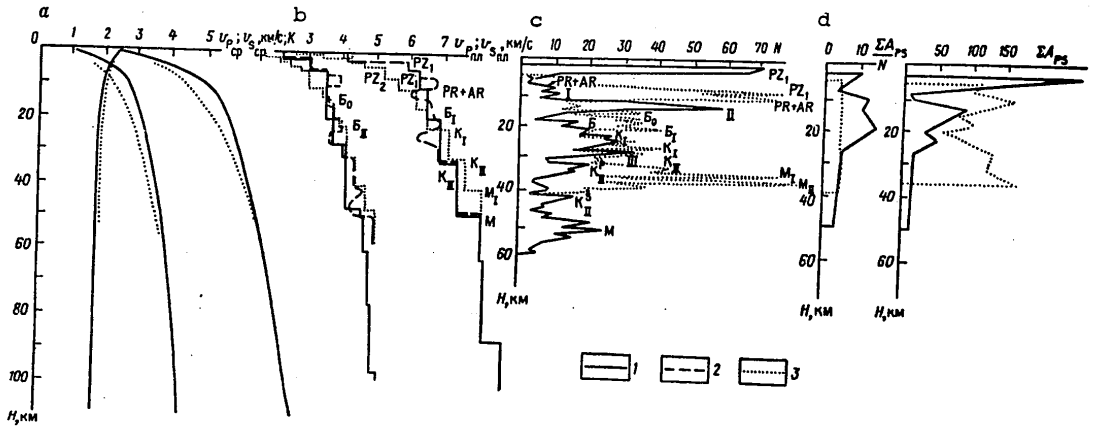

Figure 63. Velocity (a and b), Time (c) and Dynamic (d) Models of the Earth's Crust of the Northern Part of the North German Depression and Rayons of Tashkent: 1 and 3--data of "Zemlya" stations for rayons of Tashkent and the northern part of the North German Depression, respectively; 2--data of seismology (according to Ye. M. Butovskaya) by rayons of Tashkent; PZ_1--Caledonian basement; PZ_2--Variscian basement; PR + AR--Precambrian; B_0, B_I and B_{II}--roof and bottom of transition zone from granite to basaltic layer and boundary within the basaltic layer, respectively; K_I and K_{II}--Conrad-I and Conrad-II discontinuities; M, M_I and M_{II}-- Mohorovicic discontinuities; I and II--roof and bottom of layer with increased velocity of wave propagation; III--boundary within basaltic layer

APPROVED FOR RELEASE: 2007/02/08: CIA-RDP82-00850R000200030043-9

APPROVED FOR RELEASE: 2007/02/08: CIA-RDP82-00850R000200030043-9

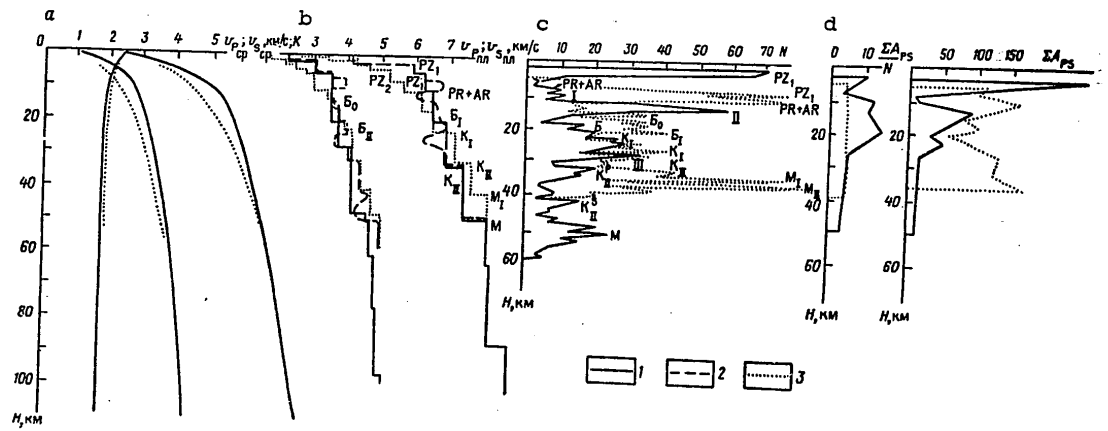

Figure 63. Velocity (a and b), Time (c) and Dynamic (d) Models of the Earth's Crust of the Northern Part of the North German Depression and Rayons of Tashkent: 1 and 3--data of "Zemlya" stations for rayons of Tashkent and the northern part of the North German Depression, respectively; 2--data of seismology (according to Ye. M. Butovskaya) by rayons of Tashkent; PZ_1--Caledonian basement; PZ_2--Variscian basement; PR + AR--Precambrian; B_0, B_I and B_{II}--roof and bottom of transition zone from granite to basaltic layer and boundary within the basaltic layer, respectively; K_I and K_{II}--Conrad-I and Conrad-II discontinuities; M, M_I and M_{II}-- Mohorovicic discontinuities; I and II--roof and bottom of layer with increased velocity of wave propagation; III--boundary within basaltic layer

APPROVED FOR RELEASE: 2007/02/08: CIA-RDP82-00850R000200030043-9

APPROVED FOR RELEASE: 2007/02/08: CIA-RDP82-00850R000200030043-9

The essence of correlation of PS waves by the regions of common (deep) points includes the following. Depth distribution diagrams to the interfaces are constructed (see Chapter 7). As a result of the fact that the sources are located at different points with respect to the stopovers of the recording stations, one can obtain recordings of PS waves at several stations and from different earthquake foci from the same point or closely located points of the interface. The condition of equivalent depths (with error permissible for the composite wave method) obtained for the same region of points, but at different stations and from different earthquakes, permits one to relate the considered composite waves to the same interface. A chart of the surface of the basaltic layer compiled for the region of Tashkent is presented in Figure 64. The error of determining the depths comprises approximately $\pm$ 1 km. The regions of various depths outlined in Figure 64 by the thin closed lines were obtained during recording of PS waves at different stations and from different earthquakes. A single region of common points permits one to note the same exchange surface, but obtained on recordings from different earthquakes on the time profile. Analysis of PS waves obtained in these regions and combination of them on separate sections of the time profile into a single boundary permit one to draw a single continuous boundary, selecting the common deep points of the overlapping sections of time profiles by regions. The coincidence of the obtained boundary with that constructed during phase correlation of PS waves indicates the correctness of the constructions. This check is especially necessary upon transition through fault zones where phase correlation of PS waves undergoes separation.

PS waves related to different crustal interfaces have a somewhat different amplitude expression which is determined by the structure of the interface, the size of the jump of velocities and the angle of incidence of the P wave on it. PS waves corresponding to the same interface in regions of their common points are easily sustained by intensity for earthquakes with different values of Δ (but $\Delta > 10°$) and α. PS waves of the same type on recordings from earthquakes with similar values of Δ and α are easily sustained in regions with complex salt-dome tectonics.

The sequence of recording reference PS waves on a recording of components of the same type and their number on recordings of different stations, but from the same earthquake, are usually maintained.

Additional composite waves traced between the main reference waves may appear in some cases at some recording stations of the same stopover, but from different foci. However, they are usually less intensive under simple platform conditions and do not strongly interfere with recording of the main reference composite waves of the investigated region.

Polarization of PS waves exchanged at the same interface (if its slope does not change to the opposite) and the polarity of their rivals with respect to P waves remain constant for each earthquake. If the angles of inclination of the interfaces vary by even 10°, the azimuths of the polarization planes

APPROVED FOR RELEASE: 2007/02/08: CIA-RDP82-00850R000200030043-9

APPROVED FOR RELEASE: 2007/02/08: CIA-RDP82-00850R000200030043-9

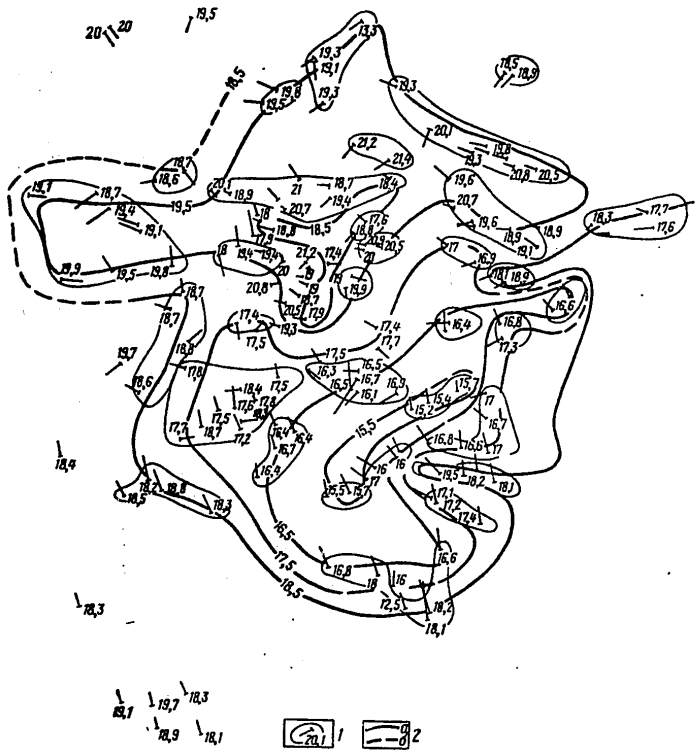

Figure 64. Diagram of Depths to Surface of Basaltic Layer in the Region of Tashkent from Data of "Zemlya" Stations: 1--regions of common depths (km) with direction of arrival or waves from earthquakes to the recording stations; 2--confident (a) and doubtful (b) isolines of depths.

of PS waves may deviate from the azimuths of the polarization planes of P waves impinging on the interface up to 60°. As a result, PS waves may approach from quadrants different from those for P waves and the polarity of their arrivals with respect to P waves will differ from that of the arrivals of PS waves recorded at adjacent stations with different orientation of the interfaces.

The Wave Pattern on Recordings from Local Earthquakes (Δ = 0-40km)

Tremors of the soil surface from the aftershocks of the Tashkent earthquake of 26 April 1966 during the summer season were recorded in Tashkent itself

APPROVED FOR RELEASE: 2007/02/08: CIA-RDP82-00850R000200030043-9

APPROVED FOR RELEASE: 2007/02/08: CIA-RDP82-00850R000200030043-9

at intervals from 3 minutes to several hours. Adjacent tremors frequently followed within fractions of a second, as a result of which several P and S waves were seemingly registered from the same aftershock on the recordings (Figure 65). Clear packets of direct P and S waves (see Figures 51 and 65) were recorded and PS and SP waves were sporadically recorded on recordings from the aftershocks of the Tashkent of 26 April 1966. The time interval between the arrival of P and S waves was short and varied from 0.8 to 1.5 second. The total length of recording all P and S waves reached 250 seconds and dependent on the energy class K of the earthquake.* The length was increased by an average from 10 to 250 seconds with an increase of K from 5.7 to 11.5. The magnitudes of the aftershocks of the Tashkent earthquake comprised an average of 5.5 and the intensity was 4-7 units (from data of the Tashkent Seismological Station). Microscopic earthquakes (with intensity less than 2 units) apparently having foci in the sedimentary mantle were also recorded by the "Zemlya" stations (Figure 66). The intensity of S waves is 3-5 times higher than that of P waves on recordings from the aftershocks (2-4 units), while the frequency is 2-4 times lower. The frequencies of P waves varied from 8 to 10 Hz (Figures 67 and 68) and those of S waves varied from 3 to 8 Hz.

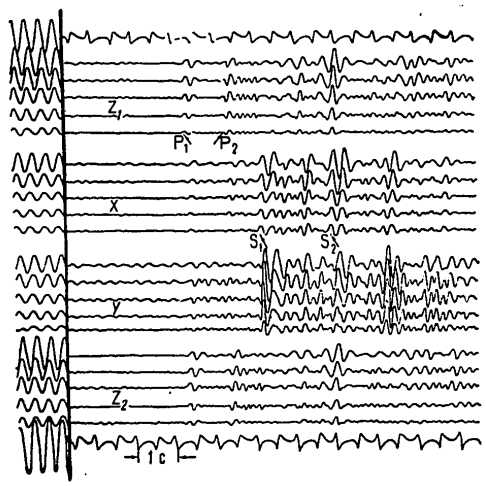

Figure 65. Recordings of Weak Aftershocks of Tashkent Earthquake of 26 April 1966 with P and S Waves

*The energy class of earthquakes is K = lgE, where E is the seismic energy of the earthquake focus in joules.

APPROVED FOR RELEASE: 2007/02/08: CIA-RDP82-00850R000200030043-9

APPROVED FOR RELEASE: 2007/02/08: CIA-RDP82-00850R000200030043-9

The Wave Pattern on Recordings from Near Earthquakes (Δ = 50-500 km)

Direct or refracted P and S waves are determined on recordings from near earthquakes as a function of the relationship of Δ and h_{och} and clear PS and SP waves are frequently present (see Figures 54 and 60). Direct waves are recorded first on the recordings of P and S waves at $\Delta \leqslant h_{och}$ and refracted waves are recorded at $\Delta \geqslant h_{och}$. P waves have frequencies of 3-5 Hz and S waves have frequencies of 1-2 Hz (see Figures 67 and 68). The total length of recording P and S waves is different and is greater by approximately an order than that of S waves. The intensity of S waves is also approximately an order greater than that of P waves (see Figure 54).

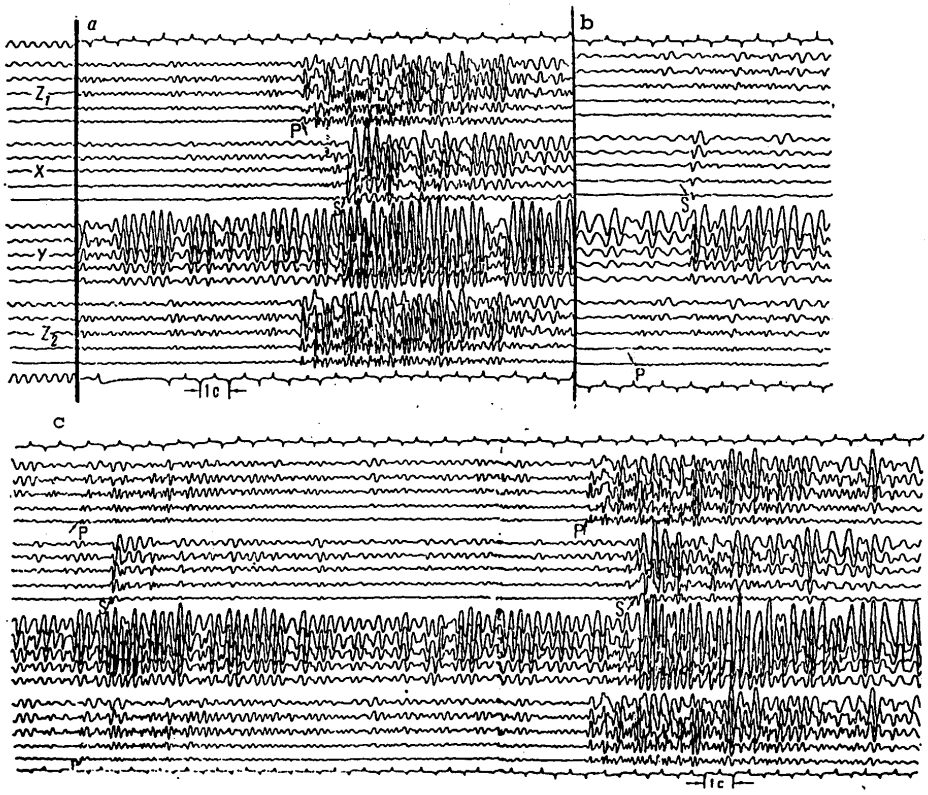

Figure 66. Recordings of Weak Aftershocks of Tashkent Earthquake of 26 April 1966 (b and c) During the Interval Between Recordings of Aftershocks with Intensity 2 (a and d)

The nature of the wave pattern on recordings from near earthquakes varies with variation of h_{och} and Δ. Deep-focus ($h_{och} \approx$ 200 km) earthquakes in

APPROVED FOR RELEASE: 2007/02/08: CIA-RDP82-00850R000200030043-9

APPROVED FOR RELEASE: 2007/02/08: CIA-RDP82-00850R000200030043-9

the Pamirs and Tyan'-Shan' have the simplest shape of recording of P and S waves and sharp arrivals. Waves from these earthquakes frequently have 2-3 periods (see Figure 60). Complication of the recording of P and S waves the same as for remote earthquakes is observed with a decrease of the focal depth, especially when it is displaced into the crust: an increase of their length and the appearance of various types of waves reflected from the crust and refracted in the crust occur. The clarity of P and S wave arrival and the nature of interference of P waves and especially of S waves vary with variation of Δ. Arrivals of P waves are more clearly noted at short epicentral distances and those of S waves are noted at long distances. This is related to the fact that S waves are recorded on a background of intensive subsequent P waves at small values of Δ (0-70 km). P and S waves are already separated by a time interval with an increase of epicentral distance and, beginning at $\Delta \approx$ 100-500 km, S waves are essentially recorded after attenuation of all oscillations caused by P waves (see Figure 54).

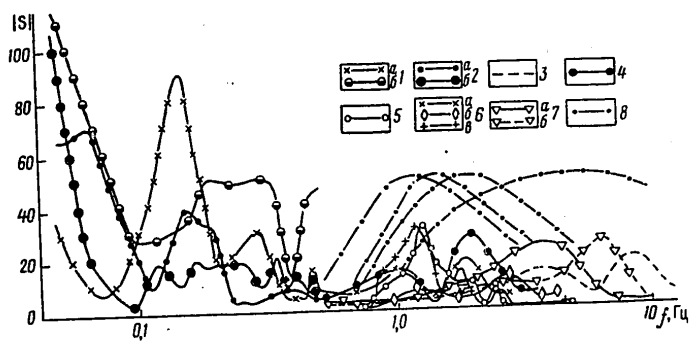

Figure 67. Amplitude-Frequency Spectra of P Waves Recorded by Seismological Apparatus (1 and 2) from Earthquakes and by "Zemlya" Stations from Earthquakes (3-6) and Explosions (7):
1-- $\Delta < 10°$; 2-- $\Delta = 60°$; a--h_{och} = 30-60 km; 6--h_{och} = 150 km; b-- $\Delta = 1°$; 4-- $\Delta = 20°$; $h_{och} = 0$; 5-- $\Delta = 40°$, h_{och} = 30 km; 6-- $\Delta = 70°$; a--h_{och} = 200 km; b--h_{och} = 100 km; c--h_{och} = 580 km; 7--P waves from explosions: a-- Δ = 50 km; b-- Δ = 60 km; 8-- frequency characteristics of "Zemlya" apparatus

The general nature of variation of the wave field can be followed on the summary hodograph and the graph $v_k = f(\Delta)$ of the first P and S waves (Figure 69 and 70). The value of v_k increased rapidly from 1.5 to 5.8-6.2 km/s for longitudinal waves at distances from 0 to 10 km from the focus. At Δ = = 10-45 km, the value of v_k of P waves increases slightly from 5.8 to 6.4 km/s; at Δ = 60-150 km, the value of v_k remains essentially constant and is equal to 6.4-65. km/s; a decrease in the values of v_k to 6 km/s is observed at

APPROVED FOR RELEASE: 2007/02/08: CIA-RDP82-00850R000200030043-9

APPROVED FOR RELEASE: 2007/02/08: CIA-RDP82-00850R000200030043-9

Δ = 150-180 km. A sharp jump of values from 6 to 8 km/s is observed at Δ = 180-200 km. Some decrease of velocities to 7.6-7.8 km/s is then observed at Δ = 180-300 km. Velocity v_k increases from 7.6 to 9 km/s at distances from 300 to 600 km. A jump of velocities to 10-15 km/s is observed at distances from 450 to 500 km. This sharp increase of velocities is difficult to explain; it is not excluded that it is caused by failure to consider some factor and is an error caused by the effect of the focal depth.

The values of the velocities of S waves vary within the following range. The value of v_k comprises 0.6-3.6 km/s at distances of Δ = 0-165 km. A jump of v_k from 3.6 to 4.65 km/s is observed at Δ = 165-180 km. The value of v_k decreases to 4.3 km/s at distances of Δ = 260-370 km. The value of v_k increases to 5 km/s at Δ = 370-500 km and is equal to 5-5.3 km/s at Δ = 500-600 km.

The Wave Pattern on Recordings from Explosions (Δ = 0-700 km)

Longitudinal and transverse waves are determined and PS and SP composite waves are sporadically determined on recordings from explosions (see Figure 53). Clearn intensive surface R_1 and R_2 Rayleigh waves, 5-10 times more intensive than P waves (see Figure 50), are determined in regions with the presence of a low-velocity mass of sedimentary rock, for example, within the Azov-Kuban' Depression and Tashkent, on recordings from explosions. The intensity of S waves is either comparable or 2-3 times higher than that of P waves. S waves frequently are not determined by intensity among subsequent oscillations of P waves. The frequencies of P waves depend on Δ and vary from 5 to 8 Hz (see Figures 67 and 68) and the frequencies of S waves vary from 3 to 5 Hz. The first phases of Rayleigh waves ($f \approx$ 0.6-1.2 Hz) have the lowest frequencies. The last phases have frequencies of 1-5 Hz. R_1 and R_2 waves have a clearly marked dispersion. The length of the recordings of packets of individual P, S and R waves from explosions is different: it is maximum (5-25 phases) for R waves and minimum (5-10 phases) for P waves.

The nature of the wave pattern on recordings from explosions can be followed on summary hodographs compiled for the regions of the Southeastern Russian Platform, the North German and Azov-Kuban' Depressions. R waves were not recorded in the first two regions. They were clearly determined on the recordings in the third region (see Figure 50).

A summary hodograph of the Southeastern Russian Series (Figure 71) consists of two branches: a summary hodograph of explosions and subsurface earthquakes with focal depth of $h_{och} \approx 0$ and a summary hodograph of earthquakes with h_{och} = 30-50 km. The points of the hodograph at $h_{och} \approx 0$ are easily averaged by straight lines along which five different values of v_k can be determined.

The dips of the hodographs correspond to distances of 160, 200-220, 400 and 500 km from the point of the explosion.

APPROVED FOR RELEASE: 2007/02/08: CIA-RDP82-00850R000200030043-9

APPROVED FOR RELEASE: 2007/02/08: CIA-RDP82-00850R000200030043-9

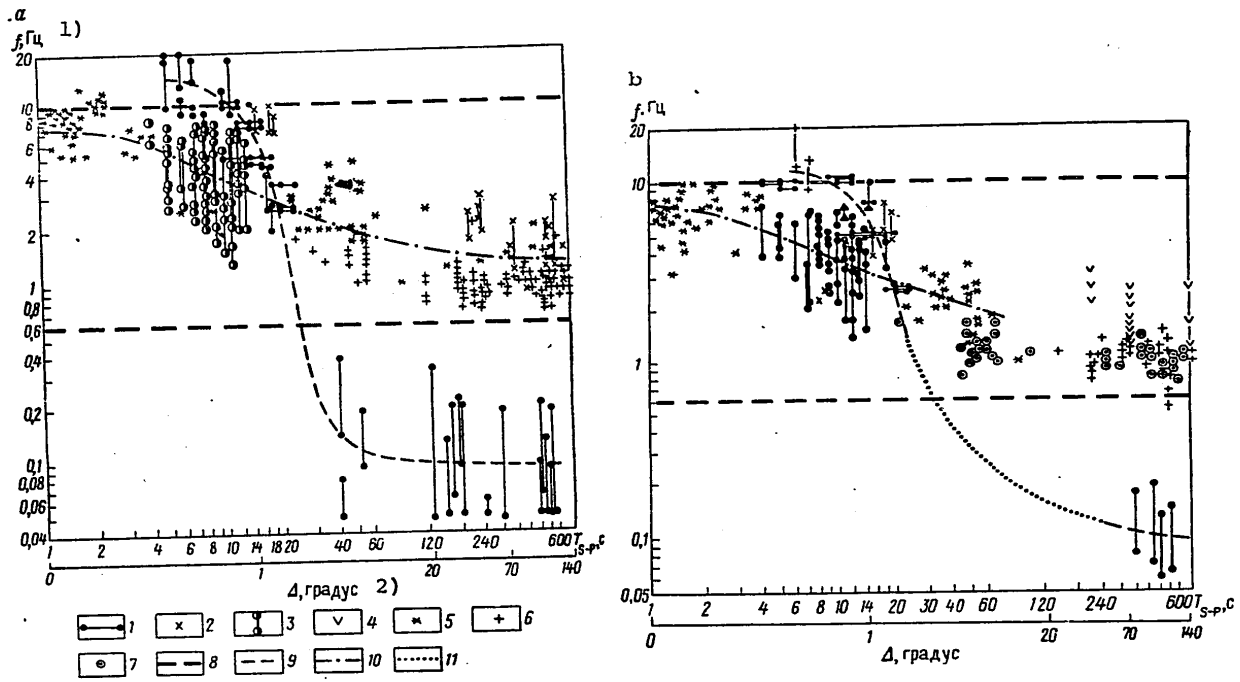

Figure 68. Maximum Frequency Spectra and Values of Visible Frequencies of P(a) and P and PS (b) Waves Recorded by Seismological Apparatus and "Zemlya" Stations: maximum frequency spectra: 1--seismological data [153, 157]; 2 and 3--data from "Zemlya" stations from earthquakes and explosions, respectively; 4--data of "Zemlya" stations from remote earthquakes; 5 and 6--values of visible frequencies of P and S waves from data of "Zemlya" stations from local, near and remote earthquakes, respectively; 7--values of visible frequencies of PS waves from data of "Zemlya" stations from remote earthquakes; 8--bandpass of "Zemlya" device at 0.7 of maximum frequency characteristic; 9--curve which averages seismological data; 10--curve which averages data obtained by "Zemlya" device; 11--proposed position of curve 9

Key:
1. Hertz
2. Degree

APPROVED FOR RELEASE: 2007/02/08: CIA-RDP82-00850R000200030043-9

APPROVED FOR RELEASE: 2007/02/08: CIA-RDP82-00850R000200030043-9

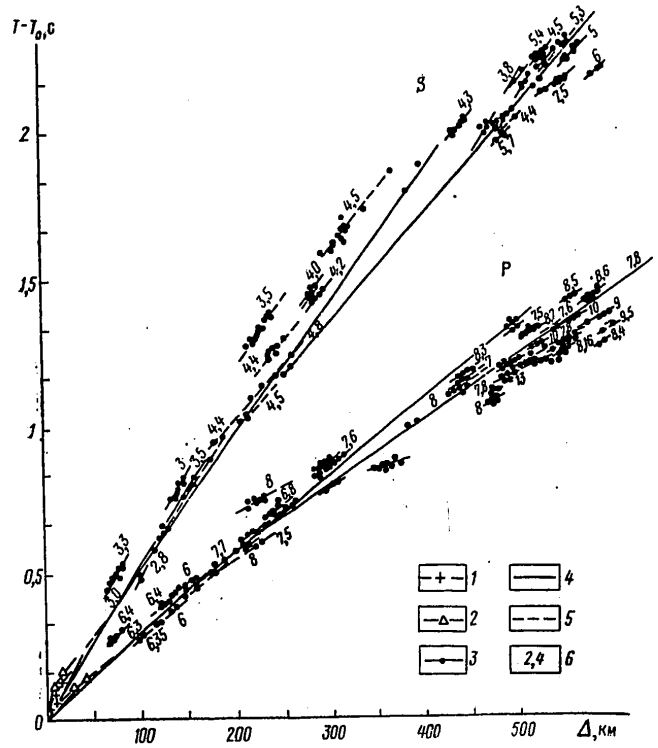

Figure 69. Summary Hodograph of P and S Waves Compiled by Recordings from Near Earthquakes and Explosions for Tashkent (1-3) and Rayons Around Tashkent(4): 1--hodographs of first arrivals of P and W waves from seismological data of Ye. M. Butovskaya; 2 and 3--hodographs of P and S waves from data of "Zemlya" stations compiled by explosions and local earthquakes, respectively; 4--hodographs of first arrivals of P and S waves compiled from seismological data of Ye. M. Butovskaya at $h_{och} = 0$; 5--averaging lines for individual earthquakes; 6--values of apparent velocities in km/s

A summary hodograph of the first arrivals of P and S waves of the North German Depression was compiled from recordings from special explosions at known coordinates and at the moment of the explosion (Figure 72).

Averaging of the points by the least squares method made it possible to obtain linear hodographs of P and S waves with the values shown in Figure 72. The points of the dips of the hodographs of P and S waves arrive at approximately

APPROVED FOR RELEASE: 2007/02/08: CIA-RDP82-00850R000200030043-9

APPROVED FOR RELEASE: 2007/02/08: CIA-RDP82-00850R000200030043-9

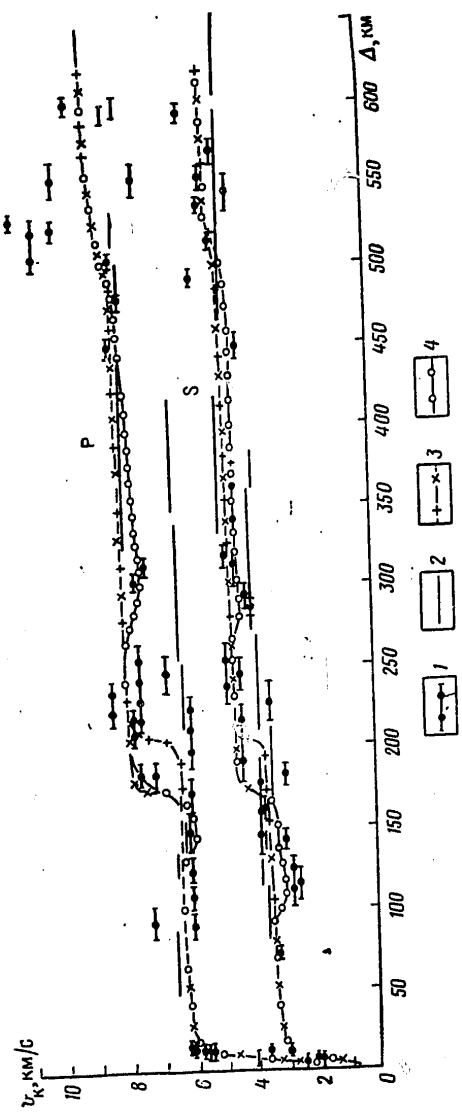

Figure 70. Graphs of $v_k = f(\Delta)$ from Summary Hodograph of Figure 69: 1--from hodographs of P and S waves in the region of first arrivals; 2--from hodographs of P and S waves in subsequent part of recording; 3 and 4--different versions of curve averaging

APPROVED FOR RELEASE: 2007/02/08: CIA-RDP82-00850R000200030043-9

APPROVED FOR RELEASE: 2007/02/08: CIA-RDP82-00850R000200030043-9

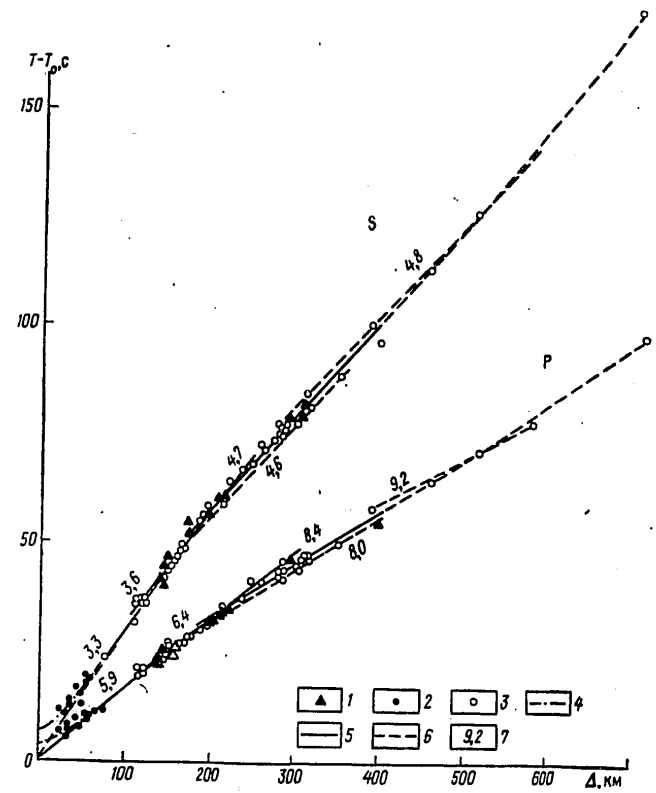

Figure 71. Summary Hodograph of First Arrivals of P and S Waves Compiled from Recordings from Explosions, Near and Local Earthquakes for Regions of Southeastern Russian Series:

1--arrival times of P and S waves from explosions; 2 and 3--arrival times of P and S waves from earthquakes at h_{och} = 20-50 km and $h_{och} \approx 0$; 4--theoretical hodographs of direct waves at h_{och} = = 23 km; 5--certain sections of summary hodographs; 6--uncertain sections of summary hodographs; 7--values of apparent velocities in km/s

the same distances from the point of the explosion: 2.5, 18, 28, 62, 83, 126, 135.5 and 178 km.

The following group waves: direct P waves related to the sedimentary mantle (v_{Pk} = 0.78 km/s), refracted P waves (v_{Pk} = 6.5 km/s) and refracted S waves

APPROVED FOR RELEASE: 2007/02/08: CIA-RDP82-00850R000200030043-9

APPROVED FOR RELEASE: 2007/02/08: CIA-RDP82-00850R000200030043-9

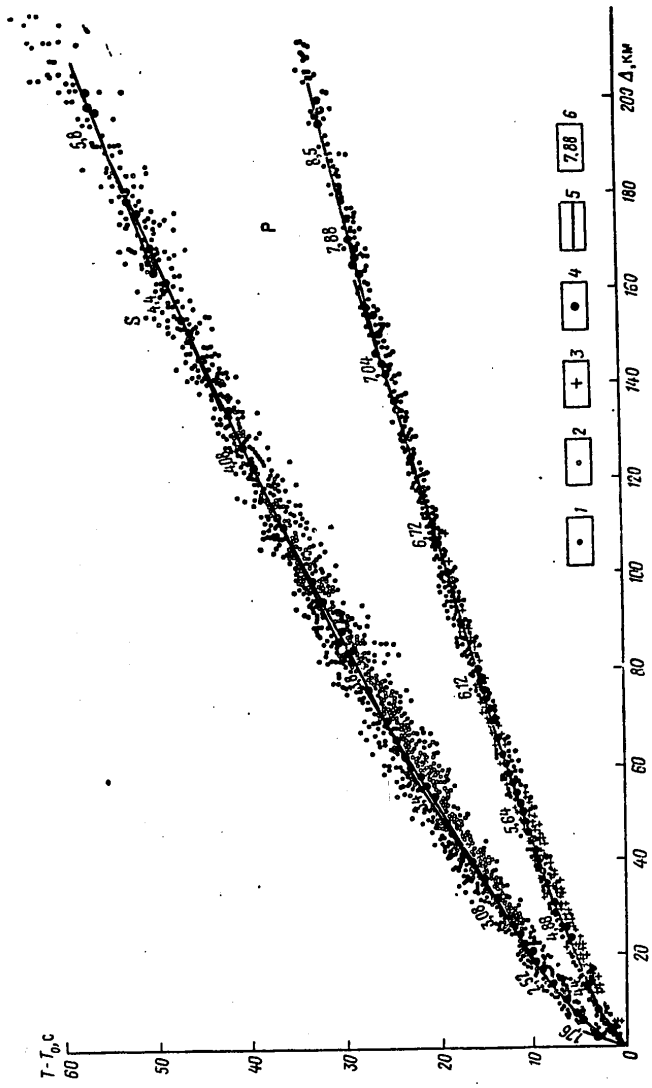

Figure 72. Summary Hodograph of First Arrivals of P and S Waves from Explosions for the North German Depression:
1 and 2--data of "Zemlya" stations for P and S waves, respectively; 3--KMPV data for P waves; 4--points of averaged summary hodograph; 5--averaged summary hodograph; 6--values of apparent velocities in km/s

APPROVED FOR RELEASE: 2007/02/08: CIA-RDP82-00850R000200030043-9

APPROVED FOR RELEASE: 2007/02/08: CIA-RDP82-00850R000200030043-9

(v_{Sk} = 3.6 km/s) related to the Paleozoic Basement and surface R_2 (v_k = 2 km/s) and R_1 (v_k = 200-500 m/s) waves, are determined on the summary hodograph from explosions obtained on the longitudinal profile within the Azov-Kuban' Depression [59].

The Wave Pattern on Recordings from Remote Earthquakes (Δ = 10-160°)

P and PS waves are registered on recordings from remote earthquakes and S waves are registered at $\Delta \approx 70°$. The foci of the remote earthquakes recorded by "Zemlya" stations during 1962-1974 are presented in Figure 56. Most of them are located in the Pacific Ocean seismically active zone and within the Central Asian and Mediterranean Sea seismically active belts. The foci distribution of these earthquakes in depth are presented in Figure 58. The magnitudes of the remote earthquakes determined by "Zemlya" recording stations are presented in Figure 73 for five regions: the Pre-Caspian, North German and Azov-Kuban' Depressions, the transition zone from the Southeastern Russian Series to the Pre-Caspian and in the region of Tashkent. A similar nature of the graphs was also found for other regions of the Soviet Union where investigations were carried out with the "Zemlya" device. Earthquakes with magnitude from 4 to 7 have been recorded at all epicentral distances. The greatest number of earthquakes was found with magnitudes from 4.5 to 6.5.

A graph of the distribution of the number of earthquakes N from their epicentral distance, recorded and accepted for processing in these regions, is presented in Figure 74. The largest number of recorded earthquakes for all the regions was found at epicentral distances of 50-76° from the foci located in Japan, in the Kurile Islands and on Kamchatka. A rather high maximum during recordings from earthquakes in the region of Tashkent is noted at Δ = = 1.5-8° and corresponds to earthquakes with foci in the Tyan'-Shan' and Pamir Mountains. The maximum values of N are noted at Δ equal to 100, 130 and 150°. They correspond mainly to earthquakes with foci in the Pacific Ocean, the Kermadec Depression, the Tonga Islands and so on. And finally, a maximum of N at $\Delta \approx 18-20°$ has been noted during observations within the North German Depression. It corresponds to earthquakes with foci in the Mediterranean and specifically in the Aegean Seas. The depths of the earthquake foci within all the maximums determined in Figure 74 are located in the mantle.

The azimuths of the P wave approach from remote earthquakes α for all regions are presented in Figure 75. As can be seen, the waves from the earthquakes approach the recording stations from all directions. But their maximum number for all regions is observed at α = 20-35° and corresponds to earthquakes of the Pacific Ocean zone with epicenters in Japan, in the Kurile Islands, on Kamchatka and so on. An additionally increased number of recorded earthquakes with α = 110-170°, corresponding to the seismically active zones of the Tyan'-Shan' and the Pamirs, was observed for the rayons of Tashkent.

APPROVED FOR RELEASE: 2007/02/08: CIA-RDP82-00850R000200030043-9

APPROVED FOR RELEASE: 2007/02/08: CIA-RDP82-00850R000200030043-9

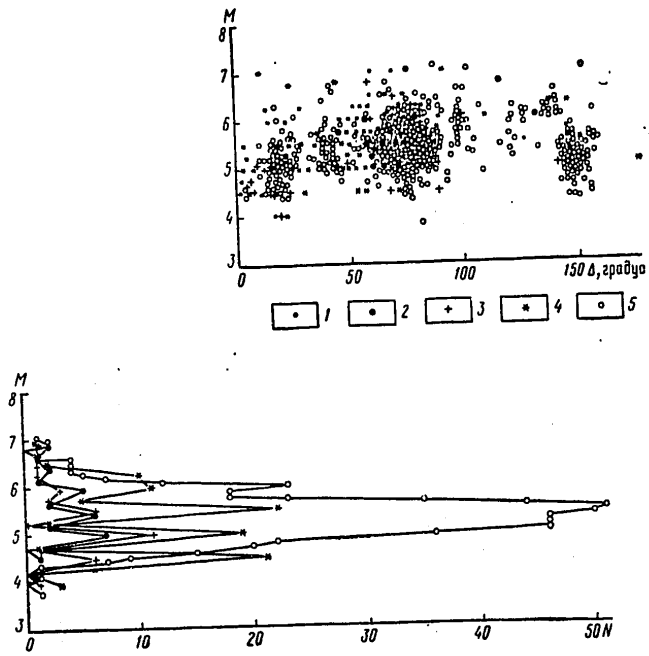

Figure 73. Graphs of the Dependence of Magnitude M of Remote Earthquakes on Δ and N:
1--Pre-Caspian Depression; 2--transition zone from Southeastern Russian Series to Pre-Caspian Depression; 3--Azov-Kuban' Depression; 4--rayons of Tashkent; 5--North German Depression;

The wave fields on recordings from remote earthquakes can be represented in the form of statistical time profiles--time models of the crust for Tashkent and the North German Depression (see Figure 63). Maximum numbers of PS waves corresponding to the main velocity boundaries of the earth's crust are observed on these profiles for both regions. The nature of the maximums, their distribution and the number N of PS waves with an increase of Δt_{PS-P} and H vary for each region in their own way. The maximums for the regions of the North German Depression (a yound series) are clear and narrow. Their values decrease only for the intermediate interfaces of the earth's crust with an increase of Δt_{PS-P} and H. They remain comparable for the basement surface and the Mohorovicic discontinuity. The maximum PS waves with an increase of Δt_{PS-P} and H become indistinct and their amplitude decreases for the region of Tashkent located in the transition zone to the mountains. This is especially evident for the transition zone from the crust to the mantle. These factors may qualitatively indicate the different structure of the crust and the transition zone from the crust to the mantle within the series of formations and the geosinclinal zones.

APPROVED FOR RELEASE: 2007/02/08: CIA-RDP82-00850R000200030043-9

APPROVED FOR RELEASE: 2007/02/08: CIA-RDP82-00850R000200030043-9

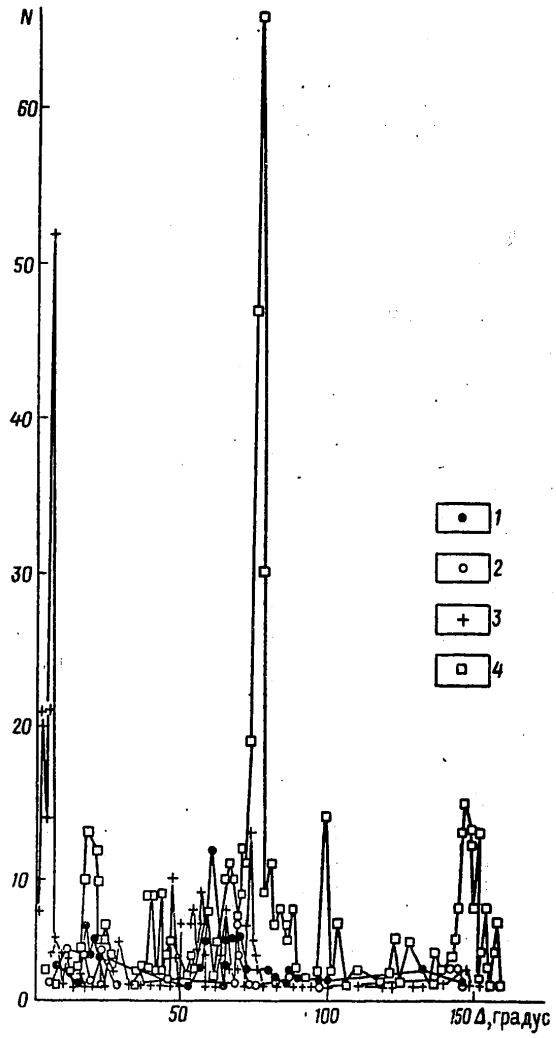

Figure 74. Graph of Distribution of Number of Earthquakes N Recorded from Foci with Different Values of Δ : 1--Pre-Caspian Depression; 2--Azov-Kuban' Depression; 3--rayons of Tashkent; 4--North German Depression

APPROVED FOR RELEASE: 2007/02/08: CIA-RDP82-00850R000200030043-9

APPROVED FOR RELEASE: 2007/02/08: CIA-RDP82-00850R000200030043-9

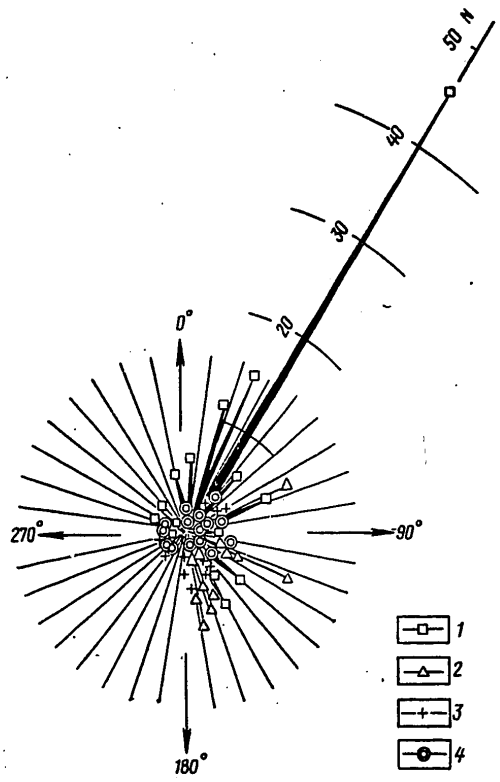

Figure 75. Graphs of Approach Azimuth Distribution α of P Waves to Recording Stations from the Number of Earthquakes N:
1--North German Depression; 2--rayons of Tashkent; 3--Pre-Caspian Depression; 4--Azov-Kuban' Depression

The Nature of the Wave Field in Fault Zones and in the Presence of Subvertical Contacts of Media of Different Petrographic Composition

Clear separation of the fault zones and subvertical contacts is a complex problem which requires consideration of all the factors outlined above for all types of P, S, PS, R and other waves. The fault zone and media contacts have the greatest effect on transient composite PS waves, which are not formed upon disappearance of the boundary in the fault zone. Lateral PS waves may appear in the presence of a sloping contact. Transient P and S waves and also R waves may only be attenuated somewhat in intensity, while their arrival times are deflected from the normal hodographs of these waves.

APPROVED FOR RELEASE: 2007/02/08: CIA-RDP82-00850R000200030043-9

APPROVED FOR RELEASE: 2007/02/08: CIA-RDP82-00850R000200030043-9

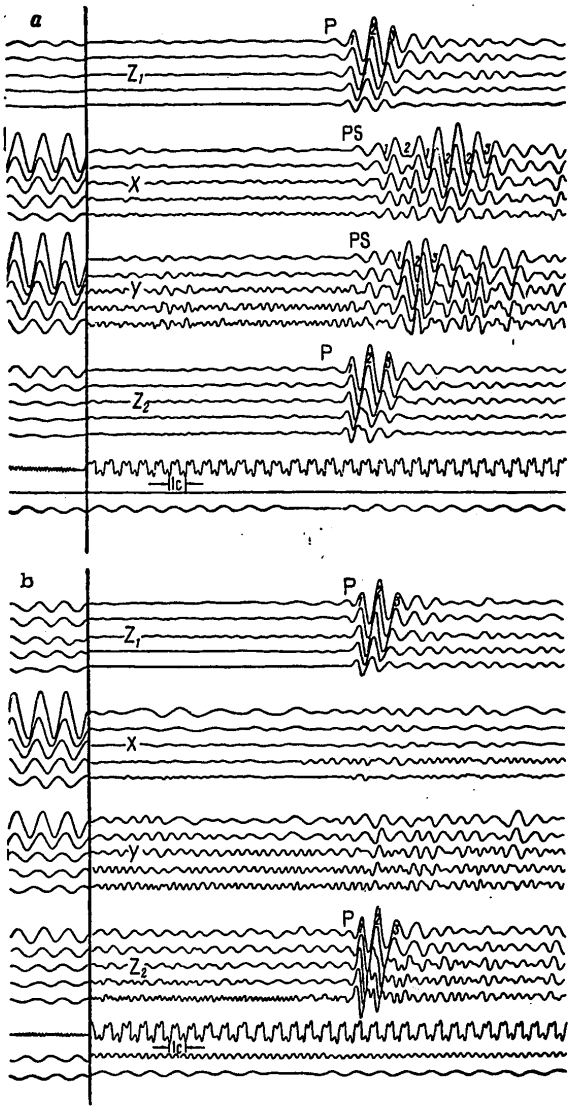

Figure 76. Seismograms Obtained Above Sections of Normal (a) and Disturbed (b) Structure of the Earth's Crust in the Rayons of Tashkent:
T = 0819, 15 Oct 1969, Δ = 170.5° and α = 318.2°

APPROVED FOR RELEASE: 2007/02/08: CIA-RDP82-00850R000200030043-9

APPROVED FOR RELEASE: 2007/02/08: CIA-RDP82-00850R000200030043-9

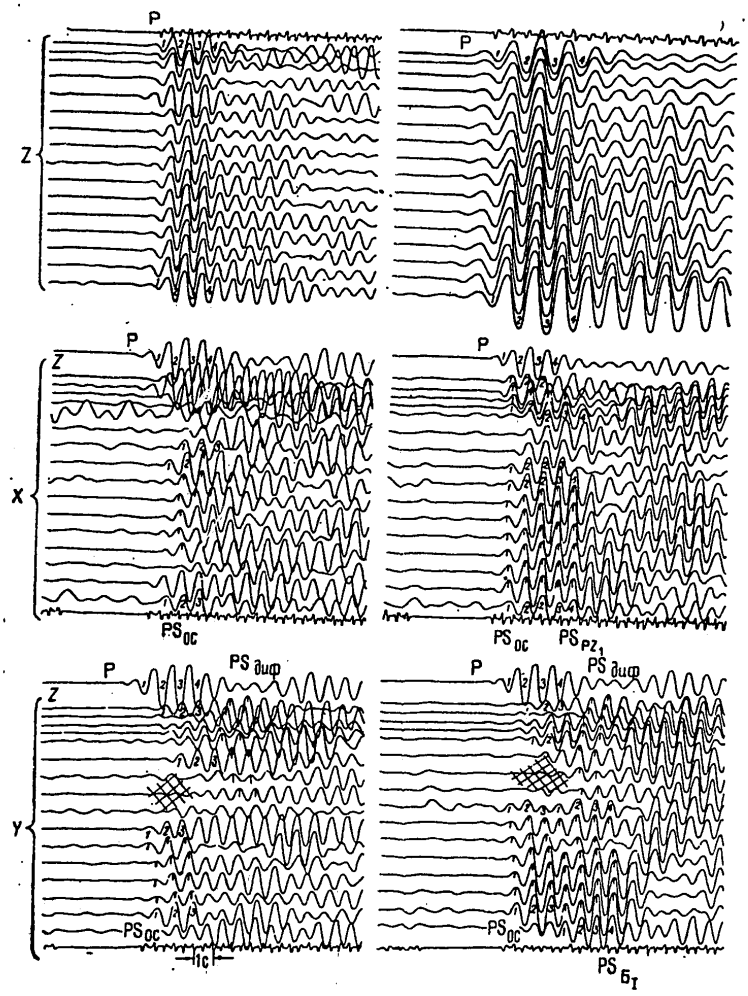

Figure 77. Correlation Seismogram Obtained by Using SS-24-61M Stations in the Region of the North German Depression. The cross-hatching denotes the location of the main North German Fault

APPROVED FOR RELEASE: 2007/02/08: CIA-RDP82-00850R000200030043-9

APPROVED FOR RELEASE: 2007/02/08: CIA-RDP82-00850R000200030043-9

Analysis of P, S, PS and R waves showed that the fault zones are determined by the following features: a) by sharp decrease of the PS wave amplitude until total disappearance baove the fault zone* (Figure 76); b) by the complexity of shape of the recording of composite and sometimes of longitudinal waves (by the appearance of a "broken," higher frequency recording); c) by the presence of a shift in the recording times of PS waves on the X and Y components; d) by the appearance of lateral PS waves which are transient diffracted and transient reflected PS waves from contacts of rock different in petrographic and physical composition upon re-recording on the SS-24-61M station (see Figure 62, a and Figure 77); e) by the presence of a time jump of Δt_{PS-P} upon transition through the fault zone; f) by variation of the polarity of arrival of PS waves; g) by the presence of a large number of PS waves which fill the entire time space; h) by attenuation of the P and S wave intensity during passage through the fault zone; i) by deviation of the recording times of P, S and R waves from the normal hodograph and k) by the presence of foci of current movements of the earth's crust.

*Disappearance of PS waves may be caused not only by the fault zone, but also by a larger angle of inclination of the interface.

APPROVED FOR RELEASE: 2007/02/08: CIA-RDP82-00850R000200030043-9

APPROVED FOR RELEASE: 2007/02/08: CIA-RDP82-00850R000200030043-9

THE DYNAMIC CHARACTERISTICS OF EXPERIMENTAL P AND PS WAVES AND THEIR COMPARISON TO THEORETICAL DATA

Moscow SEISMICHESKIYE ISSLEDOVANIYA S APPARATUROY "ZEMLYA" in Russian 1977 signed to press 31 Jan 1977 pp 134-160

[Chapter 6 from the book "Seismicheskiye issledovaniya s apparaturoy 'Zemlya' by I. V. Pomerantseva and A. N. Mozzhenko, Izdatel'stvo Nedra, 1,400 copies, 256 pages]

[Text] The dynamic characteristics of P and PS waves for earthquakes with 1.5-160° include the shape of the recording, the ratio of the PS to P wave intensity and its dependence on the parameters of the medium, the visible periods, the frequency spectra and the polarization of PS waves. Based on study of experimental data on the dynamics of P and PS waves and comparison of them to theoretical calculations, the criteria for determination of P and PS waves on earthquake recordings have been formulated.

Most dynamic graphs were constructed for P and PS waves for two regions: the North German Depression (600 earthquakes) and the rayons of Tashkent (400 earthquakes), since the channels of the "Zemlya" recording stations were reliably calibrated by their sensitivity in these very two regions (see Chapter 3). The erros of channel calibration by sensitivity did not exceed 10 percent, while the phase shifts did not exceed 1/20 of the period (0.05 second). The amplitudes of P and PS waves were masured by phases not distorted by interference phenomena for construction of the dynamic graphs. Seismograms with the presence of remodulated P and PS waves were eliminated from processing.

The Shape of Recording of P and PS Waves

It was noted during experimental studies with the "Zemlya" device in the presence of clean, noninterference recordings that the shape of the PS wave recording easily repeats the shape of the P wave recording (Figure 78).

The values of the coefficients of the cross-correlation function between amplitudes of the same type of P and PS waves were determined to determine the degree of similarity of the shape of P and PS wave recordings. Wave recordings outside the interference zones and usually in the region of the first arrivals were used in this case. The cross-correlation function coefficients were determined by

APPROVED FOR RELEASE: 2007/02/08: CIA-RDP82-00850R000200030043-9

APPROVED FOR RELEASE: 2007/02/08: CIA-RDP82-00850R000200030043-9

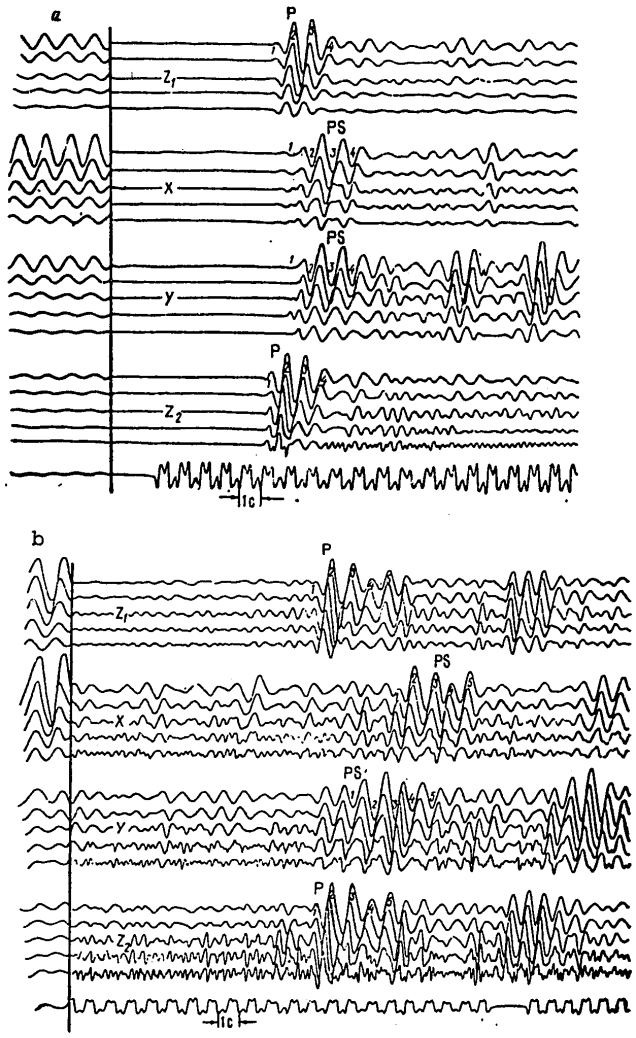

Figure 78. Shape of PS Wave Recording from Near and Remote Earthquakes Recorded in the REgions of Tashkent (a-c) and the North German Depression (d and e):
a--T = 0113, 23 Sep 1967, Δ = 4.6° and α = 158.6°; b--T = 0408, 24 Sep 1967, Δ = 64.5° and α = 107.4°; c--T = 2032, 18 Dec 1967, Δ = 4.5° and α = 103.5°; d--T = 0203, 3 Oct 1969, Δ = 71.5° and α = 23°; e--1220, 10 Jan 1970, Δ = 98.5° and α = 66.4°

[Figure continued on following page]

APPROVED FOR RELEASE: 2007/02/08: CIA-RDP82-00850R000200030043-9

APPROVED FOR RELEASE: 2007/02/08: CIA-RDP82-00850R000200030043-9

[Continued from preceding page]

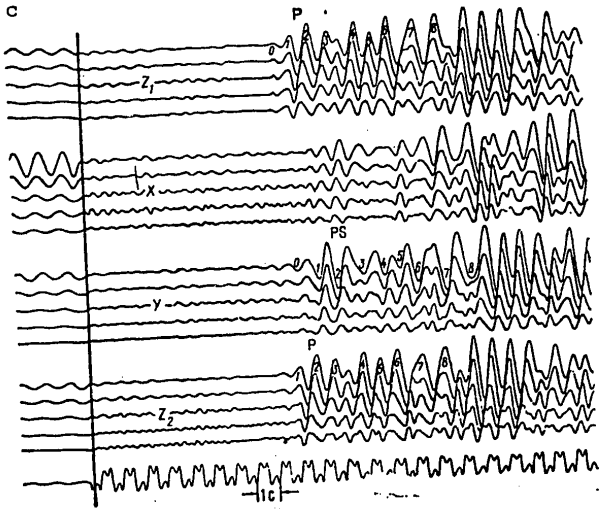

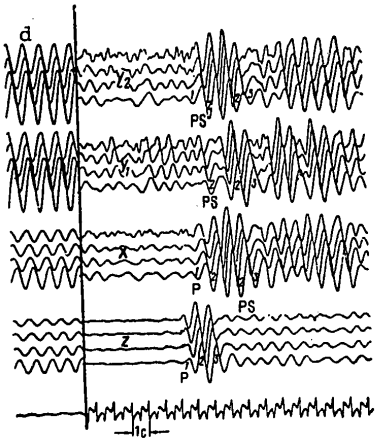

Figure 78 (Continued)

[Figure continued on following page]

APPROVED FOR RELEASE: 2007/02/08: CIA-RDP82-00850R000200030043-9

APPROVED FOR RELEASE: 2007/02/08: CIA-RDP82-00850R000200030043-9

[Continued from preceding page]

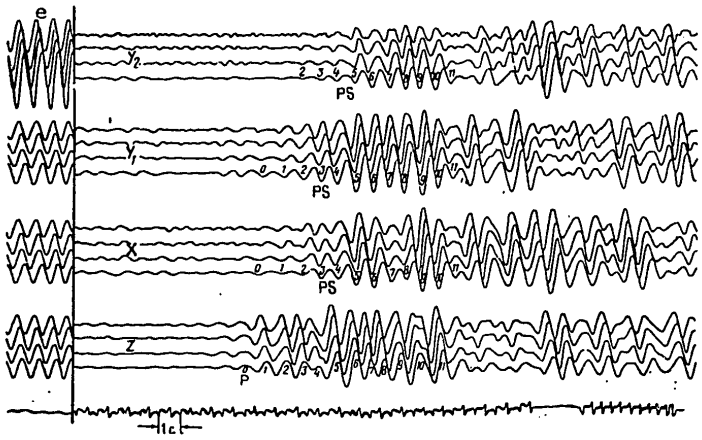

Figure 78 (Continued)

by ordinary formulas of mathematical statistics [71]. The dependence between the amplitudes of phases of the same type of P and PS waves was linear for the greater part of the material, while the correlation coefficient was included in the range of 0.8-1. Similar values of the cross-correlation function coefficients were found upon analysis of the shapes of P and PS wave recordings, theoretically calculated for different models of the interfaces of the crust and the transition zones between its layers (see Table 4). This permits one to assume that a similar shape of P and PS waves recordings is a sufficiently stable and reliable criterion for determining PS waves on the recordings.

Ratios of the Amplitudes of PS to P Waves and Their Dependence on the Parameters of the Medium

The ratios of the amplitudes of experimental PS to P waves (A_{PSq}/A_{Pw}), the first of which (A_{Pq}) were recorded on the horizontal components and the second of which (A_{Pw}) were recorded on the vertical components for the regions of the North German Depression, vay from 0.1 to 0.7, sometimes reaching unity (Figure 79). Values of A_{PSq}/A_{Pw} which exceed 1.5-2 are rarely encountered.

Graphs of A_{PSq}/A_{Pw} were analyzed for each crustal interface as a function of the epicentral distance Δ, the azimuth of the P wave approach to the recording stations α determined by the formulas of [136], the angle of incidence of the P wave to the interface i, the angle of inclination of the boundary φ at values up to 15° and depth H and structural shapes of the interfaces (Figures 79-81). A wide variation of the values of A_{PSq}/A_{Pw} is observed on all the graphs $A_{PSq}/A_{Pw} = f(\Delta, \alpha, i, \varphi, H)$. An irregularity is poorly determined,

APPROVED FOR RELEASE: 2007/02/08: CIA-RDP82-00850R000200030043-9

APPROVED FOR RELEASE: 2007/02/08: CIA-RDP82-00850R000200030043-9

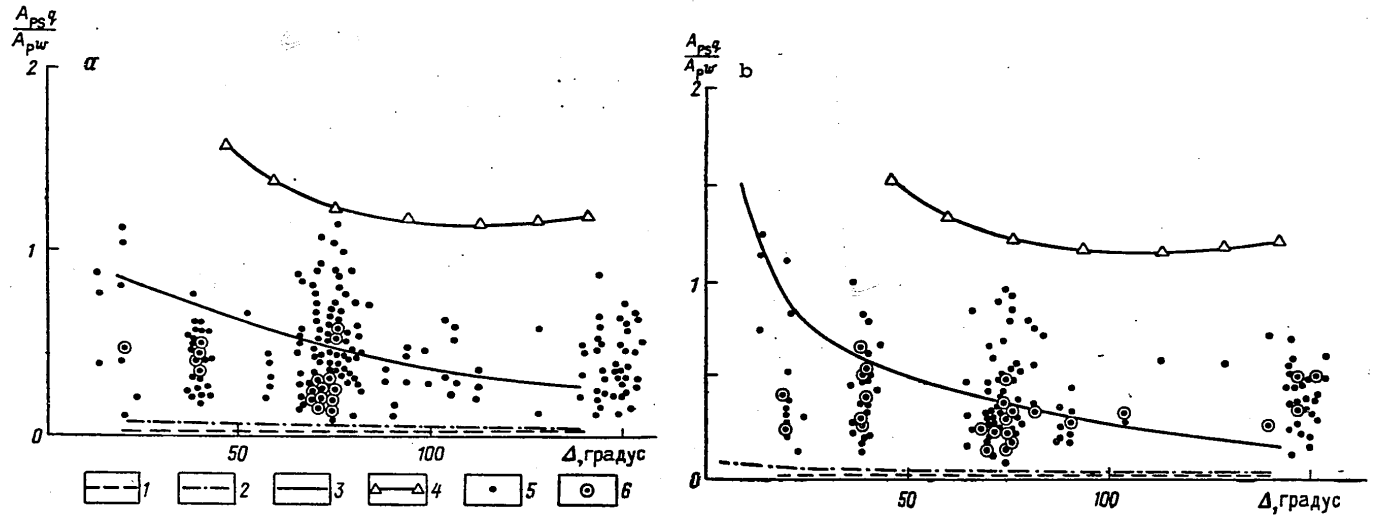

Figure 79. Experimental and Theoretical Graphs of Dependence of A_{PSq}/A_{Pw} on Δ: The experimental data were compiled for: a--the surfaces of Variscian and Caledonian Basements; b--the Pre-Cambrian Basement; c--the transition zone from the granite to the basaltic layer; d--the Conrad-I and Conrad-II surfaces; e--the transition zones from the crust to the mantle; 1-3--theoretical curves for model of medium of Figure 3 without regard to P and S wave absorption, with regard to P and S wave absorption at $\alpha_P = \alpha_S$ and with regard to P and S wave absorption at $\alpha_P = 2\alpha_S$; 4--theoretical curves for model of Figure 6 without regard to absorption of P and S waves; 5 and 6--experimental data for individual seismograms and for a series of seismograms, respectively, with number of determinations for each point of the graph greater than three.

[Figure continued on following page]

APPROVED FOR RELEASE: 2007/02/08: CIA-RDP82-00850R000200030043-9

APPROVED FOR RELEASE: 2007/02/08: CIA-RDP82-00850R000200030043-9

[Continued from preceding page]

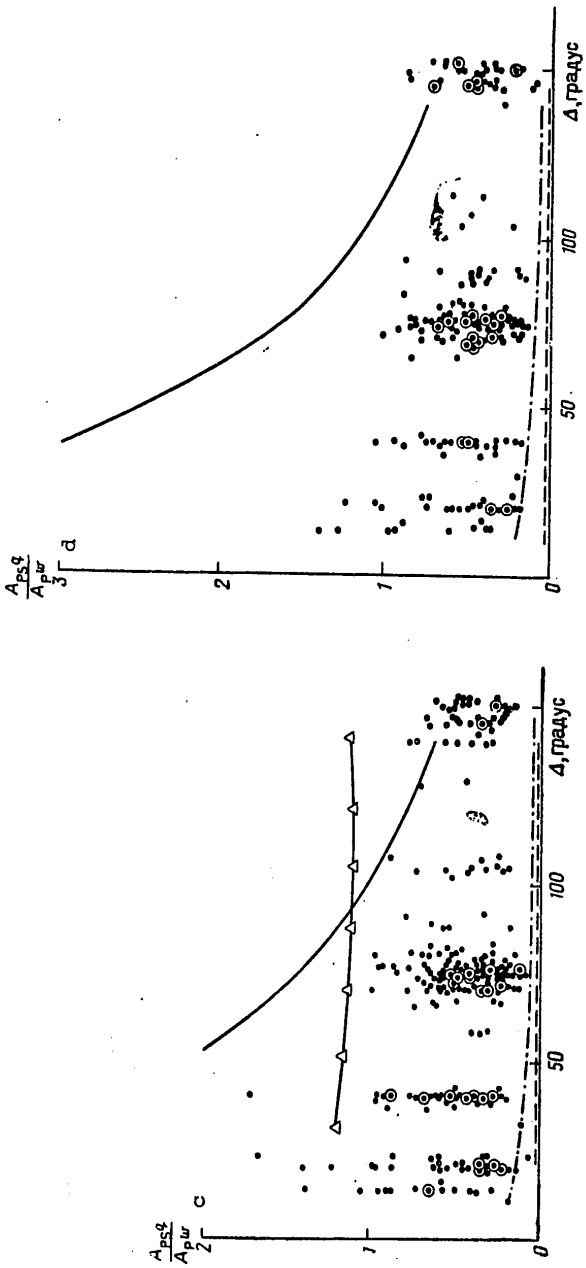

Figure 79 (Continued)

[Continued on following page]

APPROVED FOR RELEASE: 2007/02/08: CIA-RDP82-00850R000200030043-9

APPROVED FOR RELEASE: 2007/02/08: CIA-RDP82-00850R000200030043-9

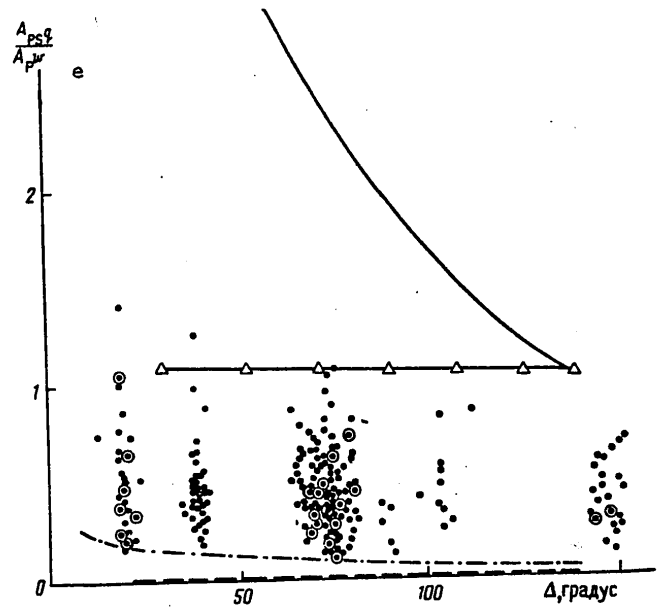

Figure 79 (Continued)

although a slight decrease in the value of A_{PSq}/A_{PW} is noted with an increase of the epicentral distance and depth of deposition of the interface. This may be related both to the absence of any common regularities and to the fact that a large amount of material obtained under similar, but still different geological conditions was used in the analysis.

The corresponding theoretical curves calculated both with and without regard to the absorbing properties of the medium were plotted on the experimental graphs. The values of the absorption coefficients for P and S waves were assumed equal to $\alpha_P = \alpha_S$ and $\alpha_P = 2\alpha_S$. The derived experimental values of A_{PSq}/A_{PW} on the graphs of the dependence on Δ (see Figure 79, a-e) and i (see Figure 81) are mainly located between the theoretical curves of A_{PSq}/A_{PW} calculated for thick-walled media with interfaces of first kind at $\alpha_P = \alpha_S = 0$ and $\alpha_P = 2\alpha_S$. the theoretical values of $A_{PSq}/A_{PW} = f(\Delta)$, also calculated for thick-walled media but for the zones between the crustal layers represented by benches of thin layers (see Figure 6), even without regard to the absorbing properties of the medium, are located above the experimental values of A_{PSq}/A_{PW}. The derived data permit one to assume that good agreement between the theoretical and experimental values of A_{PSq}/A_{PW} is observed. This coincidence may be the result of the effect of two factors: the absorbing properties of the medium and the structure of the boundary (zone) between the crustal layers. Each of the factors can be reduced to a significant divergence of the experimental values of A_{PSq}/A_{PW}.

APPROVED FOR RELEASE: 2007/02/08: CIA-RDP82-00850R000200030043-9

APPROVED FOR RELEASE: 2007/02/08: CIA-RDP82-00850R000200030043-9

Figure 80. Graphs of Dependence of Apsq/Apw on Approach Azimuths α of PS Waves to Recording Stations in the Regions of the North German Depression:
1--for PS waves related to surfaces of the Variscian, Caledonian and Pre-Cambrian Basements; 2--for PS waves formed at the interfaces of the earth's crust from the surface of the basaltic layer to the Mohorovicic discontinuity

APPROVED FOR RELEASE: 2007/02/08: CIA-RDP82-00850R000200030043-9

APPROVED FOR RELEASE: 2007/02/08: CIA-RDP82-00850R000200030043-9

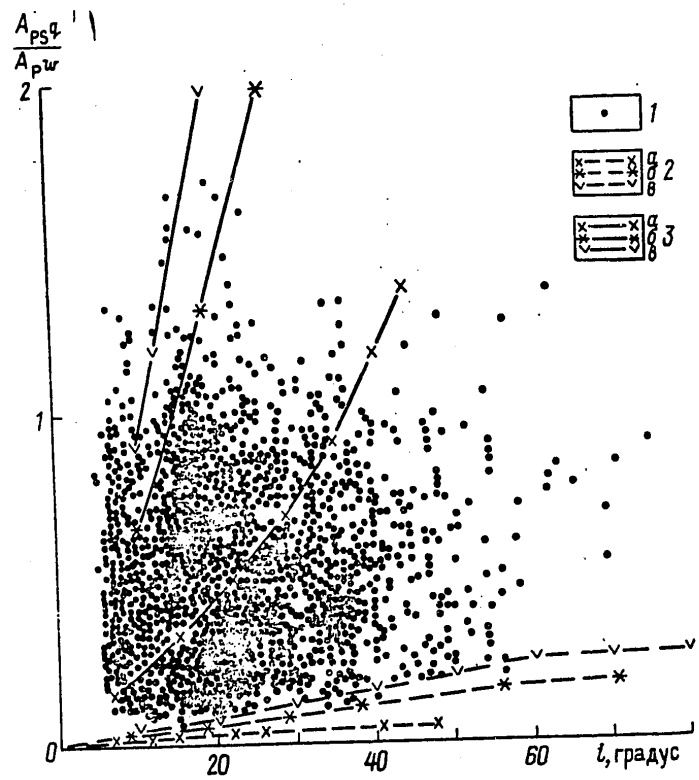

Figure 81. Graphs of Dependence of A_{PSq}/A_{Pw} on the Angle of Incidence of the P Wave on the Interface i for the Regions of the North German Depression: 1--experimental data for PS waves related to all the interfaces of the earth's crust; 2 and 3--theoretical curves of A_{PSq}/A_{PSw} calculated for different epicentral distances with and without regard to absorption of P and S waves of the real medium; a-- $\Delta = 20°$; b-- $\Delta = 72°$; c-- $\Delta = 140°$

Visible Periods and Frequency Spectra of P and PS Waves

The visible periods of P and PS waves for earthquakes with different epicentral distances vary at $\Delta \approx 1.5°$ from 0.3 to 1.1 and sometimes to 1.5 seconds at $\Delta = 160°$. The average value of the visible period of P and PS waves on recordings from remote earthquakes ($\Delta > 10°$) is equal to unity. The difference in the periods of P and PS waves is observed very rarely and mainly for recordings from near earthquakes with low values of Δ (up to 1.5-2°).

APPROVED FOR RELEASE: 2007/02/08: CIA-RDP82-00850R000200030043-9

APPROVED FOR RELEASE: 2007/02/08: CIA-RDP82-00850R000200030043-9

The frequency spectra of P and PS waves were analyzed by experimental materials obtained during seismological investigations with standard seismological apparatus [11, 66, 136] and with the "Zemlya" device. The frequency spectra of P and PS waves recorded by "Zemlya" stations were determined at the CDC-3300 processing center installed at Leipzig and at the Sigma-5 processing center at Kiev by using the standard programs of these centers. The determination was made for the channel with bandpass of 0.5-10 Hz. Several maximums are determined on the amplitude-frequency spectra of P waves (see Figure 67) from remote earthquakes: the first highest in value at frequencies less than 0.048 Hz, the second at frequencies of 0.157-0.180 Hz and the third, minimum in value, at a frequency of 1.025 Hz. The maximum frequency spectra of P waves from seismological materials with variation of Δ from 0 to 140° are shifted from frequencies of 8-10 Hz to frequencies of 0.05-0.3 Hz (see Figure 68, a and b). According to data of "Zemlya" stations, the maximum frequency spectra for these same values of change from frequencies of 8-10 Hz to frequencies of 0.6-2 Hz. The coincidence of the maximum frequency spectra of P waves recorded by the "Zemlya" device and by seismological apparatus is observed in the range of Δ = 0-8°. The maximum frequency spectra of P waves begin to diverge gradually with a further increase of Δ, reaching the highest value at Δ = 20-140°. This is related to the difference of the frequency characteristics of the "Zemlya" device and seismological stations, the first of which cut off frequencies below 0.5 Hz. It is interesting to note that, beginning at $\Delta \approx$ 2-4°, the maximum frequency spectra of P waves cease to vary with an increase of epicentral distance.

The same pattern is observed for S waves as for P waves: the frequencies of S waves recorded by seismological apparatus are lower than those of S waves recorded by the "Zemlya" device. The maximum frequency spectra of PS waves at Δ = 2-140° are located at the same frequencies as the maximum frequency spectra of P waves.

Polarization of PS Waves

Graphs of the displacement of soil particles in the horizontal plane were constructed to determine the polarization properties of PS waves from approximately 15,000 recordings of waves of remote earthquakes for regions of the North German Depression and the Tashkent Depression.

The graphs of the motion of soil particles in the horizontal plane at one of the "Zemlya" recording stations for earthquakes with different recording times T: 1) 2316, 28 Feb 1970; 2) 1700, 3 Mar 1970; 3) 0510, 10 Mar 1970; 4) 1105, 10 Mar 1970; 5) 1303, 14 Mar 1970; 6) 0033, 23 Mar 1970; 7) 0203, 23 Mar 1970; 8) 1227, 23 Mar 1970; 9) 2106, 23 Mar 1970; 10) 1912, 26 Mar 1970; 11) 1436, 31 Mar 1970; 12) 1546, 31 Mar 1970; and 13) 0024, 1 Apr 1970, are presented in Figure 82.

Seismograms with P and PS waves and graphs of displacement of soil particles after the arrival of PS waves are presented in Figure 83. In all cases the plots were made for PS waves registered first on the recordings. Analysis

APPROVED FOR RELEASE: 2007/02/08: CIA-RDP82-00850R000200030043-9

APPROVED FOR RELEASE: 2007/02/08: CIA-RDP82-00850R000200030043-9

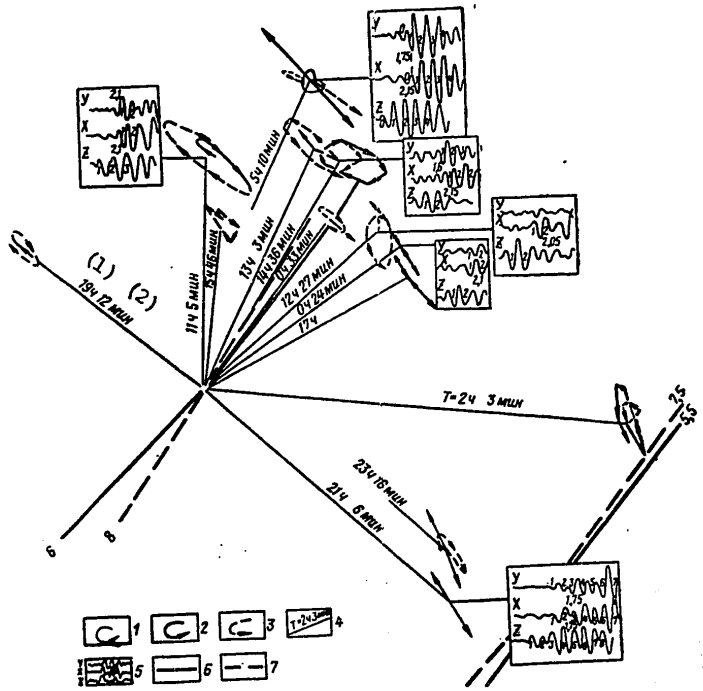

Figure 82. Graphs of Displacement of Soil Particles and Shapes of Recordings of P and PS Waves from Different Boundaries for Earthquakes Recorded at the Same Recording Station:
1-3--graphs of displacement of soil particles and shape of PS wave recording related to surfaces of Variscian and Caledonian Basements, respectively, and by sections of interference zones; 4--approach azimuths of P waves to recording station, calculated by formulas [136] with earthquake recording times; 5--shape of P wave recording on the Z component and PS wave recording on the X and Y components; 6 and 7--depth isolines (in km) along surfaces of Variscian and Caledonian Basement, respectively

Key:
1. Hour 2. Minutes

of the seismograms, similar to those presented in Figures 83 and 84, and the graphs of displacement of soil particles in the horizontal plane permit one to note the following principles. If the PS waves were determined outside the interference zone, they had linear polarization both upon exchange at the horizons in the sedimentary level and at the interfaces in the crystalline

APPROVED FOR RELEASE: 2007/02/08: CIA-RDP82-00850R000200030043-9

APPROVED FOR RELEASE: 2007/02/08: CIA-RDP82-00850R000200030043-9

mass of the crust: the surfaces of the basement and Conrad and Mohorovicic discontinuities (see Figure 83). If the PS waves were registered in the interference zone, the polarization of PS waves usually became elliptical (Figure 84, a) or even circular (Figure 84, b). Elliptical polarization is also observed when the time displacement by the X and Y components comprises 0.05 second, i.e., is located within the range of accuracy of taking the times Δt_{PS-P} from the seismograms (see Figure 82). Moreover, clear elliptical polarization is observed in the case when a PS wave is recorded on one component and the low-frequency background is recorded on the other and when waves frequently called PS_V and PS_H actually formed at different boundaries of the crust and registered on different horizontal components of the recording, are related to the same boundary. For example, a PS wave with Δt_{PS-P} = = 2.15 second was recorded on the X component and a PS wave with Δt_{PS-P} = = 1.6 second was recorded on the Y component for the same recording stations on earthquake seismograms with T = 1436 and $\Delta \approx 76.8°$ (see Figure 82). These waves [52] could be related to PS_V and PS_H waves from the same interface. At the same time, linearly polarized PS waves with Δt_{PS-P} = 1.6-1.75 seconds were determined on earthquake recordings with T equal to 2106, 2316, 2100 and 0203 and $\Delta \approx 18°$, while linearly polarized PS waves with Δt_{PS-P} = 2.1 seconds were determined on earthquake recordings with T = 1912, 1105 and 1700 with $\Delta \approx 50-86°$. The wave pattern obtained for all the earthquakes cannot be explained by the presence of PS_V and PS_H waves with time delays of 1.75 and 2.1 seconds, as was possible in the presence of only a single earthquake recording at 1436.

The only possible version of explanation in this case which makes it possible to relate the simultaneously linear and apparent elliptical polarization of PS waves includes the following. In all cases PS waves with Δt_{PS-P} equal to 1.6-1.75 and 2.1 seconds are linearly polarized, but are related to different boundaries. These interfaces are oriented differently in space. As a result, PS waves whose polarization planes do not coincide with the vertical plane passing through the station-epicenter (see Chaper 2) are formed upon approach of the P waves to the interface. In this case deviations of the azimuth of the polarization plane of PS waves for the upper boundary occur counterclockwise and those for the lower boundary occur clockwise, as a result of which PS waves from the upper boundary are recorded on the X component and those from the lower boundary are recorded on the Y component. Theoretical calculations of the deviation of the azimuths of displacement vectors of PS waves from the upper boundary for earthquakes with T = 0510 and 1303 yielded values of 60-70°, which is in good agreement with the given experimental material. The analyzed example is not the only one. Graphs were constructed (Figures 35-88) for statistical evaluation and analysis of the dynamic characteristics of PS waves.

Only those seismograms where the PS waves were registered simultaneously on the Z and Y components were used to plot these graphs. This comprises approximately 50-60 percent of all the PS wave recordings used to construct the deep profiles of the crust. The PS waves related to one boundary are recorded either on the X or on the Y component on the remaining 40-50 percent of the

APPROVED FOR RELEASE: 2007/02/08: CIA-RDP82-00850R000200030043-9

APPROVED FOR RELEASE: 2007/02/08: CIA-RDP82-00850R000200030043-9

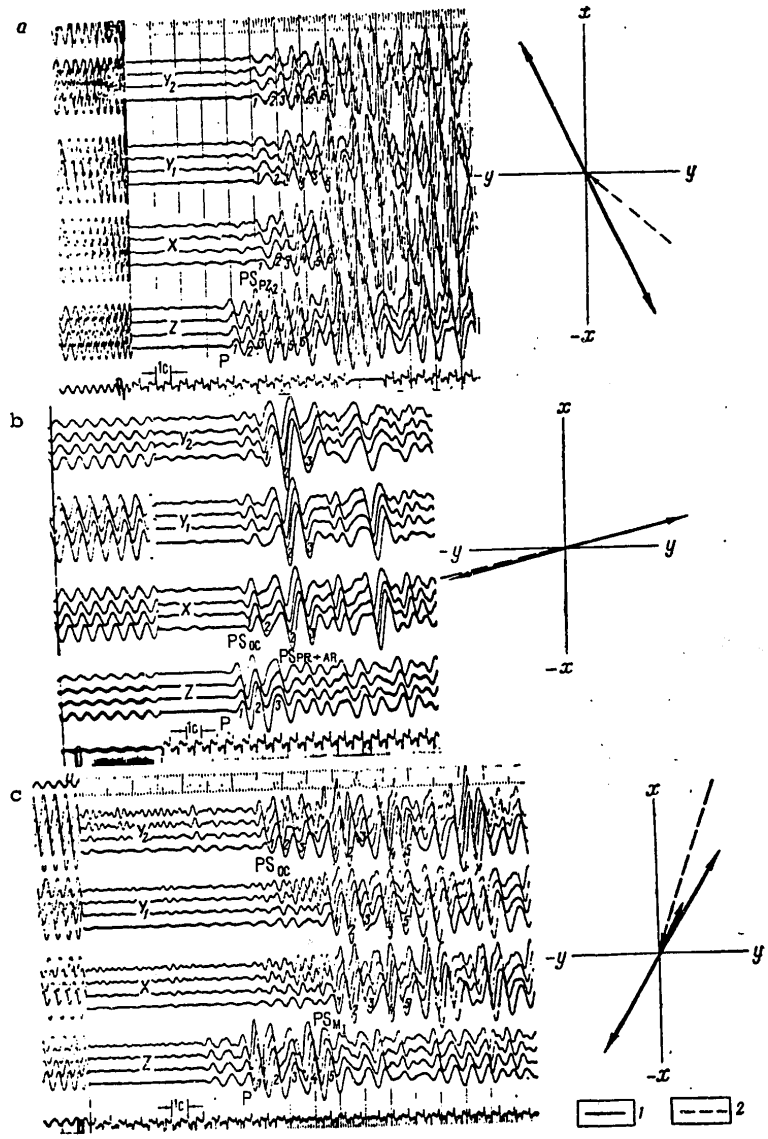

Figure 83. Seismograms and Graphs of Displacements of Soil Particles Under Seismographs for PS Waves Registered in the Range of the First Arrivals and Formed on the Surfaces of the Variscian (a) and Pre-Cambrian (b) Basements and the Mohorovicic Discontinuity (c):

1--azimuths of displacement vectors of PS waves determined by their amplitudes; 2--approach azimuths of P waves from earthquakes calculated by the formulas of [136]

APPROVED FOR RELEASE: 2007/02/08: CIA-RDP82-00850R000200030043-9

APPROVED FOR RELEASE: 2007/02/08: CIA-RDP82-00850R000200030043-9

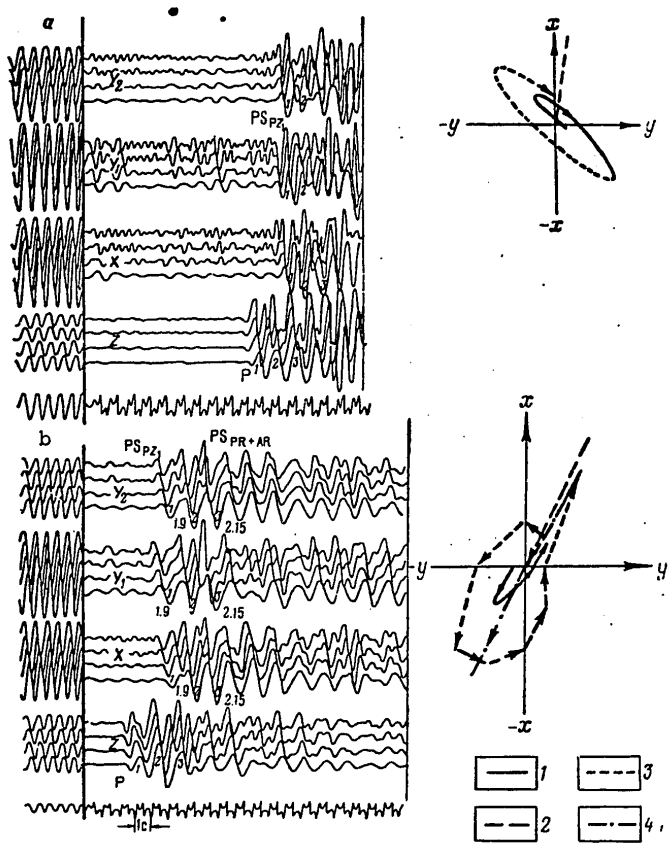

Figure 84. Seismograms and Graphs of Displacement of Soil Particles Under Seismographs for PS Waves Recorded in the Interference Zone:
1--graphs of soil particle displacement from first phases of PS waves related to surface of the Caledonian basement; 2--approach azimuths of P waves recorded by formulas of [136] to the stations; 3--interference zone; 4--section of soil particle displacement from subsequent phases of PS waves related to surface of the Pre-Cambrian basement

seismograms. This is explained both by the approach of the PS waves only in the corresponding (X and Y) directions or by deviation of the azimuth of the displacement vector of PS waves due to the angle of inclination of the interface. The total number of PS waves for each of the boundaries used to

APPROVED FOR RELEASE: 2007/02/08: CIA-RDP82-00850R000200030043-9

APPROVED FOR RELEASE: 2007/02/08: CIA-RDP82-00850R000200030043-9

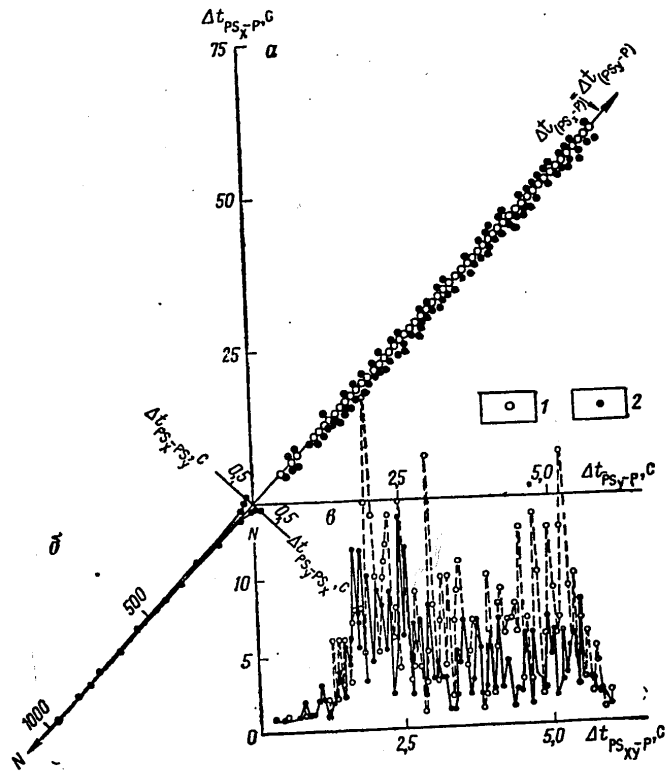

Figure 85. Graphs of Dependence of Recording Times of PS Waves on X Components $\Delta t_{PS_{X-P}}$ on their Recording Times on the Y components $\Delta t_{PS_{Y-P}}$ (a) and Distribution of the Number of PS Waves as a Function of the Shift of Recording Times (Dephasing) on the X and Y components (b) and Recording Time of Δt_{PS-P} (c):
1--values of $\Delta t_{PS_{X,Y-P}}$ and N for PS waves without dephasing on the X and Y components; 2--values of $\Delta t_{PS_{X,Y-P}}$ and N for PS waves with dephasing on the X and Y components

construct the graphs of Figures 85 and 86 vary from 160 to 400. The following principle can be traced in Figures 85 and 86. The time shift of recording PS waves on the X and Y components varies from 0 to 0.4 seconds. However, the majority of PS waves (approximately 96 percent) has shifts on the X and Y components of ± 0.1 second, 4 percent of PS waves have shifts up to ± 0.2 second and less than 1 percent of PS waves have shifts of ± (0.3-04) second. On the whole the experimental points of the graph of the function Δt_{PS_X-P} =

APPROVED FOR RELEASE: 2007/02/08: CIA-RDP82-00850R000200030043-9

APPROVED FOR RELEASE: 2007/02/08: CIA-RDP82-00850R000200030043-9

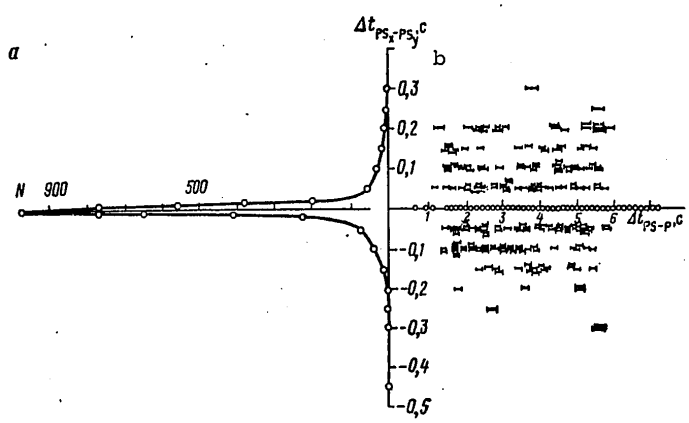

Figure 86. Graphs of Dependence of $\Delta t_{PS_X-PS_Y}$ on the Number of Composite Waves N and Δt_{PS-P} for Regions of the North German Depression:
a--curve $\Delta t_{PS_X-PS_Y} = f(N)$; b--values of $\Delta t_{PS_X-PS_Y} = f(\Delta t_{PS-P})$ for waves related to the interfaces of the earth's crust in the presence (plateaus) and absence (circles) of their dephasing on the X and Y channels, respectively

$= f(\Delta t_{PS_Y-P})$ are grouped (see Figure 85) with standard deviation of $\pm$ 0.1-0.15 second around a straight line drawn from the origin of the coordinates at an angle of 45° and which is the theoretical straight line of this graph for linearly polarized PS waves [52,54]. Analysis of the distribution of shifts equal to 0.2-0.4 second, jointly with geological materials for the rayons of Tashkent, the North German and the Azov-Kuban' Depressions, showed that they are confined to regions of deep faults of the earth's crust.

A graph of the dependence of the ratio of the major axis a of the figure (in some cases of ellipses) to its minor axis b on the time shift between the components of PS waves registered on the X and Y components of the recording and the number of waves and also graphs of displacement of the soil particles in the horizontal plane, obtained for PS waves on three stopovers of the recording stations is presented in Figure 87. Those waves in which $a/b \geqslant 3$ can be taken as linearly polarized waves with regard to the possible phase shifts by the X and Y components determined by the apparatus (up to 0.05

APPROVED FOR RELEASE: 2007/02/08: CIA-RDP82-00850R000200030043-9

APPROVED FOR RELEASE: 2007/02/08: CIA-RDP82-00850R000200030043-9

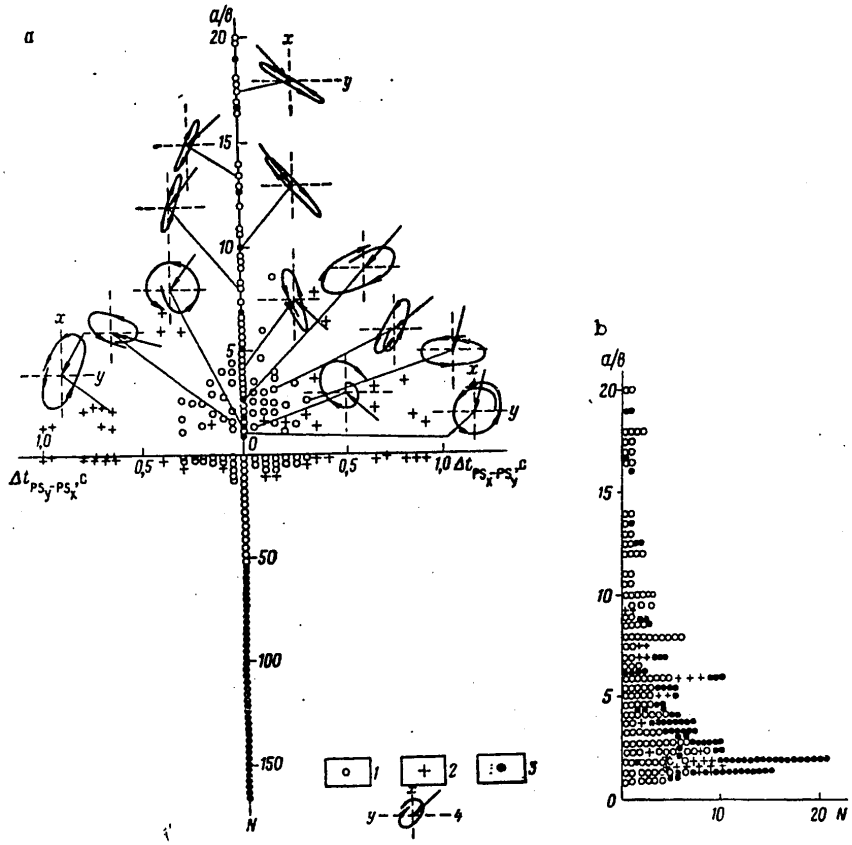

Figure 87. Graphs of the Dependence of Ratios (a/b) on the Value of Dephasing of PS Waves on the X and Y Components (a) and the Number N of PS Waves (b) Compiled for Regions of the North German Depression: 1 and 2--PS waves determined on the X and Y components and related to one or different boundaries, respectively; 3--PS waves separated either on the X or on the Y component; 4--nature of displacement of soil particles in the horizontal plane with direction of approach azimuth of P waves from earthquakes

second) and also by the error of dynamic constructions. The number of these PS waves for a crystalline crust (Figure 87, b) is small, since they are traced mainly in the region of subsequent arrivals. The graphs a/b = f(N) are interesting by their contradictory nature: displacements of the recording times of PS waves by the X and Y components do not exist, while the soil

APPROVED FOR RELEASE: 2007/02/08: CIA-RDP82-00850R000200030043-9

APPROVED FOR RELEASE: 2007/02/08: CIA-RDP82-00850R000200030043-9

particles describe oscillations close to an ellipse or even to a circle. This phenomenon can be explained by different factors, mainly from those by which the times t_{PS-P} of PS waves mainly having 3-5 phases or more were recorded by the central, least distorted interference phase while the graphs of the motion of soil particles were constructed by the phases of PS waves distorted by superposition of adjacent oscillations.

The dependence of the angle of polarization δ on the values of Δt_{PS-P} for regions of the North German Depression are presented in Figure 88. As can be seen from Figure 88, the value of δ varies from 0 to 360° regardless of the value Δt_{PS-P}. A similar curve from [52] is plotted in Figure 88. The small number of data from which this curve is constructed (30-40 determinations) permits one to assume that its nature is random.

The data obtained in Figures 82-88 permit one to assume that polarization of PS waves related to the interfaces of the earth's crust is linear or elliptical with time signals on the X and Y components no greater than $\pm$ 0.1 second and rarely, $\pm$ 0.2 second. An exception is fault zones where the values of the time shifts of PS waves on the X and Y components may reach $\pm$ 0.3-0.4 second.

It was determined for PS waves with time shifts on the X and Y components up to 0.1-0.2 second that their approach azimuths to the recording stations, determined by the amplitudes of PS waves and formulas used in seismology for horizontally layered media [136], do not coincide with each other. Graphs (Figure 89) were constructed for statistical analysis of the values of these deviations $\Delta\alpha$ and to determine their dependence on α and the number N of recorded PS waves. As can be seen from 89, a, $\Delta\alpha$ does not depend on α. The nature of the graphs $\Delta\alpha = f(N)$ themselves was rather unique (Figure 89, b). It is identical for interfaces of the crystalline mass of the earth's crust. A maximum number of PS waves is noted at $\Delta\alpha = 0$. The number of PS waves decreases to zero with an increase of $\Delta\alpha$ from 0 to 100°. Additional maximum numbers of PS waves are observed on a background of a gradual decrease of N at specific values of $\Delta\alpha$. The graph $\Delta\alpha = f(N)$ is seemingly subordinate to normal distribution law of $\Delta\alpha$ with maximum at $\alpha = 0$. On the whole, these distributions of the data of $\Delta\alpha$ indicate that PS waves are polarized in the plane of the ray (PS_V) although significant deviations of the polarization plane of PS_V waves from the vertical plane passing through the recording station-epicenter are also observed. Maximum values near $\pm$ 90° should have been observed in Figure 88 with the presence of PS_H waves.

The values of the phase shifts of PS waves register on the X and Y components and the ratios of their displacement vectors for these same components of composite PS waves with horizontal and sloping interface were compared to determine the degree of similarity of the theoretical and experimental data on the polarization characteristics of PS waves.

Comparison of the values of $\Delta t_{PS_X-PS_Y}$ showed that the theoretical and experimental data are in good agreement with each other: the values of $\Delta t_{PS_X-PS_Y}$ for platform conditions ($\varphi < 10°$) do not exceed $\pm$ 0.15 second in both cases.

APPROVED FOR RELEASE: 2007/02/08: CIA-RDP82-00850R000200030043-9

APPROVED FOR RELEASE: 2007/02/08: CIA-RDP82-00850R000200030043-9

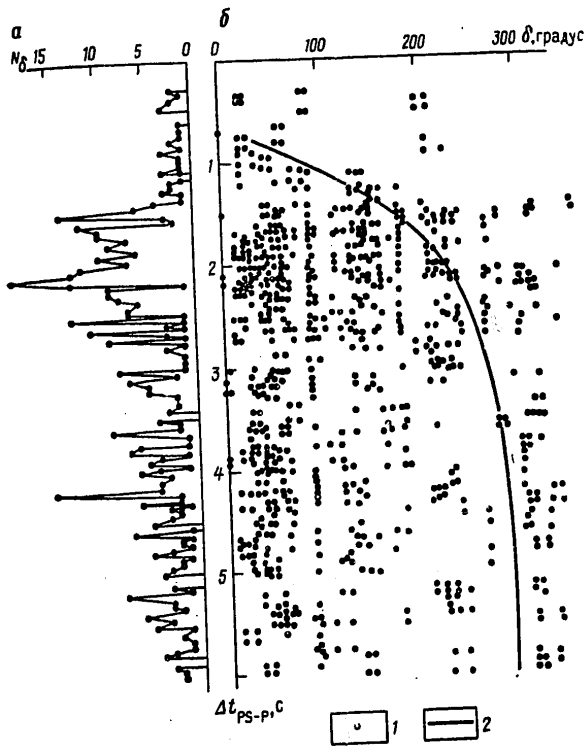

Figure 88. Graphs of Dependence of Polarization Angle δ of PS Waves on Δt_{PS-P} and Their Distribution on the Number N_δ from Regions of the North German Depression:
1--experimental data for approximately 600 earthquakes; 2--curve from [52]

The experimental values of the ratios of the displacement vectors of PS waves registered on the X and Y components (see Figure 21) are included among the theoretical curves of $\bar{U}_{PS_Y}/\bar{U}_{PS_X}$ for interfaces with angles of inclination from 0 to 20° and Δ = 20°.

The derived theoretical and experimental data on the polarization characteristics of PS waves make it possible to explain a number of phenomena observed during registration of them on recordings from remote earthquakes. The first phenomenon includes the fact that PS waves from different boundaries are registered on different horizontal components of the recording. This characteristic was explained [52] by the anisotropy of the medium which

APPROVED FOR RELEASE: 2007/02/08: CIA-RDP82-00850R000200030043-9

APPROVED FOR RELEASE: 2007/02/08: CIA-RDP82-00850R000200030043-9

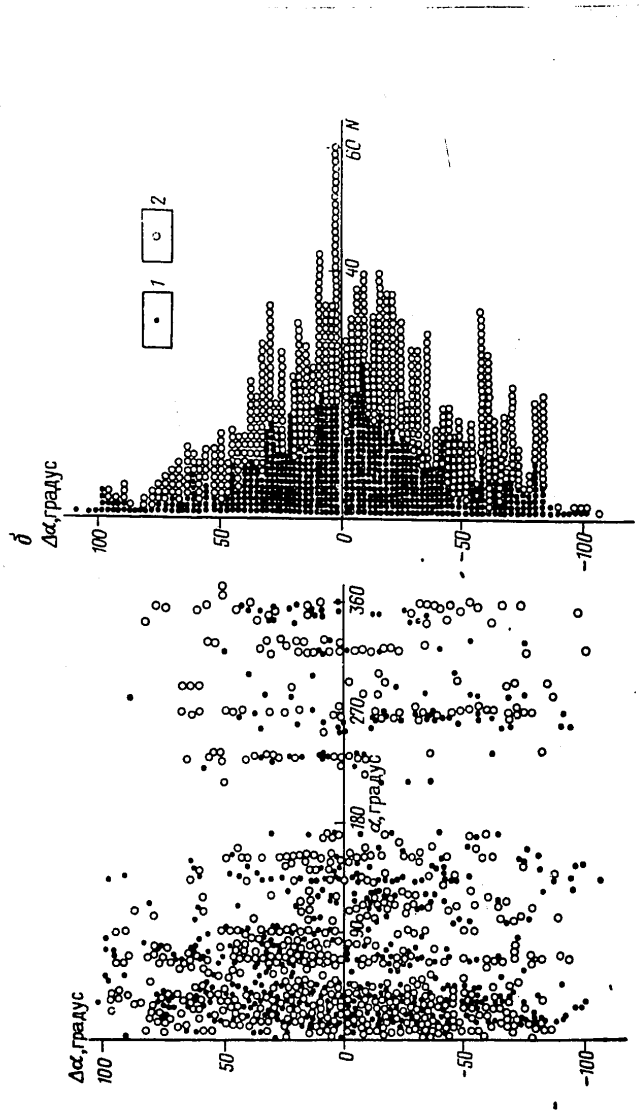

Figure 89. Graphs of Dependence of $\Delta\alpha$ on α (a) and N (b) for Regions of the North German Depression

1--for PS waves related to the surfaces of the Variscian, Caledonian and Pre-Cambrian basements; 2--for PS waves related to all the remaining interfaces of the earth's crust from the surface of the basaltic layer to the Mohorovicic discontinuity

APPROVED FOR RELEASE: 2007/02/08: CIA-RDP82-00850R000200030043-9

APPROVED FOR RELEASE: 2007/02/08: CIA-RDP82-00850R000200030043-9

determines the presence of PS_V and PS_H waves. However, as the study presented above showed, this fact can be regarded linked to the deviation of polarization planes of PS_V waves formed at the interfaces of the earth's crust with different spatial position in different directions. The second phenomenon observed on recordings of PS waves from earthquakes includes the fact that in some cases the PS waves, judging by the very typical shape of the recording, have polarity distinguished from that which should be observed at a given azimuth determined by formulas [136] (Figure 90). Construction of the motion trajectories of soil particles in the horizontal plane for PS waves shows in these cases that the azimuths of the displacement vectors of PS waves are located in a different quadrant that the approach azimuth of P waves and accordingly of PS waves, determined by the formulas of [136]. Hence, it follows that the polarity of the PS wave arrival can be distinguished from that of the P wave arrival and does not correspond to the traditional seismological distribution of the polarity of arrivals of P wave components by quadrants.* It is more correct in these cases to determine the quadrant from which the PS wave came, constructing the graph of soil particle motion in the horizontal plane. Strict consideration of the motion trajectories of soil particles and the polarity of PS wave arrivals affects to a significant degree the results of interpretation. Specifically, it may be that composite waves determined with a time shift on the X and Y components and related either to a single boundary (PS_V and PS_H) or to different boundaries, may be the components of a single wave without phase shifts upon variation of the polarity of one of the components.

The Nature of PS Waves of Different Groups and the Criteria for Separating Them on Recordings

The following groups of PS and P waves may exist on recordings from earthquakes at Δ = 5-180° and T = 0-11 seconds after the arrival of P waves: a) PS waves passing horizontal or near-horizontal ($\varphi < 10°$) interfaces of the earth's crust; b) PS waves passing through sloping (φ = 10-80°) interfaces of the earth's crust; c) lateral PS waves--transient refracted and transient diffracted; d) the horizontal components of P waves; e) incomplete (under some special conditions) P and PS waves in the sedimentary mantle.

Separation of PS waves into these groups by the shape of their recording and by the frequency spectrum is essentially impossible at the modern level of development of studies. The most optimum approach may apparently by separation of PS waves into groups according to the aggregate of their kinematic and dynamic characteristics.

PS waves which pass through the horizontal interfaces of the crust may be distinguished among the surrounding PS waves by the following features.

*Deviation of polarity from the traditional may also be caused by exchange of P and S waves on the top of the waveguide.

APPROVED FOR RELEASE: 2007/02/08: CIA-RDP82-00850R000200030043-9

APPROVED FOR RELEASE: 2007/02/08: CIA-RDP82-00850R000200030043-9

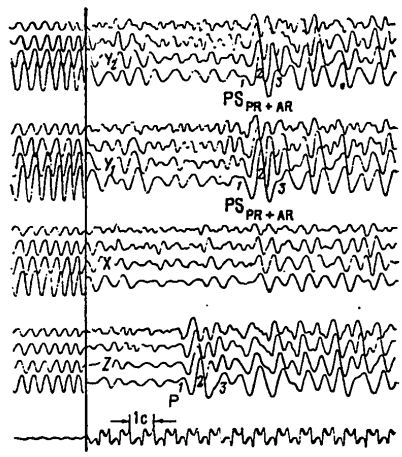

Figure 90. Seismogram with Clear Reverse Polarity of PS Wave on Y Component for Region of North German Depression:
T = 0229, 27 Jun 1969, Δ = 76.3° and α = 34.3°

1. The azimuth of the PS wave displacement vector (the major axis of an ellipse or a straight line) should coincide with the approach azimuths of P waves from earthquakes calculated by the formulas of [136]. According to theoretical calculations, the errors in determining the azimuths of the displacement vectors by their amplitudes with dynamic calibration error of 10-15° should not exceed $\pm$ 6° at any approach azimuths.

2. The angle of emergence of the seismic radiation of PS waves coincides with the theoretical angle calculated for a horizontally layered profile under the recording station.

3. The delay times of PS waves with respect to P waves from earthquakes with different approach azimuths, are registered by a single recording station and corresponding to the same interface of the crust up to the M discontinuity, should not have a spread of more than $\pm$ 0.1-0.15 second (if this is not a fault zone). As a result of this, clear maximums corresponding to the main interfaces of the earth's crust are determined on the statistical time profiles $\Delta t_{PS-P} = f(N)$. PS waves related to different interfaces of the earth's crust are easily separated in time between each other t_{PS-P} on time profiles $\Delta t_{PS-P} = f(R)$.

PS waves passing through sloping interfaces can be separated by the following features.

APPROVED FOR RELEASE: 2007/02/08: CIA-RDP82-00850R000200030043-9

APPROVED FOR RELEASE: 2007/02/08: CIA-RDP82-00850R000200030043-9

1. The azimuths of the PS wave displacement vectors (the major axis of an ellipse or a straight line) usually do not coincide with the approach azimuth of P waves from an earthquake calculated by the formulas of [136]. The discrepancies should be greater than 6 percent with dynamic channel calibration error of ± 10-15 percent.

2. The angle of emergence of seismic radiation may not coincide with the angle of emergence calculated for a horizontally layered profile under the recording station.

3. The delay times of PS waves with respect to P waves, corresponding to the same interface at a single recording station, from earthquakes with different approach azimuths yield a spread of 10 to 100 percent or more. As a result, the maximums on the statistical time profiles are indistinct or white noise is observed instead of them for all the interfaces of the crust with sufficiently large number of earthquake recordings with different approach azimuths and with an increase of Δt_{PS-P} (Figure 91).

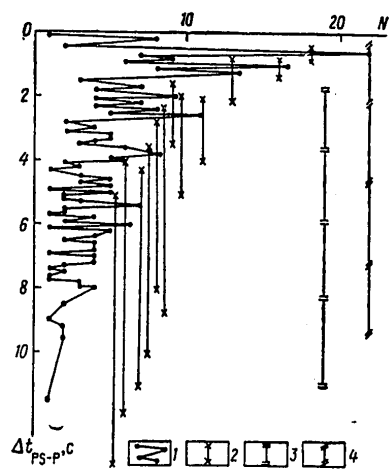

Figure 91. Statistical Time Profile of the Crust of a Mountainous Region Compared to Theoretical Times t_{PS-P} for Transient and Lateral PS Waves:
1--time profile; intervals of Δt_{PS-P}; 2--for PS waves formed on sloping interfaces of the earth's crust; 3--for transient diffracted PS waves; 4--for transient reflected PS waves

Lateral PS waves are distinguished from transient PS waves by the following features.

APPROVED FOR RELEASE: 2007/02/08: CIA-RDP82-00850R000200030043-9

APPROVED FOR RELEASE: 2007/02/08: CIA-RDP82-00850R000200030043-9

1. The cophasality axes on correlation seismograms with location of the profile transverse to the disturbance or contact have smaller values of v_k than the v_k of transient PS waves and intersect all the remaining axes (see Figure 62, a and b). The time profiles Δt_{PS-P} for these same waves intersect all the time profiles compiled for P waves for horizontal interfaces at large angles of inclination.

2. The angles of emergence of seismic radiation determined by PS waves differ from similar angles for PS waves calculated for a horizontally layered structure of the crust under the recording station.

3. The azimuths of the PS wave displacement vectors may differ from the approach azimuths of P waves to the recording stations, determined by the formulas of [136] for any values.

The horizontal components of P waves are distinguished among PS waves by the angles of emergence of seismic radiation e. In this case the waves registered on the horizontal component of the recording are initially assumed to be composite waves and then components of P waves. In the case of recording PS waves on the X and Y components, angle e is determined by the formula (Figure 92).

$$e = \operatorname{arctg} \frac{A_{PS_X}}{A_{PS_Z}}.$$

In the case of recording P waves on the Z, X and Y components, angle e is determined by the formula (see Figure 92).

$$e = \operatorname{arctg} \frac{A_{P_Z}}{A_{P_X}}.$$

Thus, for example, the following data were found for the regions of the Pre-Caspian Depression and for Tashkent. Based on the assumption that the waves on the X and Y components can be either horizontal components of P waves or PS waves, angles of e equal to 10-15 and 60-80°, respectively, were found. The theoretically calculated angles of e for PS waves registered on the X and Y components in these regions were equal to 70-80°. This made it possible to relate most experimental waves recorded on the X and Y components in these regions to composite PS waves.

Multiple waves approaching the earth's surface as P waves are determined on the recordings as the horizontal components of these waves (according to angle e). Complete and incomplete PS waves, if they exist, can be separated from single P waves by the following features.

1. A wave is assumed single if no other waves of any kind are noted on recordings of all registered earthquakes with similar values of Δ earlier than this PS wave on the horizontal component (see Figure 83, c).

APPROVED FOR RELEASE: 2007/02/08: CIA-RDP82-00850R000200030043-9

APPROVED FOR RELEASE: 2007/02/08: CIA-RDP82-00850R000200030043-9

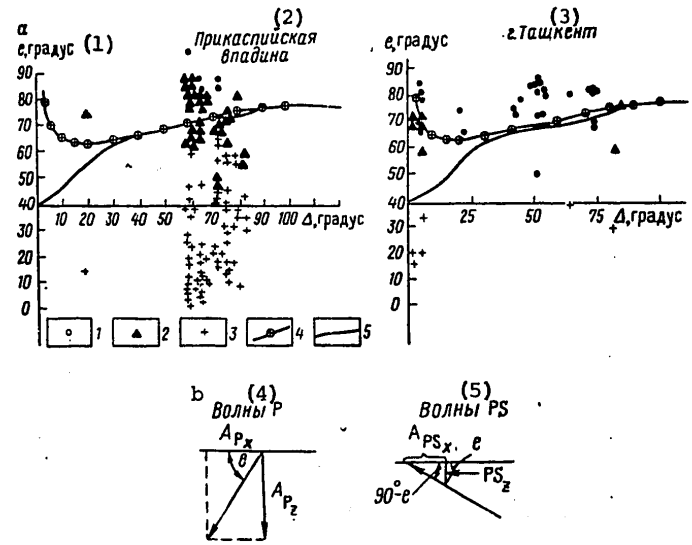

Figure 92. Graphs of Dependence of e on Δ (a) and Diagram of Ray Path of PS and P Waves in the Plane of the Ray Used When Determining Angle e (b):
1--angles e determined by the ratios of the P wave amplitude components (A_{P_Z}/A_{P_X}); 2--angles e determined by the waves registered on the X and Y components of the recording, assuming they are composite waves; 3--angles e determined by the waves registered on the X and Y components, assuming that they are components of P waves; 4--the curve e = f(Δ) according to S. D. Kogan at h_{och} = = 700 km; 5--the curve e = f(Δ) according to S. D. Kogan at h_{och} = 0

Key:
1. Degree
2. Pre-Caspian Depression
3. Tashkent
4. P waves
5. PS waves

2. All the determined PS waves may be assumed single in regions with the absence of a broken sedimentary layer. This is based on the fact that the layer in which the occurrence of intensive multiple waves is possible is absent. Waves multiple in the crystalline layers of the crust, as was demonstrated above, even without regard to the absorbing properties of the medium, have extremely low intensity and are actually not distinguished on the recordings.

APPROVED FOR RELEASE: 2007/02/08: CIA-RDP82-00850R000200030043-9

APPROVED FOR RELEASE: 2007/02/08: CIA-RDP82-00850R000200030043-9

3. The nonconformity of the delay times Δt_{PS-P} of subsequent PS waves to the theoretical times of existence of multiple waves for the region of the investigation.

A specific dependence between the recording time on the horizontal components of recording the first composite PS wave and epicentral distance was observed in many regions during work with "Zemlya" stations (Figure 93). Waves related to the deeper interfaces of the earth's crust are registered first on the recording of horizontal components with an increase of Δ. Thus, waves related to the Conrad or Mohorovicic discontinuity and having a value of Δt_{PS-P} = 3-5 seconds (see Figure 93) were registered first on recordings in many regions at Δ = 140-160°. The dependence of Δt_{PS-P} of these waves on Δ was explained by means of theoretical calculations of the intensities of the first PS waves on the X and Y components. Theoretical calculations were made for one of the models of the media of the North German Depression at absorption coefficients of $\alpha_P = 2\alpha_S$. The overall nature of the theoretical and experimental graphs is in good agreement. These data and also analysis of the experimental material of five regions permit one to assume that multiple PS waves are either absent on the recordings or their intensity is so small that they cannot have a significant effect on the wave pattern created by remote earthquakes in the initial part of the seismogram recording. This conclusion is similar to that with respect to multiple waves during GSZ [75].

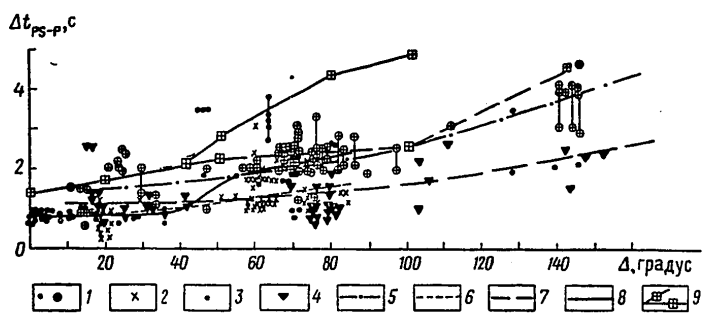

Figure 93. Graphs of Dependence of Arrival Times Δt_{PS-P} of First PS Waves on Recordings of the X and Y Components on Δ:

1--Azov-Kuban' Depression; 2--Pre-Caspian Depression; 3--Rayons of Tashkent; 4--North German Depression; 5-8--averaging curves for the Azov-Kuban', Pre-Caspian and North German Depressions and rayons of Tashkent, respectively; 9--theoretical curves for model of the crust of the North German Depression presented in Figure 3.

APPROVED FOR RELEASE: 2007/02/08: CIA-RDP82-00850R000200030043-9

APPROVED FOR RELEASE: 2007/02/08: CIA-RDP82-00850R000200030043-9

Proof of the absence of multiple PS waves may be the presence of clear maximums on the curves $\Delta t_{PS-P} = f(N)$ and $A_{PS} = f(N)$ plotted for different platform regions [113] and their persistence on large areas. Moreover, the times Δt_{PS-P} of the first PS waves registered at large values of Δ on the recordings of horizontal components correspond well to the maximum waves $\Delta t_{PS-P} = f(N)$. The persistence of the graphs $\Delta t_{PS-P} = f(N)$ within individual regions and even upon transition from region to region cannot occur in the presence of multiple PS waves on the recordings. The absence of intensive multiple waves on recordings from earthquakes and their existence on MOV seismograms from explosions are determined by the presence of P, S and PS waves at the angles of incidence to the interfaces and possibly at the frequencies from these two different types of seismic sources. Whereas the angles of incidence to the upper horizons of the sedimentary mantle do not exceed 2-8° for PS waves reom remote earthquakes, they are close to 45° for reflected waves in the regions of their initial points. As a result, the product of the reflection coefficients for multiple PS waves from earthquakes rapidly approaches zero and this product hardly differs from unity for P and S waves from explosions since the angle of incidence of the ray is similar to the critical angle in this case. Thus, the reflection coefficient of S waves will be approximately equal to 0.3 for the first layer of the model of the crust presented in Figure 3. The product of the reflection coefficients will be equal to 0.09 for a multiply reflected PSSS wave in the first layer and it will be equal to 0.0081 for a triply reflected PSSSSS wave.

APPROVED FOR RELEASE: 2007/02/08: CIA-RDP82-00850R000200030043-9

APPROVED FOR RELEASE: 2007/02/08: CIA-RDP82-00850R000200030043-9

METHOD OF INTERPRETING TRANSIENT COMPOSITE PS WAVES ON RECORDINGS FROM NEAR AND REMOTE EARTHQUAKES

Moscow SEYSMICHESKIYE ISSLEDOVANIYA S APPARATUROY "ZEMLYA" in Russian 1977 signed to press 31 Jan 1977 pp 160-183

[Chapter 7 from the book "Seysmicheskiye issledovaniya s apparaturoy 'Zemlya'" by I. V. Pomerantseva and A. N. Mozzhenko, Izdatel'stvo Nedra, 1,400 copies, 256 pages]

[Text] The method of interpreting PS waves on recordings from near and remote earthquakes includes separation and correlation of P and PS waves, construction of the time profile, determination of the velocity parameters of the medium required to transform the time profile to a depth profile, stratification of the time profiles by deep drilling data and explosions, calculation of the depths to interfaces and seismic deflections, construction of depth charts and profiles and analysis of their accuracy. Analysis of wave fields, methods of calculating depths, seismic deflection and construction of depth profiles differ somewhat from each other for regions with subhorizontal ($\varphi < 10°$) and subvertical ($\varphi > 10°$) interfaces.

Compilation of Time Profiles

Time profiles are compiled for the purpose of statistical accumulation of material from different earthquakes. They are the difference of arrival times of PS and P waves Δt_{PS-P} to the recording stations along the profile lines (Figure 94) or concentrated in one place. In the first case the distances between the recording stations R is plotted along the horizontal and in the second case the number of distinguished composite waves N. Direct accumulation of recordings from earthquakes at the observation points is impossible without preliminary conversion of signals due to the significant difference in the shape of the P and PS wave recordings from different earthquakes.

The value of Δt_{PS-P} depends, according to formulas (2.5) and (2.7) on the angle of incidence of the P wave downward to the interface i, which in turn is determined by Δ. With large differences in Δ, the times Δt_{PS-P}, especially for deep interfaces of the crust, may differ significantly from each other. Thus, for the Mohorovicic Discontinuity, if $\Delta t_{PS-P} = 6$ seconds at $\Delta = 70-140°$, then $\Delta t_{PS-P} \approx 7$ seconds at $\Delta = 3-5°$. This

APPROVED FOR RELEASE: 2007/02/08: CIA-RDP82-00850R000200030043-9

APPROVED FOR RELEASE: 2007/02/08: CIA-RDP82-00850R000200030043-9

circumstance forces one to construct the time profiles of the earth's crust from near (Δ = 3-5°) and remote (Δ = 10-160°) earthquakes separately or to introduce the corresponding corrections following from formulas (2.5) and (2.7) into the values of Δt_{PS-P} of near earthquakes.

Formulas for Determining Depths to the Interfaces H of Seismic Deflections (L), Approach Azimuths (α), Epicentral Distances (Δ) and Angles of Emergence of Seismic Radiation (e) for Horizontally Layered Media

Analysis of the formulas $\Delta t_{PS-P} = f(H, \bar{i}_{P1}, v)$, derived for horizontally layered media, showed that they may also be used with permissible errors for slightly sloping interfaces at $\varphi \leqslant 10°$ and $\Delta \geqslant 20°$ and at $\varphi \leqslant 20°$ and $\Delta \geqslant 70°$.

The depth (along the vertical) to the interface for a two-layered medium at Δ = 0-140° is determined by the formula.*

$$H_1 = \frac{\Delta t_{PS-P} v_{P_{cp}}}{K_{cp} \cos i_{S1} - \cos i_{P1}}. \tag{7.1}$$

Seismic deflections are determined by the formulas

$$L_S = H_1 \operatorname{tg} i_{S1}, \qquad L_P = H_1 \operatorname{tg} i_{P1}. \tag{7.2}$$

At $\Delta > 10°$, formula (7.1) can be reduced to a Hasegawa formula (see Chapter 2)

$$H_1 = \frac{\Delta t_{PS-P} v_{P_{cp}}}{(K_{cp}-1)\left\{1+\frac{K_{cp}}{2}\sin^2\frac{\bar{i}_{P_1}}{2}\right\}}, \tag{7.3}$$

or after slight transformations

*For the first layer in a two-layered medium, the values of v_{P1} and K_1 are equal to the mean velocity v_{PSR} and to the mean value of K_{SR}, respectively, to the interface. Therefore, let us use v_{PSR} and K_{SR} instead of v_{P1} and K_1 everywhere in the formulas.

APPROVED FOR RELEASE: 2007/02/08: CIA-RDP82-00850R000200030043-9

APPROVED FOR RELEASE: 2007/02/08: CIA-RDP82-00850R000200030043-9

$$H_1 = \frac{\Delta t_{PS-P} v_{P_{cp}}}{(K_{cp}-1)\left\{1+\frac{1}{2K_{cp}}\cos^2 e_{P1}\right\}}. \tag{7.4}$$

Seismic deflection at $\Delta > 10°$ is determined by the same formulas (7.2).

The values of α and Δ are determined by the following formulas [136]:

$$\left.\begin{aligned} \cos\Delta &= \cos\lambda_P \sin\theta \sin\theta_e + \cos\theta\cos\theta_e; \\ \sin\alpha &= \sin\lambda_P \frac{\sin\theta_e}{\sin\Delta}; \\ \cos\alpha &= \frac{\cos\theta_e - \cos\theta\cos\Delta}{\sin\theta\sin\Delta}, \end{aligned}\right\} \tag{7.5}$$

where θ is the complementary angle to the station latitude (90° - φ), θ_e is the complementary angle to the epicenter latitude (90° - φ_e); Δ is the epicentral distance, α is the azimuth to the epicenter, λ_P is the difference of station and epicenter longitudes ($\lambda - \lambda_e$), φ is the latitude of the recording station and φ_e is the latitude of the epicenter.

The error of calculating α and Δ on a computer by formulas (7.5) comprises $\pm$ 0.01°. An error in determination of Δ and α of $\pm$ (1-2°) is frequently permissible in practice. A Vul'f grid [136] is used in this case.

Angle e_{P1} is determined by recalculation of angles $e_K = f(\Delta)$ presented in [64] by the formula

$$\cos e_{P1} = \frac{v_{P_{cp}}}{v_K}\cos e_K, \tag{7.6}$$

where v_K and e_K are the velocity and angle of emergence of the seismic radiation for the earth with average parameters [64].

Construction of Depth Charts and Profiles for Horizontally Layered Media

When working with the "Zemlya" device, unlike other seismic methods of investigating the earth's crust (GSZ, KMPV and MOV), depth charts are initially constructed, from which depth profiles are then compiled. This unique production of resulting materials is determined by the approach of waves from earthquakes from different directions to the recording stations, as a result of which the derived data indicate the structure of the boundary in space rather than in the plane of the profile. To convert a three-dimensional image to a two-dimensional image (in profile), its image is constructed on a chart and then on the profile.

The entire process of constructing depth charts and profiles include the following steps.

APPROVED FOR RELEASE: 2007/02/08: CIA-RDP82-00850R000200030043-9

APPROVED FOR RELEASE: 2007/02/08: CIA-RDP82-00850R000200030043-9

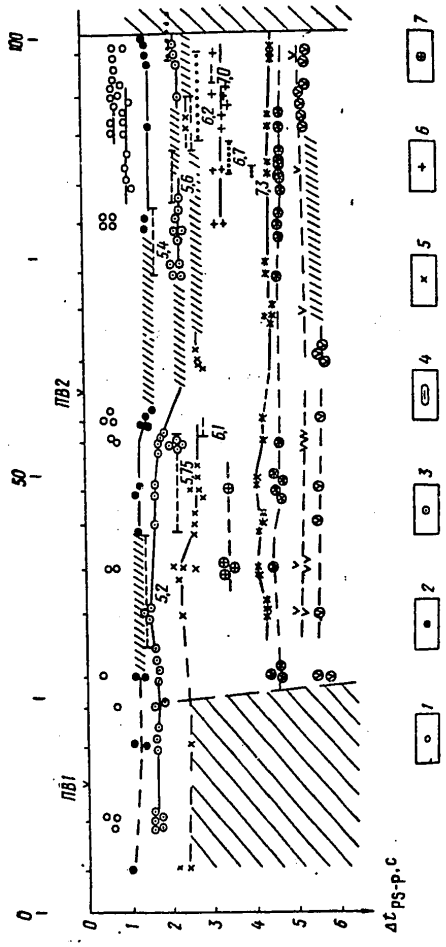

[Caption for Figure 94 on following page]

APPROVED FOR RELEASE: 2007/02/08: CIA-RDP82-00850R000200030043-9

APPROVED FOR RELEASE: 2007/02/08: CIA-RDP82-00850R000200030043-9

FOR OFFICIAL USE ONLY

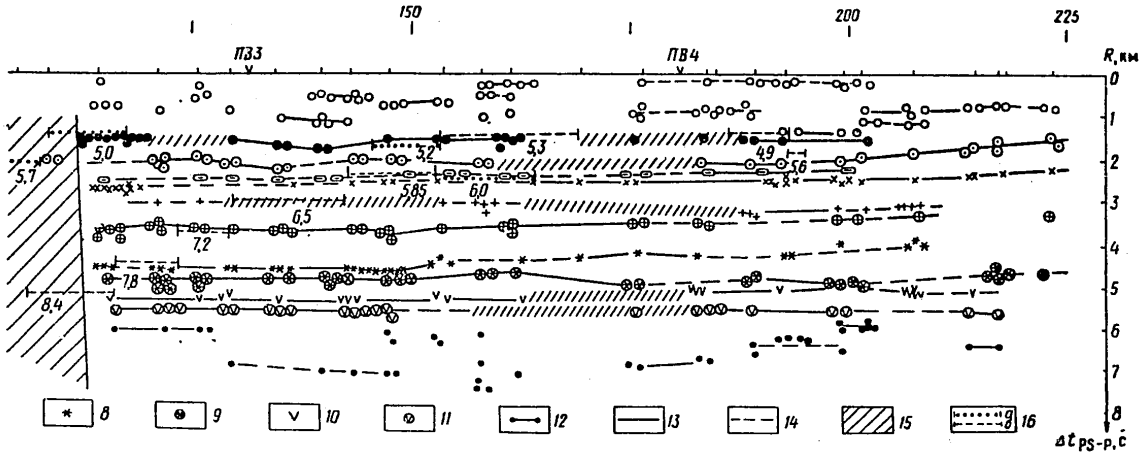

Figure 94. Comparison of Experimental (1-15) and Theoretical (16) Time Profiles of Earth's Crust by One of the Profiles of the North German Depression:
The PS waves were formed: 1--on horizons in the sedimentary mantle; 2 and 3--on surfaces of the Variscian and Caledonian Basements; 4--on surfaces of effusive-intrusive bodies; 5--on the Pre-Cambrian surface; 6 and 7--at the top and bottom of the transition zone from the granitic to the basaltic layer; 8 and 9--on Conrad-I and Conrad-II Discontinuities; 10 and 11--at the top and bottom of the transition zone from the crust to the mantle; 12--boundaries in the mantle; 13--sections of certain correlation of PS waves; 14--sections of uncertain correlation of Ps waves; 15--fault zones; 16--theoretical time profile calculated from data of P and S waves registered by "Zemlya" stations from explosions with values of $v_{P_{pl}}$ (in km/s) under the boundary; a--for PV 3; b--for PV 1, 2 and 4

FOR OFFICIAL USE ONLY

APPROVED FOR RELEASE: 2007/02/08: CIA-RDP82-00850R000200030043-9

APPROVED FOR RELEASE: 2007/02/08: CIA-RDP82-00850R000200030043-9

1. Selection of the velocity parameters of the medium and calculation of the curves $v_{P_{sr}} = f(H)$ and $K_{sr} = f(H)$ under each recording station or for individual regions of investigation necessary to convert the time profile to a depth profile.

2. Calculation of the theoretical values of Δt_{PS-P} using the derived curves $v_{P_{sr}} = f(H)$ and $K_{sr} = f(H)$.

3. Construction of graph paper of Δt_{PS-P} and determination from them of depths H_1, mean velocities $v_{P_{sr}}$ and mean values of K_{sr} to the interfaces.

4. Determination of seismic deflections by P and S waves.

5. Construction of depth charts and profiles.

The velocity parameters of the medium $v_{P_{sr}} = f(H)$ and $K_{sr} = f(H)$ are selected either for each recording station or for a series of them with an error of not more than $\pm$ 5-10 percent. The curves $v_{P_{sr}} = f(H)$ are compiled from seismic logging, MOV and KMPV data, special and incidental explosions and from near earthquakes registered by the "Zemlya" device. Seismic logging and MOV data are used as the initial materials for compilation of the curve $v_{P_{SR}} = f(H)$ to construct the surface of the crystalline base with high accuracy, especially at shallow depths of deposition (from 0.7 to 2 km). Data on coefficient K are usually absent in the region of the investigation. They are calculated by using S wave recordings from explosions and earthquakes registered by the "Zemlya" device. Methods of calculating $v_{P_{sr}} = f(H)$ and $K_{sr} = f(H)$ are presented in Chapter 9.

The theoretical values of Δt_{PS-P} are calculated by formula (7.4). The values of $v_{P_{sr}}$ and K_{sr} are calculated for each recording station with strongly variable seismological conditions by area. They are calculated for a series of stations in regions of gradual variation of these parameters. The values of Δt_{PS-P} are accordingly calculated for each station or series of stations. The value of Δt_{PS-P} is calculated on a computer for a series of stations. Special graph paper is compiled if necessary to calculate Δt_{PS-P} for each recording station.

The value of Δt_{PS-P} is calculated by a computer program in two steps. The value of H is first determined by the simplified Hasegawa formula $H = v_{P_{sr}} \Delta t_{PS-P}/(K_{sr} - 1)$ in the presence of curves $v_{P_{sr}} = f(H)$ and $K_{sr} = f(H)$ and the derived values of H are then refined by formula (7.4) by introduction of angle e_{P_1}. The theoretical values of $\Delta t_{PS-P} = f(H_1, K_{sr}, v_{P_{sr}}$ and $e_{P_1})$ are derived as a result of calculates for the given curves $v_{P_{sr}} = f(H)$ and $K_{sr} = f(H)$.

Theoretical graph papers can be calculated on the computer or by hand. They permit one to take into account with far fewer volumes of calculations all the possible variants of curves $v_{P_{sr}} = f(H)$ and $K_{sr} = f(H)$ compiled for each recording station. Theoretical graph papers (Figure 95) consist of three series

APPROVED FOR RELEASE: 2007/02/08: CIA-RDP82-00850R000200030043-9

APPROVED FOR RELEASE: 2007/02/08: CIA-RDP82-00850R000200030043-9

of the following curves: a) $v_{P_{sr}} = f(H)$; b) $K_{sr} = f(H)$; and c) $\Delta t_{PS-P} = f(H)$ at different values of e_K. Specifically, for regions of the North German Depression, the values of e_K dependent on Δ of the earthquakes registered here were selected as equal to 55, 65 and 82°, which correspond approximately to the values of Δ equal to 18, 76 and 140°. The curves $\Delta t_{PS-P} = f(H_1)$ and the corresponding curves $v_{P_{sr}} = f(H_1)$ are denoted by identical numbers. One theoretical graph paper corresponds to one interface. Since the curves $\Delta t_{PS-P} = f(H_1$, $v_{P_{sr}}$, K_{sr} and e_K are calculated by formula (7.4) which includes cos e_{P_1}, dependent on $v_{P_{sr}}$ according to (7.6), when it is considered for each boundary and station, the corresponding number of graph papers would have to be constructed. With a large number of observations (this comprised 650 points in the North German Depression), these constructions become unfeasible. To reduce the number of graph papers and to reduce them to a single paper for each interface, the values of cos e_{P_1}, different for each recording station and each earthquake, were replaced by the average value of cos e_{P_1} corresponding, according to (7.6) to the mean value $v_{P_{sr}}$ to each interface of the entire region. The effect of $v_{P_{sr}}$ on the value of cos e_{P_1} was first analyzed prior to this substitution. It turned out that even for a surface of the Caledonian Basement (the North German Depression), where the greatest variation of $v_{P_{sr}}$ was observed (from 3.2 to 4.1 km/s), the use of the averaged value of $v_{P_{sr}}$ = 3.7 km/s leads to errors in determination of angle e_{P_1} from 12 to 4° and Δt_{PS-P} = 0.005-0.01 second, which is within the bounds of accuracy of reading the times Δt_{PS-P} from the seismograms. For the remaining interfaces of the crust, replacement of interval $v_{P_{sr}}$ by the mean value $v_{P_{sr}}$ leads to even smaller errors in determination of Δt_{PS-P}.

The method of construction and use of graph papers includes the following. The values of $v_{0P_{sr}}$, $K_{0_{sr}}$ and H_{01} at any boundary in the sedimentary mantle, below which the values of $v_{0P_{po}}$ and $K_{0_{pl}}$ are known to us, are initially determined for all recording stations by the curves $v_{P_{sr}} = f(H)$ and $K_{sr} = f(H)$.

For the derived values of $v_{0P_{sr}}$, K_{0sr} and H_{01} at the boundary in the sedimentary mantle to depths somewhat greater (by approximately 5 km) than the depth to the next determined interface calculated approximately by Δt_{PS-P}, the curves $v_{P_{sr}} = f(H)$ and $K_{sr} = f(H)$ are calculated by the formulas

$$v_{P_{cp}} = \frac{H_{01}+\Delta H}{t_{01}+\frac{\Delta H}{v_{0P_{пл}}}}, \qquad (7.7)$$

where H_{01} is the depth to the boundary in the sedimentary mantle, T_{01} is the travel time of the P wave along the vertical to this boundary, ΔH is the increment of depth under the boundary in the sedimentary mantle and $v_{0P_{pl}}$ is the stratal velocity under the boundary in sedimentary deposits.

The following is then calculated

APPROVED FOR RELEASE: 2007/02/08: CIA-RDP82-00850R000200030043-9

APPROVED FOR RELEASE: 2007/02/08: CIA-RDP82-00850R000200030043-9

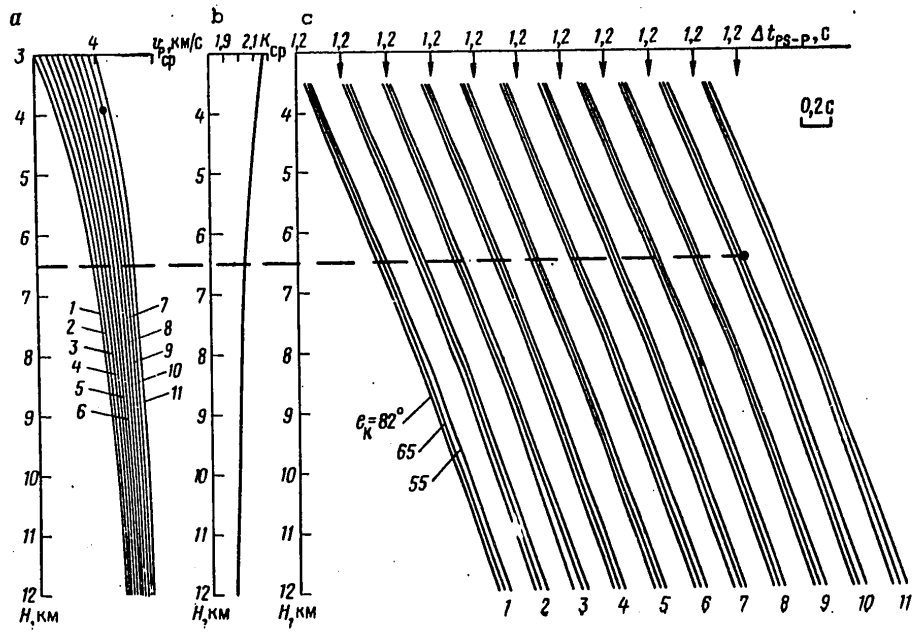

Figure 95. Theoretical Graphs For Determination of Depth to Surface of Varisican Basement for Regions of the North German Depression:
a--curves of mean velocities; b--curves $K_{sr} = f(H)$ for the upper part of the crust; c--strictly theoretical graphs of $\Delta t_{PS-P} = f(H_1, v_{P_f}, K_{sr}$ and $e_K)$ calculated for each curve of graph a.

$$K_{cp} = \frac{K_{0\,cp}\dfrac{H_{01}}{v_{0P_{cp}}} + K_{0\,пл}\dfrac{\Delta H}{v_{0P_{пл}}}}{\dfrac{H_0}{v_{0P_{cp}}} + \dfrac{\Delta H}{v_{0P_{cp}}}}, \tag{7.8}$$

where $K_{0_{sr}}$ and $v_{0P_{sr}}$ are the mean value of K and the velocity of the longitudinal waves to the boundary in the sedimentary mantle and $K_{0_{pl}}$ is the stratal value of K under the interface in the sedimentary mantle.

The set of curves Δt_{PS-P} is calculated simultaneously with curves $v_{P_{sr}} = f(H)$ and $K_{sr} = f(H)$. The values of H_1, $v_{P_{sr}}$ and K_{sr} to the first interface are then determined by the experimental values of Δt_{PS-P} and e_{P_1} from the graphs of Figure 95, c. The depth charts are constructed by the values of

APPROVED FOR RELEASE: 2007/02/08: CIA-RDP82-00850R000200030043-9

APPROVED FOR RELEASE: 2007/02/08: CIA-RDP82-00850R000200030043-9

H_1 and deflections L, by which the depth profile is compiled. The values of vp_{sr} and K_{sr} are determined to find the values of H_1 under each recording station on the depth profile, beginning from which the curves $vp_{sr} = f(H)$ and $K_{sr} = f(H)$ and Δt_{PS-P} are calculated for the next, deeper interface. The entire process of calculating the graphs and determining the values of H, vp_{sr} and K_{sr} from them is then repeated. With complex tectonics of the sedimentary mantle (of the salt-dome type), the value of H_1 must be determined with regard to the deflection and approach azimuth of the waves from earthquakes at the corresponding distance and azimuth from the recording station rather than under the recording station.

Seismic deflections by P and S waves are determined either directly by formulas (7.2) or in the presence of extensive experimental material with strongly variable seismological conditions--by graphs (Figure 96). As can be seen from formula (7.2), the tangents of angles i_{P_1} and i_{PS_1} are considerably dependent on the velocities of the P and S waves in the first medium. On the whole, the extent of deflection depends on H_1 and on tgi_{P_1} and tgi_{S_1}. Therefore, formula (7.2) can be divided into two parts, each of which can be depicted in the form of a graph. Graph II (see Figure 96) is the graph of the dependence of tgi_{P_1} and tgi_{S_1} on vp_{sr} in the covering medium for angles e_K from 50 to 83°. Graph I is the graph of the dependence of tgi_{P_1} and tgi_{S_1} on H_1. Both graphs have a common scale of tgi_{P_1} and tgi_{S_1}. The values of tgi_{P_1} and tgi_{S_1} are determined by a single tangent scale, but with different scales of vp_{sr}. The tangent of angle i_{P_1} is determined by means of the external scale and the tangent of i_{S_1} is determined by the internal scale. The process of determining L_P and L_S includes the following. By knowing the value of vp_{sr} to the point of exchange and e_K, the graph tgi_{P_1} and tgi_{S_1} on the right side is determined. The point with the given tangent and depth H_1 to the interface is then determined along the corresponding tangent curve. The extent of deflection for this point is taken from the scale LR,LS (Figure 96, I). The described sequence of determining deflections L_P and L_S is shown in Figure 96 by the dashed lines.

If one proceeds strictly from derivation of formula (7.4), the depth to the interface should be plotted on the charts or diagrams on the approach azimuths of P waves to the recording station in the range of distances from the recording station to the point of separation of the P wave from the interface, i.e., in the range of seismic deflection of the P wave. The values of deflections depend significantly on the depth of deposition of the boundary. If the deflections do not exceed 100-200 m for the surface of a basement at deposition depth of 5 km, they may reach 10 km ($\Delta \approx$ 60-70°) for the M discontinuity at a depth of 33 km. Therefore, it is more feasible, especially with regard to the dynamic properties of P and S waves determined in the region of their separation from the interface, to plot the depth on the section between the points of separation of the P and S waves from the interface rather than on the entire length of deflection of the P waves. This section will be a point for shallow-lying boundaries and will be a line measuring 3-5 km for deeply lying boundaries. Thus, the depths to the interfaces are related to the point located on the approach azimuth of P waves to the recording stations at distance $(L_P + L_S)/2$ from it when constructing depth charts by the interfaces of the earth's crust for theupper boundaries (from the surface of the basement and

APPROVED FOR RELEASE: 2007/02/08: CIA-RDP82-00850R000200030043-9

APPROVED FOR RELEASE: 2007/02/08: CIA-RDP82-00850R000200030043-9

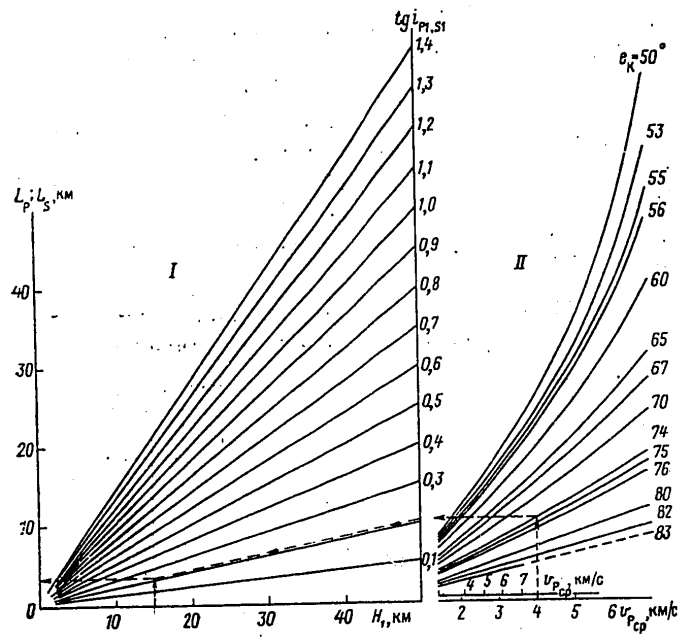

Figure 96. Graphs for Determination of Seismic Deflections Calculated for Boundaries from the Surface of the Variscian Basement to the Surface of the Basaltic Layer

approximately to the surface of the basaltic layer). Beginning from the surface of the basaltic layer and to the Mohorovicic Discontinuity, the depths to the interfaces are related to the line segment of length LP - LS, located on the approach azimuth of the P wave to the recording station at distance LS from it.

Depth charts are constructed sequentially from top to bottom from the surface of the basement to the M discontinuity. Regions with similar values of depths lying within the range of accuracy of their determination are distinguished from the data plotted on the plotting boards. For example, the values of depths 16.4-16.7, 17.5-18.7 and so on are similar with an error of ± 0.1 km in determining the depths to the surface of the basaltic layer (see Figure 64). Isolines are plotted through the centers of the regions with similar depths. They do not have to be located at equal depth intervals. The derived values of all depths to the interface along the perpendicular or in directions parallel to the isolines are projected onto the line of the profile as a function of the completeness of the derived data and are plotted on the profile where they are also averaged with regard to the accuracy of determining the depth to the interface. The charts and profiles are averaged simultaneously.

APPROVED FOR RELEASE: 2007/02/08: CIA-RDP82-00850R000200030043-9

APPROVED FOR RELEASE: 2007/02/08: CIA-RDP82-00850R000200030043-9

The Method of Comparing the Data of PS Waves to Materials of Explosions and Deep Drilling

The data of PS waves are tied into the materials of explosions and drilling by the times Δt_{PS-P} and time profiles using the formulas and calculations given below.

Comparison to materials of explosions by time profiles is made in the presence of curves $v_{Psr} = f(H)$ and $K_{sr} = f(H)$ derived in processing the explosions by recalculating them to time profiles Δt_{PS-P} by formula (7.4). The recalculated profiles of Δt_{PS-P} for their stratification are compared to the graphs v_{Ppl} and v_{Spl}, also derived by the curves $v_{Psr} = f(H)$ and $K_{sr} = f(H)$. Comparison of the time profiles constructed from PS waves at $\Delta > 70°$ and theoretically calculated by the curves $v_{Psr} = f(H)$ and $K_{sr} = f(H)$ for one of the profiles of the North German Depression is shown in Figure 94. As can be seen from this figure, the boundaries for the PS waves correspond to the velocity boundaries of P and S waves registered by "Zemlya" stations from explosions with velocity of v_{Ppl} equal to 5.3-5.4, 5.6-5.8, 6-6.2, 6.5-6.7, 7.8 and 8.4 km/s.

The interfaces constructed by PS waves are compared on the depth profiles (see Chapter 5) to the sections of refracting boundaries separated by P and S waves from explosions. Good agreement of similar profiles for the entire region indicates agreement of processing the materials by PS, P and S waves.

Comparison of Δt_{PS-P} to the times t_{0P} and t_{0S} from explosions is accomplished by using the Visser-Berlage formula [185]:

$$\Delta t_{PS-P} = \frac{H_1}{v_{P1}}(K_1 - 1)\left[1 + \left(\frac{v_{P1}}{v_{P2}}\right)^2 \frac{1}{2K_1}\sin^2 i_{P1}\right]. \qquad (7.9)$$

Formula (7.9) can be found by two methods. The first method is described in [108]. The second method includes determination of the difference $t_{0S} - t_{0P}$, where t_{0S} and t_{0P} are the times intercepted by the hodographs of refracted S and P waves above the point of the explosions through the parameters of the medium. If there is dispersion of the seismic velocities (or a low value of it) or if the PS, P and S waves are recorded at the same frequencies and also for refracted P and S waves obtained close to their initial points, the values of t_{0S} and t_{0P} for refracted P and S waves can be expressed, as for the leading waves, in the form [67].

$$t_{0S} = \frac{2H_1 \cos i_{S1}}{v_{S1}}; \quad t_{0P} = \frac{2H_1 \cos i_{P1}}{v_{P1}}. \qquad (7.10)$$

Hence,

$$\frac{t_{0S}}{2} - \frac{t_{0P}}{2} = \frac{H_1 \cos i_{S1}}{v_{S1}} - \frac{H_1 \cos i_{P1}}{v_{P1}}. \qquad (7.11)$$

APPROVED FOR RELEASE: 2007/02/08: CIA-RDP82-00850R000200030043-9

APPROVED FOR RELEASE: 2007/02/08: CIA-RDP82-00850R000200030043-9

As a result of simple transformations of (7.11), we find

$$\frac{t_{0S}}{2}-\frac{t_{0P}}{2}=\frac{H_1}{v_{P1}}(K_1-1)\left[1+\left(\frac{v_{P1}}{v_{P2}}\right)^2\frac{1}{2K_1}\sin^2 i_{P1}\right]. \tag{7.12}$$

The equality of the right sides of equations (7.9) and (7.12) permits one to write

$$\Delta t_{PS-P}=\frac{t_{0S}}{2}-\frac{t_{0P}}{2}. \tag{7.13}$$

Thus, the refracting boundaries and interfaces can be compared by knowing the delay times of the composite wave-- Δt_{PS-P} and the times t_0 for P and S waves.

The interfaces are compared to boundaries by seismic logging data using the formula

$$\Delta t_{PS-P}=\frac{t_{0S}}{2}-\frac{t_{0P}}{2}\approx t^{B}_{0S}\cos i_{S1}-t^{B}_{0P}\cos i_{P1} \tag{7.14}$$

t^{V}_{0S} and t^{V}_{0P} are the travel times of S and P waves along the vertical.

Assuming $\cos i_{S1} \approx \cos i_{P1}$, we find

$$\Delta t_{PS-P}\approx\left(t^{B}_{0S}-t^{B}_{0P}\right)\cos i_{P1}. \tag{7.15}$$

Characteristics of Interpreting Composite Transient PS Waves Formed on Sloping Interfaces of the Earth's Crust

The difference of the method of interpreting PS waves for sloping interfaces ($\varphi > 10°$) includes the need for additional analysis of wave fields by correlation and ordinary seismograms and to use three-dimensional constructions which take into account the larger angles of inclination of the interfaces.

The method of interpreting lateral PS waves has essentially not been developed. However, taking into account the dynamic and kinematic characteristics of lateral PS waves, one can use all the methods of interpretation for them valid for diffracted and planoreflected waves (methods of intersections, time fields and so on) [45, 116, 131]. Interpretation of lateral waves permits one to find data about the propagation velocities of P and S waves directly from composite waves.

The method of interpreting transient PS waves formed on sloping interfaces includes separation of these waves on the recordings of earthquakes, construction of the time profile and grouping of the points on it by boundaries, construction of the first depth profile by the method for a horizontally layered

APPROVED FOR RELEASE: 2007/02/08: CIA-RDP82-00850R000200030043-9

APPROVED FOR RELEASE: 2007/02/08: CIA-RDP82-00850R000200030043-9

medium, determination of the line of the strike and dip of the interface and also the azimuths of the displacement vectors of the incident and refracted P and PS waves, construction of theoretical graphs, determination of the angles of inclination of the interface and construction of the exchange surfaces in the profile and in space.

Separation of PS waves formed on sloping interfaces of the crust among PS waves occurring on the horizontal sections of the boundaries and also separation of transient and lateral (transient reflected and transient diffracted) PS waves is accomplished by using the criteria outlined in Chapter 6.

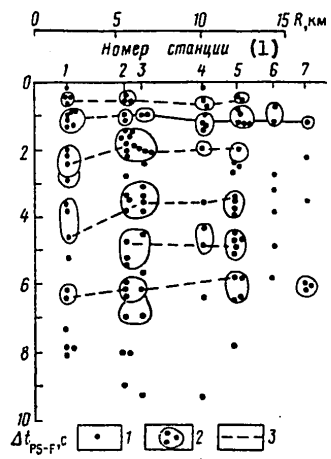

Figure 97. Time Profile for Region with Projections of the Paleozoic Basement onto the Earth's Surface: 1-- Δt_{PS-P} from different earthquakes; 2--regions in which the values of Δt_{PS-P} related to the same interface can be located; 3--assumed correlation of PS waves on the basis of horizontally layered model of the medium

Key:
1. Number of stations

The time profile is constructed by the ordinary method described for a horizontally layered medium. Despite the presence of a large dispersion of exchange points on the time profiles, grouping of points with similar values of Δt_{PS-P} is observed (Figure 97). These regions of points are related in the first approximation to the same interface. The values of the possible dispersions of Δt_{PS-P} and accordingly the range of Δt_{PS-P} in which the exchange points related to the same interface can be found are determined for the region of investigation by formulas (2.11) and (2.12). The maximum values of dispersion of Δt_{PS-P}, corresponding to the case of approach of P waves to the interface along its dip-rise line, are usually determined.

APPROVED FOR RELEASE: 2007/02/08: CIA-RDP82-00850R000200030043-9

APPROVED FOR RELEASE: 2007/02/08: CIA-RDP82-00850R000200030043-9

The preliminary depth profile is constructed by the method for a horizontally layered medium. In this case the mean value of Δt_{PS-P} from the dispersion of points related to the same boundary is used for each recording station and for each interface.

The strike and dip of the interface are determined in the following manner. Graphs of the displacement of soil particles along the horizontal components of the PS wave recording are constructed with regard to calibration of the channels. The graphs of displacement for the first interface are also constructed by the horizontal components of P waves. The graphs of oscillation of soil particles from PS waves registered at the same station and conditionally related to the same interface are plotted on the same plotting board (Figure 98). The oscillations of the soil particles in the horizontal plane from the P wave are plotted on this same board for the first interface. The direction of the dip-rise of the boundary is determined where the azimuths of the displacement vectors of PS waves determined by their amplitudes and calculated by the formulas of [136] coincide. The direction of the strike of the boundary is characterized by the maximum difference between these azimuths. The azimuths of the displacement vectors of the incident P wave and the P and PS waves refracted on the boundary are understood as the directions in the horizontal plane which comprise angles ψ_2, ψ_1' and ψ_1 with axis Ox of the right-handed coordinate system xyzo (see Figure 20). The extent of deviation of the azimuths of displacement vectors of the P waves impinging on the boundary P (ψ_2) and the P (ψ_1') and PS (ψ_1) waves approaching the recording stations (see Figure 20) can be determined either directly by the drawing of Figure 98 or by formulas (2.48) and (2.49).

Theoretical graphs of the dependence of ψ_1 and ψ_1' on ψ_2 at parameters of φ, Δ and K' are calculated for each interface constructed on the preliminary depth profile. The graphs of $\psi_1 = f(\psi_2)$, calculated for the following parameters of the media: $i_{P_1}' = 16°$ ($\Delta = 60°$), K' = 0.425 and φ = 0.10, 20, 30 and 50° $|q_S| \approx 2$, which corresponds to angles of i_{0S} up to approximately 20°, are presented in Figure 99. The process of determination of the angles of φ by the graphs of ψ_1 and $\psi_1' = f(\psi_2)$ includes the following. The directions of the dip and strike of the interface and the values of ψ_2, ψ_1 and ψ_1' are determined by the aggregate of points for a single recording station, related to a single interface. The value of ψ_1 is determined by the horizontal components of the PS waves and that of ψ_1' is determined by the horizontal components of the P waves.

Knowing the value of Δ for earthquakes (and accordingly of i_{P_1}') and also of K' and K^{II} by the values of ψ_1, ψ_1' and ψ_2, the angles of φ in the dip-rise direction of the interface are determined.

The depth of deposition of the interface at $\Delta > 10°$ is determined by the formulas which take into account angle φ :

$$H' = \frac{\Delta t'_{PS-P} v_{P_{cp}}}{(K_{cp}-1)\left\{1+\frac{1}{2K_{cp}}\cos^2 e'_{P1}\right\}}, \qquad (7.16)$$

APPROVED FOR RELEASE: 2007/02/08: CIA-RDP82-00850R000200030043-9

APPROVED FOR RELEASE: 2007/02/08: CIA-RDP82-00850R000200030043-9

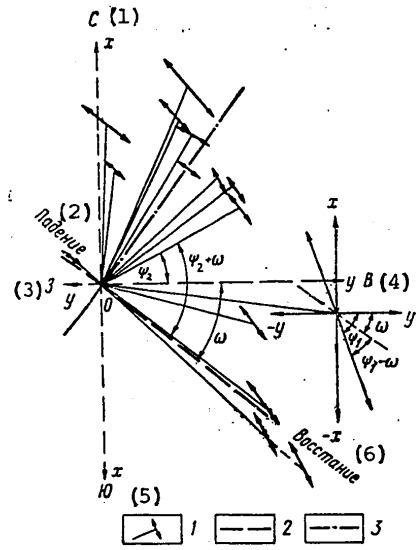

Figure 98. Diagram which Illustrates Determination of the Line of Dip and Rise of the Interface and the Values of ψ_1, ψ_2 and ω by Oscillations of Soil Particles from PS Waves in the Horizontal Plane:
1--displacement vectors of PS waves determined by their amplitudes; 2 and 3--dip-rise lines and lines of strike, respectively, of the interface

Key:

1.	North	4.	East
2.	Dip	5.	South
3.	West	6.	Rise

or

$$H_{P1} = \frac{\Delta t'_{PS-P} v_{P_{cp}}}{(K_{cp}-1)\left\{1+\frac{1}{2K_{cp}}\cos^2 e'_{P1}\right\}} + X_P \sin\varphi. \tag{7.17}$$

At $\Delta < 10°$, the formula for calculating depth is written in the form

$$H'' = \frac{\Delta t_{PS-P} v_{P_{cp}}}{K_{cp}\cdot\cos i_{S1} - \cos i_{P1}}. \tag{7.18}$$

Formula (7.17) is most convenient for determination of H. The values of the seismic deflections for H' and H'' are determined by the formulas

APPROVED FOR RELEASE: 2007/02/08: CIA-RDP82-00850R000200030043-9

APPROVED FOR RELEASE: 2007/02/08: CIA-RDP82-00850R000200030043-9

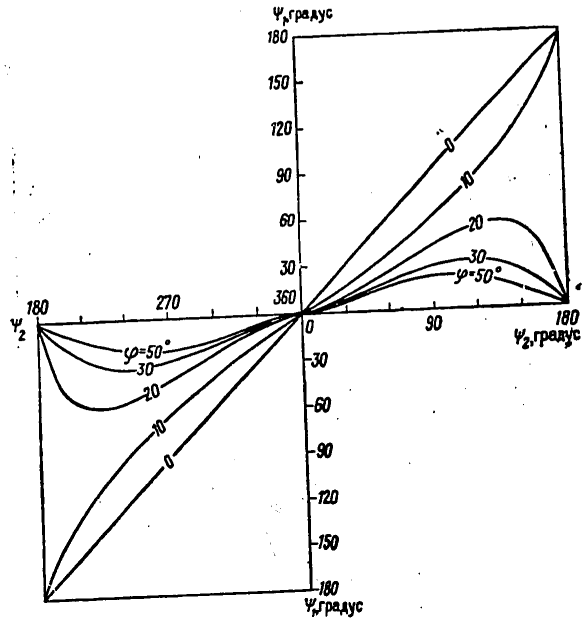

Figure 99. Theoretical Graphs of Dependence of ψ_1 on ψ_2

$$L_S = \frac{H \sin(\varphi \mp i_{S1})}{\cos i_{S1}},$$
$$L_P = \frac{H \sin(\varphi \mp i_{P1})}{\cos i_{P1}}, \tag{7.19}$$

where H = H' at $\Delta > 10°$ or H" at $\Delta < 10°$.

The seismic drift for H_{P1} is determined by the formula

$$L_P = \sqrt{(a \sin \beta' + x_{0P})^2 + b^2 \sin^2 \beta'}. \tag{7.20}$$

Recalculation of depths by the perpendicular to the interface (H' and H") to depths along the vertical is accomplished by the formulas

$$H_S^{в} = \frac{H}{\cos i_{S1}} \cos(\varphi \mp i_{S1}),$$
$$H_P^{в} = \frac{H}{\cos i_{P1}} \cos(\varphi \mp i_{P1}). \tag{7.21}$$

APPROVED FOR RELEASE: 2007/02/08: CIA-RDP82-00850R000200030043-9

APPROVED FOR RELEASE: 2007/02/08: CIA-RDP82-00850R000200030043-9

1978 YA 3 of

APPROVED FOR RELEASE: 2007/02/08: CIA-RDP82-00850R000200030043-9

APPROVED FOR RELEASE: 2007/02/08: CIA-RDP82-00850R000200030043-9

Having found the value of depth H by formulas (7.16)-(7.18), the entire process of determination by graphs $\psi_2 = f(\psi_1, \psi_1')$ and H by formulas (7.16)-(7.18) is again repeated. The cycles of determining φ and H are repeated until the discrepancies of their values found in the last two cases do not exceed the error of determining them by the described method.

Sloping interfaces are constructed in the plane and in space by PS waves in the following manner. If the line of the profile coincides with the dip-rise direction of the interface, the values of H, L and φ calculated by formulas (7.16)-(7.20) and by graphs $\psi_2 = f(\psi_1, \psi_1')$ are plotted in the plane of the profile. If the profile passes at angle γ rather than along the interface dip-rise line, then angles φ_k for this direction are determined by the formula

$$\sin \varphi_k = \sin \varphi \cos \gamma. \tag{7.22}$$

In this case the values of φ_k calculated for the given direction of the profile are substituted into formulas (7.16)-(7.18) for calculation of H. The values of H' and H" from the recording station are drawn at angle φ_k to the vertical. The boundary is drawn perpendicular to this straight line. Sloping sections are limited by the points of separation of P and PS waves from the interface, determined by formulas (8.19). The entire sloping surface is included between L_S and L_P. Its length is equal to $(L_P - L_S)/\cos \varphi_k$.

The boundaries are constructed in space by means of a special isometric scale--a protractor [114]. The values of H are calculated for this purpose by formulas (7.16)-(7.18) at the corresponding values of φ_k and are plotted in space on the approach azimuths of PS waves from earthquakes determined by formulas of [136].

The results of processing PS waves for some observation points by the method for horizontal and sloping interfaces are presented in Figure 100. The divergence of the results of processing, even for upper, shallow-lying horizons of the crust, is significant. Shifting of the boundaries in depth and in the plane comprises 30-100 percent of the real depth of deposition of the interface. Moreover, separated plateaus or even entire sections of sloping boundaries when processing by the method with regard to the angle of inclination of the interface instead of the isolated points or horizontal plateaus when using the method for horizontally layered media. For example, a composite boundary with $\Delta t_{PS-P} = 0.2$ second is determined at station 2 from recordings of four earthquakes. The use of the method of interpretation for a horizontal interface yields a single point at a depth of approximately 1 km under the station. When processing by the method for sloping boundaries, a curvilinear boundary emerging in the region of station 3 to the daytime surface is found.

The horizontal plateau under station 3 with $\Delta t_{PS-P} = 0.55$ second is shifted under station 4, being inclined at an angle of 60° to the horizon. The plateau of this same station with $\Delta t_{PS-P} = 0.3$ second is shifted under station 4 and

APPROVED FOR RELEASE: 2007/02/08: CIA-RDP82-00850R000200030043-9

APPROVED FOR RELEASE: 2007/02/08: CIA-RDP82-00850R000200030043-9

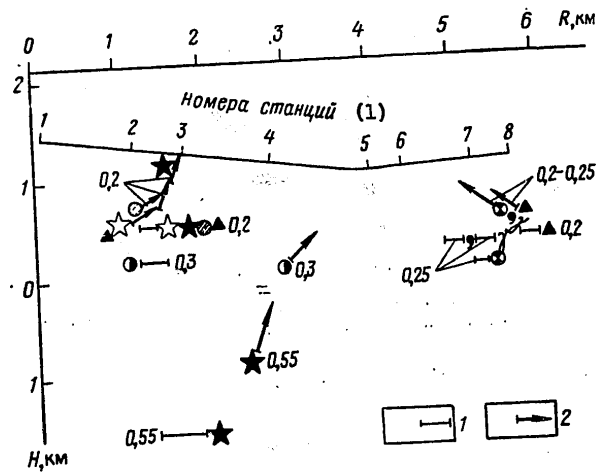

Figure 100. Results of Processing Separate Exchange Points with Δt_{PS-P} = 0.2-0.55 Second by the Method for Horizontal (1) and Sloping (2) Boundaries. The identical symbols near the plateaus cor-espond to a single earthquake and the numbers correspond to Δt_{PS-P} in seconds.

Key:
1. Numbers of stations

is inclined at an angle of 45° toward thehorizon. And finally the series of points under stations 7 and 8 with Δt_{PS-P} = 0.2-0.25 second is transformed to sloping plateaus located between stations 7 and 8. The errors of construction may increase significantly for deeper interfaces of the crust.

The described method of constructing the interface in a two-layered medium can also be used when constructing the boundaries in multilayered media. In this case the most shallow-lying interface is initially constructed. The medium from the earth's surface to the next boundary is then replaced by a layer with mean parameters and all the processing for the deeper interface is again carried out as for a two-layered medium. Thus, the overlying medium is replaced by a layer with mean values of all its parameters each time when constructing the next interface. The error of plots is 5-10 percent in this case. If necessary to increase the accuracy of the plots for deeper horizons, one should take into account the effect of refraction of rays of P and PS waves on the overlying sloping boundaries.

The Resolution and Accuracy of the Method of Composite Waves from Earthquakes

Resolution of the Method

APPROVED FOR RELEASE: 2007/02/08: CIA-RDP82-00850R000200030043-9

APPROVED FOR RELEASE: 2007/02/08: CIA-RDP82-00850R000200030043-9

Resolution of the composite wave method can be analyzed by a method known in ordinary seismic prospecting [10]. In this case the main parameter which characterizes the resolution of the method of investigation is the minimum difference of the depths of the two interfaces at which waves corresponding to each of the boundaries can be traced separately outside their zone of interference with each other and consequently can be used for further interpretation.

The nature of the zone of interference of adjacent PS waves and the degree of the reliability of determining them on the recordings depend on the value of the ratio of useful signal to background, the pulse length of the P wave from which PS waves are formed, the structure of the interfaces, the frequency of the recorded signals and other factors.

As was shown above, the use of various methodical and apparatus procedures permits one to obtain recordings of composite waves with high signal to noise ratio (more than 5-10). Let us determine the minimum thickness of the layers, study of the boundaries between which causes no difficulties by means of composite waves, as a function of the two main factors: a) the length of the initial pulse of the P wave from which the composite PS waves are formed and b) the frequencies of the recorded signals.

Let us make use of the following simplified formula to determine the minimum thickness of the layers as a function of the length of the P wave signal

$$\Delta t_{PS-P} = \frac{H_1}{v_{P1}}(K_1 - 1). \tag{7.23}$$

For the two interfaces one may write

$$\Delta t_{(PS-P)_1} = \left[\frac{H_1}{v_{P1}}(K_1 - 1)\right]_1, \quad \Delta t_{(PS-P)_2} = \left[\frac{H_1}{v_{P1}}(K_1 - 1)\right]_2. \tag{7.24}$$

Assuming the ray of the composite wave is close to the vertical and assuming in the first approximation that K_1 and v_{P1} for both boundaries are equal, let us write the difference

$$\Delta t_{(PS-P)_2} - \Delta t_{(PS-P)_1} = \frac{\Delta H_1}{v_{P1}}(K_1 - 1). \tag{7.25}$$

The waves from the two interfaces will be separated from each other if

$$\frac{\Delta H_1}{v_{P1}}(K_1 - 1) \geqslant nt, \tag{7.26}$$

where t is the period of oscillation and n is the number of periods which comprise the pulse of the PS wave.

APPROVED FOR RELEASE: 2007/02/08: CIA-RDP82-00850R000200030043-9

APPROVED FOR RELEASE: 2007/02/08: CIA-RDP82-00850R000200030043-9

The maximum value of ΔH_1 at which separation of composite waves from the two boundaries is possible if they are recorded on the same components and if they have equal intensities, is determined by the formula

$$\Delta H_1 = \frac{nt}{K_1 - 1} v_{P1}. \qquad (7.27)$$

Estimates by this approximation formula yield the following values of H. The sedimentary thickness is v_{1P} = 2 km/s, n = 2, t = 0.5 and 1 second (f = 2 and 1 Hz), K_1 = 2.7, ΔH_1 = 1.2 and 2.35 km. The crystalline crust is v_{1P} = = 6 km/s, n = 2, t = 0.5 and 1 second, K_1 = 2 and ΔH_1 = 6 and 12 km.

Recording of PS waves from different interfaces on different horizontal components, registration of PS waves first on recordings of horizontal components with an increase of Δ related to the deep interfaces of the crust and the different intensity of PS waves formed at different interfaces contribute to an increase of resolution of the composite wave method. Moreover, the resolution of the composite wave method is increased due to the fact that earthquakes with different parameters (α, λ, and so on) may produce composite waves at different interfaces. The aggregate of the given factors permits one to separate interfaces in the sedimentary mantle located at intervals of 100-200 m by depths and those in the crystalline crust at 200-500 m.

PS waves from the surfaces of the Variscian (Δ = 18°) and Caledonian (Δ = = 70°) basements, the time interval between which on the time profile comprised 0.1-0.2 second, while the value of ΔH_1 on the depth profile comprised 0.5 km, were separated in the first arrivals due to different values of Δ (18 and 70°) when working within the North German Depression. Accumulation of experimental material by PS waves from earthquakes with different values of Δ made it possible to find PS waves in the region of the first arrivals which were exchanged on the surfaces of the Variscian (Δ t_{PS-P} = 1.6-1.9 seconds), Caledonian (Δ t_{PS-P} = 1.7-2.2 seconds) and Pre-Cambrian (Δ t_{PS-P} = 2.1-2.5 seconds) Basements in the transition zone from the granitic to the basaltic layer (Δ $t_{PS-P} \approx$ 2.9-3.2 seconds) at each of 650 observation points from recordings of 1-3 earthquakes within the North German Depression. Waves exchanged at deeper interfaces of the earth's crust, including the Mohorovicic Discontinuity (Δ t_{PS-P} = 4, 4.6, 5.0-5.4 seconds) were registered at approximately half of the observation points on earthquake recordings with Δ = 140°. PS waves formed on the Mohorovicic Discontinuity were 2-10 times more intensive than PS waves related to the shallower interfaces of the earth's crust in some sections of the North German Depression. This provided confident separation of them on the recordings upon overlapping of signals up to 50 percent and good correlation along the profiles.

The dependence of the resolution of the composite PS wave method on the frequency of the recorded signals can be manifested for sharp interfaces due to the large P wavelengths, as a result of which exchange of these waves for S waves may occur in some zone near the interface rather than directly on it and also due to the fact that the boundary is a transition zone or bench of

APPROVED FOR RELEASE: 2007/02/08: CIA-RDP82-00850R000200030043-9

APPROVED FOR RELEASE: 2007/02/08: CIA-RDP82-00850R000200030043-9

layers. In both cases the dependence of Δt_{PS-P} on the frequency of the recorded signals should be observed with a dip of P waves of different frequency to the interface or exchange layer. To study this effect, we set up experimental studies near a deep borehole which exposed a Paleozoic Basement (Tashkent). Nine recordings of aftershocks of the Tashkent earthquake of 26 April 1966 with frequency of P waves of 8-10 Hz, 10 recordings of near earthquakes with frequency of P waves of 3-4 Hz and 12 recordings of remote earthquakes with frequency of P waves of 1-2 Hz were registered. According to the materials obtained, a graph of the dependence of Δt_{PS-P} on the period of the P wave on which it was clearly obvious that Δt_{PS-P} is not dependent on the periods and accordingly on the frequencies of the P waves, was constructed. This made it possible to conclude that P waves are exchanged for S waves for sharp boundaries (of the type of the Paleozoic Basement) on its surface and it not dependent on the P wavelength. Therefore, the use of P and PS wave recordings from remote earthquakes with frequencies of approximately 1 Hz does not reduce the accuracy of constructing the surface of the basement and consequently does not reduce the resolution of the composite wave method.

With a dip of P waves to transition zones [121], Δt_{PS-P} will also not depend on frequency if the structure and thickness of the bench of layers comprising the transition zone remain unchanged. In the opposite case, variation of Δt_{PS-P} as a function of frequency will vary within the range of values which comprise the difference of the travel time by P and S waves of the bench of layers which form the transition zone. According to materials of remote earthquakes with similar values of frequencies ($f \approx$ 1-2Hz) for the boundary which is unchanged in thickness by the bench of layers, Δt_{PS-P} should not vary by more than 0.1 second for the same common point at the interface [121] (due to the possible effect of the anisotropy of the medium) and either the roof or the bottom of the transition zone should be traced when tracking the PS waves from station to station by recordings of remote earthquakes. Actually, the values of Δt_{PS-P} correspond either to its roof or bottom or they have intermediate values between the room and bottom upon correlation of deep PS waves from station to station for the transition zone from the crust to the mantle. This indicates, first, that we are dealing with transition zones in the crust and separation of them by individual earthquakes may lead to significant errors. To avoid these errors, P waves from the exchange zone of not more than 5-7 earthquakes. This makes it possible to profile rather reliably the exchange zone. Second, P waves are replaced by S waves in different parts of the transition zone. Moreover, the resolution of the composite wave method also remains independent of frequency in this case (since essentially identical frequencies are observed from remote earthquakes) and is determined mainly by the length of the P waves.

The Accuracy of Constructing Interfaces by PS Waves

The accuracy of constructing interfaces of the crust by PS waves is determined by the quantity and quality of the initial material, by the correctness of determining the nature of PS waves registered on recordings, by their correlation from station to station, by the validity of the formulas used to calculate

APPROVED FOR RELEASE: 2007/02/08: CIA-RDP82-00850R000200030043-9

APPROVED FOR RELEASE: 2007/02/08: CIA-RDP82-00850R000200030043-9

depths and also by the errors in determining the parameters of the media used to construct the depth profiles. Since two types of profiles: time and depth, are used during investigations with "Zemlya" stations, let us estimate the accuracy of constructing each of these profiles.

The time profile. The accuracy of constructing the time profile is determined by the reliability of the correlation of PS waves and the dependability of identifying phases of P and PS waves of the same type. The main errors of separation and correlation of PS waves occur in those cases when PS waves comparable in amplitude are separated and correlated in the subsequent interference part of the recording. In this case errors by 1/2 or a single phase may occur when separating PS waves, which comprises 0.5 or 1 second, respectively, for recordings for remote earthquakes. Since the time profiles are compiled by a series of earthquakes (10-30) in investigations with "Zemlya" stations, the errors by one and one-half phase in separation and correlation of PS waves by any 1-2 earthquakes are easily detected and eliminated from subsequent constructions.

Let us estimate the possible time confidence intervals of the existence of interfaces of the earth's crust when they are constructed from PS waves. Let us assume that the law of error distribution is normal, the probability distribution density for which is determined by the formula

$$\psi(X)=\frac{1}{\sigma\sqrt{2\pi}}e^{\frac{(x-a)^2}{2\sigma^2}}, \tag{7.28}$$

where x is the observed value of Δt_{PS-P}, a is the selective mean value of

$$\Delta t_{PS-P}=\frac{1}{n}\sum_{i=1}^{n}(\Delta t_{PS-P});$$

and σ^2 is the standard deviation of Δt_{PS-P} determined by the formula

$$\sigma^2=\frac{1}{n}\sum_{i=1}^{n}[(\Delta t_{PS-P})_1-(\Delta t_{PS-P})]^2.$$

The confidence interval of the existence of Δt_{PS-P} is calculated by the formula

$$\varepsilon=\pm t(1-\beta,\ n-1)\sqrt{\frac{\delta^2}{n}},$$

where $t(1-\beta, n-1)$ is the Student t-distribution and n is the number of samples (earthquakes or PS waves) [71].

The estimate of parameters α, σ and ε was made for 1-30 earthquakes at values of probability P = 0.9, 0.95 and 0.99 for the following interfaces of

APPROVED FOR RELEASE: 2007/02/08: CIA-RDP82-00850R000200030043-9

APPROVED FOR RELEASE: 2007/02/08: CIA-RDP82-00850R000200030043-9

crust of the North German Depression and the rayons of Tashkent: the surface of the Pre-Cambrian and Paleozoic Basements, the transition zone from the granitic to the basaltic layer and from the crust to the mantle. The error reading the times on the seismograms comprised 0.05 second. The initial spread of times for the surface of the basements comprised $\pm$(0.05-0.1) second, for the surface of the basaltic layer it comprised $\pm$ 0.2 second and for the Mohorovicic Discontinuity it comprised 0.2 second. The time confidence intervals of the existence of the surfaces of the basements at P = 0.9 and n = 7-8 comprised +0.05 second (3-5 percent) and those for interfaces of the earth's crust comprised $\pm$ 0.1 second (1-3 percent) (see Figure 39). If errors by one-half phase or one phase remained upon construction of the time profile for any earthquake, this will increase the confidence interval of the existence of the basement surface by only 0.1-0.2 second at n = 15 and P = 0.9.

The depth profile. The error of constructing the depth profile is caused by the error in determining the nature of PS waves, by the time dispersion of Δt_{PS-P} observed on the time profiles, by the error caused by distinction of real from theoretical media and by the error of determining the different parameters of the medium (v_{Psr} and K_{sr}) used in constructing the depth profiles. Incorrect determination of the nature of PS waves may lead to significant errors in constructing the profiles and is the cause of the appearance of intermediate interfaces unrelated to anything. Processing the PS waves formed on sloping interfaces by the method for a horizontally layered medium leads to additional false boundaries--interfaces of the crust--due to the incorrect determination of the polarity of PS waves by the quadrant system. Moreover, errors in the arrangement of the boundaries in the plane and on the profile may reach 30-100 percent (see Figure 100). Errors in determining the angles of inclination of the interfaces may reach 45° or more. In platform regions where the angles of inclination of interfaces do not exceed 10°, the use of accumulation of PS waves by receiving points, jointly with their dynamic analysis, permits one to sufficiently clearly separate transient composite PS waves. All remaining types of waves yield dispersion at depths which may comprise 100 percent or more.

The confidence intervals of the existence of deep interfaces of the earth's crust, dependent on the time dispersion Δt_{PS-P}, comprise $\pm$ (100-200) m ($H_f \approx$ $\approx$ 5 km) at P = 0.9 and n = 7-8 and they comprise 400 m (H up to 33 km) for interfaces of the earth's crust.

The error caused by distinction of real from theoretical media includes the error caused by failure to consider the effect of angles of inclination of the interfaces of the crust, the error due to the use of the simplified Hasegawa formula and the error occurring upon approximation of multilayered media by two-layered media. Failure to consider the effect of the angle of inclination of the interface for a two-layered medium at φ = 0-10° and Δ = 10-140° can be disregarded and the depth to the interfaces can be determined by formulas for horizontally layered media. Formulas for horizontally layered media may also be used at φ = 0-30°, Δ = 70° and φ = 0-60° and Δ = 140°. At $\varphi > 10°$, $\Delta \leqslant 20°$ and $\varphi >$ 20-30° and Δ = 20-70°, the use of formulas for

APPROVED FOR RELEASE: 2007/02/08: CIA-RDP82-00850R000200030043-9

APPROVED FOR RELEASE: 2007/02/08: CIA-RDP82-00850R000200030043-9

horizontally layered media may lead to errors in determination of the depths of interface deposition which comprise 10-100 percent or more.

Replacement of the complete Hasegawa formula by a simplified formula is possible if the time difference in Δt_{PS-P} does not exceed $\pm$ 0.1 second by the two given formulas. This is possible at $\Delta < 30°$ for the basement surface* at $\Delta > 40$-$50°$ for the surface of the basaltic layer and at $\Delta > 100°$ for the Mohorovicic Discontinuity.

The following values of errors caused by replacement of multilayered media by media with a smaller number of layers, were obtained for the model of the crust in Figure 3. There are essentially no errors in determination of Δt_{PS-P} when a three-layered model of the sedimentary mantle is replaced by a single-layer for earthquakes with $\Delta = 140°$ and the error comprises 0.07 second for earthquakes with $\Delta = 20°$ and 0.12 second for those with $\Delta = 10°$. The error in determining the depths of deposition of the basement surface for earthquakes with $\Delta = 10°$ comprises 0.3 km. Replacement of a nine-layered model of the crust sequentially by a 4-, 3- and 2-layered model increases the error of determination of Δt_{PS-P} and the depths of deposition of the Mohorovicic Discontinuity from 0.1 to 1 second and from 0.65 to 6.5 km, respectively, for earthquakes with $\Delta < 70°$. The errors upon replacement of a multilayered by a two-layered medium can be disregarded at $\Delta = 140°$.

The relative error of determining the depth of deposition of the interface when using the simplified Hasegawa formula at separate points and by unit recordings can be calculated by the formula

$$\frac{\Delta H}{H} = \frac{\Delta(\Delta t_{PS-P})}{\Delta t_{PS-P}} + \frac{\Delta v_{P_{cp}}}{v_{P_{cp}}} + \frac{\Delta K_{cp}}{K_{cp}}.$$

The errors in determination of depth to the interface do not exceed 8-10 percent with errors in determination of Δt_{PS-P} equal to 2-3 percent, $v_{P_{Sr}}$ = = 2-3 percent and K_{Sr} = 4-5 percent. The use of the aggregate of recordings of PS waves from many earthquakes at each observation point and the use of statistical methods of processing the materials reduces the relative error in determining the depths to the interface of the earth's crust. As was indicated above, the relative error of determining the depth to the basement surface will comprise 5 percent with the number of PS waves equal to 7.8 and probability of P = 0.9, it will comprise 3 percent to the surface of the basaltic layer and 1 percent for the Mohorovicic Discontinuity.

*Estimates of the confidence intervals and errors due to failure to consider angle i were made from materials of the rayons of Tashkent and the North German Depression.

APPROVED FOR RELEASE: 2007/02/08: CIA-RDP82-00850R000200030043-9

APPROVED FOR RELEASE: 2007/02/08: CIA-RDP82-00850R000200030043-9

METHOD OF DETERMINING THE COORDINATES OF THE FOCI OF EARTHQUAKES AND INCIDENTAL EXPLOSIONS

Moscow SEYSMICHESKIYE ISSLEDOVANIYA S APPARATUROY "ZEMLYA" in Russian 1977 signed to press 31 Jan 1977 pp 183-193

[Chapter 8 from the book "Seysmicheskiye issledovaniya s apparaturoy 'Zemlya'" by I. V. Pomerantseva and A. N. Mozzhenko, Izdatel'stvo Nedra, 1,400 copies, 256 pages]

[Text] The method of determining the coordinates of focal zones is essentially identical for explosions and earthquakes. It includes separation of the first arrivals of P and S waves on the recordings, construction of the Vadati graphs from them, which are the dependence of the delay times of S waves with respect to P waves ($\Delta t_{S-P} = T_S - T_P$) on the absolute time of their recording (T_S and T_P), isochronic charts, determination of the time of occurrence of earthquakes at the focus T_0 and the location of the focus. The type of the source--an explosion or earthquake--is also additionally determined under specific conditions. Different methods of determining these values are used as a function of the ratio of the depth of the focus hoch and the epicentral distance Δ. Methods of intersections, the Vadati method and methods of solving a system of three-dimensional equations of hyperbolas are used in the relation $\Delta \leqslant$ hoch [70, 15]. Methods of intersections, hyperbolas, Golenetskiy and others are used $\Delta >$ H.

The method described below was tested upon determination of the coordinates of foci from recordings of 356 aftershocks of the Tashkent earthquake, 125 special explosions, 650 incidental explosions and 200 near earthquakes within Tashkent, the Azov-Kuban', Pre-Caspian and North German Depressions and on the Southeastern Russian Series.

Determining the Moment of Occurrence of an Explosion or Earthquake

The moment of occurrence of an explosion or earthquake T_0 is determined mainly by two methods developed in the seismology for direct waves: by the Vadati method [137-151] and by the arrival time of P and S waves. To determine T_0 by the Vadati method in the presence of n stations, n equations of the following type are compiled and solved:

APPROVED FOR RELEASE: 2007/02/08: CIA-RDP82-00850R000200030043-9

APPROVED FOR RELEASE: 2007/02/08: CIA-RDP82-00850R000200030043-9

$$T_S - T_P = (K-1)(T_P - T_0), \qquad (8.1)$$

The system of equations (8.1) is solved by the graphical method. The absolute arrival times of P and S waves to different recording stations T_P and T_S are plotted on the x-axis (Figure 101, a) and the difference of the arrival of P and S waves to the recording stations ($T_S - T_P = \Delta t_{S-P}$) is plotted on the y-axis. The straight lines $T_S = f(\Delta t_{S-P})$ and $T_P = f(\Delta t_{S-P})$ intersect on the T_P and T_S axis at point T_0 since at the moment of occurrence of the explosion or earthquake $T_P = T_S = T_0$. The value of $K = v_P/v_S$ on the path from the focus to the observation station was determined simultaneously when constructing the Vadati graphs. The times T_P for all the recording stations were plotted along the x-axis and T_S were plotted along the y-axis when determining T_0 by the arrival times of P and S waves. The derived points were averaged by a straight line whose point of intersection with the bissectrix of the coordinate angle yielded a value of T_0, read both along the T_P axis and the T_S axis. The second method with the presence of the value of K made it possible to determine the time T_0, having data only for one recording station. A straight line with angular coefficient $K = v_P/v_S$ was drawn from the point with coordinates T_P and T_S and the point of intersection of this straight line with the bissectrix of angle (B) yielded values of T_0. The Vadati graphs and the graphs $T_S = f(T_P)$ had a small time dispersion and were averaged easily by straight lines when direct waves approached the recording stations. Breaks appeared on the Vadati graphs in the case of approach of refracted (refracted in two- and three-layered media) waves to the recording stations. The errors in the recording times of P and S waves led to deviation of the points on the Vadati graphs and the $T_S = f(T_P)$ graph for different values from the straight line. The points on the Vadati graph and the graph $T_S = f(T_P)$ did not lie on a single straight line in the case of an error in determining the arrivals of P or S waves. All the points could be averaged only by means of a series of broken lines in the case of transition during correlation from one type of P and S waves to another, for example,

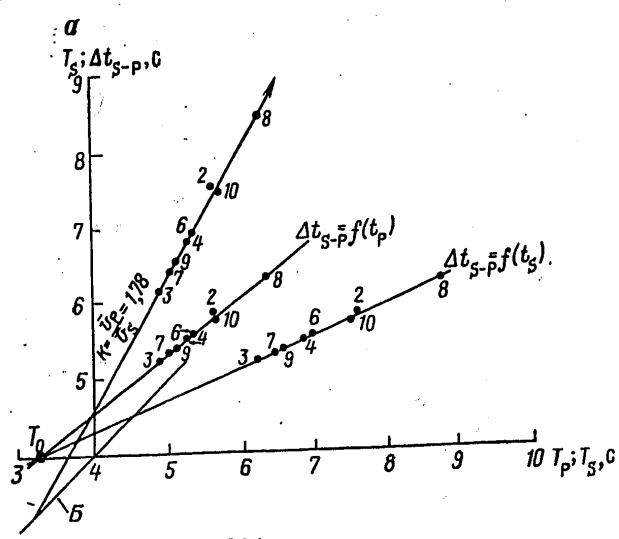

[Caption for Figure 100 on following page]

APPROVED FOR RELEASE: 2007/02/08: CIA-RDP82-00850R000200030043-9

APPROVED FOR RELEASE: 2007/02/08: CIA-RDP82-00850R000200030043-9

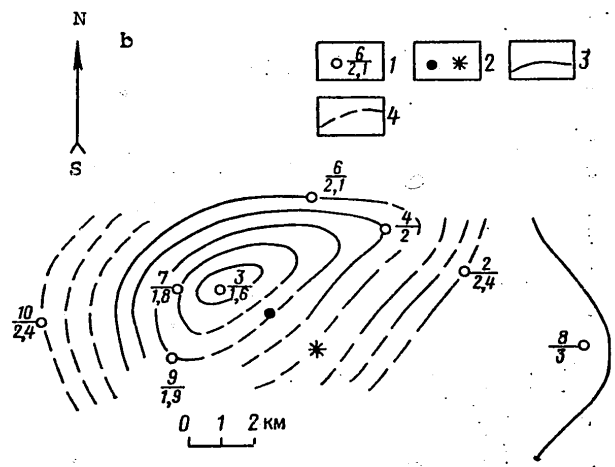

Figure 101. Example of Processing Recordings of P and S Waves from a Single Aftershock of the Tashkent Earthquake. The recording stations surround the focus, T_0 = 1717 03.24, 2 Oct 1966:
a--Vadati graphs; b--isochronic lines from P wave; 1--"Zemlya" recording stations, the number of the station is in the numerator and the arrival time of the P wave from the focus (in seconds) is in the denominator; 2--epicenter of earthquake determined on computer with h_{och} = 6.8 km and by the method of intersections with h_{och} = 2.3 km; 3--certain behavior of isochronic line of P waves; 4--assumed behavior of isochronic lines

APPROVED FOR RELEASE: 2007/02/08: CIA-RDP82-00850R000200030043-9

APPROVED FOR RELEASE: 2007/02/08: CIA-RDP82-00850R000200030043-9

from straight lines (by stations installed in the immediate vicinity to the focus) for refracted waves (for stations installed far from the focus) on the Vadati and $T_S = f(T_P)$ graphs.

Determining the Location of the Focus of an Explosion and Earthquake

The position of the epicenter of an explosion or earthquake is determined by ordinary methods outlined in seismology. When working with the "Zemlya" device, the method of intersections, the Vadati method and to a lesser extent the average Golenetskiy lines and hyperbolas were most frequently used [151]. A method of determining the foci of local earthquakes by solving a system of equations of three-dimensional hyperbolas was proposed in 1967 [70].

The method of intersections made it possible to determine the epicenter of the earthquake and the depth of the focus simultaneously by the arrival times of direct and refracted P and S waves or by the difference of the arrival times of S and P waves to the recording stations. The number of observation stations was not more than three when using this method. Theoretical or experimental hodographs compiled for the region of investigation at different focal depths were necessary when determining the epicenter and depth of the focus by the method of intersections. The position of the epicenter was determined at the point of intersection of arcs of circles with centers at the points of installation of the recording stations. The depth of the focus was taken as that, the theoretical or experimental hodographs for which yielded minimum triangles of lack of tie-ins for intersections made from the points of location of the recording stations. The most accurate results were obtained by P waves fro earthquakes with low value of Δ (up to 100 km) since separation of them on the recordings was more reliable. In the absence of T_0 or inaccurate determination of it, the radii of the intersections were determined by the difference of the arrival times of longitudinal and transverse waves (t_{S-P}) to the recording stations. To determine the explosion epicenter ($h_{och} = 0$), we suggested that reflected and refracted P and S waves be used. The radii of intersections for refracted waves in multilayered media were determined by the formula*

$$\Delta = \left[t_S - t_P - \sum_{q=0}^{m} \left(t_{0S_q} - t_{0P_q} \right) \right] \frac{1}{v_{\phi.r.}}, \tag{8.2}$$

where t_S and t_P are the travel times of the P and S waves from the focus to the recording station, $v_{f.g}$ is the imaginary boundary velocity

$$v_{\phi.r} = \frac{v_{P_r} - v_{S_r}}{v_{S_r} v_{P_r}};$$

*Formula (8.2) is strictly valid for leading waves.

APPROVED FOR RELEASE: 2007/02/08: CIA-RDP82-00850R000200030043-9

APPROVED FOR RELEASE: 2007/02/08: CIA-RDP82-00850R000200030043-9

v_{P_g} and v_{S_g} are the boundary (or apparent) velocities of the transverse and longitudinal waves.

For reflected waves propagated in a two-layered medium with horizontal interface, the equation of the radius of intersections (Δ) has the form

$$\Delta = \sqrt{(t_S - t_P)^2 \frac{1}{v_\Phi^2} - 4h_{\text{эф}}^2}, \tag{8.3}$$

where $v_f = v_{P_{eff}} - v_{S_{eff}}/v_{P_{eff}} v_{S_{eff}}$ and h is the depth of the reflecting boundary.

The Vadati method was used only for direct waves. It was used to determine the position of the epicenter and the depth of the focus of only the nearest earthquakes (but not explosions) for which the epicentral distances Δ exceeded the depths of the foci by not more than a factor of 1.5. The basis of the Vadati method was the proportional dependence between the epicentral distance and the time Δt_{S-P}. The advantage of the Vadati method is that a knowledge of the wave propagation velocity in the medium is not necessary and there is no need to be given the theoretical hodographs when determining the location of the focus by it [151].

The method of average Golenetskiy lines was used in those cases when the wave front approaching the observation stations could be assumed flat. In this case the linear isochrone was found by three recording stations. The average line which gave the direction to the epicenter was constructed for this isochrone. The same operation was repeated with the next station. Intersection of two or more average lines yielded the location of the epicenter. The focal depth was not determined in this case.

The method of hyperbolas uses the main property of a hyperbola determined as the aggregate of points for which the difference of distances from two points, called the foci of the hyperbola, is a constant value [151]. The hyperbolas were constructed sequentially for a pair of stations. Moreover, the recording stations are the foci of the hyperbola and the hyperbola itself is the geometric location of the possible epicenters. Intersection of several hyperbolas determines the location of the epicenter. The limitation of this method included the fact that v_P was supposed to be constant, i.e., the recorded waves at all the recording stations were supposed to be related to a single boundary, for example, to the surface or basement, the Mohorovicic Discontinuity and so on. No fewer than three stations must be used in the method of hyperbolas. Satisfactory results were obtained with four or more stations. The properties of the asymptote of the hyperbola rather than the hyperbola itself were frequently used for remote earthquakes [17].

APPROVED FOR RELEASE: 2007/02/08: CIA-RDP82-00850R000200030043-9

APPROVED FOR RELEASE: 2007/02/08: CIA-RDP82-00850R000200030043-9

The location of the epicenter was determined by plotting* the isochrones of direct P and S waves by the aftershocks of the Tashkent earthquake of 26 April 1966 (see Figure 101). The arrival times of the P and S waves were taken from the seismograms with an error of 0.02 second. The isochrones were made every 0.1 second. The earthquake epicenters were located within the isolines with minimum time. This method also makes it possible to determine the propagation velocities of P and S waves in the medium above the focus.

The method of solving three-dimensional hyperbolas was used to determine the parameters of foci by the arrivals of P and S waves without using theoretical hodographs. An algorithm was developed and a corresponding program was compiled [70]. The entire process of determining the coordinates of the foci and the velocity characteristic in the focal zones is divided into two steps. The value of T_0 is determined during the first step by solving equations of the following form for a series of stations

$$T_{S\,n} - T_{P\,n}K + T(K-1) = 0, \tag{8.4}$$

where T_{Pn} and T_{Sn} are the arrival times of P and S waves at the n-th recording station and K is the coefficient of the velocity ratio of longitudinal and transverse waves in the medium covering the focus.

The parameters of the focus are determined in the second step by solving a system of equations of the following form for a minimum of four stations

$$T_{P\,n,\,S\,n} - T_0 = \frac{1}{v_{P,\,S_{cp}}}\sqrt{(x_n - x)^2 + (y_n - y)^2 + h_{oq}^2}, \tag{8.5}$$

where x_n and y_n are rectangular coordinates of the n-th recording station, x and y are the rectangular coordinates of the earthquake focus and v_P, S_{sr} is the mean propagation velocity of longitudinal and transverse waves.

The Accuracy of Determining the Focal Coordinates of Earthquakes and Explosions

The accuracy of determining the focal coordinates of earthquakes and explosions was estimated for the focal zone of the Tashkent earthquake of 26 April 1966 from recordings of its aftershocks with Δ = 0-20 km and also for the foci of local earthquakes and explosions with Δ = 0-500 km, determined during studies on the Southeastern Russian Series, the Northern Pre-Caspian Depression and within Tashkent. Accuracy was evaluated both by direct calculation of the errors of time determination and construction of theoretical hodographs and by comparison of the coordinates of epicenters and foci determined by different methods.

*This method was used in studies with the "Zemlya" stations since high accuracy of reading the times from the seismograms is necessary for it.

APPROVED FOR RELEASE: 2007/02/08: CIA-RDP82-00850R000200030043-9

APPROVED FOR RELEASE: 2007/02/08: CIA-RDP82-00850R000200030043-9

The accuracy of determining the focal coordinates of the aftershocks of the Tashkent earthquake when using formulas (8.4) and (8.5) was evaluated in the following manner. Using different combinations of initial times of the first P wave arrivals for the same earthquake by alternate exclusion of one or two stations from the calculations, regions of the possible existence of earthquake foci were estimated, i.e., the accuracy of determining the focal coordinates in the horizontal plane (x, y) and their depth was estimated, depending on the location of the station and the focus, the distance from the focus to the recording station and so on.

The regions of the possible location of the epicenters of the aftershocks of the Tashkent earthquake registered by different stations (Table 8) are presented in Figure 102. The regions of the possible existence of epicenters vary from 0.8 X 0.5 to 2 X 2 km^2 and depend mainly on two factors: the neutral location of the recording stations and the focus and epicentral distances. The region of the possible existence of the epicenter decreases to 100 X 100 or 200 X 200 m^2 when using recording stations located around the focus at a distance up to 7-8 km from it.

Table 8. Data on Aftershocks of Earthquake Used for Construction of Figure 102.

(1) Номер афтершока Ташкенского землетрясения	(2) Время регистрации афтершоков	(3) Номер станций записи афтершоков	Стоянка (4)
79	(5) 2 ч (6) 06 мин, 2.XII. 1966 г.	1, 3, 6—10, 13	
80	20 ч 33 мин, 2.XII. 1966 г.	1, 3, 4, 6—13	
81	20 ч 37 мин, 2.XII. 1966 г.	1, 3—13	
83а	15 ч 26 мин, 3.XII. 1966 г.	1—10, 12, 13	a
83б	15 ч 26 мин, 3.XII. 1966 г.	1, 2—4, 6—10, 12, 13	
84	20 ч 7 мин, 4.XII. 1966 г.	1, 2—6, 8—10, 12, 13	
85	13 ч 48 мин, 6.XII. 1966 г.	1—7, 9, 12	
36	1 ч 29 мин, 31.VII. 1966 г.	2, 3, 5, 6, 9, 10	
37	1 ч 23 мин, 31.VII. 1966 г.	2, 3, 5, 9, 10	
39	1 ч 31 мин, 31.VII. 1966 г.	2, 3, 5, 6, 9, 10	
42	23 ч 07 мин, 1.VIII. 1966 г.	1—3, 5, 6, 8	
47	3 ч 14 мин, 12.VIII. 1966 г.	1, 3, 5, 6, 8, 10	b
48	5 ч 04 мин, 12.VIII. 1966 г.	1, 3, 5, 6, 8	
50	2 ч 05 мин, 16.VIII. 1966 г.	1—4, 6—10	
51	21 ч 44 мин, 16.VIII. 1966 г.	2—5, 7, 8	
52	4 ч 33 мин, 16.VIII. 1966 г.	1—5, 7—9	
53	20 ч 27 мин, 16.VIII. 1966 г.	1, 3, 5—9	
54а	3 ч 38 мин, 17.VIII. 1966 г.	1, 3, 4—10	
54б	3 ч 38 мин, 17.VIII. 1966 г.	1, 3—10	

Key:

1. Number of aftershock of Tashkent earthquake
2. Time of recording aftershocks
3. Number of stations recording aftershocks
4. Stopover
5. Hours
6. Minutes

APPROVED FOR RELEASE: 2007/02/08: CIA-RDP82-00850R000200030043-9

APPROVED FOR RELEASE: 2007/02/08: CIA-RDP82-00850R000200030043-9

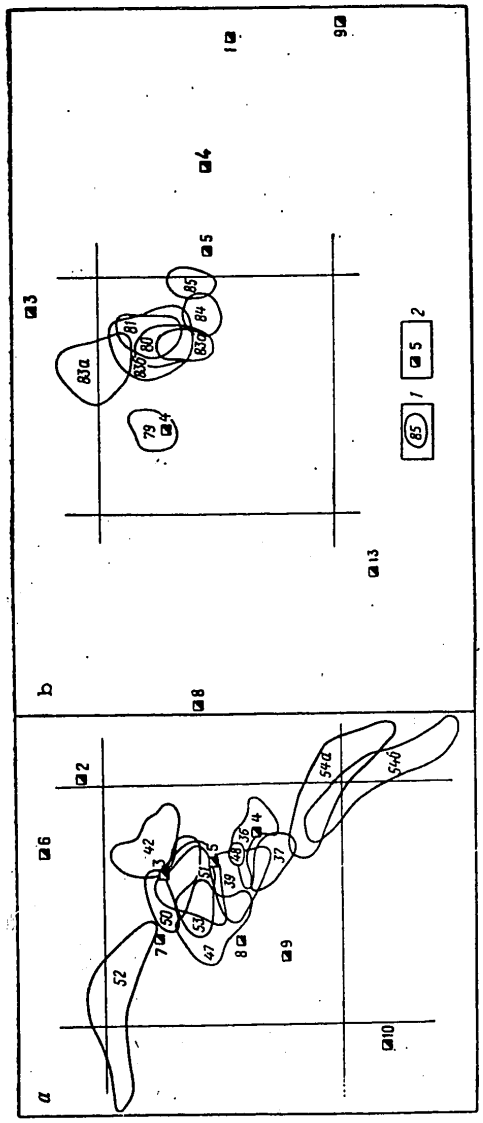

Figure 102. Regions of Possible Locations of Aftershocks of Tashkent Earthquake Registered by "Zemlya" Stations at Two Stops (a and b): 1--region of possible location of epicenters of different aftershocks of Tashkent earthquake of 26 April 1966 and their numbers (see Table 8); 2--location of recording stations and their numbers

APPROVED FOR RELEASE: 2007/02/08: CIA-RDP82-00850R000200030043-9

APPROVED FOR RELEASE: 2007/02/08: CIA-RDP82-00850R000200030043-9

The error in determining the depths of the foci calculated by remote stations may vary from 2 to 4 km. If the stations are located around the focus and if the epicentral distances are not more than 7-8 km, the error with which the focal depth is determined decreases to ±(500 meters-1 km). The best results for the aftershocks of the Tashkent earthquake were found when the distances to the foci were equal to 6-8 km at h_{och} = 3-9 km. Location of the stations at greater distances and installation of them directly in the focal zone lead to distortion of the results. To determine the focal coordinates, it is necessary that the number of stations be no less than four. The optimum number for processing is 8-9 stations.

Comparison of the locations of the epicenters of aftershocks of the Tashkent earthquake of 26 April 1966, determined by the method of intersections, the method of three-dimensional hyperbolas and the method of isochrones showed that all the epicenters generally depict the same zone. However, their location, determined by methods of isochrones and three-dimensional hyperbolas, is more compact than by the method of intersections (Figures 103 and 104). Moreover, epicenters determined by the method of three-dimensional hyperbolas are located closely to the isochrone centers with minimum time and have 3-4 times fewer triangles of lack of tie-ins than epicenters determined by the method of intersections for a theoretical hodograph (Figure 105).

Table 9. Values of h_{och} (in Kilometers) Determined by Different Methods

Номер землетрясения (см. рис. 104) (1)	(2) Способ засечек	Способ пространственных гипербол (3)	Номер землетрясения (см. рис. 104) (1)	(2) Способ засечек	Способ пространственных гипербол (3)
3	1	5,28	15	4,0	5,55
4	2	4,2	18		4,77
7	2,6	4,7	22	2,0	6,78
8	7,5	6,4	23	3,0	4,59
9	6,0	4,21	24б	3,5	6,15
11	4,0	5,9	24в	5,4	5,17
13	7,0	8,6	25а	6,0	4,6
14	3,0	6,86	25б	4,0	4,0

Key:
1. Number of earthquake (see Figure 104)
2. Method of intersections
3. Method of three-dimensional hyperbolas

The derived data permit one to assume that the most optimum and accurate method is solution of three-dimensional hyperbolas (Table 9) when determining the location of the foci of aftershocks of the Tashkent earthquake of 26 April 1966.

The accuracy of determining the focal coordinates of explosions was also estimated as a function of the location of the stations and focus. A number of

APPROVED FOR RELEASE: 2007/02/08: CIA-RDP82-00850R000200030043-9

APPROVED FOR RELEASE: 2007/02/08: CIA-RDP82-00850R000200030043-9

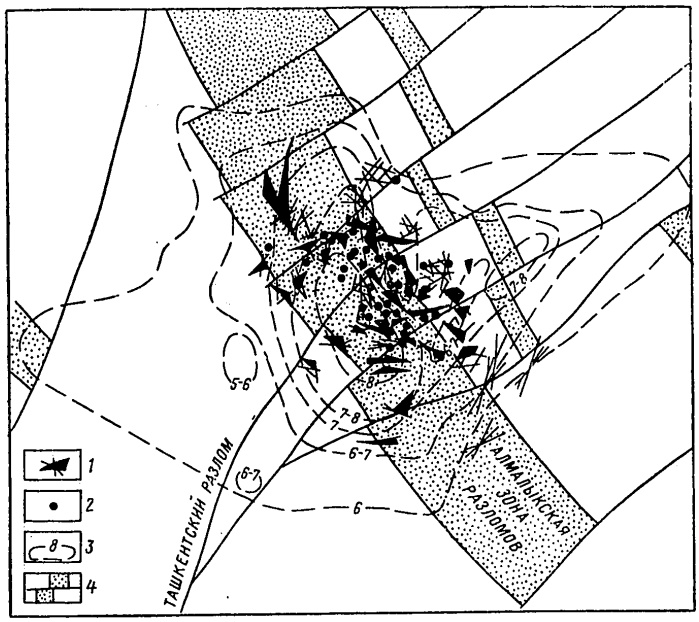

Figure 103. Location of Epicenters of Aftershocks of Tashkent Earthquake of 26 April 1966 Determined by Method of Intersections (1) and Method of Three-Dimensional Hyperbolas (2) with Isoseismal Lines of Destruction in Units (3) and Fault Zones (4) Determined by A. G. Khvolovskiy and N. B. Vol'fson by Aeromagnetic Data

Key:
1. Tashkent Fault
2. Almalyk Fault Zone

estimates was made from explosions with known coordinates and moments of the explosions. The derived results showed that the error of determining the location of the point of the explosion comprises 5-10 percent with the presence of a sufficiently accurate of P and S waves the investigated region and with the location of 4-9 recording stations in one direction from the point of the explosion at distances up to 200 km.

APPROVED FOR RELEASE: 2007/02/08: CIA-RDP82-00850R000200030043-9

APPROVED FOR RELEASE: 2007/02/08: CIA-RDP82-00850R000200030043-9

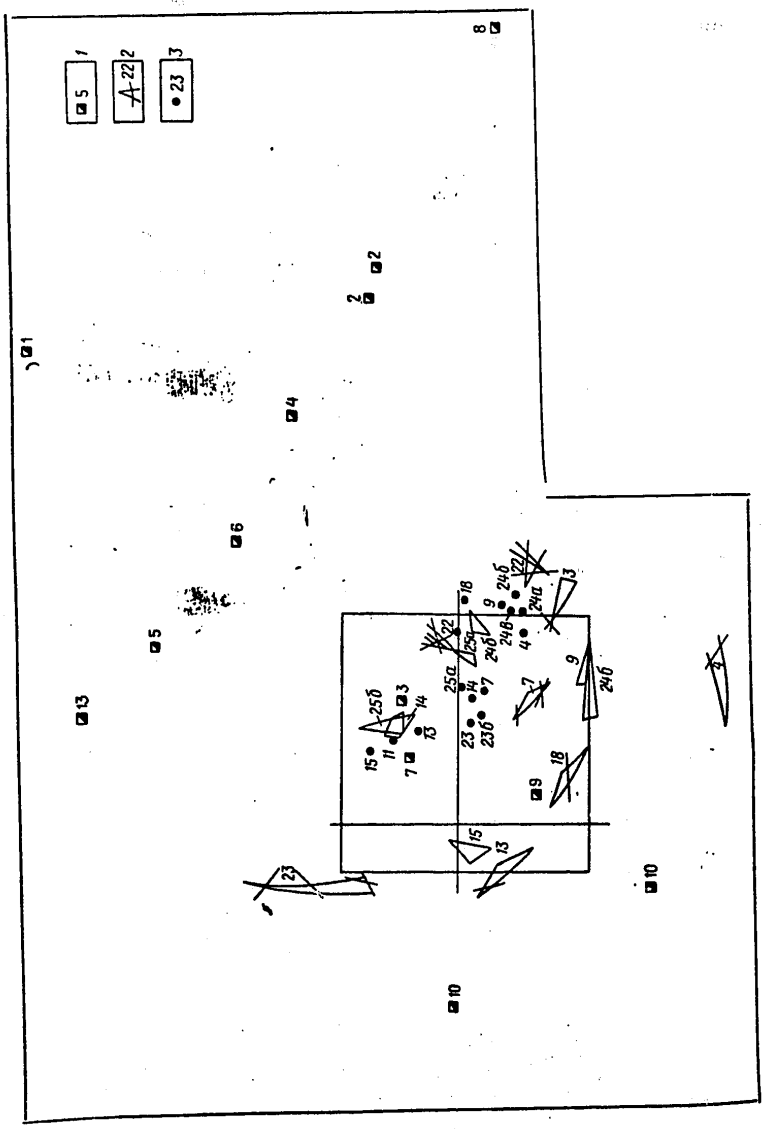

Figure 104. Comparison of the Epicenters of Aftershocks of the Tashkent Earthquake at One Stopover, Determined by the Method of Intersections from a Theoretical Hodograph (see Figure 105) and by the Method of Three-Dimensional Hyperbolas: 1--locations of installation of "Zemlya" recording stations with station number; 2 and 3--epicenters determined by the method of intersections and by the method of three-dimensional hyperbolas, respectively, with number of earthquakes from Table 9.

APPROVED FOR RELEASE: 2007/02/08: CIA-RDP82-00850R000200030043-9

APPROVED FOR RELEASE: 2007/02/08: CIA-RDP82-00850R000200030043-9

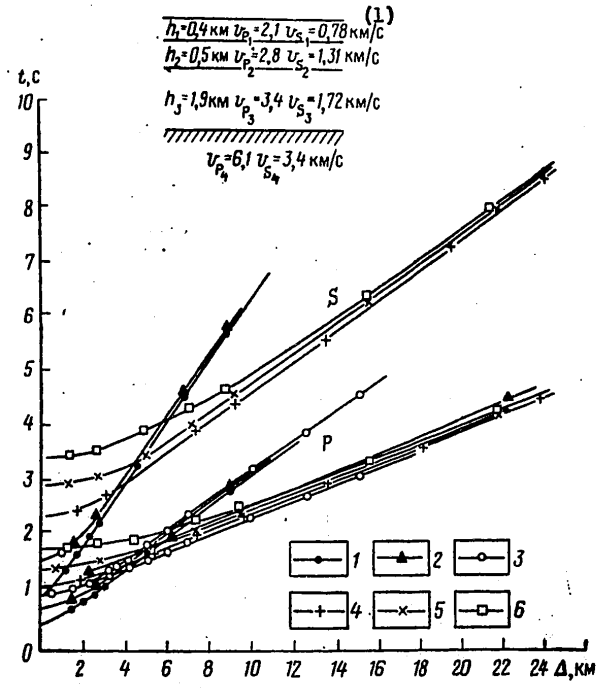

Figure 105. Theoretical Hodographs of P and S Waves for Region of Tashkent at Different Values of h_{och} and Model for Which They Were Calculated:
1--h_{och} = 1 km; 2--h_{och} = 2 km; 3--h_{och} = 2.8 km; 4--h_{och} = 4 km; 5--h_{och} = 6 km; 6--h_{och} = 8 km

Key:
1. km/s

APPROVED FOR RELEASE: 2007/02/08: CIA-RDP82-00850R000200030043-9

APPROVED FOR RELEASE: 2007/02/08: CIA-RDP82-00850R000200030043-9

METHOD OF DETERMINING THE VELOCITY PARAMETERS OF THE MEDIUM BY RECORDINGS OF EARTHQUAKES AND EXPLOSIONS (Δ = 10°)

Moscow SEYSMICHESKIYE ISSLEDOVANIYA S APPARATUROY "ZEMLYA" in Russian 1977 signed to press 31 Jan 77 pp 194-201

[Chapter 9 from the book "Seysmicheskiye issledovaniya s apparaturoy 'Zemlya'" by I. V. Pomerantseva and A. N. Mozzhenko, Izdatel'stvo Nedra, 1,400 copies, 256 pages]

[Text] The curves of variation of the velocities of longitudinal and transverse waves with depth necessary to interpret PS waves and the curves of distribution of stratal velocities of P and S waves with depth, used for stratification of the interfaces of the earth's crust and upper mantle, are determined from recordings of the first arrivals of refracted P and S waves from earthquakes and explosions. The velocity characteristic of the medium at the focal zone is determined by direct P and S waves. The velocities found from them frequently differ significantly from the propagation velocities of P and S waves outside the focal zones and, therefore, cannot be used to interpret PS waves formed beyond these regions.

Calculating the Propagation Velocities of Longitudinal and Transverse Waves by Recordings from Explosions and Near Earthquakes

The propagation velocities of P and S waves in the earth's crust are determined by the first arrivals of the refracted waves propagated from explosions and near earthquakes. The Wiechert-Herglotz-Chibisov method [147, 159, 186] is used as the main method of interpretation. Reflected P and S waves from the crustal interfaces are usually not employed to determine velocities due to their poor correlation in subsequent arrivals with spacing of observations of 5-6 km.

The method of determining velocities includes separation of the first arrivals of P and S waves on the seismograms, construction of single or summary longitudinal hodographs and graphs of the dependence of v_k on Δ by them, calculation of the curves of variation of the stratal velocities with depth at points of maximum penetration of P and S rays and mean stratal velocities and construction of vertical hodographs of P and S waves.

APPROVED FOR RELEASE: 2007/02/08: CIA-RDP82-00850R000200030043-9

APPROVED FOR RELEASE: 2007/02/08: CIA-RDP82-00850R000200030043-9

The principles of determining the first arrivals of P and S waves on the seismograms are described in Chapter 5.

Longitudinal hodographs of P and S waves are constructed along the linear profiles by ordinary methods used in KMPV and GSZ [38, 67]. Moreover, if there is a small volume of material or if it is necessary to average small inhomogeneities of the medium, summary hodographs of P and S waves are constructed. They are compiled from hodographs obtained both from special and incidental explosions and from near earthquakes. For this purpose, all the hodographs obtained in a region from special explosions and sections of hodographs from incidental explosions and earthquakes obtained at different values of Δ are constructed in a unified time and distance scale. The epicentral distances from the focus to each recording station are plotted along the horizontal and the difference of the absolute time $T_{P,S}$ of recording the P or S waves and the times at the focus T_0, the method of determination of which is given in Chapter 8, $(T_{P,S} - T_0)$, is plotted along the vertical. A summary hodograph of the first arrivals of P and S waves registered by "Zemlya" stations from special explosions on twelve profiles* is presented in Figure 72. A summary hodograph of P and S waves constructed by earthquakes is presented in Figure 69. Each section of the hodograph corresponds to an individual earthquake and does not coincide in time with surrounding hodographs. This is related to the fact that earthquakes, unlike explosions, have different values of $T_{P,S} - T_0$, determined by the different focal depth. To combine all segments of the hodographs into a single summary hodograph, they are reduced to a unified focal depth. This summary hodograph of P and S waves, compiled by Ye. M. Butovskaya for $h_{och} = 0$, is presented in Figure 69. When determining the velocity distribution with depth by S. V. Chibisov's method, one does not have to compile summary hodographs by earthquakes since one only needs to know the distribution of the apparent velocities as a function of Δ.

The graphs of $v_{P_k} = f(\Delta)$ and $v_{S_k} = f(\Delta)$ of Figure 70 were compiled by single and summary hodographs of the first arrivals of P and S waves. The graphs of $v_k = f(\Delta)$ were averaged by two methods. The first method includes averaging by the method of equal sums [17]. This method permits one to obtain a continuous curve of the true velocities at points of maximum penetration of rays as a function of depth as a result of processing by the Wiechert-Herglotz-Chibisov method. The second method includes averaging by a graduated line with artificially given gradient $\pm$ 50 m/s on the edges of the areas of apparent velocities. The second method is no less convenient for calculations, but corresponds more closely to experimental data of a layered profile of the earth's crust. The curves of stratal velocities calculated by both methods of averaging the graphs $v_k = f(\Delta)$ for a profile of the crust (see Figure 3) showed their good convergence. The difference in the curves does not exceed 3-8 percent.

The velocity distribution function with depth $v(H_{pr})$ is determined by the given hodograph of the refracted wave to calculate the greatest depth of

*This hodograph was constructed and processed by A. I. Minin.

APPROVED FOR RELEASE: 2007/02/08: CIA-RDP82-00850R000200030043-9

APPROVED FOR RELEASE: 2007/02/08: CIA-RDP82-00850R000200030043-9

penetration of the ray H_{pr}, $v_{P_{sr}}$, $v_{S_{sr}}$ and K_{sr} by the Wiechert-Herglotz-Chibisov method. The dependence of H_{pr} on v_k is expressed by the integral

$$H_{np} = \frac{1}{\pi} \int_{x=0}^{x=\Delta H_{np}} \operatorname{arcch} \frac{v_K(\Delta h_{np})}{v_K(\Delta H_{np})} d\,\Delta h_{np}, \tag{9.1}$$

where ΔH_{pr} is the distance from the point of the explosion to the point of emergence of the ray penetrating to depth H_{pr} onto the surface of observations, Δh_{pr} is the distance from the point of explosion to the point of emergence of the ray penetrating to lesser depth h_{pr} onto the surface of observations, $v_k(\Delta h_{pr})$ is the apparent velocity of the waves at the point of the hodograph obtained at distance Δh_{pr} from the point of the explosion and $v_k(\Delta H_{pr})$ is the apparent velocity of the waves at the point of the hodograph obtained at distance ΔH_{pr} from the point of the explosion.

Solution of integral (9.1) is possible by approximate methods by replacing the integral by a finite sum of rectangles, trapezoids or parabolas [17]. The formula of parabolas yields the greatest accuracy and the formula of rectangles yields the least accuracy at the same values of n (n is the equal parts into which the integration interval is divided). An estimate of the accuracy of calculations of vp carried out for a profile of the crust (see Figure 3) by formulas of parabolas and rectangles showed the following. The values of vp calculated by the formula of rectangles differ from those of vp determined by the formula of parabolas by $\pm$ 30 m/s at depths less than 3 km. The values of vp determined by the two methods coincide at depths greater than 3 km. The latter permits one to use the formula of finite sums of rectangles in calculations of vp. It has the form

$$H_{np} = \frac{1}{\pi} h \sum \operatorname{arcch} \frac{v(\Delta h_{np})}{v(\Delta H_{np})}, \tag{9.2}$$

where $h = (\Delta H_{pr} - \Delta h_{pr})/n$ is the elementary segment of summation.

The curves $v_{P_{pl}} = f(H_{pr})$ and $v_{S_{pl}} = f(H_{pr})$, calculated by formula (9.2), are rearranged into the curves $v_{P_{sr}} = f(H)$ and $v_{S_{sr}} = f(H)$ using the following formulas:

$$v_{cp} = \frac{\sum_1^n \Delta z}{\sum_1^n t_v}, \tag{9.3}$$

where Δz is the thickness of individual layers and t_v is the vertical travel time of the P or S waves in each layer.

APPROVED FOR RELEASE: 2007/02/08: CIA-RDP82-00850R000200030043-9

APPROVED FOR RELEASE: 2007/02/08: CIA-RDP82-00850R000200030043-9

Since the curve of variation of velocity with depth can be approximated by a straight line in each sufficiently small segment Δz, the value of t_v is determined by the formula [116] for the linear law of variation of velocity with depth

$$t_в = \frac{1}{v_н \beta} \ln(1 + \beta \Delta z), \tag{9.4}$$

where v_n is the velocity in the upper part (initial) of each layer Δz and β is the gradient of variation of velocity with depth.

Graphs of the mean velocities of P and S waves and K_{sr}, obtained on a "Zemlya" profile 260 km long from five points of explosion, are presented in Figure 106.

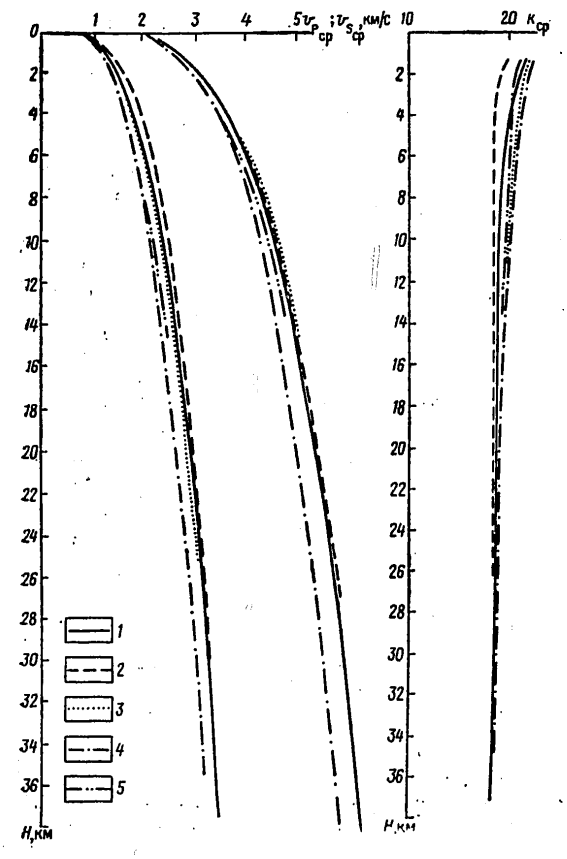

Figure 106. Curves of Dependence of $v_{P_{sr}} = f(H)$, $v_{S_{sr}} = f(H)$ and $K_{sr} = f(H)$ Compiled From Data of Five (1-5) Points of Explosion

APPROVED FOR RELEASE: 2007/02/08: CIA-RDP82-00850R000200030043-9

APPROVED FOR RELEASE: 2007/02/08: CIA-RDP82-00850R000200030043-9

The curves $v_{P_{sr}} = f(H)$ and $v_{S_{sr}} = f(H)$ are rearranged into vertical hodographs for stratification of the time and depth profiles of the crust. The times on vertical hodographs are determined by the ordinary method [45, 116]. Vertical hodographs are averaged by segments of straight lines by which the stratal velocities of longitudinal and transverse waves are calculated. The latter are rearranged into graphs of the stratal velocities of P and S waves as a function of depth H and Δt_{PS-P}. The values of Δt_{PS-P} are calculated by the Hasegawa formula [176]. Graphs of the stratal velocities of P and S waves constructed as a function of H and Δt_{PS-P} with regard to deflections are plotted on the depth and time profiles, respectively, constructed by PS waves.

The accuracy of determining the velocities and depths by the Wiechert-Herglotz-Chibisov method is estimated by the method proposed in [37]. According to the formulas of this paper, if the distance between the observation points is 5 km, the errors of tying them in are $\pm$ 100 m and the difference of the arrival times of the waves to two adjacent points is 0.9-1.0 second, the relative error of determining the values of $v_{P_{pl}}$ by single hodographs for depths from 3 to 35 km reaches 15 percent, the error of determining depths reaches 30-40 percent and the errors of determining the mean velocities and K_{sr} reach 10-15 percent. The use of opposite and overtaking hodographs to determine $v_{P_{sr}}$, K_{sr} and H permits one to significantly reduce the relative error of determining these values. Thus, if there are 3-4 direct and opposite systems corresponding to the same segment of the depth profile, the confidence interval of the existence of curves $v_{P_{sr}} = f(H)$ and $K_{sr} = f(H)$ (it decreases to $\pm$ (2-3) percent for $v_{P_{sr}}$ and $\pm$ 5 percent for K_{sr} at H = 0.9). The large relative error of determining K_{sr} by single hodographs, equal to 10-15 percent, and the small error in determination by a series of hodographs ($\pm$ 5 percent) indicate the need to find 3-4 opposite and overtaking systems for a single segment or to use supplementary data to determine the value of K_{sr}.

Methods of Determining Coefficients K

Coefficients K_{sr} are determined by data of explosions and near earthquakes registered by "Zemlya" stations, by data of seismic logging, by calculation by the Hasegawa formula, by recordings of direct P and S waves over the focus of a local earthquake, by Vadati graphs and by t_0 of hodographs of refracted P and S waves.

The mean velocity distribution curves of P and S waves with depth are found by using the formulas of N. N. Puzyrev as a result of processing the first arrivals of P and S waves by the Wiechert-Herglotz-Chibisov method. They permit one to calculate K_{sr} by direct division of the values of $v_{P_{sr}}$ by $v_{S_{sr}}$, corresponding to the same depth. The derived curves of $K_{sr} = f(H)$ are characterized by wide spreads. The values of K_{sr} for the same depths of the same profile, but found by different single hodographs may differ up to $\pm$ 0.3 (Figure 106). Summary hodographs must be compiled by regions with similar geological conditions and the values of $K_{sr} = f(H)$ must then be calculated a second time for them to reduce the spread of curves of $K_{sr} = f(H)$.

APPROVED FOR RELEASE: 2007/02/08: CIA-RDP82-00850R000200030043-9

APPROVED FOR RELEASE: 2007/02/08: CIA-RDP82-00850R000200030043-9

The data derived in this manner coincide best with the curves $K_{sr} = f(H)$ determined by other methods, including seismic logging studies.

The curve $K_{sr} = f(H)$ from data of seismic logging of deep boreholes is determined by the same method as the curve $v_{P_{sr}} = f(H)$ and $v_{S_{sr}} = f(H)$. If there are vertical hodographs found as a result of seismic logging, K_{sr} is calculated by the formula

$$K_{cp} = \frac{t_S^{\text{в}}}{t_P^{\text{в}}}. \tag{9.5}$$

Determination of K_{sr} by the Hasegawa formula is possible if the depth (from drilling data or from MOV data) and the mean velocity of longitudinal waves to this depth are precisely known and the delay time of the transient composite PS wave with respect to the P wave (Δt_{PS-P}) for this same depth is found for each level of the sedimentary mantle or basement surface. Coefficient K_{sr} is calculated by the simplified or complete Hasegawa formula (see Chapter 2). The simplified formula can be used when determining K_{sr} by earthquakes with $\Delta > 70°$. The errors of determining K_{sr} may reach $\pm$ (0.1-0.2) or more for earthquakes with lesser values of Δ .

The value of K_{sr} is calculated by recordings obtained above the focus of the local earthquake by the formula

$$K_{cp} = \frac{T_S - T_0}{T_P - T_0} \tag{9.6}$$

The value of K_{sr} is determined by Vadati graphs in the following manner. The angular coefficients of the graphs $T_S = f(T_P)$ (see Figure 101) is the mean value of K_{sr} on the path from the focus to the recording station. The graphs of the function $K_{sr} = f(h_{och})$ is compiled to find the distribution of this coefficient with depth. The spread of values with K_{sr} around the curve usually does not exceed $\pm$ (0.1-0.2) with error of determining the focal depth not below 10 percent.

The value of K_{sr} is calculated by the value of t_0 of refracted P and S waves using the following formulas. The depth of location of the refracting boundary for the hodograph of the refracted wave at short distances from x_n can be determined by the formulas for the leading waves:

$$2H = t_{0P} \frac{v_{P_{cp}}}{\cos i_{P_n}} = t_{0S} \frac{v_{S_{cp}}}{\cos i_{S_n}}, \tag{9.7}$$

where i_{P_n} and i_{S_n} are the critical angles for the rays of P and S waves emerging onto the observation surface in the regions of the initial points.

APPROVED FOR RELEASE: 2007/02/08: CIA-RDP82-00850R000200030043-9

APPROVED FOR RELEASE: 2007/02/08: CIA-RDP82-00850R000200030043-9

Assuming that $\cos i_{P_n} \approx \cos i_{S_n}$, we find

$$\frac{t_{0S}}{t_{0P}} \approx \frac{v_{P_{cp}}}{v_{S_{cp}}}. \tag{9.8}$$

Thus, having hodographs of P and S waves related to the same refraction boundary and also the conjugate points on the hodographs of these waves along the entire profile, the lines t_{0P} and t_{0S} are constructed and the values of K_{sr} are calculated. The error of determining K_{sr} does not exceed $\pm$ (0.1-0.2) second in this case.

The value of K_{pl} is determined from seismic logging data and also from materials of explosions and earthquakes registered by "Zemlya" stations. The values of K_{pl} are determined from seismic logging data as the ratio of stratal velocities of longitudinal waves to the stratal velocities of transverse waves in each layer of the sedimentary mantle. Based on materials of explosions and near earthquakes, the values of K_{pl} are determined by the ratios of the apparent or boundary velocities of P and S waves (v_{P_k}/v_{S_k} or v_{P_g}/v_{S_g}), the time ratios of P and S waves on the hodographs $((T_S - T_0)/(T_P - T_0))$ and the ratios of the stratal velocities of P and S waves calculated by the vertical hodographs of these waves. The depth for all these graphs is calculated by the Wiechert-Herglotz-Chibisov method.

Determining the Velocity Characteristics of the Medium in the Focal Zones of Modern Earthquakes

The velocity parameters of the media at the focal zones are determined by the hodographs and arrival times of direct P and S waves to the recording stations. The following methods exist in this case: selection of the theoretical model of the medium and determination of the velocities by solving a system of three-dimensional hyperbolas (see Chapter 8).

Selection of the theoretical models of the medium begins almost immediately upon determination of the focal coordinates (h_{och} of x,y) by the method of intersections from hodographs of direct waves compiled previously. Having selected the location of the focus by the triangle of lack of tie-in, the theoretical hodograph and model of the medium and consequently the curves $v_{P_{sr}} = f(H)$ and $v_{S_{sr}} = f(H)$ for which the hodograph was calculated are determined simultaneously.

The second method is more effective. It permits one, using the stations located at different distances from the focus, to determine the propagation velocity of the P and S waves in the focal zone. Comparison of curves $v_{P_{sr}}$ found for local earthquakes when solving a system of three-dimensional hyperbolas, with spacing of the recording stations at distances of 0-7 and 0-12 km from the focus to curves found for regions contiguous to the focal zone, by processing P and S waves from explosions and near earthquakes by the Wiechert-Herglotz-Chibisov method is presented in Table 10. As can be seen

APPROVED FOR RELEASE: 2007/02/08: CIA-RDP82-00850R000200030043-9

APPROVED FOR RELEASE: 2007/02/08: CIA-RDP82-00850R000200030043-9

Table 10. Mean Velocities of vp_{sr} (in km/s) Found Upon Processing of Recordings from Explosions and Local and Near Earthquakes

H, км	(1) Взрывы	(2) Местные землетрясения при различном удалении станций записи от эпицентра		(3) Близкие землетрясения
		0—7 км	0—12 км	
3,0	3,25	2,95	—	3,5
3,5	3,35	3,15	—	3,6
4,0	3,55	3,3	3,8	3,8
4,5	3,75	3,5	4,0	4,0
5,0	3,85	3,65	4,1	4,15
6,0	4,1	3,75	4,2	4,40
6,5	4,3	3,85	4,25	4,55
7,0	4,4	3,85	4,3	4,6
7,5	4,4	3,87	4,4	4,7
8,0	4,5	3,9	4,4	4,8
9,0	—	3,95	4,45	—

Key:
1. Explosions
2. Local earthquakes with different distance of recording stations from epicenter
3. Near earthquakes

from the given comparison, the minimum values are those of vp_{sr} obtained by recording stations at distances from 0 to 7 km from the focus. This permits one, knowing the locations of the recording stations and focal depths by which the reduced values of vp_{sr} were found, to limit in space the zone of reduced values of vp_{sr} and vp_{pl} with an error of 1-2 km.

APPROVED FOR RELEASE: 2007/02/08: CIA-RDP82-00850R000200030043-9

APPROVED FOR RELEASE: 2007/02/08: CIA-RDP82-00850R000200030043-9

Part 3

THE DEEP STRUCTURE OF THE EARTH'S CRUST AND UPPER MANTLE OF DIFFERENT GEOTECTONIC ZONES

THE DEEP STRUCTURE OF THE CRYSTALLINE MASS OF THE EARTH'S CRUST AND UPPER MANTLE IN THE RAYONS OF TASHKENT

Moscow SEYSMICHESKIYE ISSLEDOVANIYA S APPARATUROY "ZEMLYA" in Russian 1977 signed to press 31 Jan 77 pp 202-212

[Chapter 10 from the book "Seysmicheskiye issledovaniya s apparaturoy 'Zemlya'" by I. V. Pomerantseva and A. N. Mozzhenko, Izdatel'stvo Nedra, 1,400 copies, 256 pages]

[Text] The deep structure of the earth's crust and upper mantle was found as a result of studies with the "Zemlya" stations on the Southeastern Russian Series of formations in the Azov-Kuban', Pre-Caspian and North German Depressions and in the rayons of Tashkent.

The volume of studies on the Southeastern Russian Series (with station spacing of 5-10 km) comprises approximately 600 km of the profiles, that in the Pre-Caspian Depression comprises 400 km and that in the Azov-Kuban' Depression comprises 250 km. A total of 540 km of profiles on an area of 400 km^2 was developed in the Pre-Tashkent Depression with station spacing from 500 m to 5 km and 3,500 km of profiles were developed on an area of 50,000 km^2 with station spacing of 5-6 km within the North German Depression. The number of recordings from local, near and remote earthquakes and explosions registered in all these regions in presented in Table 7.

The deep structure of the crust and mantle was determined as a result of using P, S and PS waves registered by "Zemlya" stations from remote earthquakes (Δ = 160°) and explosions (Δ = 0-100°) of different distances in the frequency band of 0.5-10 Hz in all the named regions, the velocity characteristics of individual layers of the crust and upper mantle were determined and the zones of deep, regional faults of the crust, to part of which are confined the foci of local earthquakes, were distinguished.

Conducting the studies with the "Zemlya" device for a number of KMPV and GSZ profiles sequentially or simultaneously with these methods made it possible to compare the derived profiles and the wave patterns by the recordings from earthquakes and explosions, to determine their divergence and similarity and to formulate the bases of a rational complex of seismic and seismological investigations to study the deep structure of the earth's crust and upper mantle of different geological provinces.

APPROVED FOR RELEASE: 2007/02/08: CIA-RDP82-00850R000200030043-9

APPROVED FOR RELEASE: 2007/02/08: CIA-RDP82-00850R000200030043-9

An idea of the behavior of the interfaces of the crust in the upper mantle (H = 100 km) near Tashkent and the behavior of the interfaces in the crust to the northeast and southeast from Tashkent was obtained as a result of investigations with the "Zemlya" stations in Tashkent during 1966-1967. The velocity characteristics of the crust and mantle to depths of approximately 110 km are given from data of processing incidental and special explosions (Δ = 0-45 km) and near earthquakes ($\Delta \approx$ 600 km). The focal zone in the crust located under the center of Tashkent and the velocity characteristics of the medium in it were determined from recordings of P and S waves from aftershocks of the Tashkent earthquake. The structure of the earth's crust of the Pre-Tashkent region and adjacent Almalyk, Angren and other ore zones was determined during subsequent investigations in 1968-1970 [21]. The structure of the crust near Tashkent and the behavior of the surface of the Paleozoic basement in the direction northeast, east and southeast of Tashkent to its emergence onto the surface are eliminated in this section.

Criteria of the Intrarayon Stratification and Interrayon Correlation of Interfaces of the Earth's Crust

Until recently the main and in some cases the only criterion for relating the deep seismic boundary to some level of the crust and identification of it in different regions in the absence of deep boreholes is the value of the stratal (or boundary)* velocity. Generalization of the material by the propagation velocities of longitudinal waves in the Soviet Union and in different parts of the globe [105] permits stratification of the interfaces of the earth's crust by the values of v_{Pg} or v_{Pp1} in the following manner: a) the surface of the folded Paleozoic basement at depths of deposition from 0 to 5 km has a value of v_{Pg} which varies from 4.3 to 5.8 km/s; b) the surface of the crystalline mass of the earth's crust--the Pre-Cambrian basement--is characterized by values of stratal velocities, equal to 6-6.3 km/s on the average, at deposition depths of 5-13 km; c) the surface of the basaltic layer in different regions of the globe has a value of v_{Pp1} = 6.4-5.8 km/s; d) the boundary within the basaltic layer, conditionally named the Conrad-I surface in some regions of the USSR [41, 42, 103, 105, 110] is characterized by v_{Pp1} = 7.0-7.3 km/s; e) the boundary intermediate between the Conrad-I and Mohorovicic Discontinuities, also arbitrarily named Conrad-II, has a value of v_{Pp1} = 7.6-7.8 km/s; and f) the upper part of the mantle (the Mohorovicic Discontinuity) is determined jointly with the values of v_{Pp1} = 8-8.2 km/s; g) additional interfaces characterized by velocities of longitudinal waves of 8.4 km/s (H $\approx$ 50-60 km), 9 km/s (H = 80-90 km) and so on, were noted in the earth's mantle [123, 150].

---

*The term "boundary" velocity is conditional since the value of v_g for refracted waves corresponds to some part of the layer at the depth of maximum ray penetration. However, individual layers may characterize v_g in the overall regional layout.

APPROVED FOR RELEASE: 2007/02/08: CIA-RDP82-00850R000200030043-9

APPROVED FOR RELEASE: 2007/02/08: CIA-RDP82-00850R000200030043-9

Table 11. Velocity Profile of Crust Under Tashkent

Название слоя (1)	Индекс слоя (2)	Индекс границы (3)	$v_{P_{пл}}$, км/с (4)	$v_{S_{пл}}$, км/с	$K_{пл}$	Глубина, км (5)
Осадочный чехол (6)	ос	PZ_1	3,4	1,7—1,8	1,9—2	0—2,5
Палеозойский фундамент (7)	PZ_1	AR	5,86	3,0	1,95	2,5—5,5
Архей (8)	AR	I	6,2	3,35	1,85	5—9,5
Слой с повышенной скоростью (9)	I—II	II	6,4—6,5	3,65	1,75—1,83	9,5—14,5
Волновод (10)	$II—Б_I$	$Б_I$	6	3,2—3,4	1,8	9,5—21
Базальтовый слой (11)	$Б_I—К_I$	$К_I$	6,85—7	3,9—4	1,75	16—20
Слой глубже поверхности Конрада-I (К-I) (12)	$К_I—К_{II}$	$К^P_{II}$	7,4	4,25	1,75	20—30
Первый слой глубже поверхности Конрада-II (К-II) (13)	$К^P_{II}—К^S_{II}$	$К^S_{II}$	7,6—7,8	4,35—4,45	1,75	30—43
Второй слой глубже $К_{II}$, выделяемый только по скоростям волн S (14)	$К^S_{II}—М_I$	$М_I$	7,6—7,8	4,5—4,6	1,7	38—51
Зона перехода от коры к мантии (15)	$М_I—М_{II}$	$М_{II}$	8—8,1	4,7—4,8	1,7	45—55
Первый слой в мантии (16)	$М_I—М_{III}$	$М_{III}$	8—8,1	4,7—4,8	1,7	51—62
Второй, третий и четвертый слои в мантии (17)	$М_{III}—М_{IV}$ $М_{IV}—М_V$ $М_V—М_{VI}$	$М_{VI}$	8,2—8,4	4,8—4,95	1,7	59—86
Седьмой слой в мантии (18)	В мантии (19) $М_{VI}—М_{VII}$	$М_{VII}$	8,8—9	5,2—5,3	1,7	86—110

Key:
1. Name of layer
2. Index of layer
3. Index of boundary
4. km/s

[Key continued on following page]

APPROVED FOR RELEASE: 2007/02/08: CIA-RDP82-00850R000200030043-9

APPROVED FOR RELEASE: 2007/02/08: CIA-RDP82-00850R000200030043-9

[Key continued from preceding page]

5. Depth, km
6. Sedimentary mantle
7. Paleozoic basement
8. Archean
9. Layer with increased velocity
10. Waveguide
11. Basaltic layer
12. Layer deeper than Conrad-I discontinuity (K-I)
13. First layer deeper than Conrad-II discontinuity (K-II)
14. Second layer deeper than K_{II} determined only by velocities of S waves
15. Transition zone from crust to mantle
16. First layer in mantle
17. Second, third and fourth layers in mantle
18. Seventh layer in mantle
19. In mantle

Stratification and correlation of the crustal interfaces is also carried out by the values of the stratal velocities. The interfaces determined by PS waves are compared to the boundaries of the velocity jumps obtained from P, S and PS waves for this purpose by the methods described in Chapter 7. The results of the comparisons are presented in Figure 94 and on the depth profiles of the North German Depression (see Figures 111 and 112).

The Velocity Boundaries of the Crust and Mantle of the Tashkent Depression and Their Geological Stratification

A total of 12 boundaries was determined from data of processing P and S waves from explosions and near earthquakes and also PS waves registered by "Zemlya" stations in the crust and mantle of the Tashkent Depression (Table 11).

Besides the interfaces of the crust enumerated in Table 11, boundaries from S waves alone were noted from P and S waves at depths of 71.5, 91.4 and 107 km (see Figure 70). A waveguide has been noted from experimental material deeper than the m_I boundary. However, it was not possible to find the distribution of v_{Pp1} and v_{Sp1} in it.

The Behavior of the Interfaces of the Earth's Crust and Mantle Under Tashkent

A number of charts and disgrams of the depth distribution was compiled for the following interfaces of the earth's crust as a result of the studies of 1966-1967 [150] by means of 15 recording stations on an area of 900 km^2: surfaces of the Paleozoic (Figures 107 and 108) and Archean basements, the roof and bottom of the layer with increased velocity values (see Figure 107), the surface of the basaltic layer (see Figure 64) and the Conrad-I and Conrad-II discontinuities and the transition zone from the crust to the mantle (Figure 109).

The surface of the Paleozoic basement. The surface of the Paleozoic basement has a complex lateral structure under Tashkent (see Figure 108). On the whole, the entire basement under Tashkent can be divided into three large zones: the Chinabad projection (Tashkent rampart), the Tashkent depression

APPROVED FOR RELEASE: 2007/02/08: CIA-RDP82-00850R000200030043-9

APPROVED FOR RELEASE: 2007/02/08: CIA-RDP82-00850R000200030043-9

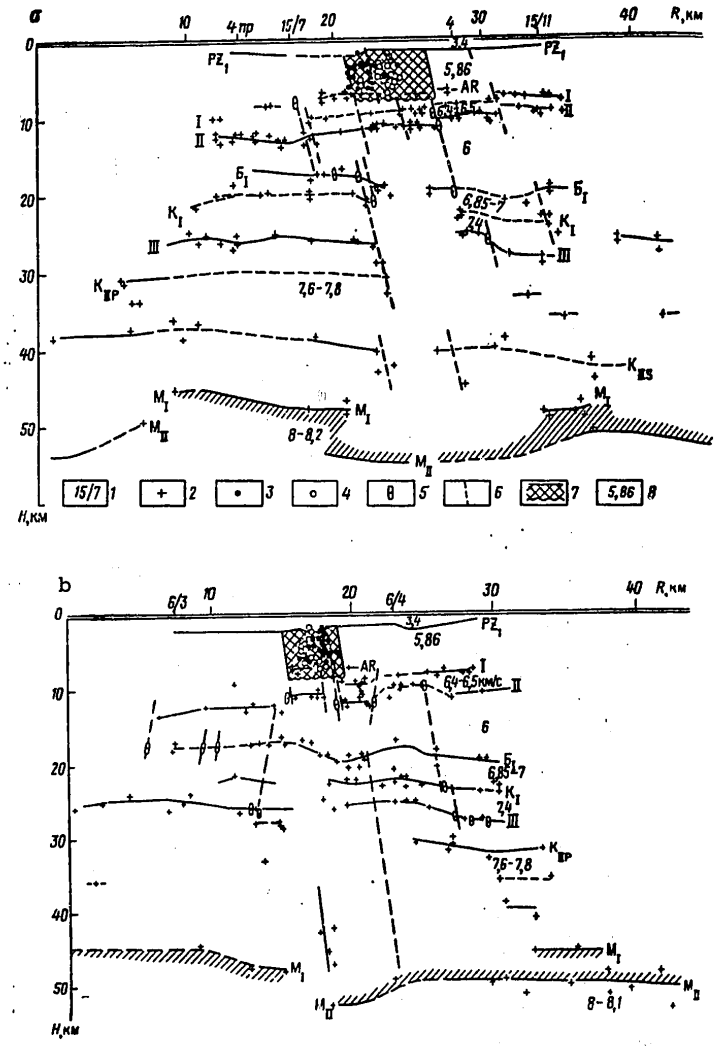

Figure 107. Profiles of the Earth's Crust Under Tashkent from Profiles 0-0 (a) and IV-IV (b) (See Figure 108): PZ_1--surface of Paleozoic basement; AR--surface of presumably the Archean basement; I and II--roof and bottom, respectively, of layer with increased velocity; B_I--surface of basaltic layer; K_I--Conrad-I discontinuity; III--boundary deeper than Conrad-I discontinuity; K_{IIIP}--Conrad-II discontinuity by P wave; K_{IIS}--Conrad-II surface by S wave; $M_I M_{II}$--roof and bottom, respectively, of transition zone

[Caption continued on following page]

APPROVED FOR RELEASE: 2007/02/08: CIA-RDP82-00850R000200030043-9

APPROVED FOR RELEASE: 2007/02/08: CIA-RDP82-00850R000200030043-9

[Caption continued from preceding page]

crust to mantle; M_{III}--section of boundary in upper mantle; 1--locations of recording stations with numbers of individual stations (in the numerator) and stopovers (in denominator); 2--points of depths from data of composite PS waves; 3--epicenters of aftershocks of Tashkent earthquake located on line of profile; 4--epicenters of aftershocks of Tashkent earthquake located at distance up to 2 km from line of profile; 5--sections of boundaries with sharp attentuation of PS waves; 6--faults from data of PS waves; 7--region of low values of velocities of longitudinal P waves (up to 4.3 km/s) and coefficient K (up to 1.61) in the focal zone; 8--value of v_{Pp1} in km/s

itself and the zone along the course of the Chirchik River. The first zone encompasses the northeastern part of Tashkent. It is characterized in the north by the most shallow absolute depths* of deposition of Paleozoic rock (700 m). Submergence of the basement from 700 m to 1.95-2.0 km is noted from the north-northeast to the south-southwest within this zone. The second zone--the Tashkent depression itself--occupies the southwestern part of Tashkent. It is characterized by deeper and smooth deposition of the surface of Paleozoic rock. The absolute depths to the surface of the basement fluctuate within very small limits--from 1.95 to 2 km. The third zone, located in the east and southeast of Tashkent, is characterized by a more complex structure (see Figure 108). All the enumerated zones are joined to each other by a series of faults. The latter converge under the central part of the city where a northeastern block of increased deposition of the basement surface is located at an absolute depth of 1.25 km. A second, more submerged block (H = 1.8 km) is observed to the southwest of it. The blocks are separated by a depression (H $>$ 2 km) inside which the isoline with depth of more than 2.4 km is formed. This is the most submerged zone under the center of the city and is a seemingly complex assembly of all the fault zones which separate the tectonic structures.

The surface of the presumably Archean basement. This surface (v_{Pp1} = 6.2 km/s) has been determined under Tashkent only in some locations. A limited amount of data probably determined by the sharpness of the interface do not make it possible to compile a chart. One can only note that this boundary is located at depths of 6-8 km (see Figure 107).

The roof and bottom of the layer with increased velocity values. The bottom of a lyer with increased velocity is traced more clearly and universally in the region of Tashkent and its roof is also determined in some sections (see Figure 107). The traced boundaries are deposited concordantly everywhere. The thickness of a layer is an average of 2 km. The same structural elements as on the surface of the Paleozoic foundation: the Chinabad outcrop, the

*The depth marks are given from sea level.

APPROVED FOR RELEASE: 2007/02/08: CIA-RDP82-00850R000200030043-9

APPROVED FOR RELEASE: 2007/02/08: CIA-RDP82-00850R000200030043-9

Tashkent depression and the zone along the course of the Chirchik River, have been determined along the bottom of the layer. The indicated zones are separated by fault systems which coincide with faults along the surface of Paleozoic rock.

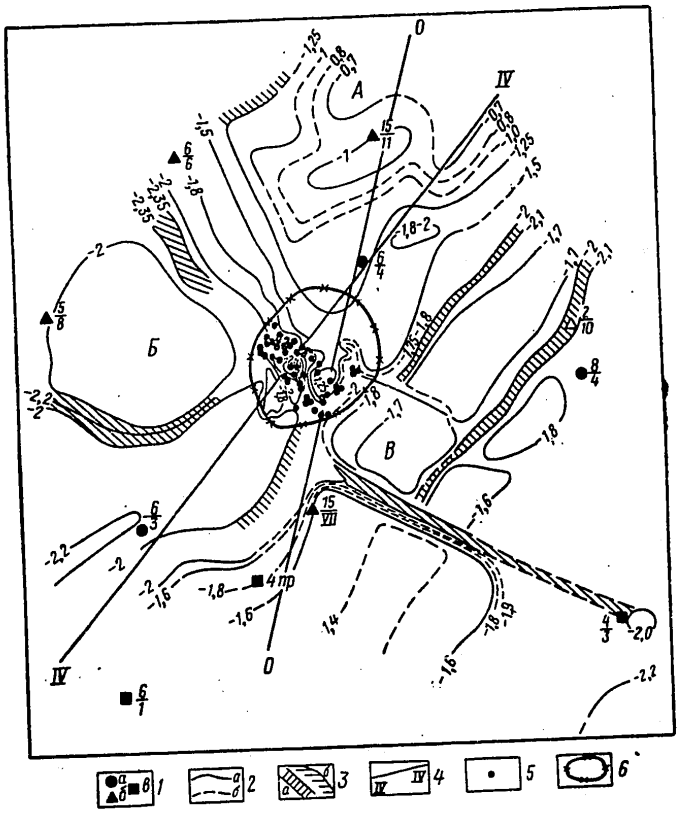

Figure 108. Relief Map of Surface of Paleozoic Basement Under Tashkent (Compiled by I. V. Pomerantseva and L. I. Kagalova):

A--Chinabad outcrop; B--Tashkent depression; C--Chirchik zone; 1--individual recording stations of 1966 (a), 1967 (b) and 1968 (c) (the number of the station is in the numerator and the number of the stopover is in the denominator); 2--certain (a) and less certain (b) isolines along the surface of the Paleozoic basement; 3--fault zones (a) and lines (b) from data of "Zemlya" stations; 4--profiles; 5--epicenters of aftershocks of Tashkent earthquake of 26 April 1966 from data of "Zemlya" stations; 6--regions where reduced values of stratal velocities of P waves up to 4.3 km/s and of coefficient K (1.61) are observed

APPROVED FOR RELEASE: 2007/02/08: CIA-RDP82-00850R000200030043-9

APPROVED FOR RELEASE: 2007/02/08: CIA-RDP82-00850R000200030043-9

The most shallow depths to the bottom of the layer (9.5-10 km) are noted in the northeast of the area of study--under the Tashkent rampart--and the deepest depths (12-14.5 km) are noted within the Tashkent depression itself and along the course of the Chirchik River. Submergence of the bottom of the layer with increased velocity occurs along the fault system of northwesterly strike (see Figure 107). A small downwarp with amplitude up to 1.5 km is located under the center of the city, which is correlated with the closed depression within the canyon along Paleozoic rock.

The surface of the basaltic layer. This surface ($v_{P_{pl}}$ = 6.8 km/s) is inversely deposited compared to the boundaries enumerated above. The most submerged region (up to 20-20.5 km) is located under the Chinabad zone (see Figure 64). The most uplifted part (up to 16 km) is noted in the southeastern part of Tashkent in the region of the course of the Chirchik River. The Tashkent depression is characterized by intermediate depths of 17-18 km. A downwarp up to 21 km deep has been determined under the center of the city with slight displacement toward the northeast (see Figure 64).

The Conrad-I Discontinuity. The Chinabad zone (20-22 km) and the zone of the Tashkent depression (24 km) is distinguished along the Conrad-I discontinuity. The most shallow depth markers along this boundary are confined to the region of the course of the Chirchik River (18-20 km) and to the northwesterly part of Tashkent (20 km). An uplifted zone (up to 21 km) is noted under the center of Tashkent.

The Conrad-II Discontinuity. This surface has been determined both by the S wave ($v_{S_{pl}}$ = 4.5-4.6 km/s) and by the P wave ($v_{P_{pl}}$ = 7.4-7.7 km/s). Extended and sustained boundaries terminate in the crust deeper than this surface (see Figure 107). The depths to this boundary vary from 30 to 34 km.

The transition zone from the crust to the mantle. Either the roof (M_I) or the bottom (M_{II}) is distinguished in the transition zone from the crust to the mantle ($v_{P_{pl}}$ = 8.0-8.2 km/s) (see Figures 107 and 109). The joint region of tracing the M_I and M_{II} boundaries is very insignificant. The roof of the transition zone (M_I) is located at depths from 45 to 47-48 km and the bottom of the transition zone (M_{II}) is characterized by depths of 49-53 km. The bottom of the zone is easily distinguished in the northwestern and southwestern parts of the city and the roof is distinguished mainly in the southeastern and northeastern parts. The boundary of the northwestern and southeastern zones has a northeasterly strike and passes through the epicentral zone under the center of the city, approximately in the direction of profile IV-IV.

The interfaces in the mantle. The boundaries are located at depths of 60, 70, 80 and 90-100 km. The boundaries in the mantle are essentially undetermined directly under Tashkent, especially under its center, since the exchange points with the spacing of the stations used were located southwesterly of Tashkent due to the large drifts. The values of depths vary from 59 to 64 km along the M_{III} boundary (H = 60 km). The zone of the southwesterly-northeasterly strike with relatively increased deposition of the boundary (up to

APPROVED FOR RELEASE: 2007/02/08: CIA-RDP82-00850R000200030043-9

APPROVED FOR RELEASE: 2007/02/08: CIA-RDP82-00850R000200030043-9

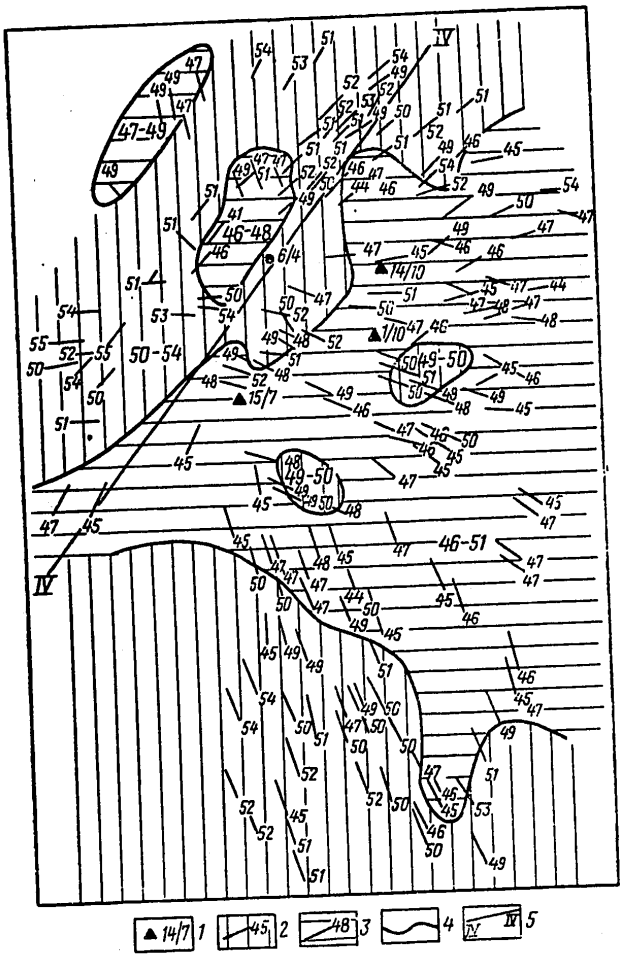

Figure 109. Relief Diagram of Transition Zone from Crust to Mantle Under Tashkent:
1--locations of "Zemlya" recording stations (the number of the station is in the numerator and the number of the stopover is in the denominator); 2 and 3--depths, in km, to the bottom and roof of the transition zone, respectively, from the crust to the mantle with directions to the recording stations; 4--profiles of distribution of M_I and M_{II} tracing zones; 5--profile IV-IV passing through the epicentral zone (see Figure 108)

56 km), which surrounds the city from the east and southeast, is distinguished in the northwestern part of the area.

APPROVED FOR RELEASE: 2007/02/08: CIA-RDP82-00850R000200030043-9

APPROVED FOR RELEASE: 2007/02/08: CIA-RDP82-00850R000200030043-9

Even fewer exchange points than along the M_{III} boundary have been found along boundaries M_{IV}-M_{VI}. It is difficult to make any judgment about the relief of these boundaries from available material. One can only determine the range of depths at which these boundaries are distinguished: 67-75 km for M_{IV}, 77-81 km for M_V and 86-100 km for M_{VI}.

Surface Structure of the Paleozoic Basement to the East and Southeast of Tashkent

Investigations with 15 "Zemlya" stations, conducted in 1968 and partially in 1969, made it possible to compile a schematic chart of depths to the surface of the Paleozoic basement to the east and southeast of Tashkent (Figure 110). This chart is easily tied in to the chart of the Paleozoic surface under Tashkent and permits one to determine the relationship of the deep structure of the Paleozoic basement of Tashkent and the mountain systems surrounding it on the east and southeast. The depth markers to the Paleozoic basement vary gradually from 0.3 to 3.2 km. The strike of the isolines is mainly northeasterly and is seemingly controlled by the location of the boundary of the emergence of the Paleozoic basement to the earth's surface. A gradual monoclinal submergence of the Paleozoic surface in a northwesterly direction, from 300 m to 2.5 km, is noted. A sharp rise to depths of 1.6 km is further observed at a distance of 4-6 km.

The Seismic Activity of the Territory of Study and its Relationship to the Deep Structure

The greatest seismic activity of the Tashkent area was observed during April-September 1966. Approximately 305 aftershocks of the Tashkent earthquake of 1966 were registered by "Zemlya" stations during this period. A graph of the distribution of earthquakes in time and their depths are presented in [110]. To establish the regularities of displacement of the foci of the aftershocks of the Tashkent earthquake, the latter were applied to a chart along the surface of the Paleozoic basement (see Figure 108) and the depth profiles of the crust (see Figure 107). The epicenters of the earthquake aftershocks are grouped on the chart in a narrow local zone in the central part of Tashkent. The area occupied by the epicenters does not exceed 2 X 3 km. The foci are located at depths from 3 to 9 km (see Figure 107) seemingly along the plane inclined toward the vertical at an angle of 15° and having a northwesterly strike. The epicentral zone along the surface of the crystalline rock is confined to sections of joining of the three large blocks of the crust determined from data of "Zemlya" stations under Tashkent: Chinabad, Tashkent and Chirchik. The propagation velocity of longitudinal waves in the crystalline mass of the crust of the epicentral zone at depths from 3 to 9 km is equal to 4.3-4.5 km/s and K_{pl} = 1.61. The velocity in the Paleozoic basement is equal to 5.8-6 km/s and K_{pl} = 1.73 in the remaining area of Tashkent and its suburbs.

Comparison of the foci of the aftershocks of the Tashkent earthquake of 26 April 1966 to the deep structure of the crust shows that the foci are located at the points of manifestation of active modern tectonic movements and

APPROVED FOR RELEASE: 2007/02/08: CIA-RDP82-00850R000200030043-9

APPROVED FOR RELEASE: 2007/02/08: CIA-RDP82-00850R000200030043-9

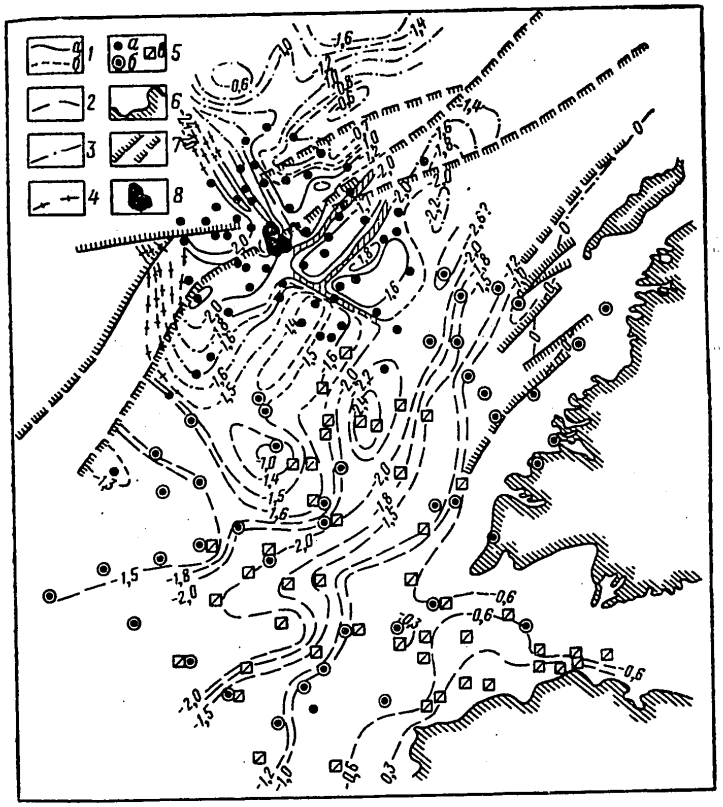

Figure 110. Relief Chart of Surface of Paleozoic Basement Under Tashkent and Within Its Southeastern Framework (Compiled by I. V. Pomerantseva and E. K. Kostrova): 1--isolines (in km) from data of I. V. Pomerantseva and L. I. Kagalova under Tashkent, confident (a) and less confident (b); 2--isolines (in km) from data of I. V. Pomerantseva southeast of Tashkent; 3--isolines (in km) from data of B. B. Tal'-Virskiy; 4--isolines (in km) from KMPV data; 5--points where the values of depths along the PS waves were found by different authors: a--data of I. V. Pomerantseva and L. I. Kagalova; b--data of L. S. Shumilina; c--data of Ye. M. Butovskaya and T. M. Gol'tseva; 6--boundary of outcrops of Paleozoic basement to earth's surface; 7--fault zones from data of B. B. Tal'-Virskiy; 8--epicentral zone of Tashkent earthquake of 26 April 1966.

APPROVED FOR RELEASE: 2007/02/08: CIA-RDP82-00850R000200030043-9

APPROVED FOR RELEASE: 2007/02/08: CIA-RDP82-00850R000200030043-9

are confined to the faults of the crust having significantly distinct structure and reduced propagation velocities of elastic longitudinal waves with reduced coefficient K. The epicentral zone is located above the deep zone of the faults which touch the entire crust and upper mantle (see Figure 107).

APPROVED FOR RELEASE: 2007/02/08: CIA-RDP82-00850R000200030043-9

APPROVED FOR RELEASE: 2007/02/08: CIA-RDP82-00850R000200030043-9

THE DEEP STRUCTURE OF THE EARTH'S CRUST OF THE NORTH GERMAN DEPRESSION

Moscow SEYSMICHESKIYE ISSLEDOVANIYA S APPARATUROY "ZEMLYA" in Russian 1977 signed to press 31 Jan 1977 pp 212-223

[Chapter 11 from the book "Seysmicheskiye issledovaniya s apparaturoy 'Zemlya'" by I. V. Pomerantseva and A. N. Mozzhenko, Izdatel'stvo Nedra, 1,400 copies 256 pages]

[Text] Studies were carried out with the "Zemlya" device in the German Democratic Republic in two stages. Experimental studies to determine the possibilities of studying the structure of the earth's crust of the German Democratic Republic by using these stations were carried out during the first stage in 1968. The conditions for reception of seismic signals were determined, the band of registered frequencies was established, the seasonal nature of the microseism background was investigated, and the technical-methodical procedures for conducting field investigations with respect to the conditions of the German Democratic Republic and so on were developed during the studies. It was established that the effect of the environment during the corresponding method and technique of the investigations could be reduced to a minimum (see Chapter 4).

Based on the results of experimental investigations during the second stage, investigations with the "Zemlya" device over the entire northern part of the German Democratic Republic were carried out from March 1969 through September 1970. A total of 3,500 km of profiles on an area of approximately 50,000 km^2 was completed and 946 remote earthquakes and 118 special explosions were registered during this period by using 25 "Zemlya" recording stations. Time profiles of the earth's crust on all the profiles were obtained from remote earthquakes from P and PS waves as a result of the field operations. Systems of direct and counter hodographs of P and S waves were obtained in addition to the time profiles 2,200 long.

Complex processing of the first arrivals of P and S waves from explosions and of P and PS waves from remote earthquakes made it possible to construct the depth charts and profiles of the crust of the North German Depression over the entire area and also to find the velocity models of the crust and to compile charts of distribution of the stratal velocities of P waves and coefficient K of the lower sedimentary mantle and the upper part of the crystalline mass

APPROVED FOR RELEASE: 2007/02/08: CIA-RDP82-00850R000200030043-9

APPROVED FOR RELEASE: 2007/02/08: CIA-RDP82-00850R000200030043-9

of the earth's crust. The mean and stratal velocity distribution curves of P and S waves with depth were found for the entire crust.

The Velocity Interfaces of the Earth's Crust and Their Stratification

Data on the propagation velocities of longitudinal waves in the crystalline mass of the crust were available in limited numbers toward the beginning of operations with the "Zemlya" stations within the North German Depression. Experimental data on the propagation velocities of transverse waves in the crystalline part of the crust are generally absent. A total of 11 layers was distinguished in the mass of the earth's crust from data of explosions and earthquakes registered by "Zemlya" stations (Table 12).

Processing the composite PS waves from remote earthquakes made it possible to significantly refine the depths and to construct the relief of the interface of the crust, to separate the lows of the sedimentary layer with the surface of the Variscian basement and to determine the transition zone from the crust to the mantle and the boundaries within the mantle.

The surface of the Variscian basement was confirmed by data of five boreholes. Taking into account the general geological concepts about the structure of the North German Depression [171] and its position between the roofs of the Variscian and Pre-Cambrian basements, the surface of the Caledonian basement was determined. The stratographic position of this boundary was confirmed by superdeep drilling 2.5 years after completion of the investigations. The surface of the Variscides was confirmed in two different locations by two boreholes drilled three years after completion of the investigations. The interfaces within the crust were stratified by values of $v_{P_{pl}}$ according to the criteria outlined in Chapter 10.

Some Data on the Nature of Propagation and the Structural Shapes of the Interfaces of the Earth's Crust

The same crustal interfaces as for P and S waves from explosions were determined as a result of processing PS waves from remote earthquakes within the North German Depression. The clearest, most marked and most easily traced of them are the surfaces of the Caledonian (PZ_1) and Pre-Cambrian (PR + AR) basements and the surfaces of the basaltic layer (B_I) itself and the layers of the Conrad-I (K_I) and Mohorovicic (M_I and M_{II}) discontinuities. The surface of the Variscian basement (PZ_2), the roof of the transition zone from the granitic to the basaltic layer (B_0) and the boundaries in the basaltic layer (B_{II} and K_{II}) were less clearly traced. A surface coinciding in depths to horizon Z (Zechstein), was traced almost everywhere in the sedimentary mantle. Tuff deposits of rotligendes (RE) and also the roof (J') and bottom (J") of stratal effusives in the lows of the sedimentary mantle were determined in some regions. Effusive-intrusive formations (J) above the Pre-Cambrian were determined within the Eastern Elbe gravitational and magnetic maximums (the Prignitskiy block) and in the northeastern area of the investigation. Structural charts were constructed for all the levels of the crystalline mass of the earth's crust.

APPROVED FOR RELEASE: 2007/02/08: CIA-RDP82-00850R000200030043-9

APPROVED FOR RELEASE: 2007/02/08: CIA-RDP82-00850R000200030043-9

Table 12. Velocity Profile of Crust of North German Depression

(1) Название слоя	(2) Индекс слоя	(3) Индекс границы	(4) Волны P и S от взрывов				Волны P, S, PS от землетрясений и взрывов (7)	
			$v_{P_{пл}}$, км/с (5)	$v_{S_{пл}}$, км/с	$K_{пл}$	Глубина, км (6)	$v_{P_{пл}}$, км/с	Глубина, км
(8) Осадочный чехол	ос (9)	PZ_2	4,0—4,4	—	—	0—4,5	4—4,4	0—6
Варисцийский фундамент (10)	PZ_2	PZ_1	5,3—5,4	2,8—2,9	1,86	4,5—7,4	5,3—5,4	2—8,5
Каледонский фундамент (11)	PZ_1	PR + AR	5,5—5,7	3,1—3,2	1,75	7,4—10,5	5,6—5,8	5,5—13
Докембрийский фундамент (12)	PR + AR	$Б_0$	6,1—6,3	3,4—3,5	1,79	10,5—13,5	6—6,3	8—20
Зона перехода от гранитного слоя к базальтовому (13)	$Б_0$—$Б_I$	$Б_I$	6,1—6,3	3,6	1,7—1,75	13,5—16,5	6,3—6,5	15—19
Первый базальтовый слой (14)	$Б_I$—$Б_{II}$	$Б_{II}$	6,5—6,7	3,75	1,73—1,79	16,5—20	6,5—6,7	16—26
Второй базальтовый слой (15)	$Б_{II}$—$К_I$	$К_I$	6,5—6,7	3,8—3,85	1,7—1,74	20—22,5	6,5—6,7	18—29
Третий базальтовый слой (16)	$К_I$—$К_{II}$	$К_{II}$	7,15	4,15	1,73	22,5—31,5	7,2—7,3	22—32
Четвертый базальтовый слой (17)	$К_{II}$—$М_I$	$М_I$	7,7	4,45	1,73	31,5—40,5	7,6—7,8	29—36
Зона перехода от коры к мантии (18)	$М_I$—$М_{II}$	$М_{II}$	8,3	4,8	1,73	40,5	8,1—8,2	32—40
Собственно мантия (19)	$М_{II}$—$М_{III}$		—	—	—	—	8,2—8,4	33—40

Key:

1. Name of layer
2. Index of layer
3. Index of boundary
4. P and S waves from explosions
5. km/s
6. Depth, km
7. P, S and PS waves from earthquakes and explosions
8. Sedimentary mantle
9. os
10. Variscian basement
11. Caledonian basement
12. Pre-Cambrian basement
13. Transition zone from granite to basaltic layer
14. First basaltic layer
15. Second basaltic layer
16. Third basaltic layer
17. Fourth basaltic layer
18. Transition zone from crust to mantle
19. Mantle itself

APPROVED FOR RELEASE: 2007/02/08: CIA-RDP82-00850R000200030043-9

APPROVED FOR RELEASE: 2007/02/08: CIA-RDP82-00850R000200030043-9

The upper part of the crystalline mass of the earth's crust of the North German Depression has a three-ti er structure according to data of the "Zemlya" stations. Surfaces of the Variscian (PZ_2), Caledonian (PZ_1) and Pre-Cambrian (PR + AR) basements, which form individual structural levels, are distinguished here. The interfaces between these levels are usually complex in shape (Figure 111, a). This indicates the repeated manifestation of folded movements which sequentially attract ever younger rock complexes.

The surface of the Variscides is noted only in the southern part of the North German Depression (Figures 111 and 112). The surfaces of the Caledonides and Pre-Cambrian, except for individual zones, are present almost universally within this depression. The disappearance of the Variscian initially and then of the Caledonian basements is observed within the North German Depression in the directon from south to north and northwest.

The boundary of tracking the Variscides passes approximately through the center of the North German Depression. The nature of its disappearance permits one to assume that the stratographic boundary related to the Variscides does not thin out, but also exists in the northern GDR, but the physical properties of the rock lying deeper than this boundary are apparently similar to the physical prcperties of the overlying Carboniferous rock. Thus, the physical boundary of the Variscides seemingly disappears and one may use the deeper boundary which we related to the surface of the Caledonian basement beyond the folded basement north of the North German Depression. A slight downwarp is observed along the surface of the Variscides toward the center of the North German Depression.

The Caledonian and Pre-Cambrian basements within the North German Depression form a synclinal structure which extends in the northwesterly direction, the central part of which coincides in layout with the Eastern Elbe gravitational and magnetic maximums (the Prignitskiy block). Another boundary (J), presumably related to the series of effusive formations which disappear into deposits of the basaltic layer in their roots (see Figure 112), is traced between the boundaries of the Caledonian and Pre-Cambrian basements in some places within the Prignitskiy block.

A diagram of the tectonic regionalization of the northern part of the GDR, compiled by depth charts of the Variscide, Caledonian and Pre-Cambrian basements, first determined and constructed in the GDR in 1971 from the results of studies with the "Zemlya" device, is presented in Figure 113. Regions with basements of different age and sections of the J boundary, directly underlying the sedimentary mantle, are plotted on this chart.

A rise and thinning in the direction toward the Prignitskiy block is noted along the transition zones from the granitic to the basaltic layer and from the crust to the mantle (Figures 114 and 115). Submergence of all the boundaries (zones) by 1-3 km is initially observed and then a rise of approximately the same amplitude is observed in all directions from the Prignitskiy block.

APPROVED FOR RELEASE: 2007/02/08: CIA-RDP82-00850R000200030043-9

APPROVED FOR RELEASE: 2007/02/08: CIA-RDP82-00850R000200030043-9

FOR OFFICIAL USE ONLY

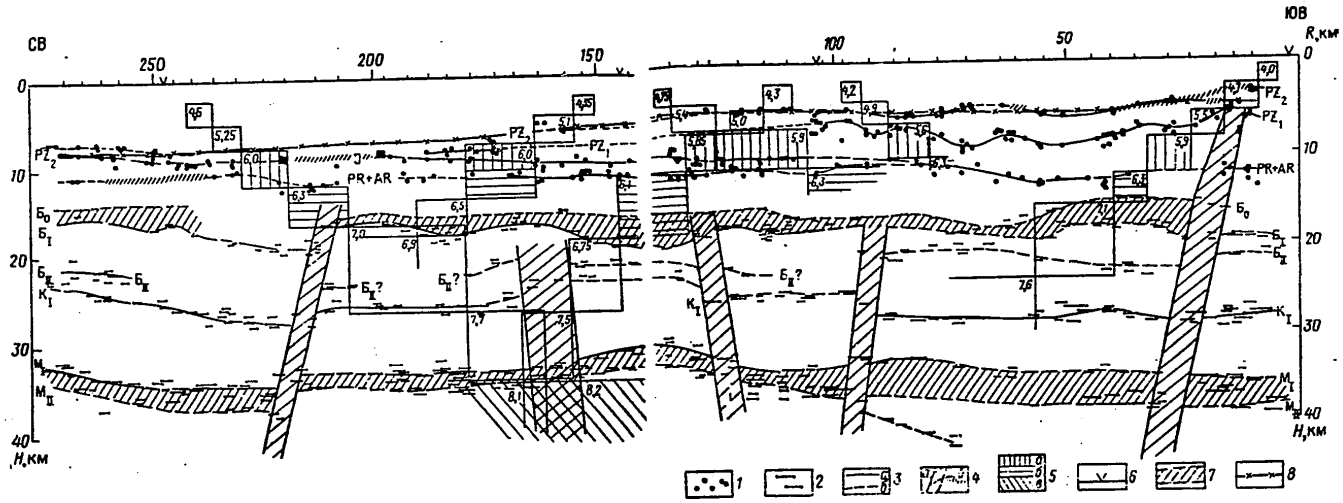

Figure 111. Depth Profile of Earth's Crust Intersecting the North German Depression from the Northwest to the Southeast, According to Data of "Zemlya" Stations (Compiled by I. V. Pomerantseva and V. P. Mavrin):
1--points of exchange of P and S waves in the upper part of the earth's crust; 2--areas of exchange of P and S waves in the middle and lower part of the earth's crust; 3--interfaces of the earth's crust, certain (a) and less certain (b); 4--deep fault zones (a) and lines (b) along the boundaries of the crust from data of "Zemlya" stations; 5--values of stratal velocities of longitudinal waves (in km/s) deeper than the surface of the Caledonian (a) and Pre-Cambrian (b) and the Mohorovicic Discontinuity (c); 6--points of explosions registered by "Zemlya" stations; 7--transition zones from granitic to basaltic layer and from crust to mantle; 8--surface of basement from KMPV data

FOR OFFICIAL USE ONLY

APPROVED FOR RELEASE: 2007/02/08: CIA-RDP82-00850R000200030043-9

APPROVED FOR RELEASE: 2007/02/08: CIA-RDP82-00850R000200030043-9

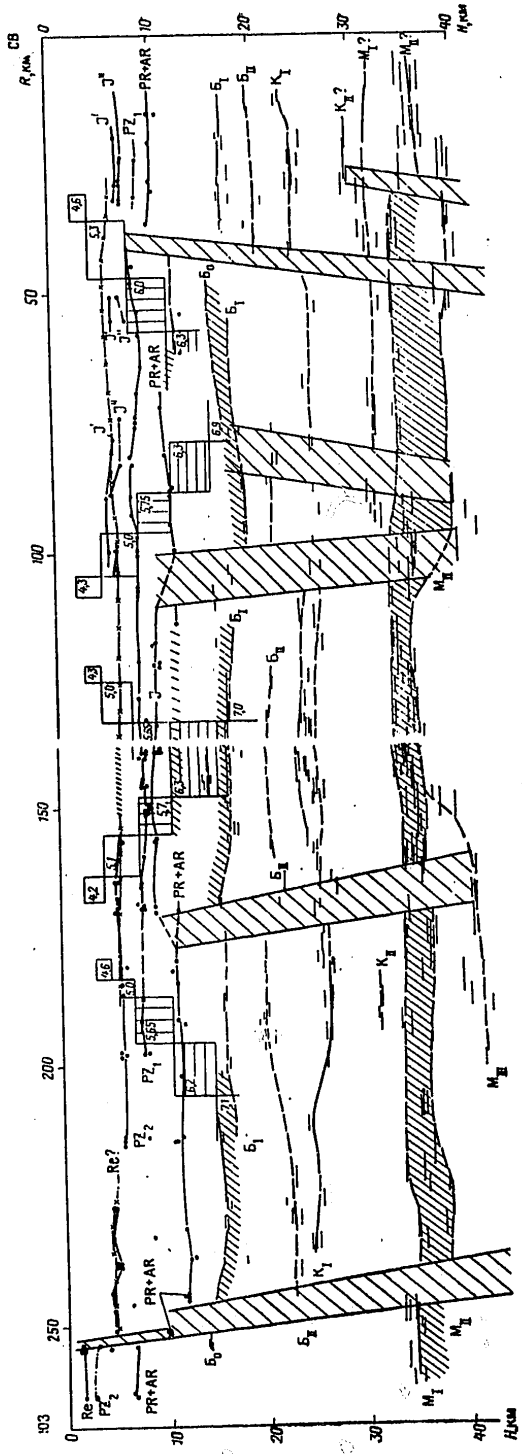

Figure 112. Depth Profile of Earth's Crust Intersecting the North German Depression From South-Southwest to North-Northeast (Compiled by I. V. Pomerantseva and L. M. Gorbach): The notations are the same as in Figure 111

APPROVED FOR RELEASE: 2007/02/08: CIA-RDP82-00850R000200030043-9

APPROVED FOR RELEASE: 2007/02/08: CIA-RDP82-00850R000200030043-9

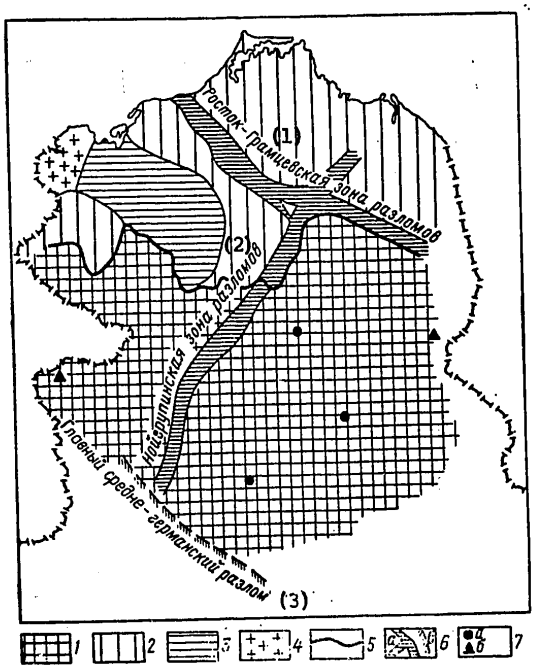

Figure 113. Diagram of Tectonic Regionalization of Northern GDR from Data of "Zemlya" Stations:
1--region of Variscide propagation; 2--region of Caledonide propagation; 3--region of propagation of effusive-intrusive formations; 4--Pre-Cambrian; 5--boundary of Variscide propagations; 6--fault zones (a) and lines (b); 7--boreholes which revealed the basement prior to working with the "Zemlya" device (a) and during operations (b)

Key:
1. Rostok-Gramzow fault zone
2. Neuruppin fault zone
3. Main Central German fault

The thickness of the sedimentary mantle of the North German Depression, according to data of "Zemlya" stations, increases from approximately 3.5 km in the south to 8 km in the north. The thickness of the granitic layer, if its composition includes the Variscides, varies from approximately 8-9 to 10-13 km. The thickness of the granitic layer without the Variscides and Caledonides comprises approximately 5-9 km.

The thickness of the basaltic layer varies from 15 to 22 km (see Figures 111 and 113). The total thickness of the crust at the center of the North German

APPROVED FOR RELEASE: 2007/02/08: CIA-RDP82-00850R000200030043-9

APPROVED FOR RELEASE: 2007/02/08: CIA-RDP82-00850R000200030043-9

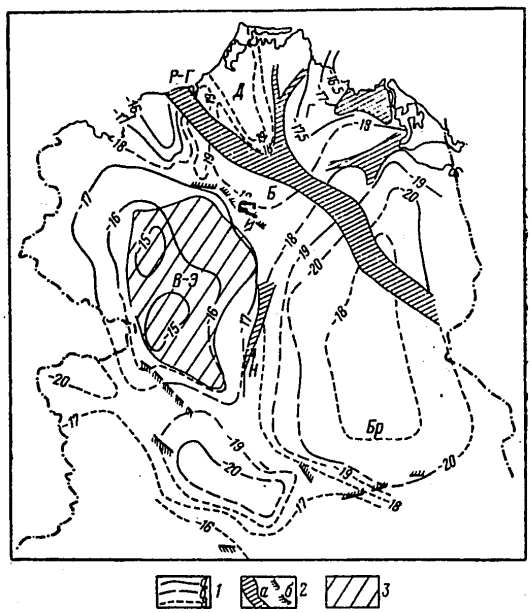

Figure 114. Chart Along Bottom of Transition Zone from Granitic to Basaltic Layer ($v_{P_{pl}}$ = 6.8-6.9 km/s) (data of "Zemlya" stations):

Different blocks of crust: D--Domgarten; G--Greifswald; B--Bartow; V-E--Eastern Elbe (Prignitskiy); Br--Berlin; R-G--Rostok-Gramzow fault zone; N--section of Neuruppin fault zone; 1--depth isoline (in km), certain (a), less certain (b) and assumed (c); 2--fault zones (a) and lines (b) from data of "Zemlya" stations; 3--region of absence or thin (up to 1 km) transition zone from granitic to basaltic layer

Depression (to the surface of the transition zone from the crust and mantle) comprises 30-33 km according to data of the "Zemlya" stations. In this case the Prignitskiy block is surrounded zones of greater thickness (2-5 km) (see Figure 115). The thickness of the crust again decreases to 30-33 km in the coastal zone and south of the Central German main fault.

The depths of deposition of the mantle itself (the bottom of the transition zone from the crust to the mantle) increase from approximately 33-34 km within the Prignitskiy block to 38-39 km to the north, south, west and east of it and again decrease to 36 km within the southern part of the Baltic Sea and south of the Central German Main fault. An exception is the region of Berlin (the Subsudenten monocline), where the depths to the mantle comprise approximately 38-39 km (Figure 115). The thickness of the transition zone itself

APPROVED FOR RELEASE: 2007/02/08: CIA-RDP82-00850R000200030043-9

APPROVED FOR RELEASE: 2007/02/08: CIA-RDP82-00850R000200030043-9

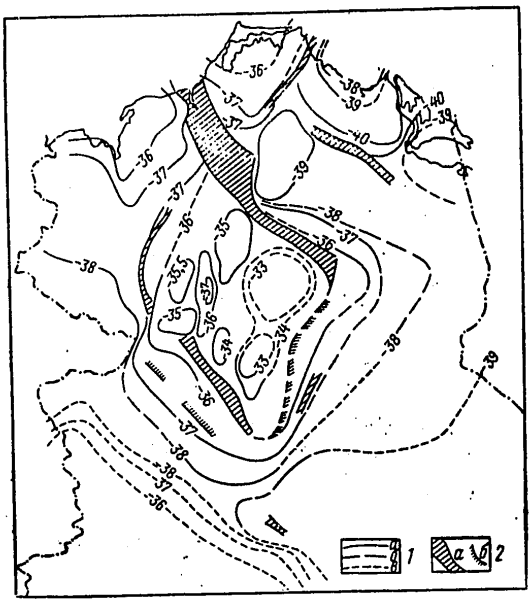

Figure 115. Relief Map of Bottom of Transition Zone from Crust to Mantle According to Data of "Zemlya" Stations: 1--depth isoline (in km), certain (a), less certain (b) and assumed (c); 2--fault zones (a) and lines (b)

from the granitic to the basaltic layer varies from 0 to 5-6 km, decreasing within the outcrops. The thickness of the transition zone from the crust to the mantle varies from 1-2 to 6-8 km. The minimum thicknesses of the transition zones are observed within the Prignitskiy block.

Comparison of the Thickness of the Sedimentary Mantle and the Crystalline Mass at the Earth's Crust of the GDR and Contiguous Countries

The derived data on the thickness of the sedimentary mantle and of the entire crust as a whole in the GDR were compared to similar materials obtained in Poland, West Germany, Czechoslovakia (from KMPV, GSZ and MOV data), Denmark, Sweden and Norway (from the results of seismology).

A relief map of the surrounding surfaces of basements of different age, determined from data of the "Zemlya" stations (see Figures 111 and 112), was constructed and it was compared to available relief maps of the basement surface of Poland and West Germany to compare the thicknesses of the sedimentary mantles of the different regions [172, 174, 183]. The isolines of the depths obtained in different countries tie in well with each other. This fact, on the one hand, permits one to assume the data on the basement surfaces obtained

APPROVED FOR RELEASE: 2007/02/08: CIA-RDP82-00850R000200030043-9

APPROVED FOR RELEASE: 2007/02/08: CIA-RDP82-00850R000200030043-9

from the "Zemlya" stations are reliable, and, on the other hand, permits one to determine the variation of thicknesses of the sedimentary mantle in the regional layout.

According to these data, two vast zones of great depths (up to 8-8.5 km) extend through northern West Germany, the German Democratic Republic and Poland. The first passes through the central part of Poland, the extreme north of the GDR and terminates in the Baltic Sea. The second zone is located somewhat to the south in the GDR. It begins to the west of the Neuruppin Fault ($H \approx 9$ km), initially proceeds to the northwest, then turns toward the south and acquires a latitudinal strike in West Germany. The depth to this boundary in the region of Hamburg comprises approximately 10 km and somewhat to the west it comprises 12 km. The most complex behavior of the isodepths of the bottom of the sedimentary mantle is noted within the GDR, which may be related both to the characteristics of the geological structure of this region and to the greater detail of the studies carried out here.

A chart of Central Europe according to the Mohorovicic Discontinuity was compiled to compare the thickness of the crust in the GDR to the thicknesses in the contiguous countries. The Mohorovicic Discontinuity, characterized by values of $v_{P_{pl}}$ = 8-8.2 km/s, was taken as the bottom of the earth's crust in most regions of the globe [105].

The boundary with $v_{P_{pl}}$ = 7.6-7.8 km/s is taken as the Mohorovicic Discontinuity in some regions, such as, for example, within the rift zones and individual regions of the Pacific Ocean. Moreover, these values of the velocities are frequently found from hodographs of limited length (50-60 km in the oceans and 150-200 km on the continents). P waves with $v_{P_{pl}}$ = 8-8.2 km/s begin to be traced in these regions with an increase of the length of the hodographs. Both boundaries with $v_{P_{pl}}$ = 7.6-7.8 km/s and 8.0-8.2 km/s were traced on the same profiles simultaneously on the Russian Series [115] and in Central Asia [110] and other regions. Their joint existence not only in the rift zones but also in regions with normal platform structure of the earth's crust permits one to assume that the boundary with $v_{P_{pl}}$ = 7.6-7.8 km/s is not the Mohorovicic Discontinuity.

Two surfaces with $v_{P_{pl}}$ = 7.6-7.8 and 8-8.2 km/s were also determined within the GDR. The first of them was related to the Conrad-II Discontinuity and the second was related to the Mohorovicic Discontinuity. The difference between them in depths comprises 2-5 km within the regions of the GDR. Two boundaries with $v_{P_{pl}}$ = 7.8 and 8-8.2 km/s have also been distinguished within Poland, according to [184]. One boundary, related to the Mohorovocic Discontinuity, was determined within West Germany, but its depth comprised 26-28 and 30-31 km for the same region according to data of different authors [168, 172, 173]. This difference permits one to assume that the Conrad-II Discontinuity is determined from the results of studies of some investigators and the Mohorovicic Discontinuity is distinguished from the results of other investigators.

APPROVED FOR RELEASE: 2007/02/08: CIA-RDP82-00850R000200030043-9

APPROVED FOR RELEASE: 2007/02/08: CIA-RDP82-00850R000200030043-9

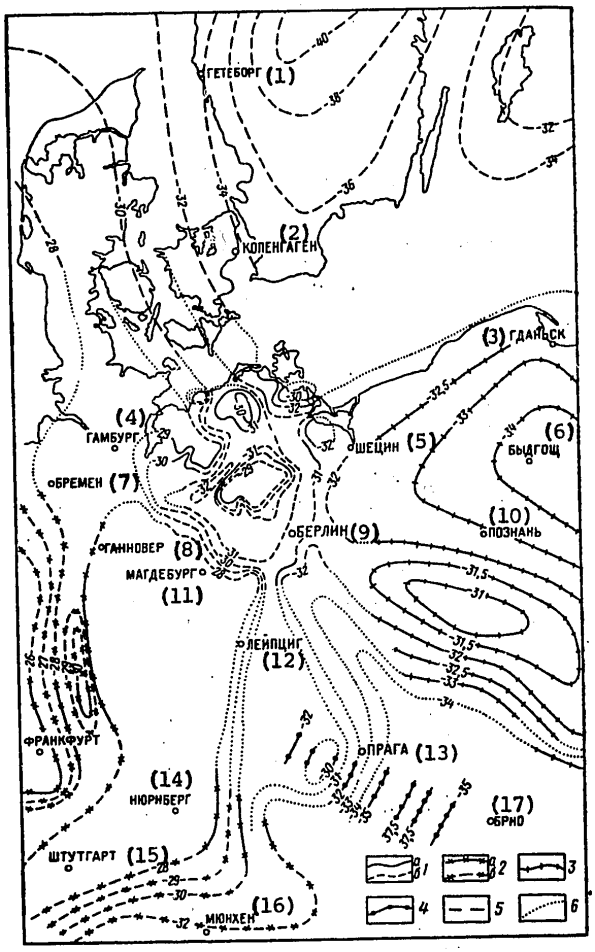

Figure 116. Map of Conrad-II Discontinuity Southwest of the Russian Series (Compiled by I. V. Pomerantseva and E. V. Kostrova):

1--isolines (in km) of Conrad-II Discontinuities from data of "Zemlya" stations, certain (a) and less certain (b); 2--isolines (in km) of Mohorovicic Discontinuity from data of recording refracted and reflected waves from explosions, certain (a) and less certain data (b); 3--isolines (in km) along the Mohorovicic Discontinuity from gravimetric data; 4--isolines (in km) along the Mohorovicic Discontinuity from GSZ data on the international profile; 5--isolines (in km) along the Mohorovicic Discontinuity from seismological data; 6--connecting isolines

[Key on following page]

APPROVED FOR RELEASE: 2007/02/08: CIA-RDP82-00850R000200030043-9

APPROVED FOR RELEASE: 2007/02/08: CIA-RDP82-00850R000200030043-9

[Continued from preceding page]

Key:

1. Goeteborg
2. Copenhagen
3. Gdansk
4. Hamburg
5. Szczecin
6. Bydgoszca
7. Bremen
8. Hanover
9. Berlin
10. Poznan
11. Magdeburg
12. Leipzig
13. Prague
14. Nuernberg
15. Stuttgart
16. Muenchen
17. Brno

Joint analysis of the materials obtained within the GDR and in contiguous countries showed that the best agreement by values of depths and the nature of the isolines is observed in the case when the Conrad-II Discontinuity is considered within the GDR, the M Discontinuity with minimum depths is distinguished within West Germany and the M Discontinuity is distinguished within other countries bounding the GDR [181]. A comparison of the chart along the Conrad-II Discontinuity, distinguished in the Northern GDR, with charts along the Mohorovicic Discontinuity in West Germany (data of explosions), Poland (gravimetric data), Czechoslovakia and the southern GDR (GSZ data), England and Sweden (seismological data), is presented in Figure 116 [170-174, 177-185]. The smooth behavior of the isolines is noted everywhere on the map. This permits one to assume that boundaries with $v_{P_{pl}}$ = 7.6-7.8 km/s and 8-8.2 km/s can be distinguished simultaneously with sufficiently detailed studies. Either the Conrad-II or the Mohorovicic Discontinuity is distinguished with less detailed seismological studies (England and Sweden).

APPROVED FOR RELEASE: 2007/02/08: CIA-RDP82-00850R000200030043-9

APPROVED FOR RELEASE: 2007/02/08: CIA-RDP82-00850R000200030043-9

THE DEEP STRUCTURE OF THE EARTH'S CRUST AND UPPER MANTLE IN THE SOUTHEAST OF THE RUSSIAN SERIES AND IN THE NORTH OF THE PRE-CASPIAN DEPRESSION

Moscow SEYSMICHESKIYE ISSLEDOVANIAY S APPARATUROY "ZEMLYA" in Russian 1977 signed to press 31 Jan 1977 pp 223-228

[Chapter 12 from the book "Seysmicheskiye issledovaniya s apparaturoy 'Zemlya'" by I. V. Pomerantseva and A. N. Mozzhenko, Izdatel'stvo Nedra, 1400 copies 256 pages]

[Text] The first ideas on the deep structure of the earth's crust and upper mantle on the Southeastern Russian Series and the Northern Pre-Caspian Depression were gained as a result of KMPV and GSZ investigations conducted by VNIIGeofizika [All-Union Scientific Research Institute of Geophysical Exploration Methods] under the supervision of Yu. N. Godin. They were subsequently supplemented by studies with the "Zemlya" device along one of these profiles and a series of crosscuts (Figure 117), see Figure 37). Specifically, no information was obtained from data of the "Zemlya" stations on the velocity characteristic of the crust for longitudinal waves in the mantle and transverse waves in the crust and mantle. Therefore, the deep structure of these regions and their characteristics are given in some cases with use of KMPV and GSZ materials.

Velocity Distribution in Crystalline Mass of Earth's Crust and Mantle from Data of "Zemlya" Stations and from KMPV and GSZ Data

The Southeastern Russian Series. The thickness of the sedimentary mantle of the Southeastern Russian Series of formations varies from 2 to 6 km and the thickness of the crystalline crust varies from 38 to 40 km. The crystalline crust consists of a number of layers (Table 13).

The Pre-Caspian Depression. The surface of the crystalline mass of the earth's crust of the Pre-Caspian Depression is characterized by values of $v_{P_{pl}}$ = 6.2-6.6 km/s, $v_{S_{pl}}$ = 3.4-3.7 km/s, K_{pl} = 1.78 and H = 4-12 km. The values of $v_{P_{pl}}$ along the surface of the crystalline crust increase to 7.0-7.2 km/s in the Central Pre-Caspian in the region of the Khobdinsk gravitational maximum where the thickness of the sedimentary mantle reaches 12-16 km (Figure 117).

APPROVED FOR RELEASE: 2007/02/08: CIA-RDP82-00850R000200030043-9

APPROVED FOR RELEASE: 2007/02/08: CIA-RDP82-00850R000200030043-9

FOR OFFICIAL USE ONLY

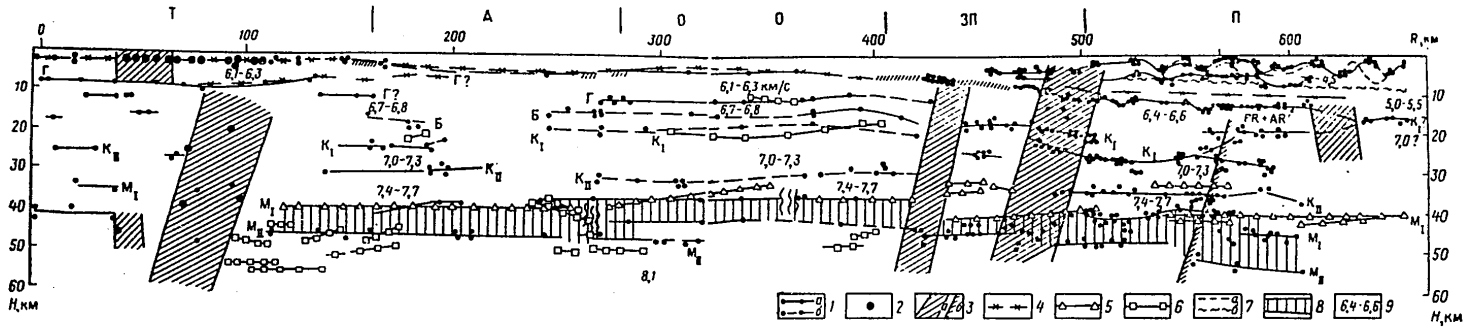

Figure 117. Comparison of Depth Profiles of Earth's Crust Constructed from KMPV and GSZ Data and From Data of "Zemlya" Station for Regions of Southeastern Russian Series and Pre-Caspian Depression (Compiled by I. V. Pomerantseva and L. P. Barskova):

PR + AR--surface of Pre-Cambrian basement; G--surface of Gabbro-Diabasic Layer; B--boundary within the basaltic layer; K_I--provisionally Conrad-I Discontinuity; K_{II}--provisionally Conrad-II Discontinuity; M_I and M_{II}--roof and bottom of transition zone from crust to mantle, respectively; T--Tatar vault; A--Abdulino Depression; O--Oremburg vault; ZP--transition zone from Southeastern Russian Series to Pre-Caspian Depression; P--Pre-Caspian Depression; 1--boundaries for data of PS waves recorded by "Zemlya" stations, certain (a) and assumed (b); 2--foci of near earthquakes; 3--fault zones (a) and lines (b) from data of "Zemlya" stations; 4--surface of Pre-Cambrian Basement from KMPV data; 5 and 6--reflecting areas along subcritical and critical reflected waves recorded by KMPV and GSZ, respectively; 7--surface of Kungurskiy (a) and Artinskiy (b) deposits of Permian from mean-latitudinal MOV data; 8--transition zone from crust to mantle; 9--value of $v_{P_{pl}}$ and km/s

FOR OFFICIAL USE ONLY

APPROVED FOR RELEASE: 2007/02/08: CIA-RDP82-00850R000200030043-9

APPROVED FOR RELEASE: 2007/02/08: CIA-RDP82-00850R000200030043-9

Two surfaces: the Conrad-II Discontinuity with velocities of v_{Pp1} = 7.8 km/s and H = 32-33 km and the Mohorovicic Discontinuity (8 km/s and H = 36-42 km) are distinguished in the Pre-Caspian according to reflected wave data obtained during subsequent arrivals during KMPV studies. Both boundaries seemingly fused together in the region of Khobda and the velocity of longitudinal waves becomes equal to 7.8 km/s deeper than the Mohorovicic Discontinuity. This may be related both to the inaccuracy of determining the velocities and to the possible thinning of the mantle rock under the Khobda gravitational maximum.

The Structure of the Earth's Crust and Upper Mantle

All the earth's crust along the Tatar Vault-Khobda profile (see Figure 117) is divided into five blocks corresponding to the following structural forms along the surface of the crystalline basement: the Tatar Vault, the Abdulino Depression, the Orenburg Vault, the transition zone to the Pre-Caspian Depression and the Pre-Caspian Depression itself (see Figure 37).

The depths of deposition of the main crustal interfaces vary from 2 km for the surface of the Pre-Cambrian Basement, 3-4 km in the region of the Tatar Vault and in the region of the Oremburg Vault, up to 5-6 km in the region of the Abdulino Depression, 6-8 km in the transition zone to the Pre-Caspian Depression and up to 12-16 km in the northern part of the depression.

The surface of the gabbro-diabasic layer [105] is submerged from 8 km in the region of the Tatar layer to 11-12 km in the transition zone to the Pre-Caspian Depression. This boundary is not traced within the Pre-Caspian.

The depths to the Conrad-I Discontinuity vary from 22 km under the Tatar Vault and 15 km under the Orenburg Vault to 28 km in the northern Pre-Caspian and up to 15-16 km in the region of the Khobda gravitational maximum.

The Mohorovicic Discontinuity or rather the transition zone from the crust to the mantle which joins either two or three boundaries at depths of 35-42 and 42-50 km on the Southeastern Russian Series (Figure 117) is also arranged non-horizontally. The minimum depths to the surface of the transition zone are observed under the Oremburg vault and comprise 34-35 km and the maximum depths (approximately 42 km) are observed in the transition zone from the Russian Series to the Pre-Caspian Depression. The depths to the surface of the transition zone from the crust to the mantle comprise 40-44 km in the Pre-Caspian Depression.

The total thickness of the transition zone from the crust to the mantle is not constant and varies from 3-12 km. The maximum depths are observed under the Orenburg vault and in the region of the Pre-Caspian Depression. Transition zones at depths of 55-60, 90-110 and 130-150 km are noted in the mantle from recording of PS waves from remote earthquakes [115].

The roof of the salt domes of the Lower Permian and the horizon in the subsaline deposits are clearly distinguished from PS waves for the Pre-Caspian

APPROVED FOR RELEASE: 2007/02/08: CIA-RDP82-00850R000200030043-9

APPROVED FOR RELEASE: 2007/02/08: CIA-RDP82-00850R000200030043-9

Table 13. Velocity Profile of Earth's Crust of Southeastern Russian Series

(1) Названия слоя	(2) Индекс слоя	(3) Индекс границы	$v_{P_{пл}}$, км/с (4)	$v_{S_{пл}}$, км/с	$K_{пл}$	(5) Глубина, км
Осадочный чехол (6)	ос (7)	PR + AR	4,25—5,45	2,12—2,87	1,9—2	0—6
Докембрийский фундамент (8)	PR + AR	Г	6,1—6,3	3,3—3,4	1,85	2—13
Габбро-диабазовый слой (9)	Г—K_I	K_I	6,7—6,8	3,8	1,76—1,79	11—30
Первый базальтовый слой (10)	K_I—K_{II}	K_{II}	7—7,3	3,7	1,89—1,97	20—32
Второй базальтовый слой (11)	K_{II}—M_I	M_I	7,4—7,7	3,9—4,1	1,88—1,9	26—40
Зона перехода от коры к мантии (12)	M_I—M_{II}	M_{II}	8,0—8,1	4,6	1,73—1,77	35—46
Первый слой в мантии (13)	M_{II}—M_{III}	M_{III}	8—8,1	4,6	1,73—1,77	42—47
Второй слой в мантии (14)	M_{III}—M_{IV}	M_{IV}	8,4	4,7	1,79	45—100
Третий слой в мантии (15)	M_{IV}—M_V		9,2	5,3	1,74	110—120

Key:
1. Names of layer
2. Index of layer
3. Index of boundary
4. km/s
5. Depth, km
6. Sedimentary mantle
7. os
8. Pre-Cambrian basement
9. Gabbro-Diabasic layer
10. First basaltic layer
11. Second basaltic layer
12. Transition zone from crust to mantle
13. First layer in mantle
14. Second layer in mantle
15. Third layer in mantle

Depression itself. It is not excluded that this horizon coincides with the bottom of the salt dome. A large vault uplift is noted somewhat to the south of the Ashchisay structure along this horizon.

On the Modern Tectonic Activity of the Southeastern Russian Series and the Northern Pre-Caspian Depression

The presence of weak tectonic activity of the Southeastern Russian Series and of the Urals folded system was established by conducted investigations [115]. The number of earthquakes registered during four months of studies did not exceed 20-25. The epicenters of local earthquakes (see Figure 37) are plotted on the relief map of the basement (from drilling data and data of

APPROVED FOR RELEASE: 2007/02/08: CIA-RDP82-00850R000200030043-9

APPROVED FOR RELEASE: 2007/02/08: CIA-RDP82-00850R000200030043-9

geophysical studies of past years and data of "Zemlya" stations), which are arranged in specific order. Moreover, the repetition of earthquakes in the same zones over a period of two years is observed. Five zones with location of epicenters of local earthquakes are distinguished. Zone A intersects the Tatar vault in the southerly and southwesterly direction. The foci of local earthquakes are grouped mainly in the crust here (H = 25-50 km) and only one earthquake epicenter is located deeper (H = 50-80 km). Zone B approaches a region bounding the steep slope of the Zhigulev-Pugachev vault from the southeast. The epicenters are localized here within a rather narrow band, extending from the northeast to the southwest. Zone C is located within the western slope of the Urals and the Pre-Urals downwarp. The epicenters of this zone are scattered over a rather broad area, although the entire zone has a meridional strike. The depths of the foci are determined less certainly here than within the first zone, since the profile of the sedimentary mantle and crust differs here from that of the Southeastern Russian Series, for which the theoretical hodographs of P and S waves were calculated. Zone D is located in the region where the Russian Series meets the Pre-Caspian Depression and is characterized by earthquake foci located deeper than the crust. The foci are located mainly in the crust in Zone E, corresponding to the Zhigulev dislocations.

The derived data on the epicenters of local earthquakes within the Tatar vault permit one to explain the wave pattern observed here during GSZ studies.

Waves from deep boundaries are easily traced south of the central part of the Tatar Vault. Determination of waves from the Mohorovicic Discontinuity was difficult to the north. Waves from the intermediate boundaries in the crust (the Conrad Discontinuity and the deeper boundaries) within the northern part of the Tatar Vault (profile II) were generally not traced continuously. They were distinguished in the form of separate not extended cophasal axes. Composite waves within this zone were also poorly registered and in some places were not distinguished at all during studies with the "Zemlya" stations.

The foci of local earthquakes plotted on the depth profile indicate an entire series of deep fractures of the crust, part of which does not reach the basement surface. It is not true that easily correlated reflected and refracted waves are difficult to anticipate in these zones. Hence, it should be concluded that the most interesting zones of the crust cannot be determined during GSZ studies and the nature of the observed wave pattern cannot be clearly explained without having data on the seismicity of the region.

Comparison of a series of faults determined with the "Zemlya" stations with locations of oil fields permits one to assume that a number of oil fields of the Southeastern Russian Series is confined to the deep fracture zone or faults contiguous with it. These may include the Mukhanovskoye and Romashkinskoye fields. The location of the latter above the zone of disturbances (within the Tatar Vault), not manifested by KMPV data in the relief of the basement surface, indicates the need to study not only the surface of the crystalline rock but also the crust for its entire thickness.

APPROVED FOR RELEASE: 2007/02/08: CIA-RDP82-00850R000200030043-9

APPROVED FOR RELEASE: 2007/02/08: CIA-RDP82-00850R000200030043-9

THE DEEP STRUCTURE OF THE CRYSTALLINE MASS OF THE EARTH'S CRUST AND UPPER MANTLE OF THE AZOV-KUBAN' DEPRESSION

Moscow SEYSMICHESKIYE ISSLEDOVANIYA S APPARATUROY "ZEMLYA" in Russian 1977 signed to press 31 Jan 77 pp 228-231

[Chapter 13 from the book "Seysmicheskiye issledovaniya s apparaturoy 'Zemlya'" by I. V. Pomerantseva and A. N. Mozzhenko, Izdatel'stvo Nedra, 1,400 copies, 256 pages]

[Text] The structure of the earth's crust of the Azov-Kuban' Depression was studied by using nine "Zemlya" recording stations. As a result of these studies with spacing of 5 km, the main profile 240 km long and a number of profiles located perpendicular to the main profile with total length of 375 km were established [125]. Studies were conducted on the main profile simultaneously with KMPV and with the "Zemlya" device. The latter, besides earthquakes, also recorded explosions during KMPV operations. The deep structure studied on the main profile which intersects the different tectonic elements is described below and a comparison of the derived data to KMPV data is also given (see Chapter 14).

The tectonic activity of the area of investigation in the Azov-Kuban' Depression was not specially studied. A total of only 40 weak local earthquakes was registered incidentally [125]. The small number of registered local earthquakes is apparently related to the very high background of industrial noise which makes it difficult to separate weak signals. On the other hand, it is possible that the profile, as shown in [5], passes through an abnormal seismic zone.

The epicenters of local earthquakes within Krasnodarskiy Kray are grouped mainly along the Black Sea coast, coinciding with the epicenters determined during seismological studies of past years. Part of the epicenters is located to the north of the area of study and part is located to the east. The accuracy of determining the epicenters of local earthquakes was low ($\pm$ 2-8 km).

APPROVED FOR RELEASE: 2007/02/08: CIA-RDP82-00850R000200030043-9

APPROVED FOR RELEASE: 2007/02/08: CIA-RDP82-00850R000200030043-9

The Velocity Interfaces of the Earth's Crust and Upper Mantle and Stratification of Them

The velocity characteristic of the crust of this region was studied by recordings from earthquakes [59, 148]. Several clear interfaces and transition zones between layers of the crust were determined within the Azov-Kuban' Depression. The first interface of the crystalline mass of the crust (vP_{pl} = 5.6-5.8 km/s) was related to the surface of the transition mass (T + I) by the velocity values and drilling data. The second boundary with vP_{pl} = 6.1-6.2 km/s was stratified as the surface of the Pre-Cambrian basement [162]. The third boundary with vP_{pl} = 6.8-7 km/s was stratified as the surface of the transition zone from the granitic to the basaltic layer. The region below which vP_{pl} = 8-8.2 km/s was related to the transition zone from the crust to the mantle. The short lengths of the hodograph of refracted and deep reflected (up to 140 km) waves did not make it possible to obtain values of vP_{pl} deeper than the Mohorovicic Discontinuity at the boundaries in the upper mantle.

The Relief and Structure of the Interfaces of the Earth's Crust and Upper Mantle

The surface of the transition mass. The surface of the transition mass within the Skifskaya series (A) is essentially deposited horizontally (Figure 118). Its absolute marks do not exceed 2.5 km. Smooth submergence of this surface to depths of 3.5 km (B and C) is observed in the southerly direction. The depth to this boundary increases sharply to 5.5 km in the region of the Timashevskaya stage (D). A depression with amplitude of approximately 1.5 km is noted to the south of the Timashevskaya stage. The surface of the transition mass lies almost horizontally at depths of 8-10 km farther to the south from this depression to the Western Kuban' trough.

The depth to the surface of the transition mass increases sharply to 18-20 km within the Western Kuban' trough; the angles of inclination of the side of the trough reach 45° or more here. The northern side of this depression is traced only in the most general lines due to the sparse spacing of the stations and their disposition along a single linear profile rather than by area. The behavior of the transition surface within the depression itself is unclear. This is explained, on the one hand, by receipt of insufficiently reliable materials and, on the other hand, by the very complex wave pattern apparently determined by a fault zone of crystalline rock (which is determined by indirect features) within the central part of the depression and by the complex structure of the lows of the sedimentary mantle. The depth of the transition surface along the southern edge of the Western Kuban' trough varies from 5 to 18 km and the angles of inclination vary from 3 to 45°.

The surface of the Pre-Cambrian basement. This surface is located at depths from 1.6 to 2.5 km within the Skifskaya series (see Figure 117). Submergence of it to 10 km in the region of the Pre-Black Sea-Kuban' downwarp is observed in the southerly direction. A fault along the Pre-Cambrian surface up to

APPROVED FOR RELEASE: 2007/02/08: CIA-RDP82-00850R000200030043-9

APPROVED FOR RELEASE: 2007/02/08: CIA-RDP82-00850R000200030043-9

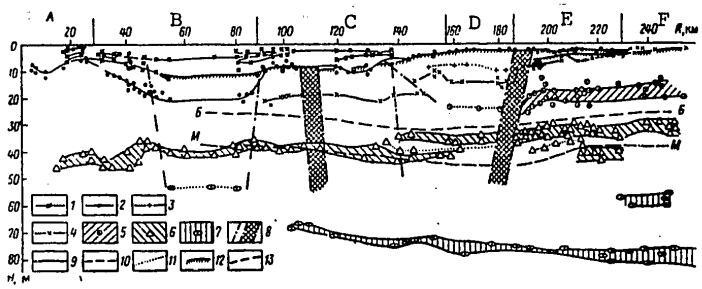

Figure 118. Profile of Crust and Upper Mantle of the Azov-Kuban' Depression from Results of Studies with "Zemlya" Stations:

A--greater Caucasus anticlinorium; B--Western Kuban' trough; C--Timashevskaya stage; D--Belogorsk-Berezanskiy megarch; E--Pre-Black Sea-Kuban' downwarp; F--Skifskaya series; 1--interfaces within sedimentary rock; 2--surface of transition mass; 3--surface of Paleozoic basement; 4--surface of Pre-Cambrian basement; 5--transition zone from granitic to basaltic; 6--transition zone from crust to mantle; 7--exchange zones in earth's upper mantle; 8--fault lines and zones of crystalline crust from data of "Zemlya" stations; 9--certain sections of interfaces; 10--uncertain sections of interfaces; 11--assumed position of interfaces; 12--surface of Paleozoic basement from KMPV data; 13--surface of basaltic layer (B) and Mohorovicic Discontinuity (M) from deep MOV data

5 km in amplitude is observed in the zone where the downwarp joins the Belogorsk-Berezanskiy megarch. The Pre-Cambrian basement lies almost horizontally at depths of 15 km within the Belogorsk-Berezanskiy megarch. A large uplift up to 5 km in amplitude, the southern edge of which is complicated by a fault of 4 km, is noted further to the south in the region of the northern part of the Timashevskaya stage along the Pre-Cambrian surface. The Pre-Cambrian surface lies almost horizontally at marks of 17-18 km in the remaining part of the Timashevskaya stage. Slight submergence of the Pre-Cambrian surface to 20-22 km is observed prior to the northern edge of the Western Kuban' trough. The surface of the Pre-Cambrian basement could not be constructed in the trough itself and south of it (in the mountainous region) since the waves exchanged at this boundary are traced in a complex interference zone on a noisy background (lateral composite PS waves which comprise P waves and so on). Phases of P and PS waves of the same type could not be certainly identified here.

The transition zone from the granitic to the basaltic layer. It is characterized in the north of the study area by depths of 14 km (see Figure 118). The depths to this boundary increase to 24-25 km south of the region where the Skifskaya platform joins the Pre-Black Sea-Kuban' downwarp. The thickness of the transition zone itself is 3.5-4 km.

APPROVED FOR RELEASE: 2007/02/08: CIA-RDP82-00850R000200030043-9

APPROVED FOR RELEASE: 2007/02/08: CIA-RDP82-00850R000200030043-9

The transition zone from the crust to the mantle. Two zones with almost horizontal deposition of boundaries are distinguished in the transition zone from the crust to the mantle. There is slight submergence of the roof of the first zone from 30 to 33 km (in the region of the Timashevskaya stage) from north to south. Sharp variation of the nature of the traceability of both zones is observed within the Timashevskaya stage, as a result of which only the lower zone, shifted downward by 3-4 km, which rises slightly toward the center of the Western Kuban' trough from marks of 40 km to 37.5 km, is traced to the south of the Timashevskaya stage. The rise of the Mohorovicic Discontinuity with a simultaneous submergence of the surface of crystalline rock leads to a sharp decrease of the thickness of the crystalline mass of the crust from 26 km within the Skifskaya series to 15-16 km within the Western Kuban' trough. The thickness of the mass of sedimentary rock increases to 20 km for these regions. The Mohorovicic Discontinuity is located at a depth of 36 km south of the Western Kuban' trough, becoming submerged under the Western Caucasus anticlinorium to 42 km. The total geological interpretation of the crustal interfaces by the "Zemlya" profile described above is given in [162].

The interface in the mantle is located at depths of 80-65 km, rising toward the Western Kuban' trough.

APPROVED FOR RELEASE: 2007/02/08: CIA-RDP82-00850R000200030043-9

APPROVED FOR RELEASE: 2007/02/08: CIA-RDP82-00850R000200030043-9

PROSPECTS FOR DEVELOPMENT OF A COMPLEX SEISMIC METHOD FOR STUDYING THE STRUCTURE OF THE EARTH'S CRUST AND UPPER MANTLE

Moscow SEYSMICHESKIYE ISSLEDOVANIYA S APPARATUROY "ZEMLYA" in Russian 1977 signed to press 31 Jan 77 pp 231-240

[Chapter 14 from the book "Seysmicheskiye issledovaniye s apparaturoy 'Zemlya'" by I. V. Pomerantseva and A. N. Mozzhenko, Izdatel'stvo Nedra, 1,400 copies, 256 pages]

[Text] The Geological Effectiveness of the Studies

The geological effectiveness of the seismic method of investigation can be established as a result of comparison with drilling data, especially carried out after operations by the given method, and also as a result of comparison with data of other geophysical studies--seismic, gravimetric, magnetometric and so on.

Comparison of Data from the "Zemlya" Stations to Deep Drilling Data

The profiles obtained with the "Zemlya" stations were compared to deep drilling data in all five regions: on the Southeastern Russian Series, in the Pre-Caspian, Azov-Kuban' and North German Depressions and in the region of Tashkent. Of greatest interest in this case is comparison to data of boreholes drilled during or after completion of operations with the "Zemlya" device. These boreholes exist in Tashkent (1) and within the North German Depression (5). Therefore, comparison to drilling data is described below for these two regions, although data on the Azov-Kuban' Depression and the Southeastern Russian Series are also presented in Table 14.

The North German Depression. Comparison of data from "Zemlya" stations and deep drilling data is presented in Table 14. By the time the operations with the "Zemlya" device were carried out, the surface of the Variscian basement in the GDR was exposed in six boreholes. Two boreholes were drilled after receipt of preliminary data with the "Zemlya" device and three boreholes were drilled 2.5-3 years after completion of the studies. The differences of the drilling data and materials of "Zemlya" stations in all the boreholes did not exceed 1-5 percent of the total depth of the basement surface.

APPROVED FOR RELEASE: 2007/02/08: CIA-RDP82-00850R000200030043-9

APPROVED FOR RELEASE: 2007/02/08: CIA-RDP82-00850R000200030043-9

Table 14. Comparison of Depths (in km) from Earth's Surface to Basement Surface from Different Data

Скважина (1)	Возраст (2)	Данные бурения (3)	Данные КМПВ (4)	Данные станции «Земля» (5)
Азово-Кубанская впадина (6)				
Старо-Минская (7)	T + J	2,1	2,1	2,05
Крыловская (8)	T + J	2,38	2,4	2,4
(9) Челбасская	T + J	2,26	2,25	2,3
Брюховецкая-1 (10)	T + J	3,22	3,2	3,1
Брюховецкая-3 (11)	T + J	4	4	4
Прикаспийская впадина (12)				
Новосергиевская (13)	AR	4,224	4,8	4,4
(14) Районы г. Ташкента				
1	PZ	1,491	1,5	1,5
2	PZ	2,385	—	2,4
3	PZ	2,356	—	2,4
4	PZ	2,443	—	2,27—2,66
5	PZ	2,27	—	2,4
6	PZ	2,375	—	2,4
7	PZ	1,57	1,54	1,64?
8 *	PZ	2,39	—	2,66
Северо-Германская впадина (15)				
1	C_1	6,58	—	6,5
2	C_1	4,445	—	4,4—4,6
3	C_1	4,87	5,8	4,9—5
4	C_1	3,536?	—	3,6?
5	Д	3,234	—	3,2—3,3
6	C_2	5,107	5,2	5,2
7 *	C_1	4,882	6,75	4,9
8 *		4,445	5	4,6—4,7
9 **	—	7	6	7
10 **	—	4,8	6	4,7—5,1
11 **	—	4,3 ***	5,5—6	4,8

* Boreholes drilled after obtaining preliminary data with the "Zemlya" device.

** Boreholes drilled 2.5-3 years after completion of operations with the "Zemlya" device.

*** The borehole is located 10 km from the profile.

Key:

1. Borehole
2. Age
3. Drilling data
4. KMPV data
5. Data of "Zemlya" station
6. Azov-Kuban' Depression
7. Staro-Minskaya
8. Krylovskaya
9. Chelbasskaya
10. Bryukhovetskaya-1
11. Bryukhovetskaya-3
12. Pre-Caspian Depression
13. Novosergeyevskaya
14. Rayons of Tashkent
15. North German Depression

APPROVED FOR RELEASE: 2007/02/08: CIA-RDP82-00850R000200030043-9

APPROVED FOR RELEASE: 2007/02/08: CIA-RDP82-00850R000200030043-9

The rayons of Tashkent. Several boreholes which revealed the surface of the Paleozoic basement were drilled before and during operations with the "Zemlya" device in the rayons of Tashkent and its environs. The differences of the drilling data and of the "Zemlya" stations for these boreholes did not exceed 50-100 m in most cases.

Borehole 8 (the epicenter) was drilled after studies with the "Zemlya" stations in 1966 in the epicentral zone and the absolute depth to the basement, according to preliminary data of "Zemlya" stations, comprised 2.2 km. The borehole exposed the surface of Paleozoic rock at an absolute depth of 1.93 km. However, as was later determined, the difference of the drilling data and the "Zemlya" stations comprises 100 m or approximately 4 percent with regard to the curvature of borehole 8 drilled on the steep slope of a canyon in the center of Tashkent.

Comparison of KMPV, GSZ and "Zemlya" Station Profiles

The North German Depression. A system of KMPV profiles with total length of approximately 1,600 km was developed and a chart was constructed by the horizon with v_{Pp1} = 6 km/s, which was regarded as the surface as the basement of different age, by the beginning of operations with the "Zemlya" stations in the GDR. Three KMPV profiles were worked out a second time by "Zemlya" stations to compare the KMPV data and the "Zemlya" station data (see Figure 111).

As can be seen from Figure 111, the basement surface according to KMPV data first passes sequentially along the surface of the Variscian basement, determined by the "Zemlya" method, and then changes to the Caledonian basement and then to the surface of the intrusive-effusive bodies within the Eastern Elbe massif (the Prignitskiy block). In other words, the surface of the KMPV basement passes along the bottom of the sedimentary mantle, being the envelope of the surfaces of basements of different ages determined by "Zemlya" stations (see Figure 111). Comparison of data for the other profile (see Figure 112) shows that the surface of the KMPV basement in the direction from south to north initially coincides with that of tuff deposits of rotligendes, then proceeds along the surface of the Variscian basement determined from data of "Zemlya" stations and passes in the north either through effusives or through other horizons in the lower part of the sedimentary mantle. Thus, the surface along the KMPV may also not reflect the basement relief in complexly structured zones when boundaries with high velocities are found in the lows of the sedimentary mantle.

Comparison was not carried out by deep boundaries within the North German Depression itself, since there were essentially no GSZ operations here. However, the thickness of the sedimentary mantle and of the entire crust of the GDR was compared to similar data of contiguous countries: Poland, West Germany and others (see Chapter 11).

The Azov-Kuban' Depression. The profiles within the Azov-Kuban' Depression were compared along the surface of the intermediate mass, partially along

APPROVED FOR RELEASE: 2007/02/08: CIA-RDP82-00850R000200030043-9

APPROVED FOR RELEASE: 2007/02/08: CIA-RDP82-00850R000200030043-9

the Pre-Cambrian and also along the deep crustal interfaces: the transition zones from the granitic to the basaltic layer and from the crust to the mantle. The surface of the intermediate mass on sections with small angles of inclination coincide rather well from materials of "Zemlya" stations with KMPV data (see Figure 118). Significant differences are observed within the Timashevskaya stage and in the Western Kuban' trough, where the angles of inclination of the surface of the intermediate mass reach 45° or more. The difference disappears within the Timashevskaya stage in the southerly direction. The boundaries diverge by almost 8 km within the Western Kuban' trough.

Theoretical calculations carried out to determine the causes for these differences show the following. Refracted waves along the dip of the northern slope of the Western Kuban' trough during KMPV operations for the T + I boundary do not emerge to the earth's surface within the profile [107]. Refracted waves along the rise of the northern slope of the Western Kuban' trough only create complication in the recordings during subsequent arrivals. These calculations permit one to state that the steep slopes of the Western Kuban' trough cannot be traced with KMPV. The KMPV boundary obtained here at depths of 10-12 km is apparently a high-velocity horizon in the lows of the sedimentary mantle.

The profiles along the surface of the Pre-Cambrian basement were compared only within zone D (see Figure 118). This boundary was not determined by KMPV operations farther south. The difference of the profiles along the Pre-Cambrian surface in this section includes only more complex behavior of it from data obtained with the "Zemlya" stations.

The surface of the transition zone from the granitic to the basaltic layer does not coincide with the boundary determined from materials of deep MOV, both in depth and in configuration. The reasons for the lack of coincidence apparently include the fact that the surface in the lows of the basaltic layer rather than the surface of the basaltic layer was constructed from MOV data since $v_{P_{sr}}$ to this surface is equal to 5.6 km/s, while the value of $v_{P_{pl}}$, determined by two reflections from D and M, is equal to 7.8-8.0 km/s. The values of $v_{P_{sr}}$ to the surface of the basaltic layer, according to data of composite waves, are equal to 5.1-5.2 km/s, which agrees with the values of $v_{P_{sr}}$ to this boundary within the Skifskaya series.

The transition zone from the crust to the mantle, according to data of PS waves, coincides with the M discontinuity from MOV data within the Western Kuban' trough and Timashevskaya stage themselves. These two boundaries diverge further north: the transition zone for composite waves is located above the M discontinuity according to MOV data. This may be caused both by the difference of $v_{P_{sr}}$ to the M discontinuity, constructed from reflected and composite waves, and by the method used to compile the summary hodographs for reflected waves. The M discontinuity, according to data of reflected waves, is constructed with a value of $v_{P_{sr}}$ = 6.2 km/s and that from data of composite waves is constructed with $v_{P_{sr}}$ = 5.8 km/s. The M discontinuity, according to MOV data, is constructed from a series of summary hodographs, each of which is compiled from a group of waves lasting several seconds,

APPROVED FOR RELEASE: 2007/02/08: CIA-RDP82-00850R000200030043-9

APPROVED FOR RELEASE: 2007/02/08: CIA-RDP82-00850R000200030043-9

reduced to any single phase. As a result, the summary hodograph coinciding at the beginning of the profile to the first phases of the observed hodograph, frequently diverges from the first phases by ± 1-3 seconds after tie-in according to the system of conjugate points toward the end of the profile. All these factors permit one to assume that the transition zone from the crust to the mantle, according to data of PS waves, coincides more to the real medium than the M discontinuity from deep MOV data.

The Southeastern Russian Series and the Northern Pre-Caspian Depression. Comparison of the interfaces constructed from data of "Zemlya" stations to KMPV and GSZ profiles after their re-interpretation with regard to the nature of the waves registered by these methods [104, 106] showed the following. The surface of the Pre-Cambrian basement and the Mohorovicic Discontinuity are clearly determined by all the methods (see Figure 117). Agreement of the basement surface to borehole data was better from data of composite waves in some cases, for example, in the Orenburg vault and in the region of the Novosergiyevskaya borehole.

Thus, according to KMPV data, the depth to the basement surface near the borehole in the Orenburg vault was 300 m less than the actual depth and according to composite wave data, it essentially coincided with drilling data. The difference of drilling and KMPV data reached approximately 1,000 m for the Novosergiyevskaya borehole and it comprises approximately 100 m for composite wave data.

In the Pre-Caspian, the basement surface surface according to composite wave data is located 4-5 km deeper than according to KMPV data. The most probable depth of the basement in the Pre-Caspian is closer to the surface constructed from composite waves according to the results of the latest KMPV studies. The differences along the Mohorovicic Discontinuity according to deep MOV and composite wave data vary from 0 to ± 2 km and they reached 4 km in one location only in the Northern Pre-Caspian. The differences are within the range of accuracy of determining depths both by MOV and by composite waves.

The matter is somewhat more complex with the intermediate boundaries. Individual boundaries constructed from GSZ data agree rather well with boundaries from composite waves (see Figure 117). However, the number of boundaries determined from PS waves is significantly greater than that from P waves. This may be related to the presence of both waveguides not determined by P waves in the crust and the presence of interfaces determined by S waves and which are clear exchange surfaces.

Comparison of "Zemlya" Station Data to the Results of Other Types of Geophysical Studies

The rayons of Tashkent. Material which permits one to gain an idea of the tectonics of the region of Tashkent and its seismic regime and to determine the possible causes of the Tashkent earthquake was obtained as a result of various geophysical studies (Kh. T. Tulyaganov, V. G. Gor'kovets, V. V. Fedynskiy, M. K. Polshkov, B. B. Tal'-Virskiy, A. G. Khvalovskiy,

APPROVED FOR RELEASE: 2007/02/08: CIA-RDP82-00850R000200030043-9

APPROVED FOR RELEASE: 2007/02/08: CIA-RDP82-00850R000200030043-9

M. A. Sadovskiy, Ye. F. Saverinskiy, Ye. M. Butovskaya, V. I. Ulomov, M. V. Kondorskaya and others), including observations with the "Zemlya" stations. Materials for all the geophysical fields were first compiled by A. G. Khvalovskiy and N. B. Vol'fson [127]. Comparison of the "Zemlya" station data on the deep structure of the earth's crust and the aftershock foci of the Tashkent earthquake to data of gravimetric, magnetometric, seismological, morphological and levelling surveys is presented below.

Comparison of the chart of the surface of the Paleozoic basement to the chart of local gravity anomalies of the rayons of Tashkent showed that the zone of conjunction of the Chinabad outcrop and of the Tashkent depression itself corresponds to the contact of positive and negative local gravity anomalies. The Chinabad outcrop is characterized by positive anomalies and the Tashkent depression is characterized mainly by negative anomalies. The region of the course of the Chirchik River is characterized by a combination of positive and negative anomalies. The aftershock foci of the Tashkent earthquake were located in the center of the city at the junction of positive and negative anomalies.

Comparison of the surface of the Paleozoic basement to the chart of the abnormal magnetic field (ΔT_a), compiled by A. N. Kotlyarovskiy and I. G. Kremnov, and to fault zones determined by N. B. Vol'fson and A. G. Khvalovskiy, showed that the epicentral zone corresponds to a region with sharp change of sign of the geomagnetic field and is located at the center of intersection of the Tashkent and Almalyk faults. There is a direct correlation relation between the chart of ΔT_a and the surface relief of the basaltic layer (see Figure 64). Positive anomalies correspond to the rises of this surface and negative anomalies correspond to the troughs.

Comparison of the surface of the Paleozoic basement to the chart of the results of morphometric surveys, compiled by A. T. Yudin, R. I. Denisov and others, showed that weak descending vertical motions were manifested during the Upper Quaternary time in the regions southeast of the main Tashkent fault. A completely different pattern is observed northwest of the Tashkent fault, where intensive uplifting (up to 10 m) and downwarping (up to 4.5 m) occurred. Moreover, linearly elongated extended structures (up to 10 km), insignificant in transverse dimensions (up to 1-2 km) were uplifted and downwarped. Especially sharp fluctuations of different sign (up to + 10 m and - 4.5 m) were noted in the epicentral zone of the Tashkent earthquake of 1966.

Comparison of the surface chart of the Paleozoic basement to the chart of results of repeated levellings carried out at Tashkent during May-September 1966 showed that a zone of a sharp rise (by 50 mm) of the earth's surface coincides with the block of increased deposition of the basement surface under the Tashkent Seismological Station (a closed isoline with mark of 1.25). This rise occurred during the period from May (the first levelling) through September (the second levelling) 1966. The earthquake epicenters are located toward the southwest, south and southeast from this uplifted block (Figure 119).

APPROVED FOR RELEASE: 2007/02/08: CIA-RDP82-00850R000200030043-9

APPROVED FOR RELEASE: 2007/02/08: CIA-RDP82-00850R000200030043-9

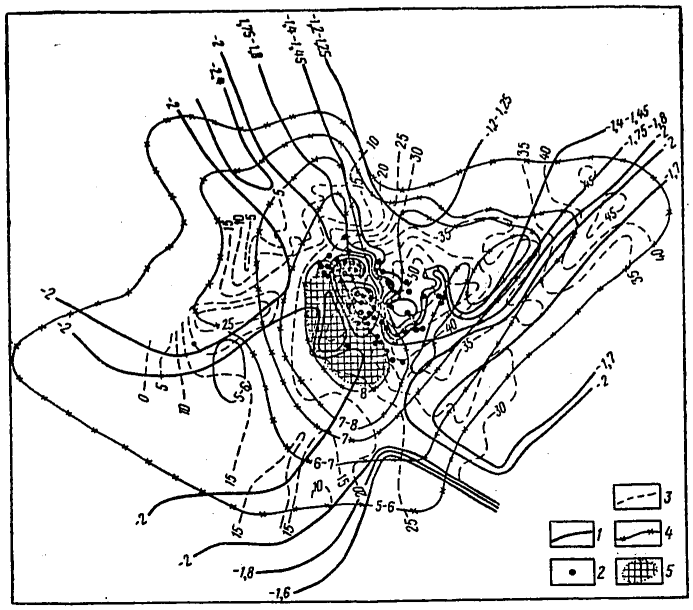

Figure 119. Surface Charts of Paleozoic Basement with Aftershock Epicenters of Tashkent Earthquake, the Results of Repeated Levellings Carried Out at Tashkent and the Isoseismal Lines of Destruction:
1--isolines (in km) along the surface of the Paleozoic basement; 2--epicenters of aftershocks of earthquake of 26 April 1966; 3--isolines of relative variation of heights of benchmarks and markers (in mm); 4--isoseismal lines of destruction; 5--epicentral zone projected onto the earth's surface at an angle of 15° to the vertical

Comparison of the surface chart of the Paleozoic and the epicenters of aftershocks of the Tashkent earthquakes to the chart of the isoseismal lines of destruction, compiled by V. I. Ulomov (1967), made it possible to determine that the earthquake epicenters are grouped somewhat to the northeast of the central isoseismal line with intensity of eight. If one takes into account that the epicentral zone for the profiles of southwesterly-northeasterly strike have an inclination to the vertical of 15° 9see Figure 107) and if the epicenters are projected onto the earth's surface along lines sloping toward the vertical at an angle of 15° rather than along the vertical, as is usually done, the epicentral zone essentially lies precisely within the isoseismal lines with magnitude of eight.

Comparison of the results of studies of different geophysical methods made it possible not only to show the relationship of different geophysical fields,

APPROVED FOR RELEASE: 2007/02/08: CIA-RDP82-00850R000200030043-9

APPROVED FOR RELEASE: 2007/02/08: CIA-RDP82-00850R000200030043-9

but also to suggest the possible cause of the Tashkent earthquake of 26 April 1966. The earthquake could occur as a result of an overthrust of the northeastern block of crystalline rock onto the southwestern block, which led to a rise of the edge of this block, to a rise of the earth's surface above it and to cracking of the crystalline rock around this block. All this caused a large number of aftershocks.

The North German Depression. The profiles of the earth's crust of the North German Depression were compared to gravimetric (Δg) and magnetometric (ΔZ and ΔT_a) data. Comparison of these data made it possible to reach the following conclusions. The main gravitational effect is created by the surface relief of the basaltic layer and the Mohorovicic layer (MII). A large gravitational maximum corresponds to the rise of these two boundaries within the Eastern Elbe massif (the Prignitskiy block). In some regions the curve Δg is affected by the surface relief of the Pre-Cambrian basement. The presence of effusive-intrusive bodies lying on the Pre-Cambrian basement within the Eastern Elbe massif and in the northeast of the area of study has the main effect on the behavior of the isolines ΔT_a and ΔZ. Their locations correspond to the maximums of ΔT_a and ΔZ. Strongly cut curves ΔT_a and ΔZ are typical for sections divided by a system of regional faults of the crust, determined by composite PS waves.

The Economic Effectiveness of the Studies

The economic effectiveness of the method is determined by comparison of its cost to the cost of other methods, which make it possible to obtain similar results, and also to the speed of the conducted studies and to the possibility of obtaining reliable geological data within short deadlines. The latter permits more active use of the results of studying the regional structure of the crust for orientation of further trends of detailed geophysical studies to search for minerals and establishing deep boreholes.

As was indicated above, the possibilities of the complex method of longitudinal, transverse and composite waves registered by the "Zemlya" device are significantly more complete than the methods based on study of the crust only by longitudinal waves (KMPV and GSZ), since, along with study of the relief of the boundaries and the velocity characteristics of the medium themselves, it permits one to study the physical characteristics of formation of different waves, the nature of the crustal interfaces, to distinguish closely located interfaces in the crust and so on.

At the same time, despite the greater spacing of observations than during KMPV and GSZ, the profiles obtained with the "Zemlya" apparatus as a result of statistical accumulation of material from different sections of the interfaces are not inferior to GSZ and KMPV profiles by their information content. Thus, recording of 15 exchange points at each recording station with spacing of 5 km for deep crustal interfaces approximately corresponds to spacing of 300 m during GSZ operations. Therefore, when evaluating the economic effectiveness of the developed method, it can be compared to KMPV and GSZ methods.

APPROVED FOR RELEASE: 2007/02/08: CIA-RDP82-00850R000200030043-9

APPROVED FOR RELEASE: 2007/02/08: CIA-RDP82-00850R000200030043-9

To do this, let us consider two indices: the length of operations and also the cost of a kilometer of profile and of ony physical observation.

The productivity of operations with the "Zemlya" stations depends on the number of stations used simultaneously and the spacing between them. With average spacing between stations of 6 km and 10-15 stations, the productivity of regional investigations comprises 2 km/day in many regions. During detailed operations where the spacing is reduced to an average of 3 km, productivity comprises 0.8-1 km/day with this same number of stations. During operations with 25 recording stations spaced at 5-6 km, productivity comprises 4-6 km/day (see Table 2). The productivity of GSZ operations with three 48-channel seismic stations operating simultaneously comprises 1-3 km/day [38, 39, 103].

The cost of operations with the "Zemlya" device is determined by the method of conducted studies and depends on the number of stations used simultaneously, the length of observations at a single stopover and the spacing between stations. The cost of the studies also depends on the region and organization of operations. The cost of operations can be estimated by the cost of 1 km of profile with given spacing of studies and by the cost of a single physical observation. During regional studies, the cost of 1 km of profile varies over a wide range in different regions from 192 rubles (spacing of 12 km) to 1,600 rubles (spacing of 5-7 km). In most regions of Central Asia, the cost of 1 km of profile during regional studies comprises 240-500 rubles (with spacing of 5-6 km) and that during detailed operations comprises 460 rubles (with spacing of 3-5 km).

In Siberia the cost of 1 km of profile increases to 1,000 rubles, which is related both to the work conditions (the use of expensive transport) and to the fact that these operations are conducted in small volumes with a small number of stations. These observations are essentially stationary seismological studies.

The total cost of one observation point, including all field and office expenses, varies from 2,500 to 17,700 rubles (see Table 2). It depends on the number of stations used simultaneously and the number of observation points. With a three-fourfold increase of the number of stations, which is equivalent to an increase of the total number of observation points, the cost of a single observation decreases by more than a factor of five.

The Direction of Further Studies with the "Zemlya" Device

The method of complex seismic study of the structure of the earth's crust and of the upper mantle, proposed and developed on its basis, is still rather young. Further improvement of the method presumes the solution of both apparatus and methodical problems.

The necessary apparatus developments may include creation of cold-resistant and marine (bottom) versions of the "Zemlya" stations which permit continuous

APPROVED FOR RELEASE: 2007/02/08: CIA-RDP82-00850R000200030043-9

APPROVED FOR RELEASE: 2007/02/08: CIA-RDP82-00850R000200030043-9

operation in the regions of Siberia and on the shelf zones of the seas and oceans. To do this, a system of portable of shelf-installed seismic detectors with natural frequency of 1 Hz, development and introduction of a unified time service which uses quartz clocks and a radio channel, development of power supply sources using thermionic generators or gas electric power plants for the use of field apparatus in difficultly accessible regions and under low temperature conditions, development of special devices which simultaneously permit receipt of signals in the form of analog recordings and in digital code and so on are necessary.

Further development of the methods of interpretation of various wavefields for complexly structured media is necessary in the methodical plan. They include the use of existing processing centers and programs for determination, correlation and separation of PS waves into groups, study of the kinematic and dynamic characteristics of lateral PS waves (transient reflected and transient diffracted), development of methods of interpreting them to determine the propagation velocities of P and S waves above the reflection and diffraction zones, development of methods of interpreting transient PS waves formed on the sloping interfaces in multilayered media, study of the effect of sloping boundaries on transient PS waves and development of methods of taking into account the distortions of the dynamics and kinematics of these waves by sloping boundaries and further development of methods of determination and stratification of the interfaces by PS waves.

APPROVED FOR RELEASE: 2007/02/08: CIA-RDP82-00850R000200030043-9

APPROVED FOR RELEASE: 2007/02/08: CIA-RDP82-00850R000200030043-9

CONCLUSIONS

Moscow SEYSMICHESKIYE ISSLEDOVANIYA S APPARATUROY "ZEMLYA" in Russian 1977 signed to press 31 Jan 1977 pp 241-243

[Conclusions from the book "Seysmicheskiye issledovaniya s apparaturoy 'Zemlya'" by I. V. Pomerantseva and A. N. Mozzhenko, Izdatel'stvo Nedra, 1,400 copies, 256 pages]

[Text] The complex seismic method of deep study of the structure of the earth's crust and upper mantle using longitudinal (P), transverse (S) and composite (PS) waves excited by earthquakes and explosions and registered by the "Zemlya" device at epicentral distances of 0-160° made it possible to solve the following problems: a) to determine the three-dimensional behavior of crustal interfaces, b) to determine the velocity characteristic of the layers of the crust by P and S waves and c) to study the seismicity of the crust in different regions. Longitudinal P and transverse S waves were used to determine the velocity characteristic of the medium and its seismicity and transient composite PS waves on recordings mainly from remote earthquakes were used to construct the relief of the crustal interfaces. Selection of PS waves to study the relief of the crustal interfaces was determined by the method of their excitation, which does not require development of special energy sources and by the approach of the rays of PS waves to the observation point from directions close to the vertical. The latter permits one to increase the resolution and accuracy of the results compared to methods of explosive seismology. Registration of PS waves from many earthquakes made it possible to use different methods of accumulating experimental data and to carry out statistical processing of them.

The "Zemlya" apparatus complex included a series of recording stations with direct magnetic recording and oscillographic re-recording of signals. The principle of frequency transformation was used during reproduction. The dynamic range of the recording and reproduction channel comprised 40-70 dB and the frequency range comprised 0.5-15 Hz. The information re-recorded from magnetic tapes of the "Zemlya" device to magnetic tapes of the SS-24-61M station or obtained by ordinary digital MOV seismic prospecting stations can be processed on analog or digital computers without any additional input devices.

APPROVED FOR RELEASE: 2007/02/08: CIA-RDP82-00850R000200030043-9

APPROVED FOR RELEASE: 2007/02/08: CIA-RDP82-00850R000200030043-9

The method of field investigations included registration of earthquakes and explosions and combined all the advantages and characteristics of seismic and seismological types of studies. The length of observations at one stop-over comprised 15-25 days, the spacing between recording stations was 5-7 km during regional studies and 0.5-3 km during detailed studies and the number of stations operating simultaneously was 10-25. The number of recordings registered during 15 days in the different regions varied: from 10 to 40 for remote earthquakes, from 2 to 85 for near and local earthquakes, from 1 to 30 for incidental explosions and from 3 to 5 for special explosions.

The existence of intensive composite PS waves on the horizontal components of recordings of remote earthquakes was proved on the basis of theoretical calculation and analysis of extensive experimental material. It is shown that PS waves may be transient and lateral by their nature: transient diffracted and transient reflected. Equations of the surface hodographs of groups of PS waves different in nature were derived and equations of the displacement vectors and azimuths of the rays of transient P and PS waves are presented. Based on theoretical calculations for the derived functions, the criteria for determination of PS waves on recordings from earthquakes and separation of them into groups were refined.

The kinematic (Δt, v_k, Δt_{PS-P}) and the dynamic (frequency spectrum, intensity, form of recording and polarization) have the characteristics of P, S and PS waves on recordings from explosions, local, near and remote earthquakes (approximately 3,000) registered in regions of the Southeastern Russian Series, the Pre-Caspian, Azov-Kuban' and North German Depressions and Tashkent were studied.

The main propositions of the method of interpreting longitudinal, transverse and composite waves for platform ($\varphi < 10°$) and mountainous ($\varphi > 10°$) regions were developed. Criteria for correlation of P, S and PS waves were formulated. Calculating formulas are presented to determine the depths of interfaces, seismic drifts, angles of inclination of crustal boundaries, epicentral distances, approach azimuths, angles of emergence of seismic radiation, average and stratal velocities of P and S waves, coordinates of the foci of local earthquakes and so on. The resolution and accuracy of the composite wave method used to construct the relief of interfaces of the earth's crust and longitudinal and transverse wave methods used to determine the velocity characteristics of the crust and its seismicity were determined.

The accuracy of constructing the crustal interfaces by PS waves is determined by the agreement of the real media to the model approximating them and to the accuracy of determining the velocity parameters of the medium. The error of constructing the boundaries comprises $\pm$ 1-5 percent with dispersion of $\Delta t_{PS-P} = \pm$ (0.1-0.2) second, the number of PS waves of 6-7, the probability $P = 0.9-0.95$ and sampling values of $\Delta t_{PS-P} = 5-1.5$ seconds. The error of determining the coordinates of local earthquake epicenters ($\Delta \approx$ 0-25 km) with eight stations or more comprises $\pm$ 100-200 m, while the error of determining the depths of foci is 0.5-1 km. The error of determining the velocity characteristics of the medium by P and S waves varies from 3 to 15 percent as a function of the observation systems.

APPROVED FOR RELEASE: 2007/02/08: CIA-RDP82-00850R000200030043-9

APPROVED FOR RELEASE: 2007/02/08: CIA-RDP82-00850R000200030043-9

The possibility of using the method to study the structure of the earth's crust, for detailed determination of the location of foci and to study the velocity characteristic of the crust outside the focal zone and within it is shown as a result of testing the developed method in aseismic (Southeastern Russian Series and North German and Pre-Caspian Depressions) and seismically active (Tashkent and Azov-Kuban' Depression) regions.

The following main data on their structure and the location of foci of modern earthquakes were found for all regions.

The structure of the earth's crust from the surface of the Paleozoic basement (vP_{pl} = 5.8-6 km/s) to the Mohorovicic Discontinuity (vP_{pl} = 8-82. km/s) and the boundaries in the upper mantle was determined under Tashkent. The location of the foci of aftershocks of the Tashkent earthquake of 26 April 1966 was determined. It is shown that the foci are located in the weakest part of the earth's crust in the zone where three of its blocks join: the Chinabad, Chirchik and Tashkent. It was determined that the focal zone is characterized by a small volume and abnormally reduced values of stratal velocities of longitudinal waves and of coefficient K_{pl}.

All the main interfaces of the earth's crust from the surface of the Variscian basement to the Mohorovicic Discontinuity were determined and constructed within the North German Depression. Charts of the stratal velocities of P waves and coefficient K_{pl} along the upper part of the crystalline mass of the crust were compiled. The three-level structure of the upper part of the crystalline mass of the crust was determined. The boundaries of the Variscian (vP_{pl} = 5.3-5.4 km/s), Caledonian (vP_{pl} = 5.7-5.8 km/s) and Pre-Cambrian (vP_{pl} = 6-6.2 km/s) phases of folding and the deeper interfaces of the earth's crust, including the Mohorovicic Discontinuity, were traced and constructed. It is shown that the Eastern Elbe gravitational and magnetic maximums are determined by a rise of the surfaces of the basaltic and subcrustal layers and by the presence of effusive formations which fill the trough along the Pre-Cambrian.

The interfaces of the earth's crust from the surface of the transition mass (vP_{pl} = 5.6-5.8 km/s) to the Mohorovicic Discontinuity (vP_{pl} = 8-8.2 km/s) and also a number of boundaries in the upper mantle to a depth of 130 km were determined and traced in the regions of the Southeastern Russian Series ($H \approx 600$ km) and the Pre-Caspian ($H \approx 400$ km) and Azov-Kuban' ($H \approx 250$ km) depressions. The presence of weak current tectonic activity of the Southeastern Russian Series, the Urals folded system and the zone where the Southeastern Russian Series and the Pre-Caspian and Azov-Kuban' depressions join was determined. The large Western Kuban' trough with amplitude of approximately 8 km, thickness of the sedimentary layer of 20 km and thickness of the crystalline crust of 17 km was determined within the Azov-Kuban' Depression along the Paleozoic surface.

The geological and economic effectiveness of the developed "Zemlya" method was evaluated. The cost of the studies, due to using the natural energy of

APPROVED FOR RELEASE: 2007/02/08: CIA-RDP82-00850R000200030043-9

APPROVED FOR RELEASE: 2007/02/08: CIA-RDP82-00850R000200030043-9

earthquakes, is considerably lower than the cost of studies by KMPV and GSZ methods with the same and with higher geological effectiveness in complex regions. This is explained by the fact that the "Zemlya" method essentially combines simplified version of KMPV and GSZ methods (by complete systems, but with greater distances between observation points) with seismological investigations.

Further development of the complex "Zemlya" seismic method should be directed along the path of developing a new device for operations at sea and in Siberia and on improving the method of interpreting wave fields and for complexly structured media.

BIBLIOGRAPHY

1. Averbukh, A. G., L, M. Gorbach and E. P. Sumerina, "The Physical Nature of Waves Registered During the First Arrivals During KMPV Observations," PRIKLADNAYA GEOFIZIKA, No. 36, Moscow, Gostoptekhizdat, 1963.

2. Alekseyev, A. S., "Some Inverse Problems of Wave Propagation Theory," IZV. AN SSSR, SER. GEOFIZ., No. 11, 1962.

3. Alekseyev, A. S., I. L. Nersesov and G. M. Tsibul'chik, "A Method of Investigating the Earth's Crust from Recordings of Composite Waves from Remote Earthquakes," IZV. AN SSSR, SER. FIZIKA ZEMLI, No. 8, 1972.

4. Alekseyev, A. S. and G. M. Tsibul'chik, "Using Inverse Filtration During Summation of Seismograms from Remote Earthquakes," GEOLOGIYA I GEOFIZIKA, No. 3, 1971.

5. Anan'in, I. V., "The Seismic Effect of Near Earthquakes in the Eastern Caucasus," in "Voprosy inzhenernoy seysmologii" [Problems of Engineering Seismology], No. 9, Moscow, IZD-VO AN SSSR, 1963.

6. Andreyev, S. S., "Study of the Deep Structure of the Earth's Crust by Means of Composite PS Waves Registered During Earthquakes," IZV. AN SSSR, SER. GEOFIZ., No. 1, 1957.

7. Andreyev, S. S. and N. V. Shebalin, "Using Short-Period Seismographs to Determine Composite Waves on Remote Earthquake Recordings," IZV. AN SSSR, SER. GEOFIZ., No. 7, 1957.

8. Afanas'yeva, N. A. and N. K. Bulin, "Determining the Velocity Profile of the Earth's Crust and Upper Mantle by the Angle of Emergence of Longitudinal Seismic Waves," IZV. AN SSSR, SER. FIZIKA ZEMLI, No. 12, 1969.

9. Akhmerov, R. Z., A. M. Nasyrov and V. A. Pak, "Using the 'Zemlya' Device to Study the Structure of the Earth's Crust," in "Zemnaya kora Uzbekistana" [The Earth's Crust of Uzbekistan], Tashkent, FAN UzSSR, 1974.

APPROVED FOR RELEASE: 2007/02/08: CIA-RDP82-00850R000200030043-9

APPROVED FOR RELEASE: 2007/02/08: CIA-RDP82-00850R000200030043-9

10. Belonosova, A. V., A. S. Alekseyev and S. S. Tadzhimukhamedova, "Nekotoryye metody i algoritmy interpretatsii geofizicheskikh dannykh" [Some Methods and Algorithms for Interpretation of Geophysical Data], Moscow, Nauka, 1967.

11. Belotelov, V. L. and N. V. Kondorskaya, "The Spectra of Composite Waves from Kamchatka Earthquakes," IZV. AN SSSR, SER. GEOFIZ., No. 4, 1964.

12. Belyayevskiy, N. A. and V. Z. Ryaboy, "The Propagation Velocities of Longitudinal Seismic Waves Along the Mohorovicic Discontinuity for the USSR," DOKL. AN SSSR, vol. 186, No. 2, 1969.

13. Belyayevskiy, N. A., "Zemnaya kora v predelakh territorii SSSR" [The Earth's Crust Within the USSR], Moscow, Nedra, 1974.

14. Berzon, I. S., "Vysokochastotnaya seysmika" [High-Frequency Seismic Studies], Moscow, IZD-VO AN SSSR, 1950.

15. Bereza, G. V. and V. Z. Ryaboy, "Measuring the Phase and Absolute Amplitude-Frequency Characteristics of Seismic Detectors," RAZVEDOCHNAYA GEOFIZIKA, No. 61, Moscow, Nedra, 1974.

16. Borisov, A. A., "Glubinnaya struktura territorii SSSR po geofizicheskim dannym" [The Deep Structure of the USSR from Geophysical Data], Moscow, Nedra, 1967.

17. Bronshteyn, I. K. and K. A. Semendyayev, "Spravochnik po matematike dlya inzhenerov i uchashchikhsya vuzov" [Mathematical Handbook for Engineers and Students of Vuzes], Moscow, Nauka, 1964.

18. Bulin, N. K., "Determining the Depth of the Folded Basement by Means of Transient Composite PS Waves Registered During Earthquakes," IZV. AN SSR, SER. GEOFIZ., No. 6, 1960.

19. Bulin, N. K. and Yu. I. Sytin, "The Experience of Using Seismological Investigations to Study the Deep Structure of the Earth's Crust in Turkmeniya," TRUDY VSEGEI, NOVAYA SERIYA, No. 42, Moscow, Gostoptekhizdat, 1960.

20. Butovskaya, Ye. M., "The PS Wave During Near Earthquakes," TRUDY GEOFIZ. IN-TA AN SSSR, No. 16 (143), 1952.

21. Butovskaya, Ye. M. and T. M. Gol'tseva, "The Deep Structure of the Earth's Crust in the Pre-Tashkent Region," in "Tashkentskoye zemletryaseniye 26 aprelya 1966 g." [The Tashkent Earthquake of 26 April 1966], Tashkent, FAN UzSSR, 1971.

22. Butovskaya, Ye. M., "Method and Results of Constructing the Velocity Profiles of Sequential Approximations on the Example of Some Regions of Uzbekistan," IZV. AN SSSR, SER. FIZIKA ZEMLI, No. 8, 1968.

APPROVED FOR RELEASE: 2007/02/08: CIA-RDP82-00850R000200030043-9

APPROVED FOR RELEASE: 2007/02/08: CIA-RDP82-00850R000200030043-9

23. Vol'vovskiy, B. S., I. S. Vol'vovskiy, A. V. Yegorkin et al, "The Possibilities of Using Large Explosions for Deep Seismic Studies," in "Geofizicheskiye polya i seysmichnost'" [Geophysical Fields and Seismicity], Moscow, Nauka, 1975.

24. Yegorkina, G. V., I. V. Garetovskaya, I. A. Sokolova et al, "The Possibilities of Using 'Zemlya' Seismic Stations During Study of Seismically Hazardous Zones in Armenia," in "Geofizicheskiye polya i seysmichnost'," Moscow, Nauka, 1975.

25. Vol'vodskiy, I. S., "Seysmicheskiye issledovaniya zemnoy kory v SSSR" [Seismic Studies of the Earth's Crust in the USSR], Moscow, Nedra, 1973.

26. "Voprosy dinamicheskoy teorii rasprostraneniya seysmicheskikh voln" [Problems of the Dynamic Theory of Seismic Wave Propagation], Vol. 1, Moscow, Gostoptekhizdat, 1957.

27. "Voprosy dinamicheskoy teorii rasprostraneniya seysmicheskikh voln," Vol. 2, Leningrad, IZD. LGU, 1959.

28. "Voprosy dinamicheskoy teorii rasprostraneniya seysmicheskikh voln," Vol. 3, Leningrad, IZD. LUG, 1959.

29. Gal'perin, Ye. I., "Vertikal'noye seysmicheskoye profilirovaniye" [Vertical Seismic Profiling], Moscow, Nedra, 1971.

30. Gal'perin, Ye. I., "Polar-Position Correlation of Seismic Waves," DOKL. AN SSSR, Vol. 222, No. 2, 1975.

31. Gal'perin, Ye. I., I. L. Nersesov and R. M. Gal'perina, "The Problem of the Effect of the Daytime Surface Relief on the Surface of Seismograms," DOKL. AN SSSR, Vol. 217, No. 3, 1974.

32. Gal'perina, R. M., "The Problem of the Physical Bases and Prospecting Capabilities of the Composite Wave Method from Data of Vertical Seismic Profiling (VSP)," DOKL. AN SSSR, Vol. 182, No. 2, 1969.

33. Gamburtsev, G. A. and P. S. Veytsman, "Compilation of Deep Seismic Sounding Data on the Structure of the Earth's Crust in the Region of the Northern Tyan'-Shan' to Seismological and Gravimetric Data," IZV. AN SSSR, SER. GEOFIZ., No. 9, 1956.

34. Gamburtsev, G. A., "Osnovy seysmorazvedki" [Fundamentals of Seismic Prospecting], Moscow, Gostoptekhizdat, 1959.

35. Gamburtseva, N. G., L. P. Vinnik and A. M. Polikarpova, "A Method of Distinguishing Composite PS Waves from Recordings of Remote Earthquakes," GEOLGIYA I GEOFIZIKA, No. 9, 1970.

APPROVED FOR RELEASE: 2007/02/08: CIA-RDP82-00850R000200030043-9

APPROVED FOR RELEASE: 2007/02/08: CIA-RDP82-00850R000200030043-9

36. Garetovskaya, I. V., "Study of the Deep Structure of Armenia from Near Earthquakes Registered by 'Zemlya' Stations," in "Geofizicheskiye polya i seysmichnost'," Moscow, Nauka, 1975.

37. Geyko, V. S., "Determining the Average and Effective Velocity by the Hodograph of the Refracted Wave with Arbitrary Law of a Gain of Velocity with Depth," IZV. AN SSSR, SER. FIZIKA ZEMLI, No. 3, 1970.

38. "Glubinnoye seysmicheskoye zondirovaniye zemnoy kory v SSSR" [Deep Seismic Sounding of the Earth's Crust in the USSR], Leningrad, Gostoptekhizdat, 1962.

39. "Glubinnoye seysmicheskoye zondirovaniye. Materialy Vtorogo Vsecoyuznogo soveshchaniya po izucheniyu kory i verkhney mantii Zemli metodami seysmologii vzryvov" [Deep Seismic Sounding. Materials of the Second All-Union Conference on Study of the Earth's Crust and Upper Mantle by Seismic Explosion Methods], Alma-Ata, Nauka, 1973.

40. Pevzner, L. A., K. A. Popov, I. K. Pushkarev et al, "Geophysical Studies with Seismic Microregionalization of the City of Alma-Ata," in "Geofizicheskiye polya i seysmichnost'," Moscow, Nauka, 1975.

41. Godin, Yu. N., "Complex Regional Geophysical Studies of the Southeastern Russian Series of Formations," GEOLOGIYA NEFTI, No. 5, 1958.

42. Godin, Yu. N., B. S. Vol'vovskiy and I. S. Vol'vovskiy, "Seismic Studies of the Earth's Crust in the Region of the Fergana Intermountain Area," DOKL. AN SSSR, Vol. 133, No. 6, 1960.

43. Golitsyn, B. B., "Izbrannye trudy. Seysmologiya" [Selected Works. Seismology], Moscow, IZD-VO AN SSSR, 1960.

44. Gol'tsman, F. M. and V. N. Troyan, "Optimum Algorithms for Separation of Interfering Seismic Waves," IZV. AN SSSR, SER. FIZIKA ZEMLI, No. 8, 1967.

45. Gurvich, I. I., "Seysmicheskaya razvedka" [Seismic Prospecting], Second edition, revised and supplemented, Moscow, Nedra, 1970.

46. Gutenberg, B., "Fizika zemnykh nedr" [Physics of the Earth's Interior], Moscow, IL 1963.

47. Demenitskaya, R. M., "Kora i mantiya Zemli" [The Earth's Crust and Mantle], Moscow, Nedra, 1967.

48. Jeffries, T., "Zemlya, yeye proiskhozhdeniye, istoriya i stroyeniye" [The Earth, Its Origin, History and Structure], Moscow, IL, 1960.

APPROVED FOR RELEASE: 2007/02/08: CIA-RDP82-00850R000200030043-9

APPROVED FOR RELEASE: 2007/02/08: CIA-RDP82-00850R000200030043-9

49. Dikgof, Yu. A., "Quantitative Interpretation of the Hodographs of Composite Waves Resulting During Earthquakes or Remote Explosions," in "Apparatura, metodika i rezul'taty interpretatsii geofizicheskikh nablyudeniy" [Apparatus, Method and Results of Interpreting Geophysical Observations], No. 4, Kazan', IZD. KAZANSKOGO UN-TA, 1970.

50. Dimakov, A. I. and A. I. Tamarov, "Glubinnaya struktura Mangyshlaka" [The Deep Structure of Mangyshlak], Leningrad, Nedra, 1973.

51. Druzhinin, V. S., V. M. Rybalka and D. A. Belikova, "The Reflecting Properties of the M Discontinuity on the Eastern Edge of the Russian Series of Formations," IZV. AN SSSR, SER. FIZIKA ZEMLI, No. 8, 1970.

52. Yegorkina, G. V., "Study of the Anisotropy of the Earth's Crust from Recordings of Composite Seismic Waves," IZV. AN SSSR, SER. FIZIKA ZEMLI, No. 9, 1969.

53. Yegorkina, G., "Some Results of Wave Polarization," in "Teoreticheskoye i eksperimental'noye issledovaniye obmennykh voln zemletryasenniy" [Theoretical and Experimental Study of Composite Waves from Earthquakes], Moscow, IZD. VNIIGeofizika, 1973.

54. Yegorkina, G., "The Nature of Phase Shifts During Registration of Transient Composite PS Waves," PRIKLADNAYA GEOFIZIKA, No. 70, 1973.

55. Yepinat'yeva, A. M., "Reflected Waves Occurring at Angles of Incidence Greater than the Maximum," IZV. AN SSSR, SER. GEOFIZ., No. 6, 1957.

56. Yepinat'yeva, A. M., "Study of Longitudinal Seismic Waves Propagated in Some Real Layered Media," TRUDY IN-TA FIZIKI ZEMLI, No. 14 (181), 1960.

57. Yepinat'yeva, A. I., "Fizicheskiye osnovy seysmicheskikh metodov razvedki" [Physical Fundamentals of Seismic Methods of Prospecting], Moscow, IZD. MGU, 1970.

58. Zhigal'tsev, A. A., "Dynamic Characteristics of Composite Waves," in "Fizika zemletryaseniy i seysmika vzryvov" [The Physics of Earthquakes and the Seismic Nature of Explosions], Moscow IZD-VO AN SSSR, 1962.

59. Pomerantseva, I. V., G. V. Yegorkina, I. A. Sokolova et al, "Recordings of Local Earthquakes and Explosions Obtained During Operations with 'Zemlya' Stations in Regions with Different Geological Structure," PRIKLADNAYA GEOFIZIKA, No. 54, 1969.

60. Zverev, S. M., "GSZ at Sea," in "Materialy mezhdunarodnogo soveshchaniya ekspertov po vzryvnoy seysmologii" [Materials of an International Conference of Experts on Explosion Seismology], Kiev, Naukova Dumka, 1969.

APPROVED FOR RELEASE: 2007/02/08: CIA-RDP82-00850R000200030043-9

APPROVED FOR RELEASE: 2007/02/08: CIA-RDP82-00850R000200030043-9

61. Ipatova, R. S. and L. N. Rykunov, "Modelling the Effect of Unevennesses of the Earth's Surface on Seismograms," IZV. AN SSSR, SER. FIZIKA ZEMLI, No. 11, 1974.

62. Klushin, I. G., "The Nature of the Series of Seismic Boundaries in the Lower Zone of the Lithosphere," GEOFIZICHESKIY SBORNIK, No. 44, 1971.

63. Knote, Kh., G. Genshel' and V. Lange, "Brief Survey of the Status of Deep Seismic Operations in the GDR," in "Geofizicheskiye issledovaniya stroyeniya zemnoy kory yugo-vostochnoy Yevropy" [Geophysical Studies of the Structure of the Earth's Crust of Southeastern Europe], Moscow, Nauka, 1967.

64. Kogan, S. D., "The Dynamic Parameters of Deep Earthquake Foci," TRUDY GEOFIZ. IN-TA, No. 30 (157), 1955.

65. Kondorskaya, N. V., "Determination of the sP Wave During Shallow Earthquakes and Its Use to Determine the Depth of the Focus," TRUDY GEOFIZ. IN-TA, No. 36 (163), 1956.

66. Kondorskaya, N. V. and N. S. Landyreva, "Characteristics of the Seismicity of Kamchatskaya Oblast from Observation Data of the Network of Stationary Stations," PRIKLADNAYA GEOFIZIKA, No. 10, 1962.

67. Gamburtsev, G. A., Yu. V. Riznichenko, I. S. Berzon et al, "Korrelyatsionnyy metod prelomlennykh voln" [The Correlation Method of Refracted Waves], Moscow, IZD-VO AN SSSR, 1952.

68. Kosminskaya, I. P and R. M. Krakshina, "Subcritical Reflections from the Mohorovicic Discontinuity," IZV. AN SSSR, SER. GEOFIZ., No. 6, 1961.

69. KOSMINSKAYA, I. P., "Metod glubinnogo seysmicheskogo zondirovanniya zemnoy kory i verkhov mantii" [The Method of Deep Seismic Sounding of the Earth's Crust and Upper Mantle], Moscow, Nauka, 1968.

70. Kuzina, D. A., "Computer Processing of Recordings of Local Earthquakes Registered by 'Zemlya' Stations," PRIKLADNAYA GEOFIZIKA, No. 62, 1971.

71. Linnik, Yu. V., "Metod naimen'shikh kvadratov i osnovy teorii obrabotki nablyudeniy" [The Least Squares Method and Fundamentals of the Theory of Processing Observations], Moscow, Fizmatgiz, 1962.

72. Lin'kova, T. M., "Transient Longitudinal and Composite Waves Formed on the Thin Layer with Reduced or Increased Velocity," in "Teoreticheskoye i eksperimental'noye issledovaniye obmennykh voln zemletryaseniy," Moscow, IZD. VNIIGeofizika, 1973.

73. Lin'kova, T. M. and B. Ye. Shcherbakova, "Transient Longitudinal and Composite Waves Formed on a Thin Inhomogeneous Layer," in "Teoreticheskoye i eksperimental'noye issledovaniye obmennykh voln zemletryaseniy," Moscow, IZD. VNIIGeofizika, 1973.

APPROVED FOR RELEASE: 2007/02/08: CIA-RDP82-00850R000200030043-9

APPROVED FOR RELEASE: 2007/02/08: CIA-RDP82-00850R000200030043-9

74. Litvinenko, I. V., S. A. Ankudinov and L. N. Platonenkova, "The Structure of the Earth's Crust of the Eastern Part of the Baltic Shield and the Barents Sea from GSZ Data," in "Trudy 10 General'noy assamblei Yevropeyskoy seysmologicheskoy komissii" [Proceedings of the 10th General Assembly of the European Seismological Committee], Vol. 1, Moscow, IZD. VINITI, 1970.

75. Lossovskiy, Ye. K., "Summarnyye mnogokratnyye volny i problema nadezhnosti seysmologicheskikh postroyeniy v GSZ" [Multiple Summary Waves and the Problem of the Reliability of Seismological Constructions in GSZ], Kiev, Naukova Dumka, 1978.

76. Lukk, A. A., I. L. Nersesov and L. S. Chepkunas, "A Method of Determining the Layer of Reduced Velocity in the Earth's Crust and Mantle," IZV. AN SSSR, SER. GEOFIZ., No. 2, 1970.

77. Lykov, V. I. and N. P. Smirnova, "The Ratio of the Velocities of Leading Waves from the Mohorovicic Discontinuity," IZV. AN TURKMEN SSR, SER. FIZ.-TEKHN., KHIM., I GEOL. NAUK, No. 3, 1966.

78. Lykov, V. I., V. A. Bezgodkov and V. S. Orlov, "Method of Interpreting the Materials of Profile Seismolgical Observations with 'Zemlya' Stations in Southern Turkmenia," in "Geologiya i poleznyye iskopayemyy e Turkmenii" [Geology and the Minerals of Turkmenia], No. 1, Ashkhabad, NTGO Turkmen. SSR, 1968.

79. Matveyeva, N. N., "Materialy kolichestvennogo izucheniya dinamiki seysmicheskikh voln" [Materials of Quantitative Study of the Dynamics of Seismic Waves], Vol. 1, Leningrad, IZD.-VO LGU, 1957.

80. Smirnova, N. S., Z. M. Kustova, M. V. Vasil'yeva et al, "Materialy kolichestvennogo izucheniya dinamiki seysmicheskikh voln" [Materials of Quantitative Study of the Dynamics of Seismic Waves], Vol. 2, Leningrad, IZD.-VO LGU, 1957.

81. Burova, A. V., Yu. A. Voronin, B. Ya. Gel'chinskiy and A. V. Manukhov, "Materialy kolichestvennogo izucheniya dinamiki seysmicheskikh voln" [Materials of Quantitative Study of the Dynamics of Seismic Waves], Vol. 3, Leningrad, IZD.-VO LGU, 1958.

82. Mishin, S. V. and N. M. Dareshkina, "Determining the Composite Components on Recordings of Remote Earthquakes," IZV. AN SSSR, SER. FIZIKA ZEMLI, No. 9, 1966.

83. Mikhota, G. G., "The Spectra and Intensity of Deep Waves," in "Materialy Mezhdunarodnogo soveshchaniya ek spertov po vzryvnoy seysmologii, Kiev, Naukova Dumka, 1969.

84. Mozzhenko, A. N., "Amplifiers for KMPV and GSZ," RAZVEDOCHNAYA I PROMYSLOVAYA GEOFIZIKA, No. 18, 1957.

APPROVED FOR RELEASE: 2007/02/08: CIA-RDP82-00850R000200030043-9

APPROVED FOR RELEASE: 2007/02/08: CIA-RDP82-00850R000200030043-9

85. Mozzhenko, A. N., "A Magnetic Recording Device for Registration of Earthquakes and Remote Explosions," IZV. AN TURKM. SSR, SER. FIZ.-TEKHN., KHIM. I GEOL. NAUK, No. 1, 1961.

86. Monastyrev, V. K. and Yu. V. Oznobikhin, "Kinematic Criteria for Determination of Multiple Waves from Earthquakes," in "Metodika seysmorazvedki v Zapadnoy Sibiri" [Method of Seismic Prospecting in Western Siberia], Tyumen', 1972.

87. Shtutin, I. V., K. A. Savinskiy, O. F. Berezhnova and I. V. Lobachevskiy, "Some Results of Studying the Deep Structure of the Northern Irkutsk Ampitheater with 'Zemlya' Stations," GEOLOGIYA I GEOFIZIKA, No. 10, 1970.

88. Nersesov, I. L. and T. G. Rautian, "The Kinematics and Dynamics of Seismic Waves at Distances Up to 3,500 km from the Epicenter," in "Eksperimental'naya seysmika" [Experimental Seismic Studies], Moscow, Nauka, 1964.

89. Oblogina, T. I., "The Dynamic Characteristics of Elastic Diffracted Waves," IZV. AN SSSR, SER. GEOFIZ., No. 4, 1956.

90. Obolentseva, I. R. and L. G. Dantsig, "Polarization of Transient Longitudinal and Composite Waves in the Case of Sloping Interfaces," GEOLOGIYA I GEOFIZIKA, No. 4, 1971.

91. Dantsig, L. G., A. A. Dergachev, V. V. Zhadin and V. A. Senyukov, "The Possibility of Separating Composite Waves on Recordings from Remote Earthquakes," in "Metodika seysmicheskakh issledovaniy" [Method of Seismic Studies], Moscow, Nauka, 1969.

92. Oznobikhin, Yu. V., "The Polarity of Arrivals of Composite and Multiple Waves from Earthquakes and Method of Calculating Their Intensities for Some Models of Media," in "Metodika seysmorazvedki v Zapadnoy Sibiri," Tyumen', 1972.

93. Oznobikhin, Yu. V., "Some Dynamic Characteristics of Composite and Multiple Waves from Remote Earthquakes by Calculations on a Model of the Profile of the Western Siberian Platform," in "Metodika seysmorazvedki v Zapadnoy Sibiri," Tyumen', 1972.

94. Oznobikhin, Yu. V., I. V. Rezvov and V. F. Chekalev, "Some Results of Using the Method of Composite Waves from Earthquakes in the Northern Part of Western Siberia," in "Materialy po tektonike glubokikh gorizontov Zapadno-Sibirskoy plity" [Materials on the Tectonics of the Deep Levels of the Western Siberian Platform], Tyumen', 1972.

95. Gal'perin, Ye. I., G. N. Aksenovich, R. M. Gal'perina and M. S. Erenburg, "The Experience of Separating Transient Composite Waves by the Polar Correlation Method (On an Example of Observations with the 'Zemlya' Stations)," IZV. AN SSSR, SER. FIZIKA ZEMLI, No. 7, 1975.

APPROVED FOR RELEASE: 2007/02/08: CIA-RDP82-00850R000200030043-9

APPROVED FOR RELEASE: 2007/02/08: CIA-RDP82-00850R000200030043-9

96. Orlov, V. S., "Identification of P and PS Waves During Operations by the Method of Composite Waves from Earthquakes with the 'Zemlya' Stations," IZV. AN TUKRM. SSR, SER. FIZ.-TEKHN., KHIM. I GEOL. NAUK, No. 6, 1971.

97. Pavlenkova, N. I., "Volnovyye polya i model' zemnoy kory" [Wave Fields and the Model of the Earth's Crust], Kiev, Naukova Dumka, 1973.

98. Pankratov, A. P., A. V. Suvilova and Zh. N. Firsova, "Glubinnoye stroyeniye Severo-Kaspiyskoy sineklizy i struktura zony Khobdinskogo maksimuma. Tezisy dokladov soveshchaniya po problemam tektoniki" [The Deep Structure of the North Caspian Syneclise and the Structure of the Zone of the Khobda Maximum. Report Topics of A Conference on Problems of Tectonics], Moscow, IZD-VO AN SSSR, 1962.

99. Parfent'yev, A. I., "Magnitnaya zapis' v kinotekhnike" [Magnetic Recording in Movie Equipment], Moscow, IZD-VO Iskusstvo, 1957.

100. Polshkov, M. K., "Teoriya analogovoy i tsifrovoy seysmorazvedochnoy apparatury" [The Theory of Analog and Digital Seismic Prospecting Apparatus], Moscow, Nedra, 1973.

101. Polshkov, M. K., M. K. Bulin and B. Ye. Shcherbakova, "Using Composite Waves from Earthquakes to Study the Earth's Crust and Upper Mantle," PRIKLADNAYA GEOFIZIKA, No. 68, 1972.

102. Pomerantseva, I. V., "The Results of Operations to Study the Structure of the Crystalline Mass of the Earth's Crust in Some Regions of the Southeastern Russian Series," PRIKLADNAYA GEOFIZIKA, No. 31, 1961.

103. Pomerantseva, I. V., "The Nature of Waves Related to the Surface of the Crystalline Basement," PRIKLADNAYA GEOFIZIKA, No. 34, 1962.

104. Pomerantseva, I. V., "The Velocity Characteristic, Structure and Possible Composition of the Crystalline Mass of the Earth's Crust," PRIKLADNAYA GEOFIZIKA, No. 38, 1964.

105. Pomerantseva, I. V., "The Nature of Waves Related to the Intermediate Interfaces in the Crystalline Mass of the Earth's Crust and the Deep Structure of the Southeastern Russian Series," PRIKLADNAYA GEOFIZIKA, No. 41, 1965.

106. Pomerantseva, I. V., "Geological Interpretation of the Deep Seismic Profiles of the Crust and Upper Mantle," in "Glubinnoye stroyeniye Urala" [The Deep Structure of the Urals], Moscow, Nauka, 1968.

107. Pomerantseva, I. V., "Method of Interpreting Transient Composite Waves Recorded by the 'Zemlya' Stations," PRIKLADNAYA GEOFIZIKA, No. 53, 1968.

APPROVED FOR RELEASE: 2007/02/08: CIA-RDP82-00850R000200030043-9

APPROVED FOR RELEASE: 2007/02/08: CIA-RDP82-00850R000200030043-9

108. Pomerantseva, I. V. and M. V. Margot'yeva, "K voprosu o prirode voln, registriruemykh pri GSZ" [The Nature of Waves Recorded During GSZ], Moscow, IZD. VNIIGeofizika, 1959.

109. Pomerantseva, I. V. and L. S. Shumilina, "The Characteristics of the Deep Structure of the Earth's Crust in the Region of Tashkent," in "Problemy stroyeniya zemnoy kory i verkhney mantii," Moscow, Nauka, 1970.

110. Pomerantseva, I. V., "Determination and Correlation of PS Waves Recorded by 'Zemlya' Stations," in "Teoreticheskiye i eksperimental'nyye issledovaniya obmennykh voln zemletryaseniy," Moscow, IZD. VNIIGeofizika, 1973.

111. Pomerantseva, I. V., "The Results of Using 'Zemlya' Stations to Study the Focal Zone of the Tashkent Earthquake," in "Seysmotektonika Sredney Azii i Dal'nego Vostoka" [The Seismotectonics of Central Asia and the Far East], Moscow, Sovetskoye Radio, 1974.

112. Pomerantseva, I. V., "The Effect of the Angle of Inclination of the Interface on the Difference of Arrival Times of Single Composite PS and Longitudinal P Waves to the Earth's Surface," PRIKLADNAYA GEOFIZIKA, No. 80, 1975.

113. Pomerantseva, I. V., L. P. Barskova and A. N. Mozzhenko, "Models of the Earth's Crust Obtained from Data of 'Zemlya' Stations in the Area of Some Series of Different Age, Platform Depressions and Foredeeps," in Glubinnoye stroyeniye zemnoy kory" [The Deep Structure of the Earth's Crust], Moscow, Nauka, 1975.

114. Pomerantsev, V. V., "The Isometric Scale-The Transporter," GORNYY ZHURNAL VYSSHIKH UCHEBNYKH ZAVEDENIY, No. 5, 1961.

115. Pomerantseva, I. V., A. N. Mozzhenko, I. A. Sokolova and G. V. Yegorkina, "Using 'Zemlya' Seismological Stations in Study of the Structure of the Southeastern Russian Series," DOKL. AN SSSR, Vol. 163, No. 1, 1965.

116. Puzyrev, N. N., "Interpretatsiya dannykh seysmorazvedki metodom otrazhennykh voln" [Interpretation of Seismic Prospecting Data By the Reflected Wave Method], Moscow, Gostovtekhizdat, 1959.

117. Puzyrev, N. N., "Some Problems of Interpreting Transverse and Composite Waves," in "Eksperimental'nye issledovaniya poperechnykh i obmennykh voln" [Experimental Studies of Transverse and Composite Waves], Novosibirsk, Izd-vo SO AN SSSR, 1962.

118. Puzyrev, N. N. and I. R. Obolentseva, "Polarization of Longitudinal and Composite Reflected Waves on the Horizontal Surface of Observations in the Case of Sloping Interfaces," in "Poperechnyye i obmennyye volny v seysmorazvedke" [Transverse and Composite Waves in Seismic Prospecting], Moscow, Nedra, 1967.

APPROVED FOR RELEASE: 2007/02/08: CIA-RDP82-00850R000200030043-9

APPROVED FOR RELEASE: 2007/02/08: CIA-RDP82-00850R000200030043-9

119. Puzyrev, N. N., S. V. Krylov and B. P. Mishen'kin, "Metodika rekognostsirovochnykh glubinnykh seysmicheskykh issledovaniy" [The Method of Deep Seismic Exploration Studies], Novosibirsk, Nauka, 1975.

120. Raitt, R. U., "Anisotropy of the Upper Mantle," in "Zemnaya kora i verkhnyaya mantiya" [The Earth's Crust and Upper Mantle], Moscow, Mir, 1972.

121. Ratnikova, L. I., "Metody rascheta seysmicheskikh voln v tonkosloistykh sredakh" [Methods of Calculating Seismic Waves in Thin-Layered Media], Moscow, Nauka, 1973.

122. Ratnikova, L. I. and A. L. Levshin, "Calculating the Spectral Characteristics of Thin-Layered Media," IZV. AN SSSR, SER. FIZIKA ZEMLI, No. 2, 1967.

123. Ratnikova, L. I. and T. B. Yanovskaya, "Approximate Calculation of the Wave Fields in Thin-Layered Media," in "Nekotoryye pryamyye i obratnyye zadachi seysmologii. Vychislitel'naya seysmologiya" [Some Direct and Inverse Problems of Seismology. Computer Seismology], Moscow, Nauka, 1968.

124. Pomerantseva, I. V., A. N. Mozzhenko, I. A. Sokolova and G. V. Yegorkina, "The Results of Regional Studies with the 'Zemlya' Seismic Stations and the Prospects of These Investigations," in "Regional'nyye geologo-geofizicheskiye issledovaniya v bortovoy zone Prikaspiyskoy vpadiny" [Regional Geological-Geophysical Studies in the Lateral Zone of the Pre-Caspian Depression], Saratov, 1964.

125. Pomerantseva, I. V., A. N. Mozzhenko, G. V. Yegorkina et al, "The Results of Studying the Structure of the Earth's Crust and Upper Mantle by Using the 'Zemlya' Stations in the Azov-Kuban' Depression," PRIKLADNAYA GEOFIZIKA, No. 55, 1969.

126. Shcherbakova, B. Ye., K. A. Savinskiy, I. V. Lobachevskiy and I. M. Shtutin, "The Results of the First Deep Seismic Studies with the 'Zemlya' Stations in the Pre-Baykal Area," in "Baykal'skiy rift" [The Baykal Rift], Moscow, Nauka, 1968.

127. Tulyaganov, Kh. T., V. G. Gar'kovets, A. G. Khvalovskiy et al, "The Results of Complex Geological-Geophysical Investigations to Study the Nature of the Tashkent Earthquake," SOVETSKAYA GEOLOGIYA, No. 1, 1968.

128. Yegorkina, G. V., I. V. Garetovskaya, I. A. Sokolova et al, "The Results of Operations of 'Zemlya' Stations on Study of the Deep Structure of the Earth's Crust of Armenia," in "Geofizicheskiye issledovaniya v seysmoopasnykh zonakh" [Geophysical Studies in Seismically Dangerous Zones], Moscow, Izd. VNIIGeofizika, 1971.

APPROVED FOR RELEASE: 2007/02/08: CIA-RDP82-00850R000200030043-9

APPROVED FOR RELEASE: 2007/02/08: CIA-RDP82-00850R000200030043-9

129. Al'ter, S. M., N. Ya. Kunin, L. M. Lysyakov et al, "The Results and Further Direction of Complex Geophysical Studies of the Seismically Dangerous Region of Alma-Ata," in "Zemnaya kora sesymoopasnykh zon" [The Earth's Crust of Seismically Dangerous Zones], Moscow, Nauka, 1973.

130. Riznichenko, Yu. V., "The Geometric Seismic Nature of Layered Media," TRUDY IN-TA TEORETICHESKOY GEOFIZIKI, Vol. 2, No. 1, 1946.

131. Riznichenko, Yu. V., "Seismic Quasi-Anisotropy," IZV. An SSSR, SER. GEOGR. I GEOFIZ., Vol. 13, No. 6, 1949.

132. Rikhter, Ch. F., "Elementarnaya seysmologiya" [Elementary Seismology], Moscow, Izd-vo IL, 1963.

133. Rogoza, O. I., "Kinematic and Some Dynamic Characteristics of Refracted-Diffracted Waves," PRIKLADNAYA GEOFIZIKA, No. 32, 1962.

134. Rudnitskiy, V. P., "The Polarized Properties of Composite Seismic Waves," GEOFIZICHESKIY SBORNIK, No. 44, 1971.

135. Rudnitskiy, V. P., "Some Problems of Ray Theory of Transient Composite Waves," in "Voprosy geofizicheskikh issledovanii na Ukraine" [Problems of Geophysical Studies in the Ukraine], Kiev, Naukova Dumka, 1972.

136. Veshnyakov, A. V., D. I. Kirnos, N. A. Linden et al, "Rukovodstvo po proizvodstvu i obrabotke nablyudeniy na seysmicheskikh stantsiyakh SSSR" [Handbook on Production and Processing of Observations at Seismic Stations of USSR], Part 1, Moscow, Izd-vo AN SSSR, 1952.

137. Arkhangel'skiy, V. G., V. N. Gayskiy, A. L. Levitskaya et al, "Rukovodstvo po proizvodstvu i obrabotke nablyudeniy na seysmicheskikh stantsiyakh SSSR" [Handbook on Production and Processing of Observations at Seismic Stations of USSR], Part 2, Moscow, Izd-vo AN SSSR, 1954.

138. Rustanovich, D. N., "The Seismicity of the Turkmen' SSR and the Ashkhabad Earthquake of 1948," in "Voprosy inzhenernoy seysmologii," Moscow, Nauka, 1967.

139. Ryaboy, V. Z. and I. N. Galkin, "The Absolute Amplitude Characteristics of Signals During Deep Seismic Studies," in "Metodika i rezul'taty issledovaniya zemnoy kory i verkhney mantii" [The Method and Results of Studies of the Earth's Crust and Upper Mantle], Moscow, Nauka, 1972.

140. Savarenskiy, Ye. F., "The Angles of Emergence of Seismic Radiation and Some Related Problems," TRUDY GEOFIZ. IN-TA AN SSSR, No. 15 (142), 1952.

141. Saverenskiy, Ye. F. and D. P. Kirnos, "Elementy seysmologii i seysmometrii" [Fundamentals of Seismology and Seismometry], Moscow, Gostoktekhizdat, 1955.

APPROVED FOR RELEASE: 2007/02/08: CIA-RDP82-00850R000200030043-9

APPROVED FOR RELEASE: 2007/02/08: CIA-RDP82-00850R000200030043-9

142. Sollogub, V. B., D. Prosen and G. Milittser, "Stroyeniye zemnoy kory tsentral'noy i yugo-vostochnoy Evropy (po dannym zrivnoy seysmologii)" [The Structure of the Earth's Crust of Central and Southeastern Europe (From Data of Explosion Seismology)], Kiev, Naukova Dumka, 1971.

143. "Stroyeniye zemnoy kory po seysmicheskim dannym" [The Structure of the Earth's Crust from Seismic Data], Moscow, Izd-vo IL, 1959.

144. Butovskaya, Ye. M., T. M. Gol'tseva, V. P. Surov et al, "The Structure of the Almalyk Ore Region from Data of Studies with the 'Zemlya' Device," in "Zemnaya kora Uzbekistana" [The Earth's Crust of Uzbekistan], Tashkent, FAN, 1974.

145. Subbotin, S. I., V. B. Sollogub and A. V. Chekunov, "The Structure of the Earth's Crust of the Main Structural Elements of the Ukraine," DOKL. AN SSSR, Vol. 153, No. 3, 1963.

146. Sumerina, E. P., "Determination of the Absorption and Dispersion Coefficients of Longitudinal and Transverse Waves Recorded by 'Zemlya' Stations," RAZVEDOCHNAYA GEOFIZIKA, No. 59, 1973.

147. Tagay, Ye. D., "Using the Wiechert-Chibisov Method to Determine the Velocity Parameters of the Medium During Deep Seismic Sounding," PRIKLADNAYA GEOFIZIKA, No. 36, 1963.

148. Tagay, Ye. D. and G. S. Padurets, "Study of the Deep Structure of Regions by Using Subsequent Recordings on Seismograms of Regional KMPV Studies," PRIKLADNAYA GEOFIZIKA, No. 51, 1968.

149. Tal'-Virskiy, B. B., "The Tectonics and Geophysical Fields of Oil- and Gas-Bearing Regions of the Central Part of Central Asia," author's abstract of dissertation for degree of doctor of geological-mineralogical sciences, Moscow, MINKh i GP imeni Gubkin, 1972.

150. "Tashkentskoye zemletryaseniye 26 aprelya 1966 g." [The Tashkent Earthquake of 26 April 1966], Tashkent, FAN, 1971.

151. Treskov, A. A., "Interpretation of Observations of Near Earthquakes," in "Voprosy seysmichnosti Sibiri" [Problems of the Seismicity of Siberia], Novosibirsk, SO AN SSSR, 1964.

152. Trigubova, K. V., "The Nature of Waves Recorded by 'Zemlya' Stations from Remote Earthquakes," in "Teoreticheskoye i eksperimentalnoye issledovaniye obmennykh voln zemletryaseniy," Moscow, Izd. VNIIGeofizika, 1973.

153. Fedotov, S. A. and S. A. Boldyrev, "The Dependence of the Absorption of Composite Waves on Frequency in the Crust and Upper Mantle of the Kurile Island Arc," IZV. AN SSSR, SER. FIZIKA ZEMLI, No. 9, 1969.

APPROVED FOR RELEASE: 2007/02/08: CIA-RDP82-00850R000200030043-9

APPROVED FOR RELEASE: 2007/02/08: CIA-RDP82-00850R000200030043-9

154. Fedorenko, A. N., "Magnitnaya sey smicheskaya zapis'" [Magnetic Seismic Recording], Moscow, Nedra, 1964.

155. Fotiadi, E. E., "Geologicheskoye stroyeniye Russkoy platformy po dannym regional'nykh geofizicheskikh issledovaniy i opornogo bureniya" [The Geological Structure of the Russian Series from Data of Regional Geophysical Studies and Support Drilling], Moscow, Gostoptekhizdat, 1959.

156. Khalevin, N. I., "The Deep Structure of the Urals and Contiguous Regions According to Geophysical Data," GEOTEKTONIKA, No. 6, 1972.

157. Khalturin, V. I., "The Amplitudes and Periods of Seismic Waves from Earthquakes," author's abstract of dissertation for degree of candidate of physicomathematical sciences, Moscow, IFZ AN SSSR, 1966.

158. Kharkevich, A. A., "Spektry i analiz" [Spectra and Analysis], Moscow, Fizmatgiz, 1962.

159. Chibisov, S. V., "Processing the Curvilinear Hodograph of Elastic Waves During Planoparallel Distribution of Their Velocities in an Elastic Medium," GEOFIZIKA, No. 4, 1934.

160. Chichinin, I. S., "A Device for Regional Seismic Studies in Difficultly Accessible Regions," GEOFIZICHESKOYE PRIBOROSTROYENIYE, No. 19, 1964.

161. Tsibul'chik, G. M., "Analyzing the Structure of Seismograms from Remote Earthquakes," GEOLOGIYA I GEOFIZIKA, No. 4, 1969.

162. Shevchenko, V. I. and I. A. Rezanov, "The Deep Geological Structure of the Western Part of the Caucasus, the Crimea and the Adjacent Black Sea Basin," IZV. AN SSSR. SER. GEOL., No. 10, 1972.

163. Shcherbakova, B. Ye., T. M. Lin'kova and T. I. Semenova, "The Nature of Waves Recorded by 'Zemlya' Stations in Regions of Eastern Siberia," SOVETSKAYA GEOLOGIYA, No. 4, 1972.

164. Shcherbakova, B. Ye. and T. M. Lin'kova, "Theoretical Seismograms of Transient Longitudinal and Composite Waves with Some Models of the Interfaces," in "Teoreticheskiye i eksperimental'nyye issledovaniya obmennykh voln zemletryaseniy," Moscow, Izd. VNIIGeofizika, 1973.

165. Shcherbakova, B. Ye. and T. M. Lin'kova, "Transient Longitudinal and Composite Waves Formed in the Transition Layer," in "Teoreticheskiye i eksperimental'nyye issledovaniya obmennykh voln zemletryaseniy," Moscow, Izd. VNIIGeofizika, 1973.

166. Yanovaskaya, T. B., Yu. A. Surkov and Ye. M. Ignashkina, "A Program for Calculating Hodographs and Amplitudes of Waves Propagated in an Axisymmetrical Inhomogeneously Layered Medium," in "Programmy dlya interpretatsii seysmicheskikh nabludeniy, [Programs for Interpretation of Seismic Observations], Leningrad, Nauka, 1972.

APPROVED FOR RELEASE: 2007/02/08: CIA-RDP82-00850R000200030043-9

APPROVED FOR RELEASE: 2007/02/08: CIA-RDP82-00850R000200030043-9

167. Berch, F., "The Velocities of Compressional Waves in Rocks to 10 Kilobars," GEOPHYSICS, No. 4, 1960.

168. Bram, K. and P. Giese, "Die Geschwindingkeits-verteilung der P-Welle in der Erdkruste im Raum Augsburg (sued-Deutschland) Ergebnisse und Vergleich zweier seismischer Messungen," Z. FUER GEOPHYSIK, No. 34, 1968.

169. Fajklewicz, Z., "Crustal Thickness in the Region of the Pre-Sudetic Monocline in the Light of Geophysical Data," Materialy i prace, Publications of the Institute of Physics of the Polish Academy of Sciences, Selected Problems of Upper Mantle Investigations, 1966-1968, Warczawa, 1970.

170. Fuchs, K. and M. Landisman, "Results of Reinterpretation of the North-South Adelegsen-Milders-South Refraction Line in West Germany," Z. FUER GEOPHYSIK, No. 32, 1966.

171. Grundriss der Geologie der Deutschen Demokratischen Republik. Bd. 1. Geologischen Entwicklung des Gesamtgebietes. Herausgegeben von Zentralen Geologischen Institut im Auftrag des Staatssekretariats fuer Geologie beim Ministerrat der Deutschen Demokratischen Republik, Berlin, Akademie Verlage, 1968.

172. "German Research Group for Explosion Seismology, Crustal Structure in Western Germany," Z. FUER GEOPHYSIK, No. 30, 1963.

173. "German Research Group for Explosion Seismology, Seismic Wide-Angle Measurements in the Bavarian Mollasse Basin," GEOPHYSICAL PROSPECTING, Vol. 14, No. 1, 1966.

174. Giese, P., Ergebnisse der bisherigen seismischen Messungen in den Alpen und Eroerterung einiges damit zusammen haengender Probleme, Clausthal-Zellerfelt, 1965.

175. Closs, H., "Der untergrund der Alpen im Lichte neuerer geophysikalischer Untersuchungen," ERDOEL UND KOHLE, Vol. 19, No. 2, 1966.

176. Hasegawa, M., "Die Wirkung der odersten Erdschicht auf die Anfangsbewegung einer erdbeden Wellen," Z. FUER GEOPHYSIK, Vol. 6, No. 2, 1930.

177. Liebscher, H. I., "Reflexionshorizonte der tieferen Erdkruste im Bayerischen Alpenvorland, abgeleitet aus Erdgebnissen der Reflexionsseismik," Z. FUER GEOPHYSIK, Vol. 28, 1962.

178. Liebscher, H. I., "Deutugsversuche fuer die Struktur der tieferen Erdkruste nach reflexionsseismischen und gravimetrishcen Messungen in Deutschen Alpenvorland," Z. FUER GEOPHYSIK, Vol. 30, 1964.

179. Meissner, R., "An Interpretation of the Wide-Angle Measurements in The Bavarian Molasse Basin," GEOPHYSICAL PROSPECTING, Vol. 14, No. 1, 1966.

APPROVED FOR RELEASE: 2007/02/08: CIA-RDP82-00850R000200030043-9

APPROVED FOR RELEASE: 2007/02/08: CIA-RDP82-00850R000200030043-9

180. Pomerantseva, I. V., A. N. Mozzhenko, C. Junge and W. Lange, "Die Methode 'Zemlja' ein neues verfahren zur regionalen untersuchung des Krusten beis Geologie," Z. FUER DAS GESAMTGEBEIT DER GEOLOGISCHEN WISSENSCHAFTEN, No. 2, 1970.

181. Morelli, C., S. Bellemo and G. de Visintini, "Non-Directional Travel-Time Anomalies for European Stations," BOLL. DI GEOFISICA TEORICA ED APPLICATA, Vol. 10, No. 38, 1968.

182. Prodehl, C., "Auswertung von Refraktionsbeobachtungen im bayerischen Alpenvorland (Steinbruchsprengungen bei Eschenlohe 1958-1961) im Heimblick auf die Tiefenlage des Grundgebirges," Z. FUER GEOPHYSIK, Vol. 30, No. 4, 1964.

183. Skorupa, J., "Morphology of the Consolidated Basement in Poland in the Light of Seismic Refraction Surveys," MATERIALY I PRACE, 34, Publications of the Institute of Geophysics of the Polish Academy of Sciences, Selected Problems of Upper Mantle Investigations, 1966-1968, Warsaw.

184. Subbotin, S, V. Sollogub, D. Prosen, T. Dragasetich, E. Mituch and K. Posgay, "Crustal Structure of Southeastern Europe According to the Data of Deep Seismic Soundings," BOLL. GEOF., Vol. 10, No. 39, 1968.

185. Visser, S. W. and J. Berlage, "Zur Trage der Ungleichzeitigkeit der P-Einsaetze bei den horizontalen und vertik len seismographen," GERLANDS BEITRAEGE ZUR GEOPHYSIK, Vol. 19, No. 1, 1928.

186. Wiechert, E., "Bestimmung des weges der Erdbebenwellen im Erdinern von E. Wiechert und Ludwig Geiger," PHYSIK Z., No. 11, 1910.

[8144/0195-5621]

COPYRIGHT: Izdatel'stvo "Nedra", 1977

6521

CSO: 8144/195 END

APPROVED FOR RELEASE: 2007/02/08: CIA-RDP82-00850R000200030043-9